MEMBRANE PROPERTIES OF CONES AND GANGLION CELLS OF THE ~~TIGER~~ SALAMANDER RETINA

Karen Elizabeth Everett

A thesis submitted for the degree of
Doctor of Philosophy
in the
University of London

Department of Physiology
University College London
January 1990

Abstract

The aim of this thesis was to investigate the membrane properties of cone photoreceptors and ganglion cells of the salamander retina and to determine their role in the processing of the visual signal.

Experimental investigations were carried out on cells in the intact retina and also in cells that had been isolated from the retina by enzymatic dissociation.

Glutamate is thought to be the neurotransmitter released from vertebrate photoreceptors. Glutamate gates channels in postsynaptic bipolar and horizontal cells, but there have been no exhaustive studies of the effects of glutamate on the photoreceptors themselves. In patch-clamp recordings from both isolated cones and cones in the intact salamander retina, glutamate was found to activate a current carried largely by chloride ions, which is localized to the synaptic terminal of the cone. This suggests that glutamate released from a cone terminal may act on "autoreceptors" on that terminal, modulating its own release. This may be important as a mechanism for increasing the gain of cone phototransduction.

The membrane properties of ganglion cells determine how visual information is coded for transmission to the brain. Ganglion cells have previously been shown to exist as at least two types, sustained and transient, in terms of the pattern of action potentials produced in response to illumination. The origin of transience in ganglion cells in unclear. Salamander ganglion cells show sustained or transient responses to the injection of current mimicking light-induced synaptic input. Using the whole-cell recording method, the properties of both voltage-gated currents and excitatory and inhibitory neurotransmitter-gated currents were investigated in voltage-clamped salamander ganglion cells. On the basis of these results, it is suggested that transience in the response of ganglion cells may in part be due to the properties of the voltage-gated membrane currents present in these cells.

Preface

The complex nature of the experiments described in Karen Everett's thesis required that some of them be carried out in collaboration with others. Apart from this necessary input (described below) all of the thesis is Karen Everett's work: she was responsible, with normal supervisorial input, for initiating the work described, doing the experiments and analysing the results. All of the writing of the thesis was done by her.

Early experiments, when the techniques were being learned, were done in collaboration with David Attwell, Monique Sarantis and Peter Mobbs.

In the chapter on the effects of glutamate on cones, some experiments were done in collaboration with Monique Sarantis and David Attwell (with one person manipulating the cells and the other controlling the electronics: having two people present speeds up the experiments). In the chapters on the voltage-gated and neurotransmitter-gated currents in ganglion cells, some experiments were performed with help from Peter Mobbs.

Throughout the thesis, all of the experimental records shown are from experiments the candidate performed herself.

David Attwell

Contents

List of Figures

In Chapter 1

In Chapter 2

In Chapter 3

List of Tables

In Chapter 2

In Chapter 6

Acknowledgements

It is a pleasure to thank both David Attwell and Peter Mobbs for their guidance and advice throughout the period of my PhD.

I would also like to thank my colleagues Helen Brew, Monique Sarantis, Boris Barbour, Marek Szatkowski and Beverley Clark, and the other members of the Physiology Department, in particular David Eisner, Sue Wray and Miguel Valdeolmillos, for continual encouragement and for making my stay so enjoyable.

I am very grateful to the Wellcome Trust of Great Britain for the award of a postgraduate scholarship.

Finally, it has been a comfort to me to have always had my family behind me.

Chapter 1
Introduction

To understand the physiological basis of visual processing in the vertebrate retina, it is important to characterize the voltage-gated and neurotransmitter-gated currents in the membrane of retinal cells.

The experiments presented in this thesis reveal evidence for a novel glutamate-gated current in cone photoreceptors, and characterize the properties of both voltage- and neurotransmitter-gated currents present in ganglion cells of the tiger salamander retina. With this knowledge, the way in which these currents contribute to various aspects of visual processing may be assessed.

This introduction gives background information on the structure of the vertebrate retina and the properties of the different retinal cell types, with particular emphasis on neurotransmitter pathways and the function of synaptic transmission in the retina.

1.1 An overview of the structure of the vertebrate retina

1.1.1 Cellular organization of the retina

The retina contains six major types of neurons; photoreceptors, horizontal cells, bipolar cells, amacrine cells, interplexiform cells and ganglion cells. The positions of these cells in the retina is shown in Fig. 1.1A (reproduced from Dowling, 1987). In addition, the diagram shows the large radial glial cell type, the Müller cell, which is found in all vertebrate retinae (Cajal, 1893), and which traverses the whole retina, extending fine processes laterally between the retinal neurones.

All vertebrate retinae have a layered organization as shown in Fig 1.1B, which is a photograph of a living slice of retina from the tiger salamander. The retina has three layers of cell bodies, the photoreceptor cell layer, the inner nuclear layer (containing the cell bodies of bipolar, horizontal and amacrine cells), and the ganglion cell layer. Synaptic connections made between the cell layers are restricted to the outer plexiform layer (where photoreceptors contact bipolar and horizontal cells) and the inner plexiform layer (where bipolar and amacrine cells contact ganglion cells). Exceptions to this cellular arrangement do occur, when

Fig. 1.1 The structure of the vertebrate retina.

A The major types of cell found in the vertebrate retina (from Dowling, 1987). The original drawing was based on observations of cells in the mudpuppy retina that had been stained by the Golgi method. The letters indicate: receptors, R; a horizontal cell, H; bipolar cells, B; an amacrine cell, A; an interplexiform cell, I; a ganglion cell, G; a Müller cell, M. All of these cell types are neuronal, except for the Müller cell, which is the main type of glial cell in the retina, extending processes all the way through the retina from the spaces between the photoreceptors and pigment cells (not shown) at the top of the diagram, to the vitreous humour at the bottom. Müller cells also have processes along the whole length of the cell which extend laterally between the neurons. The lines at the top and bottom of the diagram represent the external and internal limiting membranes respectively.

B The retinal slice preparation obtained by vertical slicing of the flattened retina on a slide, and then rotating the pieces of retina obtained, through 90^{o} so that the photoreceptor longitudinal axes were parallel to the slide. The photograph was taken with Hoffman modulation contrast optics. The photoreceptor layer (PL) and ganglion cell layer (GCL) are clearly visible in the outer and inner retina respectively. The photoreceptors normally project into the pigment epithelium, and the ganglion cell layer faces the vitreous. Between these cell layers, the outer plexiform layer (OPL) comprises the photoreceptor to bipolar and horizontal cell synapses, the inner nuclear layer (INL) contains the bipolar, horizontal and amacrine cell bodies, and the synaptic connections between bipolar, amacrine and ganglion cells make up the inner plexiform layer (IPL). Scale bar is 60μm.

A

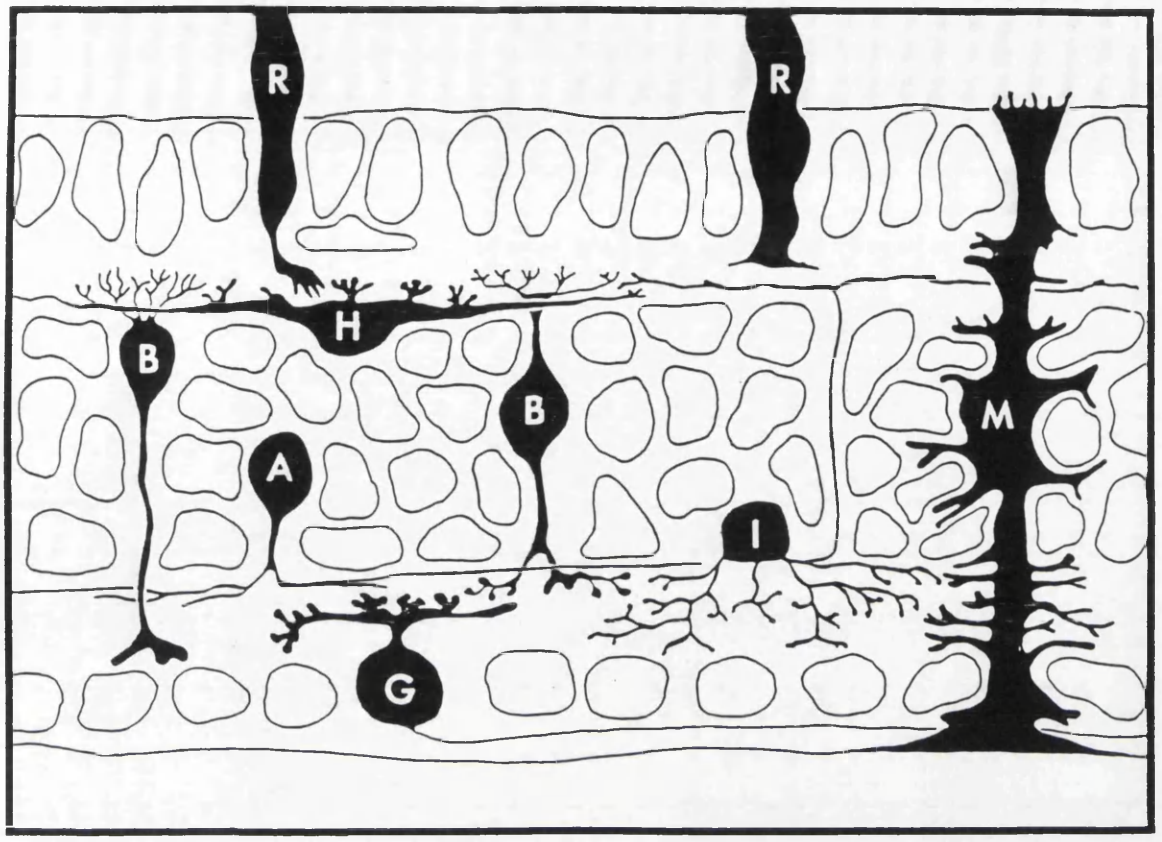

B

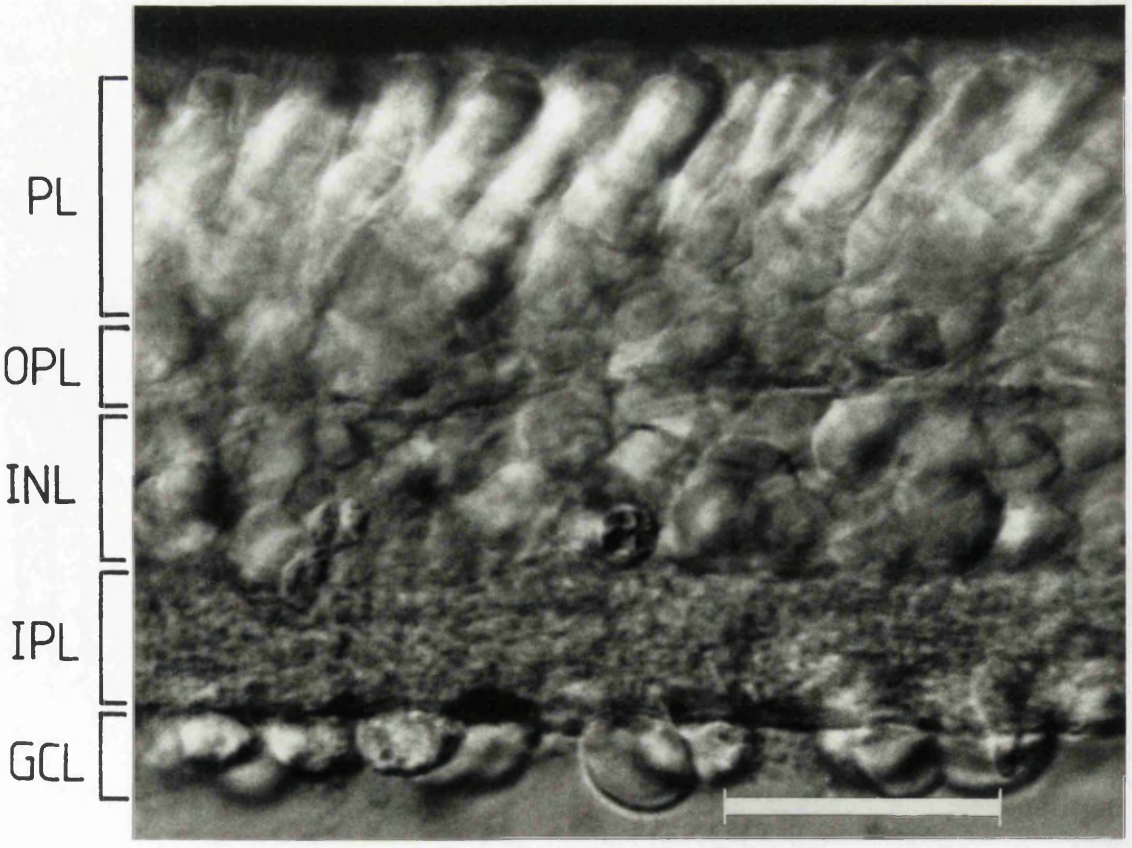

cells become "displaced" with respect to their "normal" position. For example, amacrine cells "displaced" to the ganglion cell layer are a general feature of many retinae.

1.1.2 Identification of retinal neurones

A combination of morphological (discussed here) and physiological studies (sections 1.2.3, 1.2.6) allows identification of the major retinal cell types (reviewed by Werblin, 1973), the properties of which are similar in the retinae of lower (amphibia and fish) and higher vertebrates (rat, rabbit and cat).

Much early information about retinal cell morphology came from visualization of Golgi-stained cells with light microscopy (Cajal, 1893). Later, details of the synaptic connections in the retina were revealed by electron microscopy of Golgi-stained cells or specifically labelled cells (see below). Both electrical synapses (e.g. between photoreceptors and between horizontal cells, Witkovsky et al., 1974) and chemical synapses (Lasansky, 1973) are found in the retina.

Physiological studies, particularly intracellular recording with microelectrodes and more recently patch-clamp recording (Hamill et al., 1981), suggest that there are a few basic response types for each class of retinal neuron. Cell types may be identified during recording by introducing dyes (such as Niagara Sky Blue or Procion yellow) into the cell, by injection, or by allowing them to diffuse into the cell from the recording electrode.

Complementary to the use of dyes, pharmacological studies which localize putative neurotransmitters or enzymes for their synthesis can distinguish certain retinal cell types from others. This may involve immunohistochemical techniques which use antibodies specific for particular substrates, conjugated with fluorescent markers, allowing direct visualization of the label associated with a particular cell type.

In Chapters 4 to 6 of this thesis, a staining technique which specifically labels ganglion cells has been used successfully for their identification in the intact retina and in an isolated cell preparation (see Methods, sections 2.5.1 and 2.5.2, Chapter 2).

1.2 Information transfer in the retina

1.2.1 Transmission of information in the retina occurs through vertical and lateral pathways which are subserved by different neurotransmitters.

Information is carried in two directions during visual processing, vertically and laterally through the retina with respect to the diagrams in Fig 1.1. Vertically, electrical signals generated by light in photoreceptors (see below, section 1.2.2) are transmitted via chemical synapses to bipolar cells, and from bipolar cells to ganglion cells. Ganglion cell axons form the optic nerve which projects to the optic tectum. Vertical transmission of information is thought to be mediated predominantly by excitatory amino acid neurotransmitters (see sections 1.3.2 and 1.3.8).

Laterally, information transfer is mediated mainly by inhibitory amino acid neurotransmitters from horizontal cells to cone photoreceptors and bipolar cells in the outer retina (see section 1.3.6) and from amacrine cells to bipolar and ganglion cells in the inner retina (see section 1.3.10). Interplexiform cells extend processes into both inner and outer plexiform layers, and seem to provide feedback from the inner retina (mainly from amacrine cells: Dowling and Ehinger, 1975) to bipolar and horizontal cells in the outer retina.

1.2.2 Phototransduction: the first stage of information processing in the retina

Information processing in the retina begins with the conversion of light into a voltage response (phototransduction) in photoreceptors. In the absence of light, an inward "dark" current (carried by sodium and calcium ions) flows through the photoreceptor outer segment membrane and keeps the cell depolarized.

Light causes photoreceptors to hyperpolarize. This voltage response results from absorption of light by a visual pigment, activating an enzyme cascade, which eventually leads to a drop in the concentration of cyclic GMP (cGMP) in the cytoplasm of the photoreceptor outer segment. The cGMP directly gates "dark" current channels, holding them open in the dark (Fesenko et al., 1985), so that when the levels of cGMP fall in the light the channels close,

thus reducing the inward "dark" current and hyperpolarizing the photoreceptors (Hagins et al., 1970; Lamb, 1986). The gain of phototransduction is high; for each molecule of rhodopsin isomerized, several hundred outer segment channels close.

In Chapter 3, I describe a novel neurotransmitter-gated current localized to the synaptic terminal of salamander cone photoreceptors which, when activated, may initiate a positive feedback mechanism which could increase the gain of cone phototransduction.

1.2.3 Outer retinal neurons respond to light with graded changes in voltage

The magnitude of the hyperpolarization in photoreceptors produced by light depends on the light intensity, increasing in size as the light intensity increases. The maximum change in voltage which occurs in response to bright light is between 25 and 30mV (from the photoreceptor dark potential of -40mV (see section 1.3.1) to around -65mV).

Bipolar and horizontal cells also produce graded voltage responses to light. Horizontal cells hyperpolarize, and bipolar cells can be divided into two classes, those that hyperpolarize in response to light in the centre of their receptive field ("OFF" bipolars), and those that depolarize ("ON" bipolars). These two classes probably exist as a result of different actions of the photoreceptor neurotransmitter on each cell (see section 1.3.4).

1.2.4 Formation of "OFF" and "ON" channels in the retina

Segregation of the visual information into "OFF" and "ON" channels at the bipolar cell level results in the sign of the photoreceptor response to light (classified as "OFF", because the photoreceptors are depolarized when the light goes off) being either conserved or inverted. Hyperpolarizing bipolar cells have output synapses directly onto "OFF" ganglion cells and depolarizing bipolar cells send synapses to "ON" ganglion cells (response properties of these cells are described below). It is not really known why this organization exists. Marr (1982) suggests that it provides an efficient way of signalling both increases and decreases in illumination (discussed in section 1.4.1).

1.2.5 Centre-surround organization in the receptive field of retinal neurons

The classification of response types into "OFF" and "ON" represents the effects of light falling on the centre of the bipolar or ganglion cells' receptive fields (determined by the dendritic spread of the cell). Light falling in the periphery (surround) of the bipolar cell receptive field produces a voltage change in the bipolar cell which is opposite in sign to that generated by direct input from photoreceptors. This effect is mediated by horizontal cells in the outer retina which make inhibitory synapses with bipolar cells, either directly, or via cone photoreceptors (see sections 1.3.6 and 1.3.7).

This centre-surround organization allows for signalling of differences in light intensity between the receptive field centre and the surround, rather than simply detecting the intensity at one point on the retina.

As for the segregation of information into "OFF" and "ON" channels, this centre-surround organization is maintained by ganglion cells in the inner retina as a direct result of the input they receive from bipolar cells. Amacrine cells provide an extra level of lateral inhibition to ganglion cells (either directly, or via bipolar cells) which is activated by motion in the receptive field surround (Werblin, 1972). The functions of this centre-surround organization are discussed further with respect to removal of unimportant information during retinal processing in section 1.4.2.

1.2.6 Inner retinal neurons produce action potentials

Ganglion cells convert graded changes in voltage produced by outer retinal neurons into trains of action potentials, and
outer retinal neurons into trains of action potentials, and
(Werblin & Dowling 1969) on cells produce action potentials because a regenerative signal is required to transmit information along the relatively long ganglion cell axons to the brain.

Three classes of ganglion cells were originally described in the frog by Hartline, (1938) on the basis of their responses to light. These were "ON", "OFF" and "ON-OFF" ganglion cells. The frequency of action potentials produced by "ON" ganglion cells increases when they are centrally illuminated, while the frequency

of action potentials produced by "OFF" ganglion cells increases at the offset of ilumination and is decreased by central illumination. "ON-OFF" ganglion cells produced a response at light on and light off. Ganglion cells of lower vertebrates can have a simple centre-surround receptive field or may exhibit more complex properties, such as motion-dependence or direction-selectivity.

Ganglion cells in higher vertebrates, for example, cat and rabbit, also have a centre-surround receptive field organization which may be simple (Kuffler, 1953) or more complex, e.g. direction-selective (Barlow and Levick, 1965; Levick, 1967).

In the cat, the centre-surround units formed two classes, X-cells and Y-cells, each including both the "ON" and "OFF" forms. This classification into X- and Y- is based on certain properties (Enroth-Cugell and Robson, 1966). Y-cells have a larger receptive field size, their axons have faster conduction velocities and they have a more transient light response than X-cells. The two types also respond differently to the presentation of a sinusoidal grating over the receptive field. For X-cells, a grating position could always be found such that no response occurred when it was introduced or withdrawn. No such null position could be found for Y-cells.

A third class of ganglion cells, W-cells, were found in the cat retina by Stone and Hoffman (1972). These are usually cells which cannot be classified as X- or Y-cells and which have axons with very slow conduction velocities.

1.2.7 Ganglion cells produce sustained or transient bursts of action potentials in response to light

The "ON" and "OFF" ganglion cell classes may be further subdivided into two response groups; those that produce a sustained burst of action potentials while a light is on or off and those which generate only a transient burst of action potentials in response to the onset or offset of light. Roughly speaking, "sustained" ganglion cells provide a measure of the light intensity (relative to the surround) at different points on the retina, while "transient" ganglion cells signal only that the light intensity has changed (thus signalling for example, movement of a stimulus). Amacrine cells, which show a transient response to light, are

thought to be involved in movement detection, and transience in the ganglion cell response to light may have a similar function.

The exact origin of transience in ganglion cell responses is not clear. Transience in the ganglion cell response may arise in a variety of ways;

1) By transient (i.e. not tonic) presynaptic release of the bipolar cell transmitter to ganglion cells.

2) By desensitization of ganglion cell receptors for the bipolar cell neurotransmitter (which is assumed to be released tonically when light is applied or removed).

3) Release of inhibitory neurotransmitters from amacrine cells (see section 1.3.10) starting after the start of release of the excitatory bipolar cell transmitter, may result in the effect of the excitatory transmitter on the ganglion cell membrane being counteracted at late times. This could occur because an extra synaptic delay is incurred in the amacrine cell pathway to ganglion cells (Werblin, 1977).

4) As a mechanism intrinsic to the ganglion cell itself e.g. the properties of voltage-gated currents in the ganglion cell membrane.

Of course, the generation of a transient ganglion cell response may result from a combination of the above possibilities. In Chapters 4 and 5 of this thesis, the mechanisms suggested above by 4 and 2 respectively are investigated to see how they might contribute to the generation of transience in the ganglion cell response to light. In addition in Chapter 6, the ganglion cell ionic currents gated by inhibitory transmitters (which may underlie mechanism 3 above) are investigated.

1.2.8 Signal shaping by voltage-gated currents in retinal neurons

The waveform of the voltage response to light in photoreceptors is not determined solely by the time course of suppression of the outer segment light-sensitive current. In the salamander, it is shaped further by voltage- and time-dependent currents in the membrane of the inner segment (and by current entering through electrical synapses between photoreceptors and, in the case of cones, generated by synaptic input from horizontal cells). Hyperpolarization of isolated photoreceptors produces an inward current as a result of activation of voltage-gated membrane

currents. This adds a transient component to the voltage response, which is not present in the photocurrent response (see review by Attwell, 1986). Transience in the response of retinal neurons is a mechanism by which visual signals may be temporally filtered, reducing the magnitude of low frequency signals. The importance of temporal filtering is discussed later, in section 1.4.3.

In some species (e.g. goldfish), a similar set of voltage- and time-dependent currents makes the voltage response of bipolar cells to light more transient than the waveform of the synaptic current generated in bipolar cells by the light-induced suppression of neurotransmitter release from photoreceptors (Kaneko and Tachibana, 1985).

Chapter 4 of this thesis shows that isolated ganglion cells of the salamander also have voltage-gated currents, and their possible contribution to the generation of transience in ganglion cells is discussed in section 7.3 (Chapter 7).

1.3 Synaptic transmission in the retina

Virtually every neurotransmitter or neuromodulator substance in the nervous system has been found in the retina of one species or another (Ehinger, 1982; Fain et al., 1983) The physiological actions of putative neurotransmitters at different levels within the retina have been reviewed by Ikeda (1985) and Massey and Redburn (1987). The functional significance of different types of synaptic input to various retinal cell types has been discussed in a recent review by Daw et al., (1989).

This section presents an overview of the neurotransmitter circuitry in the retina.

1.3.1 Neurotransmitter release from retinal neurons

It is well established that neurons release neurotransmitters when they are depolarized. The first indication that some retinal neurons release neurotransmitters at a high rate in the dark, and that light suppresses neurotransmitter release, appeared in the first intracellular recording of photoreceptor and horizontal cell responses (Svaetichin, 1953), which showed that the membrane potentials of these cells in the dark were more depolarized (-40mV) than those of other neurones (-70mV). Light decreases this depolarization, causing

cells to hyperpolarize from -40mV to around -65mV (the resting potential of most other neurons). Copenhagen and Jahr (1989) have shown directly that release of the photoreceptor transmitter in the turtle is indeed increased by depolarization and suppressed by hyperpolarization (see below).

Divalent cations play a fundamental role in the process of neurotransmitter release from presynaptic terminals of the neuromuscular junction and spinal cord. Calcium is generally required for neurotransmitter release, and its action is antagonized by an excess of magnesium or other divalent cations, such as cobalt (Del Castillo and Katz, 1954).

In a study of synaptic transmission between photoreceptors and horizontal cells in the perfused turtle retina, lowering external calcium or applying cobalt or magnesium hyperpolarized horizontal cells and suppressed their light response, but had little effect on the responses of photoreceptors (Dowling and Ripps, 1973). These observations suggest that a depolarizing transmitter is released in a calcium-dependent manner (but see Schwartz, 1986) from photoreceptors in the dark, and that the horizontal cell hyperpolarizing response to light results from suppression of the release of the photoreceptor neurotransmitter.

1.3.2 The photoreceptor transmitter

The best candidate for the transmitter released from photoreceptors is the excitatory amino acid, glutamate. This conclusion is based primarily on studies of the pharmacological actions of glutamate and various glutamate agonists and antagonists on the membrane potential and light responses of second order neurons (bipolar and horizontal cells; (Furukawa & Hanawa, MSS) Miller and Slaughter, 1986; Attwell *et al.*, 1987), in addition to immunocytochemical localization of glutamate synthesizing enzymes (Brandon and Lam, 1983; Sarthy *et al.*, 1986) and studies of release of neurotransmitter candidates from isolated photoreceptors (Miller and Schwartz, 1983; Ayoub *et al.*, 1988). More recently, endogenous excitatory amino acids released on depolarization of isolated turtle photoreceptors (Copenhagen and Jahr, 1989) have been demonstrated to gate "postsynaptic" glutamate-activated channels in patches of rat hippocampal neurons.

1.3.3 There are different types of receptors for glutamate

Glutamate depolarizes many neurons to which it is applied by opening non-specific cation channels which allow both sodium and potassium ions to pass (Watkins and Evans, 1981; Mayer and Westbrook, 1985). Glutamate receptors are usually classified according to their response to the selective glutamate agonists kainate, quisqualate, and N-methyl-D-aspartate (NMDA). Application of glutamate agonists to hyperpolarizing bipolar and horizontal cells has shown that glutamate receptors in these cells are of the kainate type (Shiells et al., 1981; Lasater et al., 1984; Ishida, 1984). It appears that depolarizing bipolar cells have specific receptors for glutamate (Slaughter and Miller, 1985a) which are different from other types of excitatory amino acid receptors found in the retina (see section 1.3.4 below).

1.3.4 There are two classes of bipolar cells which respond differently to glutamate

Although glutamate receptors on both hyperpolarizing and depolarizing bipolar cells are gated preferentially by kainate, and have a reversal potential around OmV, the existence of two response types is determined by the differential effects of photoreceptor transmitter (assumed here to be glutamate) on these cells (Attwell et al., 1987).

Since light hyperpolarizes photoreceptors and reduces the amount of glutamate released from them, the postsynaptic effects of glutamate are expected to be opposite to the effects produced by light in second order neurons. Hyperpolarizing (or "OFF") bipolar cells, depolarize and show an increase in membrane conductance in response to applied glutamate. Thus, glutamate appears to open channels in "OFF" bipolar cells in the dark. Suppression of the photoreceptor transmitter input in the light causes glutamate-gated channels to close, and the bipolar cell to hyperpolarize.

In depolarizing (or "ON") bipolar cells, glutamate-gated channels in the membrane are thought to be closed by the photoreceptor transmitter. Light suppression of transmitter release from photoreceptors will thus result in fewer channels being closed, explaining the light-induced depolarizaton. Isolated bipolar cells from the tiger salamander can be identified tentatively as hyperpolarizing or depolarizing from their different

responses to applied glutamate (Attwell et al., 1987).

1.3.5 Glutamate receptors on "ON" bipolar and horizontal cells are different

Application of glutamate and different glutamate agonists or antagonists to the retina and recording the responses produced in bipolar and horizontal cells, shows that glutamate activates pharmacologically distinct receptors in each cell type. The action of glutamate is blocked by antagonists PDA (cis-2,3-piperidine dicarboxylic acid) in hyperpolarizing bipolar cells and horizontal cells (Slaughter and Miller, 1983a) and by DOS (D-O-phosphoserine) in horizontal cells (Slaughter and Miller, 1985b). The glutamate analogue APB (2-amino-4-phosphonobutyric acid) mimics the action of glutamate on depolarizing bipolar cell receptors (Slaughter and Miller, 1985a), but has no effect on horizontal cells and hyperpolarizing bipolar cells. This suggests that the depolarizing bipolar cell glutamate receptor ("APB receptor") is distinct from other classes of glutamate receptors (e.g. kainate-type receptors). It has also been suggested that rod and cone inputs to depolarizing bipolar cells are mediated by two different receptors for glutamate (Nawy and Copenhagen, 1987).

Horizontal cells hyperpolarize in response to light and depolarize in response to applied glutamate. The glutamate-induced depolarization observed in isolated horizontal cells, does not seem to be accompanied by any apparent change in membrane resistance, suggesting perhaps that glutamate simultaneously opens and closes channels in the cell membrane (Lasater and Dowling, 1982; Tachibana, 1985)

1.3.6 Horizontal cells make inhibitory synapses in the outer retina

Lateral transmission of information in the outer retina is thought to be mediated by release of inhibitory amino acids from horizontal cells to bipolar cells and cone photoreceptors. This lateral inhibition probably forms the antagonistic surround of the centre-surround receptive field of both cones and bipolar cells (see section 1.3.7). Electrical coupling between horizontal cells increases the size of the receptive field surround (Lamb, 1976)

Both physiological and pharmacological lines of evidence indicate that gamma-aminobutyric acid (GABA) is a horizontal cell

transmitter. GABA is accumulated within frog horizontal cells (Voaden et al., 1974) and is synthesized in isolated axons of goldfish cone horizontal cells (Marc et al., 1978). Release of GABA from horizontal cells (in a calcium-independent way) by glutamate and its analogues, has been demonstrated in the goldfish retina (Ayoub and Lam, 1984) and GABA has been shown to gate postsynaptic $GABA_A$-type chloride channels in isolated turtle cones (Kaneko and Tachibana, 1986) and bipolar cells from the salamander (Attwell et al., 1987). Further, receptors for GABA have been morphologically localized by immunocytochemistry to cone synaptic terminals in chicken and goldfish retinae (Yazulla et al., 1987).

In the salamander retina, only about 60% of horizontal cells accumulate GABA, and a similar percentage of hyperpolarizing bipolar cells receive GABA-mediated inhibitory input (Wu, 1986). Hence, it seems likely that another transmitter (e.g. glycine) may mediate the receptive field inhibitory surround of the other bipolar cells.

Autoradiography of retinae labelled by high affinity radioactive glycine uptake has shown that horizontal cells, in addition to making postsynaptic contact with cones and bipolar cells, also receive inputs from glycine-containing interplexiform cells (Marc and Liu, 1984). This may provide an alternative pathway for horizontal cell-mediated signals to reach the inner plexiform layer.

1.3.7 Mechanisms of production of lateral inhibition

When horizontal cells are hyperpolarized by light, they will release less GABA. The effect of this change in GABA released onto postsynaptic cells (bipolar cells and cones) is dependent on a specific relationship between the chloride reversal potential (E_{Cl}) and the resting potential in those cells. When E_{Cl} is below the resting potential, GABA and glycine will evoke an influx of negative chloride ions (an outward current) at the resting potential, which will lead to a hyperpolarization. Thus light, which suppresses GABA release, will depolarize the cell (by disinhibition). There is evidence that this mechanism produces the antagonistic surround response of cone photoreceptors (Kaneko and Tachibana, 1986) and hyperpolarizing bipolar cells (Miller and

Dacheux, 1983). Miller and Dacheux (1983) also suggest that the hyperpolarizing surround response of depolarizing bipolar cells is generated by having the chloride reversal potential above the resting potential of the bipolar cell so that applied GABA will produce an inward current at the bipolar cell resting potential and removal of GABA hyperpolarizes the cell.

Inhibition may also be produced by another mechanism termed shunting inhibition, in which an increase in chloride conductance can occur without a change in the cell membrane potential. This occurs when E_{Cl} is close to the cell resting potential, so there is no net movement of chloride ions into or out of the cell in response to GABA or glycine at the resting potential, but when excitatory transmitters depolarize the cell an outward current through the chloride channels reduces the depolarization generated.

1.3.8 The bipolar cell transmitter

Glutamate is also a strong candidate for the excitatory amino acid transmitter from bipolar (and some amacrine cells) to ganglion cells (Slaughter and Miller, 1983a; Bloomfield and Dowling, 1985). Glutamate has been shown to act directly on isolated ganglion cells in the rat (Aizenman *et al.*, 1988a) and in the tiger salamander (Chapter 5 of this thesis). "ON" and "OFF" bipolar cells probably release the same excitatory amino acid transmitter (Naka, 1976; Slaughter and Miller, 1983a, 1983b).

1.3.9 Glutamate receptors on ganglion cells

The properties of ganglion cell receptors for glutamate have been investigated extensively in the intact vertebrate retina (Slaughter and Miller, 1983c; Ikeda, 1985; Ikeda *et al.*, 1989) and have been studied more recently in isolated ganglion cells (Aizenman *et al.*, 1988a; Karschin *et al.*, 1988). In both preparations receptors for glutamate were found to be most sensitive to kainate, although quisqualate and NMDA do have some effect. Responses to glutamate and glutamate analogues in isolated salamander ganglion cells are investigated in Chapter 5 of this thesis.

Ganglion cell axons form the optic nerve which relays processed visual information to the brain. In lower vertebrates glutamate is also thought to mediate transmission of information

from the optic nerve to the tectum (Langdon and Freeman, 1986), acting via kainate or quisqualate receptors (Nistri et al., 1988).

1.3.10 Amacrine cells make inhibitory synapses in the inner retina

Amacrine cells make synapses with ganglion cells and contribute to the properties of the ganglion cell receptive field surround (section 1.2.5). Probable inhibitory amino acid synapses have been demonstrated by electrophysiological and pharmacological studies (Miller et al., 1981). Amacrine cells have been shown to accumulate the inhibitory amino acids GABA and glycine (Ehinger, 1972) by a sodium-dependent high affinity uptake mechanism (Voaden et al., 1974) and to release these putative neurotransmitters by appropriate light stimulation or by increasing the external potassium concentration.

GABA and glycine have both been shown to gate postsynaptic chloride channels in isolated retinal ganglion cells from the goldfish (Ishida and Cohen, 1988; Cohen et al., 1989) with properties similar to those of conventional GABA and glycine-gated chloride channels (Bormann et al., 1987; Robertson, 1989). In Chapter 6 of this thesis I show that GABA and glycine gate similar chloride channels in isolated ganglion cells of the salamander.

Application of GABA or glycine to ganglion cells in the intact retina produces a hyperpolarization from their resting potential. This suggests that the chloride reversal potential must be below the ganglion cell resting potential (Miller et al., 1981; Miller and Dacheux, 1983). In ganglion cells, amacrine cell-mediated inhibition is produced by hyperpolarization (see section 1.3.7), but in amacrine cells, where E_{Cl} is approximately equal to the resting potential, a non-voltage generating "shunting" conductance change (see section 1.3.7) seems to be responsible for GABA or glycine-mediated inhibition (Miller et al., 1981).

Both sustained and transient inhibition are seen in ganglion cells (Belgum et al., 1982; 1983) and are thought to be mediated by separate amacrine cell inputs. In support of this hypothesis, there is evidence for independent GABA and glycine-releasing amacrine cells in the mudpuppy (Miller et al., 1977) and perfusion of the glycine anatagonist, strychnine, blocks transient but not sustained ganglion cell inhibition in the same species (Belgum et al., 1984).

1.3.11 Modulation of synaptic input to ganglion cells

There is evidence that the strength of surround inhibition in ganglion cells may be modulated directly by other amacrine cell transmitters (e.g. acetylcholine, from cholinergic amacrine cells), indirectly by the effects of amacrine cell inhibitory neurotransmitters on release of bipolar cell or amacrine cell excitatory neurotransmitters, or by putative neuromodulator substances such as peptides shown to be localized within amacrine cells (Karten and Brecha, 1980; Eskay et al., 1981).

The spontaneous activity of retinal ganglion cells with a centre-surround receptive field in higher vertebrates, is increased by acetylcholine (Schmidt et al., 1987) and direction-selectivity can be abolished by the acetylcholinesterase inhibitor, physostigmine (Ariel and Daw, 1982).

In addition to the direct effects of GABA on ganglion cells, GABA has also been shown to inhibit release of acetylcholine from amacrine cells of the rabbit (Massey and Redburn, 1982), and to modulate synaptic release from bipolar cells of the salamander (Lukasiewicz et al., 1988).

Other substances released from amacrine cells include peptides such as enkephalins and substance P (Eskay et al., 1980), which have been shown to have long-lasting postsynaptic effects on ganglion cell responses to light (Dick et al., 1980; Glickman et al., 1982). Exogenous application of enkephalins to chicken amacrine cells can inhibit their release of GABA (Watt et al., 1984). It has been previously demonstrated that enkephalins are capable of regulating acetylcholine release from mammalian sympathetic ganglia, by behaving as transmitters for long-lasting presynaptic inhibition of cholinergic transmission (Konishi et al., 1981). Thus, it is possible that similar peptides localized within retinal amacrine cells have a neuromodulatory role, changing the excitability of the ganglion cells under conditions when retinal sensitivity must be reset, for example during light or dark adaptation.

1.3.12 The actions of retinal neurotransmitters are terminated by uptake into neurons and glia

In order for neurotransmitters to function efficiently, and to prevent neuronal damage through prolonged receptor

stimulation (in the case of glutamate: Rothman and Olney, 1987), mechanisms must exist for termination of the postsynaptic action of neurotransmitters. Following synaptic release, inactivation of neurotransmitters may occur in a variety of ways such as diffusion away, binding, uptake or breakdown by extracellular enzymes.

Since there are no extracellular enzymes in synaptic clefts in the retina to inactivate many released neurotransmitters and to minimize the need for de novo synthesis of neurotransmitters, uptake of released transmitters could serve two important functions: to terminate their postsynaptic action and to recycle them for re-use.

Studies on the uptake of glutamate, GABA and glycine in the central nervous system (CNS) have shown that each is taken up by a structurally specific high affinity mechanism (Balcar and Johnston, 1973).

The extent to which uptake of glutamate, GABA and glycine occurs into retinal neurons and glial (Müller) cells seems to vary between different species (see review by Ripps and Witkovsky, 1985). Autoradiographic techniques have shown that glutamate is taken up preferentially into Müller cells rather than into neurons in the rat (White and Neal, 1976) and rabbit retina (Ehinger, 1972), although in some species there is also uptake of glutamate into photoreceptors, e.g. in goldfish retina (Marc and Lam, 1981) and rat retina (Brandon and Lam, 1983). Müller cells are the main site of localization of the enzyme glutamine synthetase (Sarthy and Lam, 1978), which converts glutamate to glutamine. Glutamine is thought to be able to diffuse freely into and out of cells, whereas glutamate cannot. Hence glutamine formed in glial cells may be passed back to neurons for re-use (e.g. converted back to glutamate, which might then be used as a transmitter or as a precursor for synthesis of GABA).

In the salamander retina, the properties of glutamate uptake into Müller cells have been detailed by Brew and Attwell (1987) and Barbour et al., (1988). These authors show that glutamate uptake is electrogenic, and occurs by a high affinity, sodium-dependent mechanism, which is similar to that observed for glutamate uptake in the CNS (Balcar and Johnston, 1972; Stallcup et al., 1979). Further, the uptake carriers for glutamate are spatially localized

to regions of the Müller cell membrane which face the neurons, and are therefore in an appropriate position for removing glutamate from the extracellular spaces.

In most retinae studied, uptake of GABA seems to occur predominantly into horizontal and amacrine cells, and glycine is taken up mainly by amacrine cells (Ehinger, 1972; Voaden et al., 1974). Immunocytochemical techniques have localized GABA-synthesizing and -degrading enzymes (L-glutamate decarboxylase and GABA-transaminase respectively) to horizontal and amacrine cells of the rat retina (Lin et al., 1983), suggesting that breakdown of accumulated GABA can occur, in addition to synthesis of GABA from glutamate. High affinity uptake of GABA and glycine in the retina is also sodium-dependent. In the absence of external sodium ions, uptake of both radiolabelled GABA and glycine in the toad retina was reduced by about 80% (Voaden et al., 1974).

This brief review shows clearly that uptake of excitatory and inhibitory neurotransmitters occurs into neurons and glia in the retina. This is probably the most powerful mechanism for terminating the actions of these transmitters. Even if neurotransmitter action is initially terminated by diffusion of the transmitter out of the synaptic cleft, this diffusion is only possible because uptake systems keep the extracellular transmitter concentration low outside the synaptic cleft.

1.4 The functions of retinal processing

The retina has two main functions. First of all it converts light into an electrical signal in rod and cone photoreceptors (see section 1.2.2) and then processes this signal to remove visual information that is unimportant. This minimizes the number of ganglion cell axons required to transmit useful information to the brain.

Neural processing of the visual signal optimizes the ability of the retinal ganglion cells (output neurons of the retina) to encode useful information. The coding capability of ganglion cells is necessarily restricted because they have an upper limit to the number of action potentials they can produce to encode a stimulus. This limit is set by the properties of the voltage-gated currents underlying the action potential and by the need for information to

be transmitted in a finite time.

A combination of mechanisms contribute to such signal shaping. These include activation of voltage- and time-dependent currents in retinal cell membranes, current flow through electrical synapses and the action of various neurotransmitters at different levels in the retina.

Below I discuss the ways in which the segregation of information into "OFF" and "ON" channels, the centre-surround receptive field organization and the enhancement of transience in the visual signal, accentuate useful information while removing that which is unimportant.

1.4.1 Segregation of information into "OFF" and "ON channels

When the "ON" pathway is blocked in the outer retina using the glutamate analogue APB (section 1.3.5), the ability of "ON" ganglion cells to detect changes in light intensity is impaired (Schiller et al., 1986). The segregation of information into "OFF" and "ON" channels is thought to providing an efficient (i.e. energy conserving) way of transmitting information about relative increases and decreases in illumination (Marr, 1982). In principle, it would seem that this could be achieved by having just one type of ganglion cell, e.g. an "ON" cell, which responded to an increase or decrease in illumination by increasing or decreasing its firing rate respectively. However, the coding of small changes in intensity superimposed on a low spontaneous firing rate (in darkness) would suffer from the problem that the change in rate of firing would not be detectable by the brain in less than the time which elapses between action potentials. This problem is avoided by having two information channels, one with a low spontaneous rate of firing in darkness, which increases as the light intensity increases ("ON) and one with a low rate of firing in the light which is increased by darkness ("OFF").

1.4.2 Centre-surround receptive field organization

The centre-surround organization in the receptive field of some retinal neurons is a mechanism by which detection of spatial changes in light intensity (i.e. differences in intensity, or contrast, between the centre and the surround) is enhanced. The advantage of comparing centre and surround signals is that the

range of signal amplitudes to which the coding range of the bipolar or ganglion cells must be devoted is then more restricted than the entire range of absolute light intensities, because images on the retina tend to be spatially correlated. Thus, a limited range of information eventually reaches the inner retina, enabling the dynamic range of ganglion cells to be devoted to only that information which is relevant (Barlow, 1981; Srinivasan et al., 1982).

1.4.3 Transience in the response of retinal neurons

Transience in the voltage response of retinal neurons is a form of temporal filtering of the visual signal. This temporal filtering starts in the earliest stages of signal generation, with voltage- and time-dependent currents changing the waveform of the photoreceptor voltage response to light (see also section 1.2.8), so that it peaks before the peak change in the light-sensitive current flowing. At the level of the second order neurons, the voltage change produced in postsynaptic bipolar and horizontal cells has a shorter duration than that of the presynaptic photoreceptor voltage response (Ashmore and Copenhagen, 1980).

The response range over which a cell can discriminate differences in light intensity is limited by membrane noise. Consequently, it is beneficial to remove voltage noise and thus improve the signal-to-noise ratio. This can occur if signals with the frequency characteristics of light-induced responses are enhanced, while noise at other frequencies is attenuated. The temporal filtering occurring at the photoreceptor-bipolar cell synapse may carry out this operation (Copenhagen et al., 1983).

The transmitted signal can become much more transient in the inner plexiform layer (Werblin & Dowling, 1969). The voltage response to light in "transient" amacrine and ganglion cells has a much shorter duration than that of bipolar cells. This enhancement of transience is thought to be involved in the detection of movement (Werblin, 1973).

The signal produced by photoreceptors often remains rather constant (if images vary only slowly), so rather than transmitting the same information on an unchanging image, it is more economical to transmit information on changes in the image.

1.4.4 Detection of edges

The centre-surround receptive field organization and the division of information into "OFF" and "ON" channels, may both contribute to the detection of edges in the visual signal.

It is thought that the centre-surround organization in bipolar and ganglion cells could contribute to the detection of edges, because cells with such receptive fields can be strongly stimulated when their centre, but not all of their surround, is placed on one side of an edge. The same cells are strongly inhibited when they are placed on the other side of the edge. Thus, appropriately placed neighbouring "OFF" and "ON" cells on either side of an edge would both be strongly stimulated (Marr, 1982). Together, these responses could be correlated and detected by higher centres.

1.4.5 Synopsis

The principle function of retinal processing is to optimize image analysis by selecting information so that the number of neural connections required to connect the eye to the brain is minimized. The maximal amount of information in images exists where the light stimulus is changing spatially at edges or boundaries between light-dark or colour, or changing temporally. Thus, the visual system uses the mechanisms described above to enhance detection of information in these regions of the image, and remove unimportant signals.

1.5 Introduction to the experiments presented in this thesis

1.5.1 Advantages of using an isolated cell preparation to study the effects of neurotransmitters on retinal neurons

Much information about the function of retinal transmitters has come from electrophysiological studies made from cells in the intact retina (Massey and Redburn, 1987). However, there are several problems associated with such *in situ* recordings. For example, it is often a problem to adequately voltage-clamp cells with many fine processes and since cells *in situ* certainly receive chemical and electrical synaptic input from other cells, it is often difficult to assign the observed effects of applied drugs to the specific cell types studied. Further, the concentrations at which drugs are applied are often high (5-50mM) and may not reflect the true physiological concentrations which reach the cells. Such high concentrations are used because the effectiveness of drugs may be reduced as a result of diffusion away from the proposed site of action, or uptake by the surrounding cells.

Recording from freshly isolated cells (section 2.1.3, Chapter 2) largely circumvents these problems. It provides a powerful method of investigating the precise mode of action of putative neurotransmitters on cell membranes, at specific concentrations. For example, in this thesis (Chapter 3) I show that isolated cone photoreceptors are sensitive to very low concentrations of glutamate (1-2μM). Isolated cells with most of their processes resorbed are more easily voltage-clamped (Chapter 4), making them more suitable for studies of voltage-gated currents present in the membrane.

1.5.2 Why study the effects of glutamate, GABA and glycine on retinal neurons?

The retina is a good preparation to study, as the constituent cells can be isolated with minimal damage, and recorded from with relative ease using patch-clamp methods (section 2.3, Chapter 2) and the anatomical and physiological organization in the retina is well established.

One disadvantage of making recordings from isolated cells is that receptors detected on these cells may be extra-synaptic and hence not used for transmission in the intact retina. For this reason, the present investigations have concentrated on the actions

of glutamate, GABA and glycine on certain retinal cell types (see below), for which there is considerable evidence that they act as neurotransmitters *in vivo* (see section 1.3).

1.5.3 Questions addressed by this thesis

The preceding sections have given an introduction to the experiments presented in this thesis. The questions addressed by each chapter of this thesis are collected here to give some idea of the organization of the thesis. These questions are presented again for discussion in Chapter 7.

In Chapter 3

Experiments presented in Chapter 3 of this thesis, reveal that glutamate, previously thought to have no effect on photoreceptors, evokes a membrane current in cone photoreceptors. The effect of glutamate on cones is different from the effects of glutamate on postsynaptic bipolar and horizontal cells in the outer retina, and may be functionally significant in the early stages of visual processing.

Questions discussed in section 7.1 which are addressed by the experiments in Chapter 3

(1) Does L-glutamate evoke a current in cone photoreceptors?

(2) Does L-glutamate activate channels or an electrogenic carrier mechanism in the cone membrane?

(3) Which ions carry the current evoked by glutamate?

(4) How does the glutamate-induced current depend on the external glutamate concentration?

(5) How does the glutamate-induced current depend on the external sodium concentration?

(6) Are the glutamate-gated channels localized to specific regions of the cone cell membrane?

(7) What might be the functional significance of receptors for glutamate at the cone synaptic terminal?

In Chapter 4

It is not known how transience in the ganglion cell response to light arises. In Chapter 4, I have investigated the possibilty that transience (in response to injected current, mimicking the light-evoked synaptic current) in the ganglion cell response arises

predominantly from voltage-gated currents which I characterize in the ganglion cell membrane.

Questions discussed in section 7.3 which are addressed by the experiments in Chapter 4

(1) What is the functional significance of the difference in response properties of sustained and transient ganglion cells in response to injected current?

(2) Can isolated ganglion cells be divided into sustained and transient cell types in response to current injection?

(3) Which voltage-gated currents are present in the isolated ganglion cell membrane?

(4) How might these voltage-gated currents account for the division of ganglion cells into sustained and transient classes?

In Chapter 5

Isolated ganglion cells of the salamander express receptors for glutamate with properties which are similar to those seen for glutamate-gated channels in isolated ganglion cells from rat (Aizenman et al., 1988a) and rabbit (Massey and Miller, 1988). The possibility that desensitization of ganglion cell receptors for glutamate contributes to ganglion cell "transience" (section 1.2.7) was investigated.

Questions discussed in section 7.5 which are addressed by the experiments in Chapter 5

(1) Do ganglion cells have receptors for L-glutamate?

(2) How do any glutamate receptors present respond to the glutamate analogues kainate, quisqualate and NMDA?

(3) Is the response to glutamate localized to appropriate regions of the ganglion cell membrane?

(4) Could different classes of glutamate receptors be localized to different regions of the ganglion cell membrane?

(5) Is it possible that desensitization of ganglion cell receptors for glutamate contributes to the generation of transience in the light response of ganglion cells?

In Chapter 6

The properties of ionic currents gated by GABA and glycine were investigated in isolated salamander ganglion cells. Their

properties were found to be similar to those observed recently in isolated ganglion cells from the goldfish retina (Ishida and Cohen, 1988; Cohen et al., 1989).

Questions discussed in section 7.7 which are addressed by the experiments in Chapter 6

(1) Do isolated ganglion cells have receptors for GABA and/or glycine?

(2) Do GABA and glycine gate conventional chloride channels in salamander ganglion cells?

(3) How are chloride ions important for inhibition in the retina?

(4) Do ganglion cells have receptors for the peptide, substance P?

(5) Is it possible that release of inhibitory amino acids from amacrine cells to ganglion cells, delayed with respect to release of glutamate from bipolar cells, may contribute to the generation of transience in the light response of ganglion cells?

Chapter 2
Methods

This chapter is divided into two sections dealing with two different retinal cell types, (I) cone photoreceptors, and (II) ganglion cells. Each section is subdivided to describe (1) cell preparations; (2) solutions; (3) methods of recording from cells; (4) data acquisition and analysis.

I CONE PHOTORECEPTORS

2.1 Cell preparations

Experiments were performed on retinae from larval tiger salamanders (Ambystoma tigrinum), 15-25cm long. Recordings were made from cells in two preparations; cells in the intact isolated retina, and cells isolated from the retina. The first step for both of these preparations involved obtaining an isolated eyecup as follows.

2.1.1 Preparation of retinal eyecups

An eye was excised from a salamander immediately following decapitation and immediate destruction of the brain. Extraneous tissue was trimmed from the eyeball under a dissecting microscope. Holding the eye loosely with blunt forceps, a cut was made in the sclera anterior to the ora serrata using a piece of broken razor blade. This cut was continued around the eye using ophthalmological scissors until the front of the eye was isolated from the rest of it. The lens and front of the eye were removed with fine forceps while scissors were used to cut any attachments between the lens and the rear half of the eye. The vitreous humour was removed by capillarity using a piece of 1mm capillary tubing with a microfilament thread in it (microelectrode glass: section 2.2.2).

The half eyecup was either used immediately or stored in a small plastic petri dish (Falcon, 3080) under Ringer's (solution A, Table 2.1) in a refrigerator at 5°C (and used within 36 hours).

2.1.2 Isolated retina preparation flatmounted receptor side uppermost

The half eyecup (section 2.1.1) was trimmed with ophthalmological scissors by cutting through the retina, choroid

and sclera all round the eye, posterior to the ora serrata. It was then cut in half through the optic disc, leaving two retinal halves still attached to the choroid and sclera.

A base for each of the retinal halves was made in advance by fixing a Millipore filter (diameter: 1cm; pore size: 0.45μm) with Vaseline stopcock grease to the bottom of the recording bath (a perspex frame with a central 15x15x3mm hole mounted on a 75x50x1mm glass slide). Using a fragment of razor blade, holes were cut in the filter to accommodate precisely two triangular chips of glass of the same thickness as the filter, and slightly smaller than the retinal halves. (These chips were obtained by scoring and breaking a glass coverslip). The purpose of the chips was to allow illumination of the preparation from below. Using fine forceps, each piece of eyecup was delicately positioned over one of the glass chips, retinal side down, sclera uppermost. The edges of the eyecup pieces that extended beyond the glass chip were pressed into the filter using fine forceps so that the retina adhered to the filter at its edges. The sclera, choroid, and retinal pigment epithelium were then easily lifted off, to leave the pieces of neural retina flatmounted receptor side upwards. The preparation was rapidly covered with Ringer's* (solution A, Table 2.1), filling the recording bath to prevent the retina from drying out.

* 20-22°C

The recording bath was then transferred to a microscope with a fixed stage (Ergaval, East Germany), fitted with Hoffman modulation contrast optics (Modulation Optics Inc., Greenvale, N.Y.). The portions of retina overlying the inlaid glass chips could be observed. Since the glass chips were about the same thickness as the filter, the retina lay flat upon the surface and sufficient light passed through the chips so that individual cells could be resolved from above when observed under high power with a x40 magnification Zeiss water-immersion lens and x10 or x16 eyepieces.

Prior to cell recording, the flatmounted retinal preparation was treated with an enzyme cocktail to remove viscous material surrounding the photoreceptors, which resists movement of the patch pipette within the photoreceptor layer and prevents recording from cells. The exact nature of this viscous substance is unknown, but it could be loosened by bathing the preparation for 8-10 minutes in

Ringer's to which the following enzymes had been added: collagenase, 2mg/ml (Cooper, L5000476); hyaluronidase, 1.2mg/ml (Sigma, H2376), and trypsin inhibitor, 0.3mg/ml (Sigma, T9253). A few cells were successfully patch-clamped without enzyme pretreatment and had similar properties to those patched after enzyme pretreatment; however, enzyme pretreatment was almost always necessary.

Monochromatic light stimuli (620nm, 300μm diameter on the retina), were applied to the preparation via the microscope objective, after being passed through a shutter, neutral density filter (for adjusting the intensity) and interference filters (to select a wavelength band). Stimuli were introduced into the microscope light path through a beam combining prism.

During experiments in which cone cell light responses were recorded, the following special precautions were taken to avoid bleaching of the retina. Animals were dark-adapted for at least two hours before an experiment. Experiments were performed in a dark room. Apart from removal of the eye from the animal (done under dim red light), all viewing of the preparation during the dissection, was with an infra-red image converter (F.J.W. Industries). During experiments, the preparation was viewed with a T.V. screen connected to an infra-red sensitive silicon diode camera (Hitachi, HV17SD) attached to the microscope.

2.1.3 Isolated cones

Cones were isolated from the retina using a method similar to that described by Bader et al., (1979), involving enzymic dissociation of the retina.

The half eyecup (section 2.1.1) was trimmed with scissors as for preparation of the flatmounted retina (section 2.1.2) and cut into quarters. One piece was transferred with forceps to a petri dish containing fresh Ringer's (solution A, Table 2.1). The remaining portions of retinal eyecup were stored in Ringer's in the refrigerator at 5°C (for later use). Eyecups stored in this way remained viable for 36 hours.

While under Ringer's, the neural retina to be used generally started to float free from the retinal pigment epithelium of the eyecup and was teased off gently using fine forceps. Detaching the neural retina is easier in a dark-adapted eye, since the rod

photoreceptor outer segments withdraw from the retinal pigment epithelium in the dark-adapted state. Using a cut-off Pasteur pipette (tip diameter 2-2.5mm), fire polished so that the sharp edges of glass did not catch the sticky retina, the piece of retina was transferred to 2ml of a dissociation solution containing (mM): NaCl 66; $NaHCO_3$ 25; NaH_2PO_4; Na-pyruvate 1; KCl 3.7; glucose 15; DL-cysteine-HCl 10; with 0.03ml papain (Sigma, P3125) added to it. This solution had a pH of around 6.5, which fell within the optimum range for the proteolytic action of papain. The retina was left in this solution for 7-8 minutes at room temperature (20-22^{o}C). These conditions gave an isolated cell population which was almost all photoreceptors, with a good yield of healthy-looking cones.

After incubation, using a cut-off pipette, the retina was washed by dropping it through three tubes (Sarstedt, 4ml plastic tubes), each containing about 3ml of Ringer's. The retina was mechanically triturated (drawn in and out of an uncut, fire polished Pasteur pipette) slowly and gently, in 1ml of Ringer's, until the retina could be seen to break up into a suspension of cells. This whole suspension was plated into the recording bath and the cells were allowed to settle for 5-10 minutes before recording. Cells tended to stick to the glass surface of the bottom of the bath and remained healthy for 2-3 hours after plating in the bath. After this length of time cells began to lose their distinctive morphology, rounding up with the cytoplasm becoming granular in appearance and their membranes more fragile, as judged by the shortened length of time for which whole-cell recordings could be made.

Cones were identified under high power magnification (x40 objective) before recording, either as double cones (consisting of a principle and accessory member; recordings usually made from the principle member) or single cones, by the presence of a cone-shaped outer segment (see Fig. 2.1A which shows a single cone). Most recordings were made from cells with visible synaptic terminals.

2.2 Solutions

2.2.1 Superfusion

Superfusion solutions used outside cells when studying isolated cones and when studying cones in the intact retina are

Fig. 2.1 Photographs of a cone and a ganglion cell isolated from the retina by enzyme dissociation (see section 2.1.3). The photographs were taken under normal illumination using Hoffman modulation contrast optics.

A An isolated cone photoreceptor. The cone outer and inner segments, cell body and synaptic terminal are labelled. Scale bar is 10μm.

B An isolated ganglion cell with an extensively branching dendritic tree (section 2.5.5). Most isolated ganglion cells have far fewer processes than this cell. Arrow indicates position of axon, most of which is out of the plane of focus. Scale bar is 50μm.

A

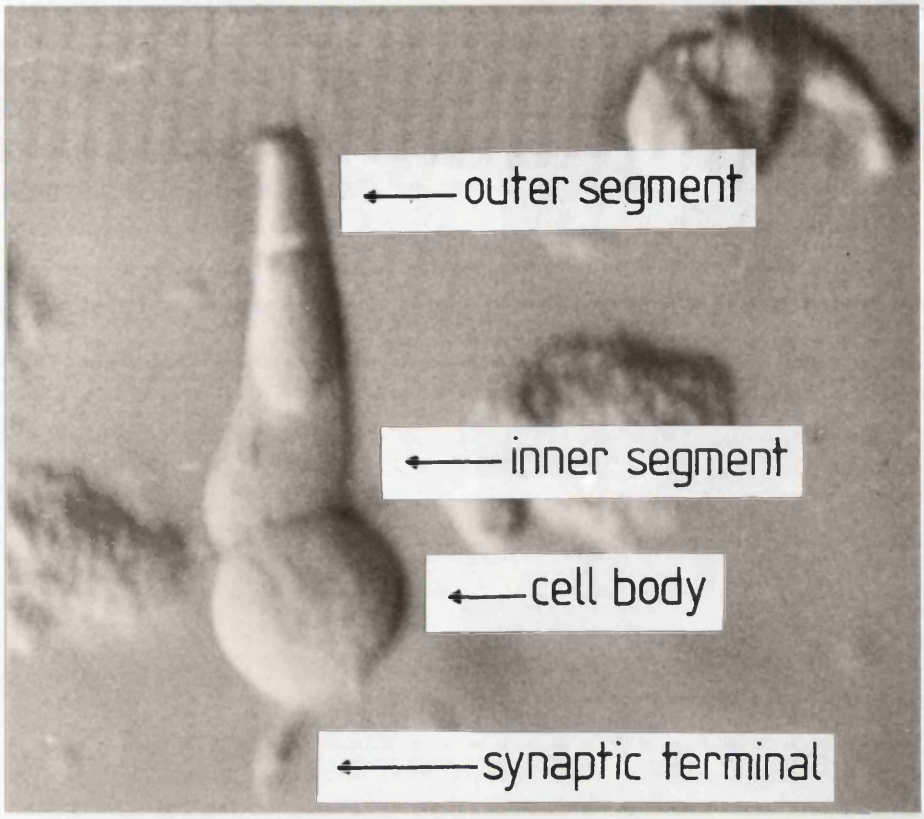

10µm

B

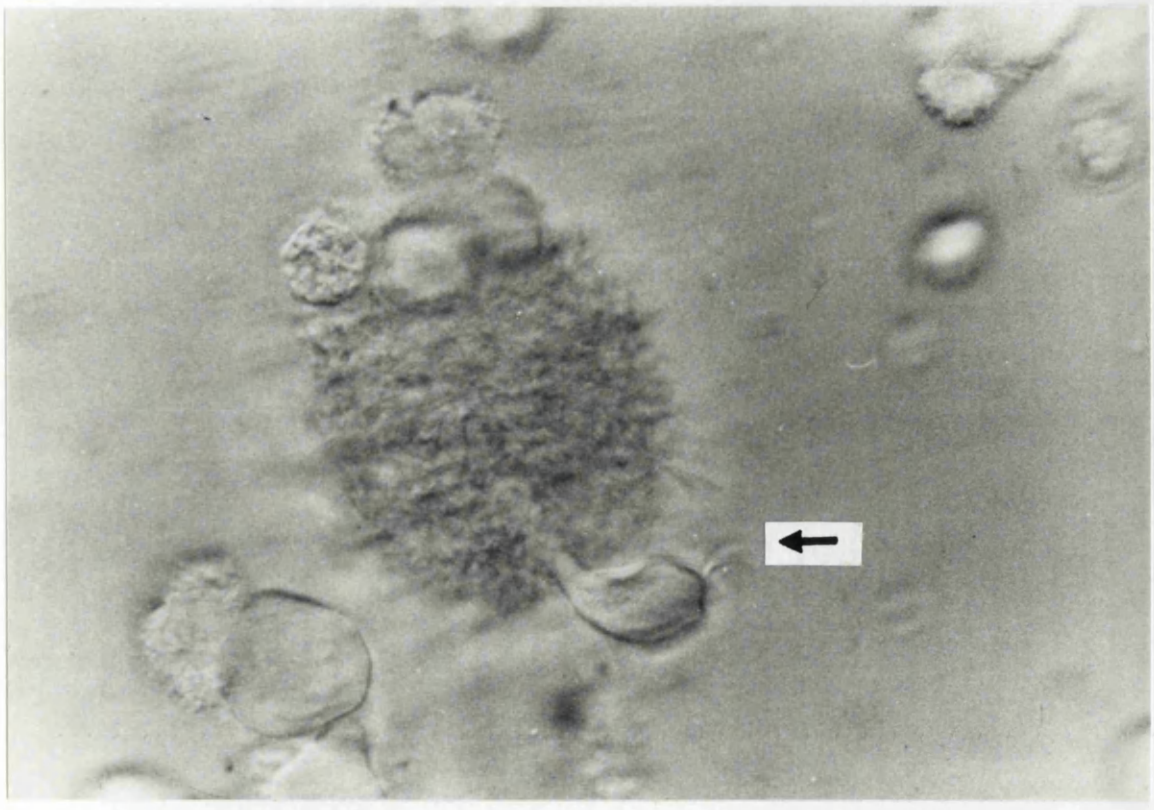

50µm

given in Table 2.1. Solutions A and B are Ringer's solutions used for studying the effects of glutamate (sodium L-glutamate; Sigma, G1626) on cones. Solution A (normal Ringer's) was used to study cones in the intact retina and for some experiments on isolated cones. Solution B was a Ringer's solution containing 6mM barium (referred to as barium Ringer's), used for most of the experiments on the glutamate-evoked current in isolated cones. Barium was used because it blocks most of the resting potassium conductance and reduces membrane noise in retinal Müller cells (Newman, 1985), and it is assumed to have a similar effect on the cone resting conductance (see section 3.3.1). All experiments were performed at room temperature (20-22°C).

In experiments where cones were exposed to a uniform concentration of a substance (as for changing the external glutamate concentration to determine the dose-response curves for glutamate), a bath perfusion system was used. Solutions were passed into the recording bath through plastic tubing by gravity flow. A continous flow (~1 ml/min) of solution through the bath was achieved by having excess solution removed by a vacuum pump sucking through a small tube. After starting whole-cell recording, cells were lifted from the bottom of the bath and moved close to the solution inlets to reduce the time taken for responses to reach a steady state. Electrical noise generated by the vacuum removal system was eliminated by grounding this system: a hypodermic needle was used for suction, a cotton thread was run down the tubing connecting the needle to the vacuum waste bottle, and the contents of the waste bottle were electrically connected to the recording bath. When pharmacological agents (e.g. Threo-3-hydroxy-DL-aspartate; Sigma, H5932) were applied by perfusion, they were simply added to solution A or B, at the concentrations required.

2.2.2 Iontophoresis

Glutamate was often applied by iontophoresis. Iontophoretic electrodes were pulled on a Livingstone-type microelectrode puller (Narishige) from borosilicate glass with a microfilament thread (Clark Electromedical Instruments, No. GC150TF10). Electrodes were connected via a platinum wire to the head stage of a recording amplifier equipped with a current pump system for iontophoresis. Electrodes were filled with 1M sodium L-glutamate (pH adjusted to

8.0, with NaOH; resistance 30MΩ, in normal Ringer's). Glutamate, which exists largely as a negatively charged ion at pH 8.0, was iontophoresed with a negative ejection current (-40nA) and a positive backing current (+30nA) was used to minimize loss of the drug when no ejection current was applied. Iontophoresis and local perfusion of glutamate gave similar results.

2.2.3 Intracellular media

The various solutions used to fill patch pipettes for experiments on both isolated cones and cones in the intact retina, are given in Table 2.2. During whole-cell recording, small ions in the patch pipette solution diffuse into the cell in 30-60 seconds (Fenwick et al., 1982). By using different pipette solutions from Table 2.2, cells with different internal concentrations of substances could be studied (for example chloride, see section 3.3.7, Chapter 3).

2.3 Methods of recording from cells

2.3.1 Methods for whole-cell patch-clamp recording

The whole-cell variant of the patch-clamp technique (Hamill et al., 1981) was used to study glutamate-induced currents in cones (Chapter 3). Patch pipettes for patch-clamp recording were pulled on a BBCH puller (Mecanex, Geneva) from borosilicate glass with a microfilament insertion (Clark Electromedical Instruments, No. GC150TF10) and coated with Sylgard resin (Dow Corning) to reduce capacitative coupling between the pipette contents and the extracellular medium (Hamill et al., 1981). Their resistance in normal Ringer's was about 10-20MΩ. On some occasions thick-walled microelectrode glass was used (Clark, No.GC150F10) and was not Sylgarded; the thicker-walled glass served the same purpose as the Sylgard resin.

To obtain a whole-cell recording, a patch-pipette was brought up to gently touch the cell membrane of the cone cell body, and gentle suction was applied to the pipette resulting in the formation of a high resistance seal (usually in the range 2-200GΩ) between the patch pipette and the cell membrane. After forming a high resistance seal, a further pulse of suction produced a low resistance pathway into the cell. The cell could then be voltage-clamped, with the current being measured as the voltage drop across

the 500MΩ resistance of a current to voltage converter (LIST EPC-7). The indifferent electrode was an Ag/AgCl pellet placed in the recording chamber, except when the chloride concentration in the superfusion solution was altered, in which case a 4M NaCl agar bridge connected the bath to the Ag/AgCl pellet to avoid changes in electrode potential.

The pipette series resistance (R_p) between the inside of the patch-pipette and the cell interior, was measured from the current response to a voltage-clamp step (see section 2.3.3). The R_p was typically 10 to 20MΩ, though values as low as 2MΩ and as high as 60MΩ were sometimes found. The pipette series resistance sometimes changed during the course of an experiment and was therefore monitored at the beginning and end of each experiment. The voltage error produced by the series resistance ($V_{error} = R_p$.peak current flowing; inward current having a negative sign and outward current, positive) could be corrected for by subtraction from the nominal voltage-clamp potential (i.e. $V_{real} = V_{nom} - V_{error}$). For example, in experiments involving glutamate application at the resting potential, the peak glutamate-induced current e.g. 80pA flowing through a 2MΩ series resistance resulted in a voltage error of 0.16mV. At potentials away from the resting potential the steady current at that voltage, in the absence of glutamate, must also be considered and added to the glutamate-induced current to obtain the peak current. The calculated voltage error was considered to be negligible if it was 1mV or less. However the series resistance correction could be significant, e.g. for a larger R_p of say 20MΩ, and taking (-)80pA to be the peak current flowing into the cell, the voltage difference between the pipette and the cell interior would be 1.6mV, with the cell interior more positive. Thus in order to calculate the true membrane potential, 1.6mV should be added to the nominal voltage-clamp potential.

Since the pipette and the recording chamber contained different solutions, a junction potential existed at the tip of the pipette when it was in the solution prior to forming a seal. This was corrected for as described by Fenwick et al., (1982). Junction potentials were measured by comparing the zero current voltage obtained when the pipette and bath contained intracellular medium, to that obtained when the bath solution was replaced by the

extracellular medium used while forming a seal. During this procedure, a 4M NaCl agar bridge connected the bath to the reference electrode to avoid changes in reference electrode potential. Junction potentials measured for various intracellular media relative to extracellular solutions are given in Table 2.2.

Nominal voltage-clamp potentials were corrected for junction potentials and any voltage error produced by the series resistance when, for example, plotting current-voltage relations (e.g. sections 3.3.2 and 6.6.3 in Chapters 3 and 6 respectively).

2.3.2 Voltage-clamp quality in cones

The non-spherical shape of cones raises the question of how non-uniform the potential is in these cells during voltage-clamping.

If the cone is treated simply as a uniform cylindrical cable (ignoring the junction between the inner and outer segments and the fine structure of the outer segment), it is possible to calculate the electrical space constant of the cell. This is the distance from the site of recording at which the cell voltage is predicted to fall to about a third of its original value.

The current applied to the patch pipette produces a voltage (V_o) at the site of recording. Assuming that current flow within the cell occurs in only one direction (towards the outer segment), that the cell is "open-ended" (i.e. that V_o falls exponentially with distance) and that cell membrane conductance is uniformly distributed, the electrical space constant, λ, is given by

$$\lambda = (a.R_m/R_i)^{1/2} \qquad (2.1)$$

where a = cell radius (m)

R_i = the specific cytoplasmic resistance of the cone (Ωm)

R_m = the specific membrane resistance of the cone (Ωm^2)

The specific cytoplasmic resistance is about 2Ωm. The specific membrane resistance can be calculated from the equation:

R_m = cell membrane resistance.cell area

The cone membrane resistance is typically around 500MΩ, and cell area was $2x10^{-9}m^2$ (assuming the cone cell has the area of an open-ended cylinder, $2\pi rh$, with r=radius, h=length, for a cone of

approximately 10μm diameter and 60μm long). The R_m was calculated to be $1 \Omega m^2$.

By inserting these values of R_i and R_m into equation 2.1 above, λ is found to be equal to 1600μm. Thus the space constant is much larger than the length of the cone (60μm), implying that it is unlikely that a voltage applied to the cell body will fall significantly over the length of the cone. Using this value of λ, it is possible to quantify what fraction of a voltage applied to the cone (V_o) will fall in a distance 60μm from the site of recording.

From the following expression,

$$\text{fractional voltage drop} = V_x/V_o = e^{(-x/\lambda)} \qquad (2.2)$$

where V_x = voltage at distance, x, from site of recording
and V_o = voltage applied at the site of recording,

it is calculated that 1% of the voltage applied to the cone (at the cell body) will fall across the cytoplasmic and membrane resistances, in a distance equal to the length of the cone. This assumes that there is an exponential drop in voltage from the region of recording, which is not the case, because the ends of the cell are sealed: correcting for this would result in even less voltage non-uniformity.

In experiments involving insertion of two microelectrodes simultaneously into the inner and outer segments of a rod, Bader et al. (1979) and Attwell & Wilson (1980) have shown that Ambystoma rod photoreceptors are effectively isopotential in the physiological range of membrane potentials. Similar measurements for cone photoreeptors cannot be made since electrodes cannot be inserted into the cone outer segment.

There are four possible causes of significant voltage non-uniformity in cones which have been ignored in the calculation above.

(1) The axial resistance along the cytoplasm of the narrow ciliary process at one edge of the lamellae of the cone outer segment, which will tend to isolate the distal portion of the outer segment from its proximal portion.

(2) The axial resistance along the cytoplasm in the narrow

outer segment lamellae, which will tend to isolate the tips of the lamellae from the ciliary process.

(3) The resistance of the junction between the inner and outer segments.

(4) The resistance of the axon connecting the cell body to the synaptic terminal, which will tend to isolate the terminal from the cell body.

Attwell et al., (1982) have calculated the non-uniformity that would arise from the first two resistances. Assuming an outer segment conductance of 1nS, the maximum non-uniformity in the cone outer segment membrane potential was calculated to be 2.2% in the physiological range of membrane potentials.

The resistance of the junction between the cone inner and outer segments, which will tend to isolate the outer segment from the inner segment, cannot be measured directly, but the experiments of Bader et al., (1979) and Attwell & Wilson, (1980) described above, show that in rods this junction does not produce significant voltage non-uniformity.

The size of any voltage drop along the axon connecting the cell body to the synaptic terminal could be estimated by calculating the space constant of the axon (making similar assumptions to those described above) from equation 2.1. Assuming the specific membrane resistance of the axon is the same as above ($1\Omega m^2$) and that the conductance in the axon is uniformly distributed, for an axon of diameter 1μm the space constant, λ, is calculated to be 500μm. If the axon is 10μm long, the calculated percentage voltage drop of 1% (from equation 2.2) shows that the voltage applied to the cell body is not significantly altered over this distance.

2.3.3 Measurement of capacitance and series resistance

The membrane capacitance (C), and series resistance (R_p) between the mouth of the patch-pipette and the cell interior were measured from the current response to a 10mV voltage-clamp step from a holding potential near to the zero current potential (-40mV in cones). At this potential there is little contribution of voltage-gated currents to the membrane current, and the cell can be treated as the parallel combination of a capacitor and a resistor, R_{in}, where R_{in} is the parallel combination of the cell membrane

resistance, R_m, and the resistance, R_{seal}, of the seal between the electrode and the cell (see inset to Fig. 2.4, which shows an example of measurement of the capacitance and series resistance in a ganglion cell). The time course of the change in current in response to a voltage-clamp step is predicted (Tessier-Lavigne et al., 1988) to have the waveform:

$$I(t) = V/(R_{in} + R_p) \times \{1 + (R_{in}e^{-t/\tau}/R_p)\} \quad (2.3)$$

where t = time after application of the voltage-clamp step,
V = amplitude of step (10mV)
τ = the decay time constant of the transient;

$$\tau = CR_{in}R_p/(R_{in} + R_p) \quad (2.4)$$

Thus the current amplitude at t = 0 (obtained by semi-logarithmic extrapolation) is:

$I_o = V/R_p$ allowing the calculation of R_p.

The steady-state current is:

$I_{\infty} = V/(R_{in} + R_p)$ allowing the calculation of R_{in}.

The membrane capacitance can then be calculated from the time constant of the current relaxation as:

$$C = \tau(R_{in} + R_p)/R_{in}R_p \quad (2.5)$$

Figure 2.4 (see section 2.7.3) shows an example of a ganglion cell capacity transient used for these calculations. The cone capacity transient is very similar. The semi-logarithmic plot of the decay of the transient in both cones and ganglion cells was linear as predicted by equation 2.3. For cones, this was the case for all isolated cells studied. The time constant of the decay of the transient in cones was generally around τ = 0.30 mseconds, but varied from τ = 0.09 to 0.41 msec, in cones with capacitances varying from 13 to 30pF and cell membrane resistances varying from 100 to 900MΩ, in normal Ringer's solution. Cones in the intact retina had larger capacitances of between 95 and 145pF (larger cell membrane area since cells were more intact) and lower membrane resistances (90 to 280MΩ).

2.4 Data acquisition and analysis

2.4.1 Data storage

All experimental records were stored on magnetic tape on a RACAL store 4DS tape recorder or on a modified video recorder. For analysis, current traces could be fed into a computer (PDP 11/73) via an analogue-to-digital converter (Cambridge Electronic Design, 502, 12-bit), numbered in blocks, and stored. Analysis of current records could then be performed, and useful data plotted using a Hewlett Packard plotter (model 7470A).

2.4.2 Noise analysis

Noise analysis was used to examine current fluctuations (produced by opening and closing of ion channels) in whole-cell patch recording due to the application of glutamate. The computer programs used for noise analysis were provided by Professor David Colquhoun and modified by Dr. Marc Tessier-Lavigne. Signals stored on magnetic tape were high pass filtered at 2 or 4Hz, and low pass filtered at 500 or 1000Hz. These signals were digitized and selected noise data was analysed.

Table 2.1 External solutions: cones

The external solutions listed below are those used for experiments on a) isolated cones, and b) cones in the intact retina. All solutions are Ringer's based, with solution A as the normal Ringer's solution used (based on Bader et al., 1979). A Ringer's solution containing 6mM barium (solution B) was often used (section 2.2.1). All concentrations given are in (mM), unless otherwise indicated.

a) Isolated cells

	A Normal Ringer's solution	B Barium Ringer's	Na60-Na2.1* Low sodium solutions
KCl	2.5	2.5	2.5
NaCl	104.5	104.5	n*
$CaCl_2$	3.0	3.0	3.0
$MgCl_2$	0.5	0.5	0.5
Glucose	15.0	15.0	15.0
HEPES	5.0	5.0	5.0
$BaCl_2$	-	6.0	6.0
CholineCl	-	-	104.5-n*
NaOH	2.5	2.5	2.5

The NaOH added brought the final pH to 7.25

* For solutions Na60-Na2.1, sodium was replaced with choline to give final sodium concentrations of 60 and 2.1mM. The total sodium concentration in Ringer's (solutions A and B) was 107mM.

b) Intact retina

Solutions were based on normal Ringer's and contained 10μM bicuculline (control), or 10μM bicuculline plus 5mM glutamate (see section 3.3.10).

Table 2.2 Internal solutions: cones

Patch pipettes were filled with the solutions listed in the table below. Solutions C101, C30 and C9 (containing 101, 30 and 9mM chloride respectively) were used to study the chloride-dependence of the glutamate-induced current in isolated cones; solution C16 (16mM chloride) was used for experiments in the intact retina. All concentrations given are in mM unless otherwise indicated. Junction potentials are indicated for the external Ringer's used (measured as described by Fenwick et al., 1982).

	C101	C30	C9	C16
$[Cl^-]$	101mM	30mM	9mM	16mM
KCl	80	9	-	-
KAcetate	15	86	95	100
K_2EGTA	5	5	5	5
NaCl	5	5	5	-
Na_2ATP	5	5	5	5
$CaCl_2$	1	1	1	1
$MgCl_2$	7	7	1	7
$Mg(Acetate)_2$	-	-	6	-
HEPES	5	5	5	5
Na_3GTP	-	-	-	0.05
cGMP	-	-	-	1
KOH	15	15	15	15

Free $[Ca^{2+}]_i$ is 1.36×10^{-7}M for all above solutions.

Cell prep.	isolated cones	isolated cones	isolated cones	intact retina
External solution	B	B	B	A
Junction potential (mV)	-6	-7	-6	-7

The KOH added brought the pH of the internal solutions to 7.0.

* K_2EGTA is actually roughly $K_{2.25}$EGTA so that 5mM will contribute about 11 mM potassium to the solution.

2.5 Cell preparations

Experiments were performed on retinae from larval tiger salamanders (section 2.1), and recordings made from two cell preparations: the intact flatmounted retina (mounted ganglion cell side up), and isolated ganglion cells.

The retinal ganglion cell layer contains ganglion cells, having long axons which project to the brain, and a small population of "displaced" amacrine cells which do not have axons. In principle ganglion cells should be identifiable simply by the presence of their axons, but in practice it is virtually impossible to distinguish visually between ganglion cells and amacrine cells in the ganglion cell layer of the intact retina, and often difficult to identify isolated ganglion cells due to loss or retraction of their axons during the isolation procedure. The technique described below, selectively labels ganglion cells so they may be unequivocally identified as such prior to recording in intact retinae or isolated cell preparations.

2.5.1 Staining of ganglion cells prior to cell preparation

To identify ganglion cells prior to recording, the cells were labelled (Cook and Mobbs, 1988) using fluorescein isothiocyanate dye conjugated to horseradish peroxidase (FITC-peroxidase).

An eye was excised from a freshly killed salamander. Excess connective tissue and muscle was removed from the eyeball and the optic nerve trimmed with ophthalmological scissors, under a dissecting microscope. While immobilizing the eye in a suitable position with fine forceps, an incision was made with a razor blade in the cornea, just above the junction between the iris and the corneal surface. The cut was carefully continued using fine ophthalmological scissors until the cornea could be lifted away from the rest of the eye, leaving the iris intact. Using fine forceps, the lens was removed, and scissors used to sever any attachments between the lens and the rear part of the eye.

A small piece of gelatin sponge impregnated with 300mg/ml Ringer's, FITC-peroxidase was held between fine forceps and applied to the cut end of the optic nerve. Using clean fine forceps, the prepared eyecup was lifted and positioned onto a pre-prepared Vaseline cup

in a petri dish (Fig. 2.2), with the iris uppermost. The Vaseline was sealed to the eyecup and to the base of the petri dish, by melting the Vaseline with a hot wire wrapped around the tip of a soldering iron and allowing it to reset. This seal keeps the gel-foam in contact with the retina in a small air-filled space, ensuring that the dye can only reach the retina by being retrogradely transported with HRP along ganglion cell axons in the optic nerve, thus selectively staining ganglion cells. The eyecup was maintained at 4°C, for 24-48 hours, under oxygenated Ringer's (solution A, Table 2.1).

2.5.2 Visualization of stained ganglion cells

The FITC-peroxidase label remains within the cell during preparation of the retina for observation (sections 2.5.4, and 2.5.5). Illumination of the cell preparation with ultra-violet (UV) light enables visualization of the green fluorescence from the fluorescein label. The UV light was directed through the objective of the microscope using an epi-illuminator. All ganglion cells studied in the intact retina and in an isolated cell preparation were identified as such prior to recording.

2.5.3 Photographing stained ganglion cells

Ganglion cells stained with FITC-peroxidase were photographed (Fig. 2.3) with an Olympus OM-2 camera mounted on the top of the microscope. Additional photographs were obtained for observing cell morphology by incorporating the fluorescent dye, Lucifer Yellow into the patch electrode. In whole-cell patch-clamp mode the Lucifer Yellow diffuses into the cell and its fine processes. Fig. 2.3 shows photographs taken at different depths of focus under high power magnification, to reveal the size and shape of a ganglion cell body and its dendritic tree in the intact retina.

2.5.4 Isolated retina preparation flatmounted ganglion cell layer uppermost

This preparation was used to study ganglion cell properties in the intact retina. The half eyecup was removed from the Vaseline cup and washed in normal Ringer's (solution A, Table 2.1). Under a dissecting microscope, using ophthalmological scissors, the iris was lifted away from the rest of the eye, by cutting carefully through the retina choroid and sclera, all around the circumference

Fig. 2.2 Schematic diagram showing the arrangement for staining ganglion cells prior to cell preparation (see section 2.5.1). The gel-foam impregnated with the FITC-peroxidase label remains in contact with the cut end of the optic nerve in a small air filled space in the eyecup preparation. This contact is maintained for at least 12 hours before preparation of cells.

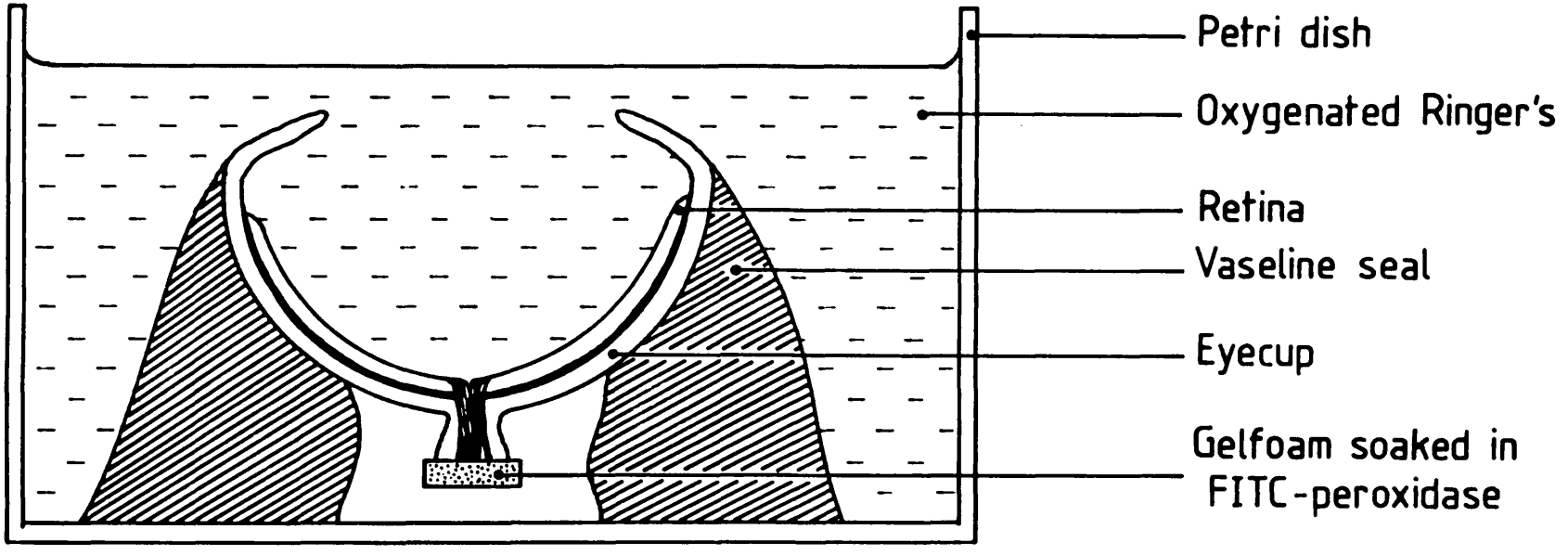
Petri dish
Oxygenated Ringer's
Retina
Vaseline seal
Eyecup
Gelfoam soaked in
FITC-peroxidase

Fig. 2.3 A series of photographs showing a whole-cell patch-clamped ganglion cell in the intact retina stained with Lucifer Yellow. The photographs are taken at different depths of focus. Ganglion cells could be identified by virtue of the fluorescent dye which was incorporated into the patch pipette (A) and diffuses into the cell soma staining the axon (B) and dendritic processes (C). The scale bar is 50μm.

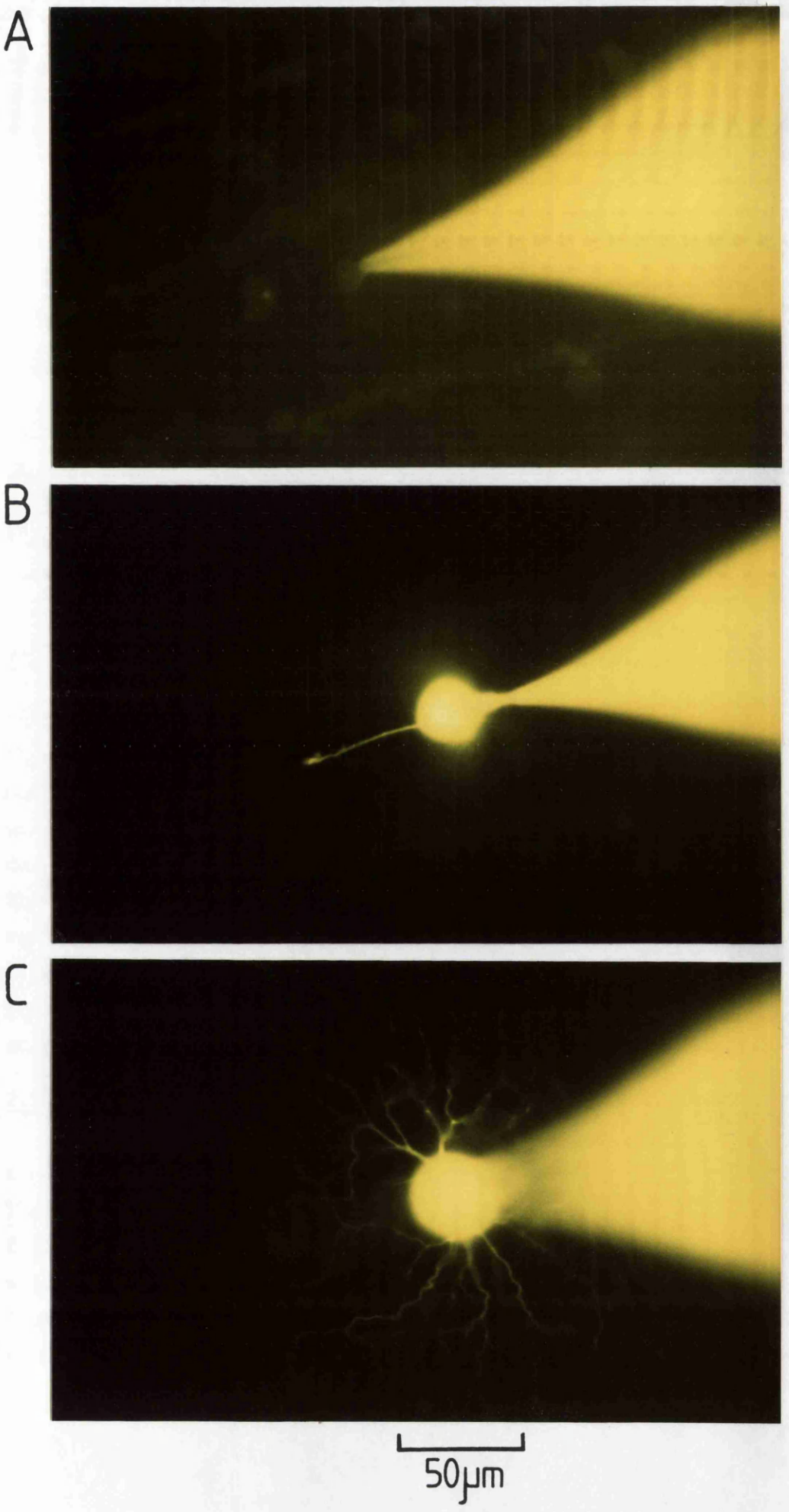
A
B
C
50µm

of the eye, posterior to the ora serrata. It was then cut into quarters and the neural retina separated from the retinal pigment epithelium in two of the retinal quarters.

A base for the pieces of retina was made in advance by inserting two glass chips into a Millipore filter as described in section 2.1.2 for cones. The recording bath was filled with Ringer's, and the retinae transferred to it using a cut-off firepolished Pasteur pipette. Then, using two pairs of fine forceps, each floating piece of retina was carefully positioned over one of the glass chips, with the ganglion cell layer uppermost (usually it is not difficult to identify which surface contains the ganglion cell layer, as the isolated retinae curl upwards with the ganglion cell layer as the concave surface). The edges of the retinae that extended beyond the glass chips were pressed into the filter using fine forceps, securing them to the filter.

The recording bath was then transferred to the microscope used for experiments. At the uppermost surface of the retina the ganglion cell axons could be clearly seen overlying the faint ganglion cell bodies. Overlying the whole ganglion cell layer is the collagenous basement membrane which greatly hinders movement of the patch pipettes to the cells. This viscous sheet of basement membrane could be loosened by treating the flatmount preparation with an enzyme cocktail (section 2.1.2) for 20-30 minutes, and then carefully lifted from the neural retina using fine forceps, leaving the ganglion cell bodies clearly visible and accessible for recording. It was always necessary to lift the basement membrane free from the ganglion cell layer prior to cell recording. Subsequent illumination of the ganglion cell layer with UV light enabled identification of stained ganglion cells.

2.5.5 Isolated ganglion cells

Ganglion cells were isolated from the retina by a method similar to that described for cone photoreceptors (section 2.1.3). The half eyecup was removed from the Vaseline cup and washed with fresh Ringer's (solution A, Table 2.1). The half eyecup was trimmed with scissors to remove the iris, as for preparation of the flatmounted retina (section 2.5.4) and cut into quarters, one piece used immediately, and the remaining portions stored in Ringer's in

a refrigerator (5°C).

The retina to be used was gently teased from the pigment epithelium and transferred to the dissociation medium (section 2.1.3), and papain was added. The retina was left in this solution for 20-25 minutes, at 33°C. After incubation the retina was washed, triturated to produce isolated cells and plated into the recording chamber as described in section 2.1.3 for cones.

Ganglion cells were identified by illumination with UV light (under high power illumination) to reveal the fluorescent FITC-peroxidase label. Healthy ganglion cells had a long axon (often running millimetres across the field of view) and sometimes very extensively branching dendritic trees (see Fig 2.1B), although more commonly, they had only a few dendritic processes. Cells with fewer processes were presumably more uniformly voltage-clamped (see section 2.7.2). Recordings were only made from ganglion cells identified with the fluorescent dye. For recording voltage-gated currents (Chapter 4), stained ganglion cells with visible axons were chosen. For recording ganglion cell responses to L-glutamate and other drugs, (Chapters 5 and 6) best responses were obtained from cells with dendritic processes, irrespective of the presence of an axon.

2.6 Solutions

2.6.1 Superfusion

The Ringer's solution used to superfuse isolated ganglion cells, and ganglion cells in the intact retina was solution A (Table 2.1). This was used to study the voltage-gated membrane currents in ganglion cells (Chapter 4), in addition to the neurotransmitter-gated currents in these cells (Chapters 5 and 6). In experiments where ganglion cells were exposed to a uniform concentration of a substance, a bath perfusion system was used (section 2.2.1). Experiments were generally performed in a cool environment (10-15°C).

When neurotransmitter candidates and pharmacological agents (used to block different membrane components) were applied by bath perfusion, they were simply added to the Ringer's solution A (Table 2.1). To study voltage-gated membrane currents, 2mM cobalt chloride (BDH Chemicals Ltd. catalogue no. 27790) was sometimes added to Ringer's to block the calcium current; 1μM Tetrodotoxin (TTX:

Sigma, T6254) was added to block the sodium current. To study glutamate-gated currents in ganglion cells, sodium L-glutamate (Sigma, G1626) was added to Ringer's. Other drugs added to Ringer's solution included: kainic acid (kainate: Sigma, K0250); quisqualic acid (quisqualate: Sigma, Q3875); N-methyl-D-aspartate (NMDA: Sigma, M3262); N-acetylaspartylglutamate (NAAG: Sigma, A6796); gamma-aminobutyric acid (GABA: Sigma, A2129); glycine (BDH Chemicals Ltd., 10119); bicuculline methiodide (Sigma, B6889); strychnine (Sigma, S7001); substance P (Sigma, S6883).

2.6.2 Iontophoresis

For iontophoresis of L-glutamate, see section 2.2.2. For iontophoresis of glycine, microelectrodes (section 2.3.1) were filled with 0.5M glycine (pH adjusted to 3.0 with HCl, resistance around 30MΩ in Ringer's solution A). For iontophoresis of gamma-aminobutyric acid, microelectrodes were filled with 0.5M GABA (pH adjusted to 3.0 with HCl, resistance around 30MΩ in Ringer's). Both glycine and GABA exist as positively charged ions at pH 3.0, and thus were iontophoresed with a positive ejection current (+40nA). A negative backing current (-30nA) was used to prevent loss of the drug when not ejecting.

2.6.3 Intracellular media

The intracellular media used to fill patch pipettes for experiments on both isolated ganglion cells, and ganglion cells in the intact retina, are given in Table 2.3. Solution G42 (42mM chloride) was used initially, but was replaced by solution G3, with a lower chloride concentration (3mM), as there is evidence that the internal chloride concentration of ganglion cells in vivo is very low (Miller and Dacheux, 1983). The ionic-dependence of the currents evoked by GABA and glycine were studied by changing the pipette chloride concentration (section 6.3.5, Chapter 6)

For studying voltage-gated currents in ganglion cells (Chapter 4), pharmacological agents were sometimes included to block different membrane current components. These were: caesium sulphate ($CsSO_4$: BDH Chemicals Ltd., 27573); tetraethylammonium ions (TEA: Sigma, T2265). In some cases, leupeptin (Sigma, L3631) was added to help prevent washout of the calcium current (Chad & Eckert, 1986).

For photographing ganglion cells stained with Lucifer Yellow (Sigma, LO259) 0.1% of the dye was incorporated into the patch pipette.

2.7 Methods of recording from cells

2.7.1 Methods for whole-cell patch-clamp recording

The whole-cell variant of the patch-clamp technique (Hamill et al., 1981) was used to study voltage-gated membrane currents (Chapter 4) and neurotransmitter-gated currents in ganglion cells (Chapters 5 and 6). Patch pipettes for patch-clamp recording were pulled from thick-walled glass with a microfilament thread (Clark Electromedical Instruments, No. GC150F10). For some experiments patch pipettes were also coated with Sylgard resin (Dow Corning) to reduce as far as possible any capacitative coupling between the pipette contents and the extracellular medium. Their resistance in Ringer's (solution A, Table 2.1) was usually about 10-20MΩ.

A whole-cell recording was obtained as described in section 2.3.2, except that capacity currents were compensated for using the electronic capacity compensation provided by the LIST EPC patch-clamp amplifier.

The pipette series resistance (R_p) was measured for ganglion cells, as described for cones in section 2.3.2, assuming the ganglion cell can be adequately voltage-clamped (see section 2.7.2). Any significant voltage error (greater than 1mV) produced by R_p was corrected for by subtraction from the nominal holding potential (see section 2.3.1 for cones).

The cell input resistance, R_{in}, shown in the inset to Fig. 2.4A, represents the parallel combination of the cell membrane resistance (R_m) and the resistance of the seal (R_{seal}) between the electrode and the cell.

When the seal resistance is high (gigaohms), there will be little or no current leak across R_{seal} and current will only flow through R_m. Thus, the measured ganglion cell resting potential (V_{app}) will approach the real cell resting potential (V_{rp}). However, if R_{seal} is low, current will leak across the seal, significantly altering the resting potential. This was especially the case in recordings made from ganglion cells in the intact retina, when it was often difficult to form a seal, in many cases

resulting in a very low seal resistance. R_{seal} (300MΩ-30GΩ) was measured in the cell-attached configuration before a whole-cell clamp was obtained (ignoring the conductance of the patch of membrane under the electrode), and was often found to be of a similar magnitude to the input resistance measured in whole-cell mode. It is likely therefore that the apparent resting potential is lower than the true resting membrane potential (V_{rp}), because of shunting by the poor seal.

The apparent membrane potential was corrected for voltage error through a low seal resistance in the following way. Treating the seal resistance as a non-selective leak to earth (Tessier-Lavigne, et al., 1988), which is assumed not to be altered during the rupturing of the membrane patch to obtain a whole-cell clamp, the relationship between the apparent and true resting potential is:

$$V_{rest}/V_{app} = R_{seal}/(R_{seal}-R_{in})$$

and the input resistance, R_{in} is related to the true membrane resistance, R_m by:

$$1/R_{in} = 1/R_m + 1/R_{seal}$$

So, for a cell having an apparent R_{in} of 300MΩ, and a low R_{seal} of say, 600MΩ, the voltage error, V_{error}, is 32mV, correcting a V_{app} of -28mV to a true V_{rest} of -60mV.

The relationship between neurotransmitter-induced currents and voltage (I-V relations) were plotted using a computer programme written by Peter Mobbs, which corrected nominal voltage-clamp potentials for junction potential and any significant voltage error produced by the series resistance.

2.7.2 Voltage-clamp quality in ganglion cells

Ganglion cells in vivo are unlikely to be voltage uniform as they have many extensive branches and a long thin axon. Thus, voltage control in the whole-cell patch-clamp mode is often difficult, if not impossible, while the cells retain their morphology. Recordings made from ganglion cells in the intact retina were often hindered by lack of voltage-clamp control, with cells producing action potentials in "voltage-clamp", preventing any useful analysis of voltage-gated membrane currents in these

cells. Isolated ganglion cells either lose or resorb many of their dendritic branches during the isolation procedure, enabling these cells to be more successfully voltage-clamped. Some indication that both isolated ganglion cells and ganglion cells in the intact retina can be adequately voltage-clamped, comes from examining the form of their capacity transients. It might be expected that injection of a square current pulse into ganglion cells which have different "cell compartments" (e.g. axon, cell body, dendrites), would result in generation of capacity transient components for each compartment which have different time courses. Thus the whole-cell capacity transient would probably be best fit by several exponentials. However, capacity transients for practically all cells studied could be fitted with a single exponential (although this does not rule out the possibility that very fast transients are not resolved). Further, Coleman and Miller (1989) have indicated that the specific membrane resistance of ganglion cells in the intact amphibian retina, is very high (around $6 \Omega m^2$), and that there is little attenuation of voltage along ganglion cell axons.

2.7.3 Measurement of capacitance and series resistance

The methods used to measure the capacitance (C) and pipette series resistance (R_p) in ganglion cells were identical to those described for cones in section 2.3.4. Fig 2.4A shows the time course of a ganglion cell capacity transient obtained during whole-cell recording. The semi-logarithmic plot of the decay of the transient is shown in Fig. 2.4B, and is linear, as predicted for a parallel combination of a capacitor and resistor (see inset to Fig. 2.4, where R_{in} is the parallel combination of cell membrane resistance and seal resistance). The time constant of the decay of the transient for the cell in Fig. 2.4 was τ = 0.51msec. This cell had a capacitance equal to 27pF and the cell membrane resistance was 570MΩ.

2.8. Data acquisition and analysis

This was carried out as described above for cones (see sections 2.4.1 and 2.4.2).

Fig. 2.4 Measurement of capacitance (C) and pipette series resistance (R_p) in an isolated ganglion cell.

A Current flow in response to a 10mV depolarization (lower trace) from a holding potential of -40mV. The inset shows the circuit used for analysis of the capacity transient. R_{in} represents the parallel combination of the cell resistance (R_m) and the resistance of the seal (R_{seal}) between the electrode and the cell (section 2.3.3). The resting potential of the cell, which could be represented in this circuit by a battery, is omitted for simplicity. The current does not rise instantaneously at t=0, as in equation 2.1, because of filtering by the tape recorder.

B Semi-logarithmic plot of the decay of current in **A** to its steady-state value $I(\infty)$. For this cell, the series resistance (calculated as described in section 2.3.3) was 19MΩ, the cell capacitance was 27pF and the cell input resistance was 570MΩ.

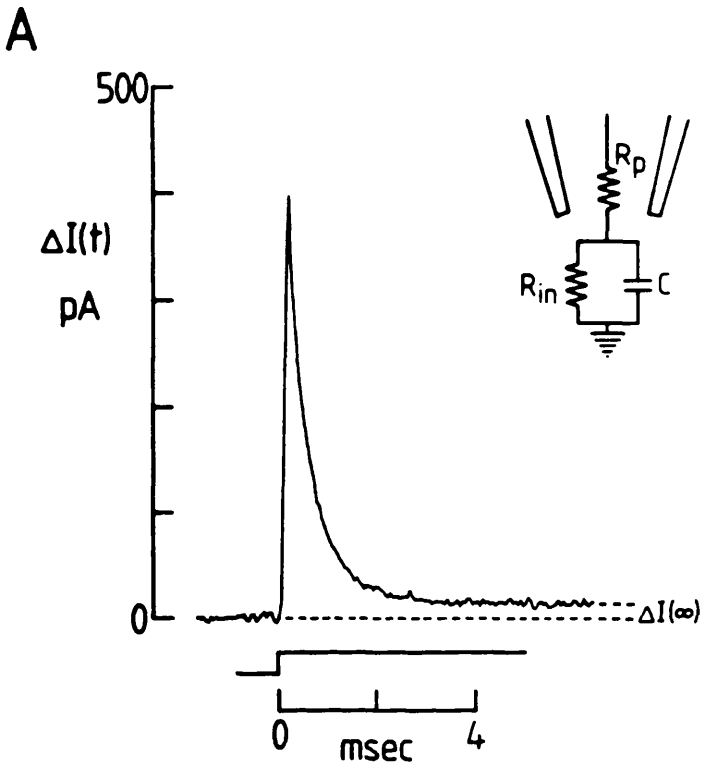
A
500
ΔI(t)
pA
0
R_p
R_{in}
C
ΔI(∞)
0
msec
4

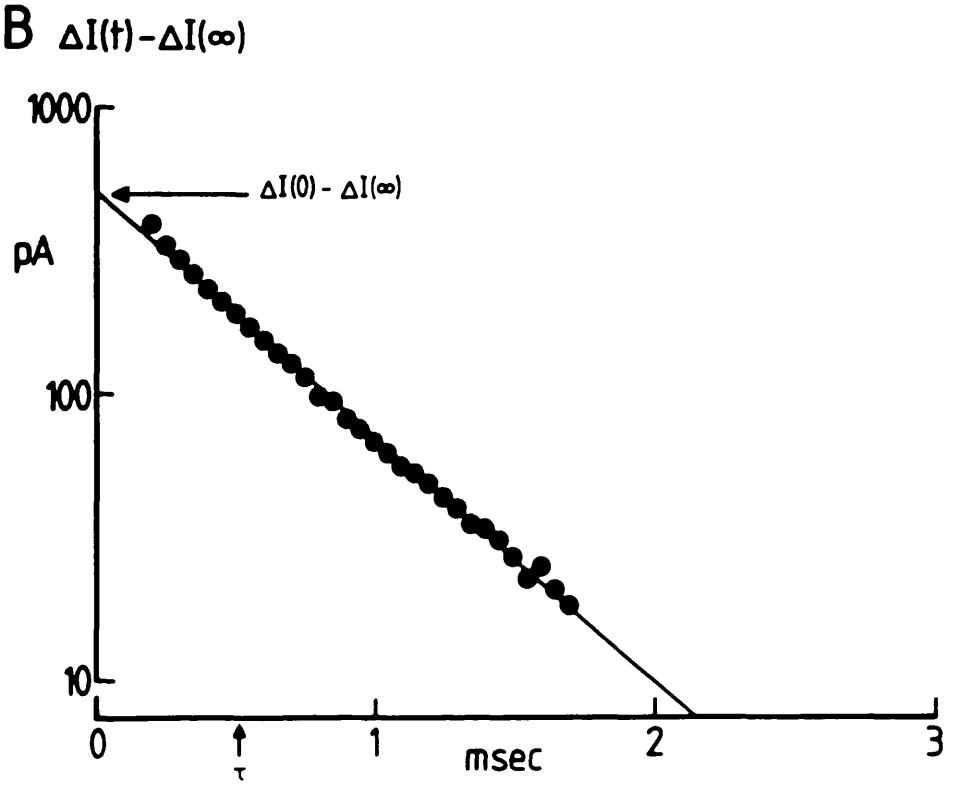
B ΔI(t)-ΔI(∞)
1000
ΔI(0) - ΔI(∞)
pA
100
10
0
τ
1
msec
2
3

Table 2.3 Internal solutions: ganglion cells

Patch pipettes were filled with the solutions listed in the table below. Pharmacological agents were added to solution G3 (3mM chloride) at the concentrations shown below. Junction potentials are indicated below, with respect to Ringer's solution A (Table 2.1).

	G3	G17	G42	G102	G3G	G42G
$[Cl^-]$	3mM	17mM	42mM	102mM	3mM	42mM
KCl	-	5	30	90	-	30
KAc	90	85	60	-	-	-
KGluc	-	-	-	-	90	60
K_2EGTA	10	10	10	10	10	10
NaCl	-	-	-	-	-	-
Na_2ATP	5	5	5	5	5	5
$CaCl_2$	1	1	1	1	1	1
$MgCl_2$	0.5	5	5	5	0.5	5
$Mg(Ac)_2$	4.5	-	-	-	-	-
$Mg(gluc)_2$	-	-	-	-	4.5	-
HEPES	13.3	13.3	13.3	13.3	13.3	13.3
KOH	15	15	15	15	15	15
Free $[Ca^{2+}]_i$ is 5.78×10^{-8}M in all of the above solutions.						
Junction potential (mV)	-11	-10	-9	-6	-12	-8

The pH was adjusted to 7.0 with 1M KOH.

* K_2EGTA is actually roughly $K_{2.25}$ so that 10mM will contribute about 23mM potassium to the solution.

Chapter 3

A presynaptic action of glutamate at the cone output synapse

3.1 Introduction

The results presented in this chapter describe the properties of the current induced by L-glutamate in isolated cone photoreceptors and in cones in the intact retina. The results are divided into ten sections; (1) Glutamate evokes a current in isolated cones; (2) Dependence of the glutamate-induced current on voltage; (3) Noise changes associated with the glutamate-induced current; (4) Dependence of the glutamate-induced current on external glutamate concentration; (5) Spatial localization of the glutamate response; (6) Dependence of the glutamate-induced current on external sodium concentration; (7) Dependence of the glutamate-induced current on patch pipette chloride concentration; (8) The glutamate-induced current in cones is blocked by threo-3-hydroxy-DL-aspartate (THDA); (9) The glutamate-evoked chloride current in cones is different from the chloride current evoked in cones by gamma-aminobutyric acid (GABA); (10) Glutamate induces a current in cones in the intact retina.

The results are used to address the questions raised in section 1.5.3 (Chapter 1). These questions are presented for discussion in section 7.1 (Chapter 7).

3.2 Methods

Experiments described in sections 1 to 9 were performed on isolated cones (section 2.1.3, Chapter 2) and those in section 10 on cones in the intact retina (section 2.1.2, Chapter 2). In all experiments cones were voltage-clamped, and recordings were made using the whole-cell variant of the patch-clamp technique. The external Ringer's solution was either normal (solution A, Table 2.1, Chapter 2) or contained barium (solution B, Table 2.1) and was applied by bath perfusion. Patch pipettes contained solution Cl01 (Table 2.2, Chapter 2) except where otherwise indicated. L-glutamate was usually applied by iontophoresis though sometimes by bath perfusion of solutions containing defined concentrations of glutamate. All experiments were carried out on cones with visible synaptic terminals.

3.3 Results

3.3.1 Glutamate evokes a current in isolated cones

Fig. 3.1A shows the response to iontophoretically applied L-glutamate in an isolated cone voltage-clamped to -84mV in normal Ringer's solution and with 101mM chloride in the patch pipette (solution Cl01, Table 2.2). In this cell, glutamate evoked an inward current of 47pA at -84mV. In 25 cells tested, glutamate produced a small inward current usually of 10-20pA, but sometimes as large as 60pA, at the cone resting potential (-40mV).

Most of the experiments described in this chapter were carried out in the presence of 6mM barium (solution B, Table 2.1). Barium was found to reduce the cone membrane noise (at potentials away from the potassium equilibrium potential, E_K), making it easier to detect small currents induced by glutamate. Hence, the currents needed to voltage-clamp cells at very positive or very negative potentials were reduced, increasing the range of voltages at which the glutamate-induced current could be studied. Barium probably acts by blocking potassium channels, as has been shown for retinal Müller cells (Newman, 1985).

Fig. 3.1 shows that the presence of barium in the external solution does not affect the size of the glutamate-induced current. The magnitude of the glutamate response in normal Ringer's (Fig. 3.1A) was compared to that in barium Ringer's (Fig. 3.1B) in the same cell. Each trace shown is an average of 5 responses. The size of the glutamate response was practically the same in both external solutions.

3.3.2 Dependence of the glutamate-induced current on voltage

The currents produced by iontophoretic application of glutamate in a cone voltage-clamped to a range of different potentials, are shown in Fig. 3.2A. The external solution was barium Ringer's and the patch pipette contained 101mM chloride (solution Cl01, Table 2.2). Glutamate increased the membrane conductance of cones, producing an inward current below 0mV, which was larger at more negative potentials. There was no net current flow at 0mV (the reversal potential) and the glutamate-induced current was outward at potentials positive to this.

The peak glutamate-induced currents were plotted against voltage in Fig. 3.2B. This current-voltage (I-V) relation showed

Fig. 3.1 Comparison of the magnitudes of currents induced by iontophoresis of L-glutamate in an isolated voltage-clamped cone, in normal Ringer's (A) or in the presence of 6mM barium (B). Patch pipette contained solution ClOl (Table 2.2, Chapter 2). Each trace is an average of five responses.

A Glutamate produced an inward current of 47pA in an isolated cone voltage-clamped to -84mV. Inward current is shown downwards. External solution is normal Ringer's (solution A, Table 2.1). Bottom trace shows timing of iontophoresis.

B In barium Ringer's (solution B, Table 2.1), the magnitude of the glutamate-evoked inward current (top trace) for the same cell as in **A**, at the same potential, was 48pA. The presence of barium does not markedly affect the size of the glutamate response at -84mV.

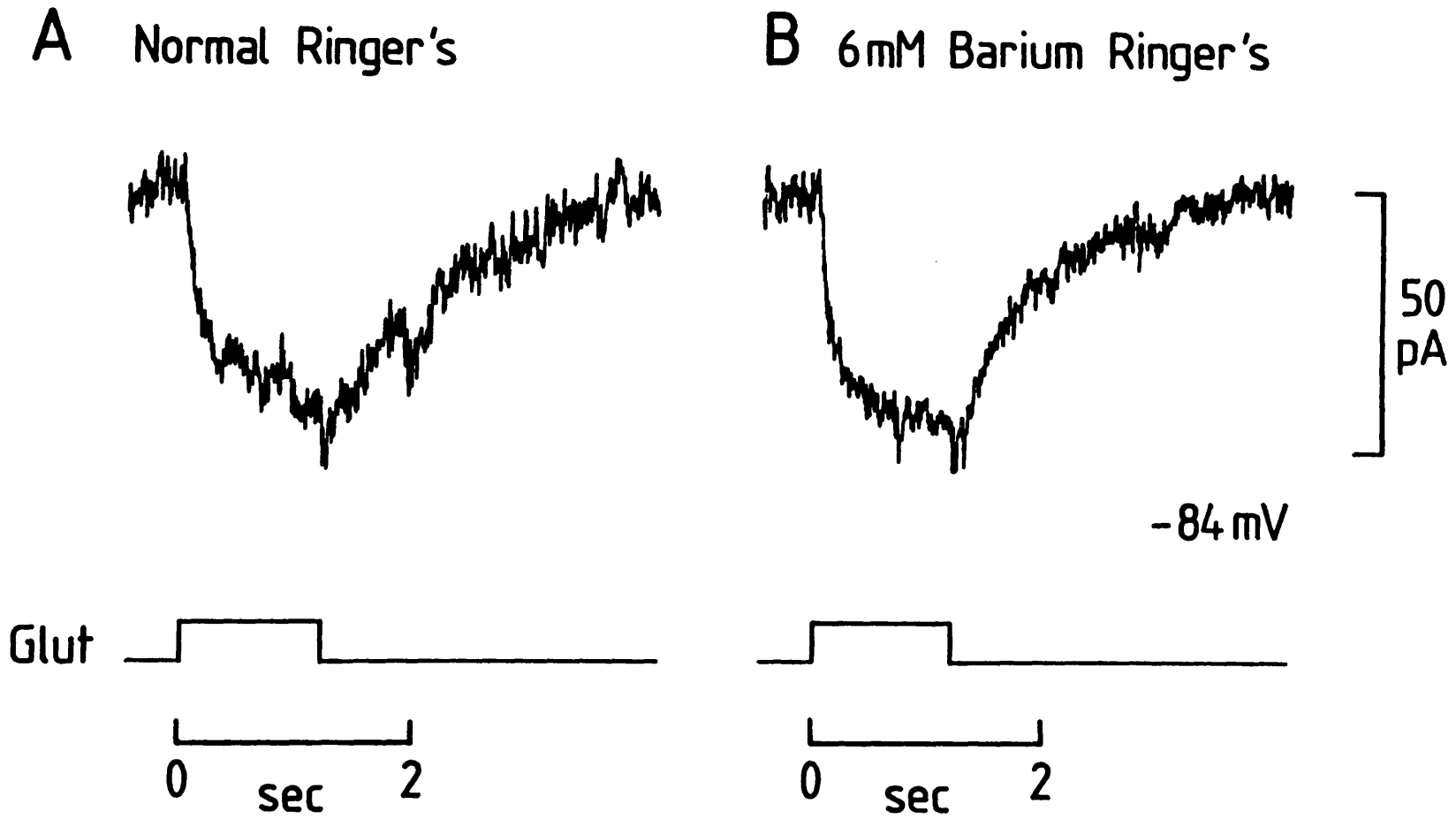
A Normal Ringer's
B 6mM Barium Ringer's
50 pA
-84 mV
Glut
0
sec
2
0
sec
2

Fig. 3.2 The voltage-dependence of currents induced by glutamate applied iontophoretically. External solution was barium Ringer's (solution B, Table 2.1). The patch pipette contained 101mM chloride (solution Cl01, Table 2.2).

A Currents induced by iontophoretic application of glutamate to an isolated cone photoreceptor, voltage-clamped to different membrane potentials (shown beside each trace). The timing of iontophoresis is shown by the square trace immediately below the current data. Currents are inward below 0mV, the reversal potential for the response, and outward above this voltage.

B Current-voltage relation for the glutamate-induced currents in **A**. Peak glutamate-induced currents are plotted as a function of membrane potential.

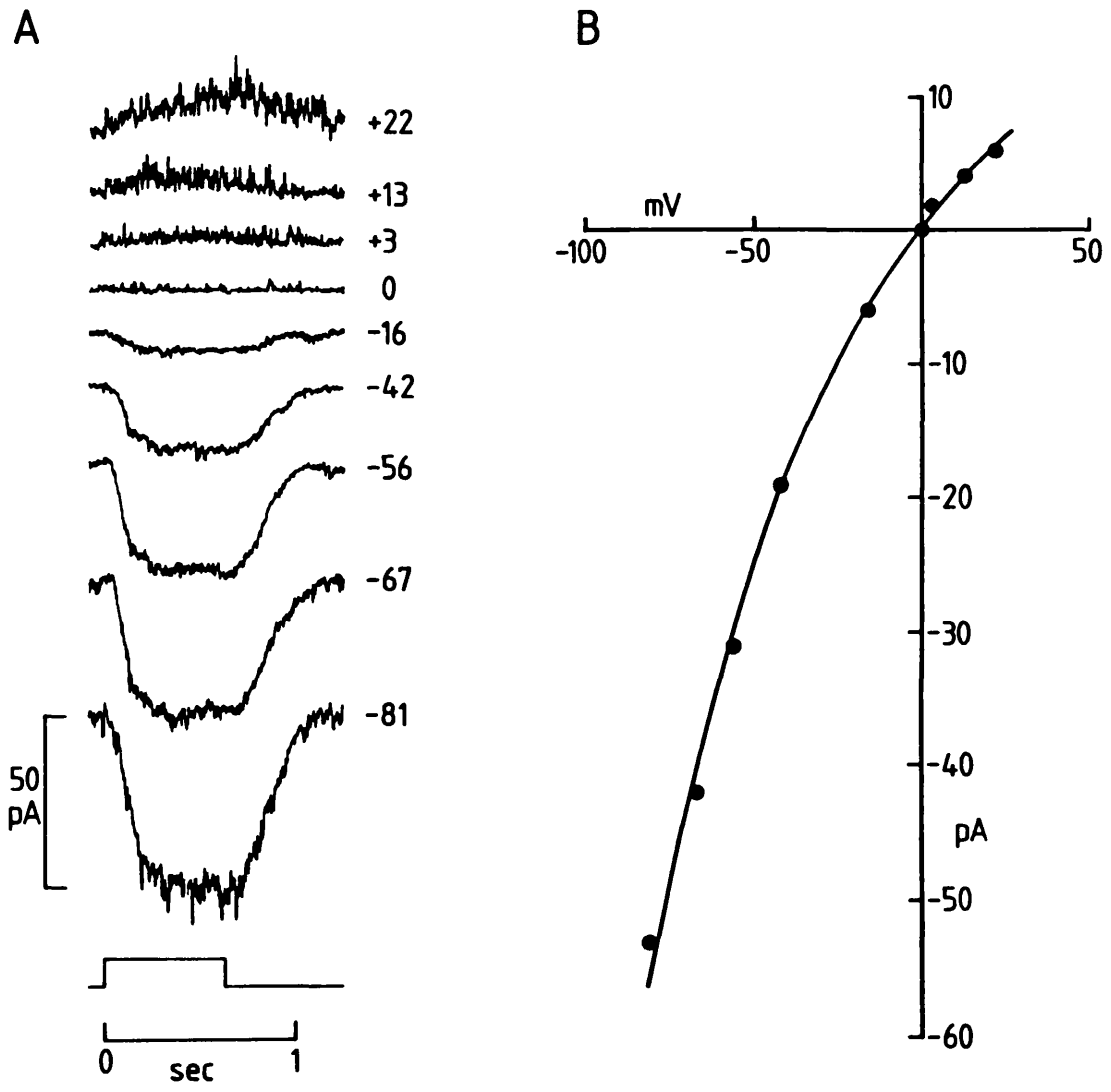
A
+22
+13
+3
0
-16
-42
-56
-67
-81
50
pA
0
sec
1
B
mV
-100
-50
50
10
-10
-20
-30
-40
pA
-50
-60

inward rectification around the reversal potential of OmV. The fact that the glutamate-evoked current had a clear reversal potential implies that at least part of the current is produced by glutamate opening ion channels (see discussion, section 7.1.2, Chapter 7).

3.3.3 Noise changes associated with the glutamate-induced current

The glutamate-induced current was usually accompanied by a small increase in current fluctuations, or noise (due to opening and closing of ion channels). Analysis of this noise in whole-cell patch-clamp recordings can give information on single channel properties without having to record from single channels.

In Fig. 3.3A, application of glutamate by iontophoresis to an isolated cone held at -76mV, produced a small inward current of about 10pA (upper trace, low pass filtered at 500Hz). The external solution was normal Ringer's and the patch pipette contained C101 (101mM chloride, Table 2.2, Chapter 2). The lower trace (high pass filtered at 2Hz) shows that an increase in current fluctuations was associated with the change in current produced by glutamate. This current noise is probably due to an increase in channels opening and closing when glutamate is applied.

The glutamate-induced inward current was associated with a small increase in the variance of the membrane current noise as shown in Fig. 3.3B.

In Fig. 3.3C, the linearity of the plot of the mean glutamate-induced current against variance of the glutamate-induced current noise in the range 2-500Hz, tested the assumption that the single channel open probability was low (Colquhoun and Hawkes, 1977). In this case, assuming there is only one type of glutamate-gated channel present, an estimate of the current flowing through a single channel can be obtained from the ratio of the increase in current variance to the mean glutamate-induced current flowing (i.e. from the slope of the line shown through the points). This gave a single channel current of 0·076pA, and a calculated single channel conductance of 1·26pS (taking into account "lost variance" at >500Hz and <2Hz, by extrapolation of a sum of Lorentzians fitted to the net power spectrum of the noise induced by glutamate).

The net power spectrum of glutamate-induced current noise for this cell was obtained by subtracting the mean control spectrum

Fig. 3.3 Analysis of current fluctuations (noise) associated with the current induced by glutamate in cones.

A Glutamate produces an inward current (upper trace, low pass filtered at 500Hz) when applied iontophoretically to an isolated cone voltage-clamped to -76mV. The external solution was normal Ringer's (solution A, Table 2.1) and the patch pipette contained solution Cl01 (with 101mM chloride, Table 2.2, Chapter 2). When the current in **A** was high pass filtered at 2Hz (lower trace), an increase in the magnitude of current fluctuations was seen to be associated with the glutamate-induced current.

B The glutamate-induced inward current (upper trace) is associated with an increase in the variance (pA^2) of the glutamate-evoked current noise, in the range 2-500Hz (lower trace).

C Relationship between the noise variance (in the range 2-500Hz), and the mean glutamate-evoked current flowing is approximately linear, implying that the probability of channel opening is low. The slope of the line (the ratio of the increase in current variance to the mean glutamate-induced current flowing) gives an value of 0·076pA, for the current flowing through a single glutamate-gated channel (making the assumptions described in section 3.3.3).

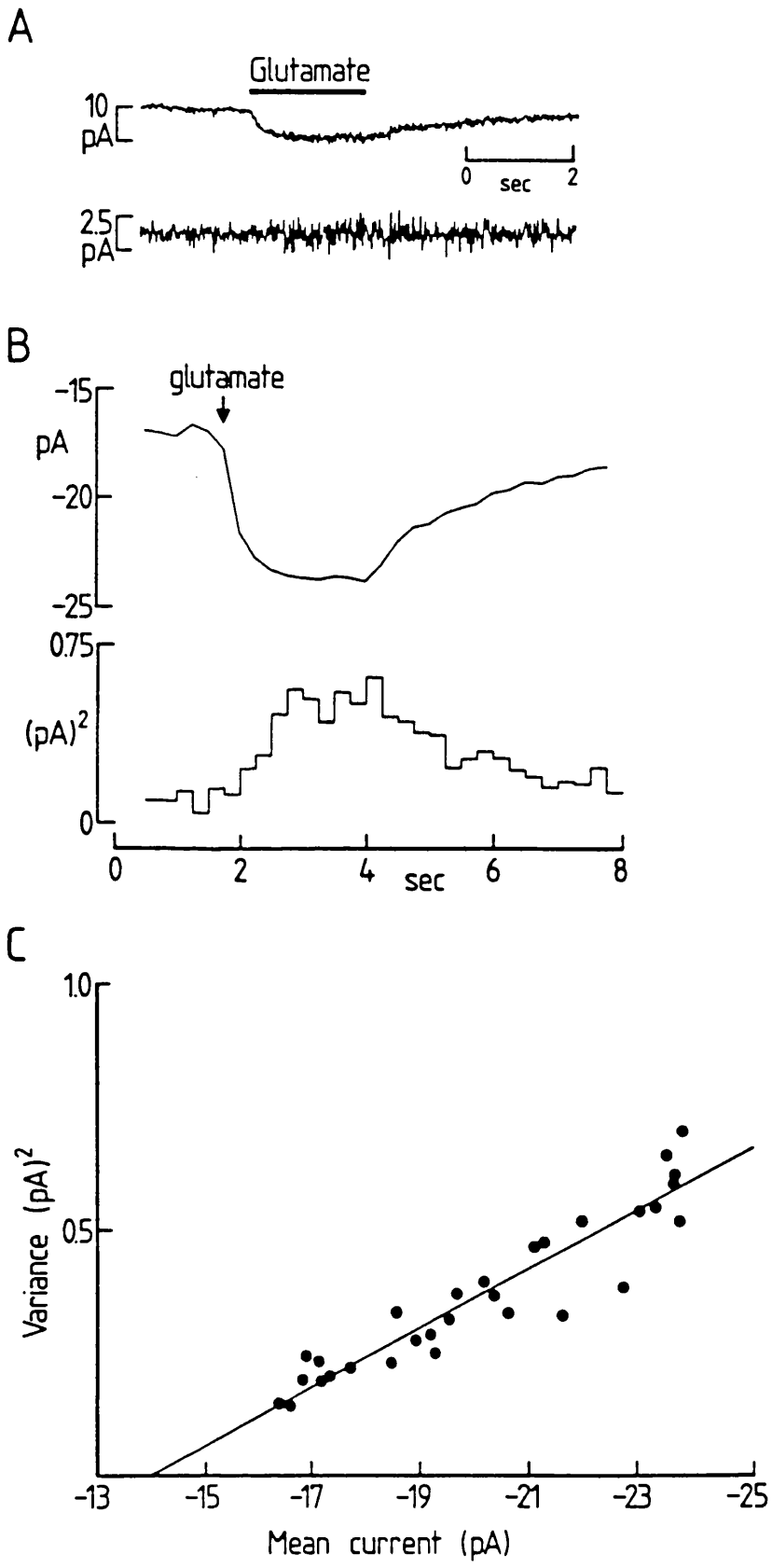
A
Glutamate
10 pA
0 sec 2
2.5 pA
B
glutamate
-15
pA
-20
-25
0.75
(pA)²
0
0 2 4 sec 6 8
C
1.0
Variance (pA)²
0.5
-13 -15 -17 -19 -21 -23 -25
Mean current (pA)

(for noise in the absence of glutamate) from the mean spectrum of noise in the presence of glutamate. This spectrum could be reasonably well fitted with the sum of two Lorentzians with half power, or "cut-off" frequencies of 45 and 282Hz. Fitting the spectrum with the sum of two Lorentzians implies that the glutamate-gated channel can exist in more than two states (e.g. there could be two closed states and one open state, or one closed and two open states). The half power frequencies can be used to obtain information about the rates of channel transitions between open and closed states.

3.3.4 Dependence of the glutamate-induced current on external glutamate concentration

The dependence of the glutamate-induced current on the external glutamate concentration was investigated by bath applying different concentrations of glutamate dissolved in barium Ringer's to isolated cones. Patch pipettes contained 101mM chloride (Table 2.2, Chapter 2).

In Fig. 3.4A, as the glutamate concentration was increased from 1μM to 100μM, the glutamate-evoked inward currents became larger, in a cone voltage-clamped to -42mV. 1μM glutamate induced a current of -28pA, which was a significant proportion (over a third) of the maximal glutamate-induced current of -70pA.

The normalized dose response curve for the data in A is shown in Fig. 3.4B. The line drawn through the points is a curve describing first order Michaelis-Menten kinetics, having the form:

$$I/I_{max} = [\text{glutamate}]/\{[\text{glutamate}] + K_m\}$$

for which the apparent K_m is 1.4μM. This low value of K_m indicates that glutamate binds with high affinity to its receptor. Fig. 3.4C shows a Lineweaver-Burke plot for the data in A and B, in which the K_m was found to be 1.4μM. In two other cones, Lineweaver-Burke plots gave K_m values of 2.6 and 5.5μM at -40mV. The linearity of the Lineweaver-Burke plots (and the fit of the Michaelis-Menten equation in Fig. 3.4) suggest that the binding of one glutamate anion activates the current.

To investigate whether the dose-response curve was affected by membrane potential, similar concentrations of glutamate were applied to the same isolated cone as in Fig. 3.4, voltage-clamped

Fig. 3.4 The currents induced by different glutamate concentrations (between 1μM and 100μM) in a cone voltage-clamped to -42mV.

A The currents induced in an isolated cone held at -42mV, by different concentrations of locally perfused glutamate. Glutamate was dissolved in barium Ringer's (solution B, Table 2.1). Solution Cl01 (Table 2.2) containing 101mM chloride was used to fill the patch pipette. From the graph it can be seen that 1μM glutamate produced a significant fraction of the current evoked by 100μM glutamate.

B The normalized dose-response curve from the data in **A**. The currents at each dose were normalized to the maximum current in 100μM for each point. The curve through the points is a Michaelis-Menten relation (see section 3.3.4) with an apparent K_m of 1.4μM.

C A Lineweaver-Burke plot for the data in **A** and **B**. 1/[glutamate] was plotted against 1/(glutamate-induced current), and the line through the points was fitted by linear regression with $1/I_{max}$ = 0.016, and the slope of the line = -0.648. The K_m is 1.4μM. A straight line fit suggests that glutamate binds with first order kinetics to its receptor.

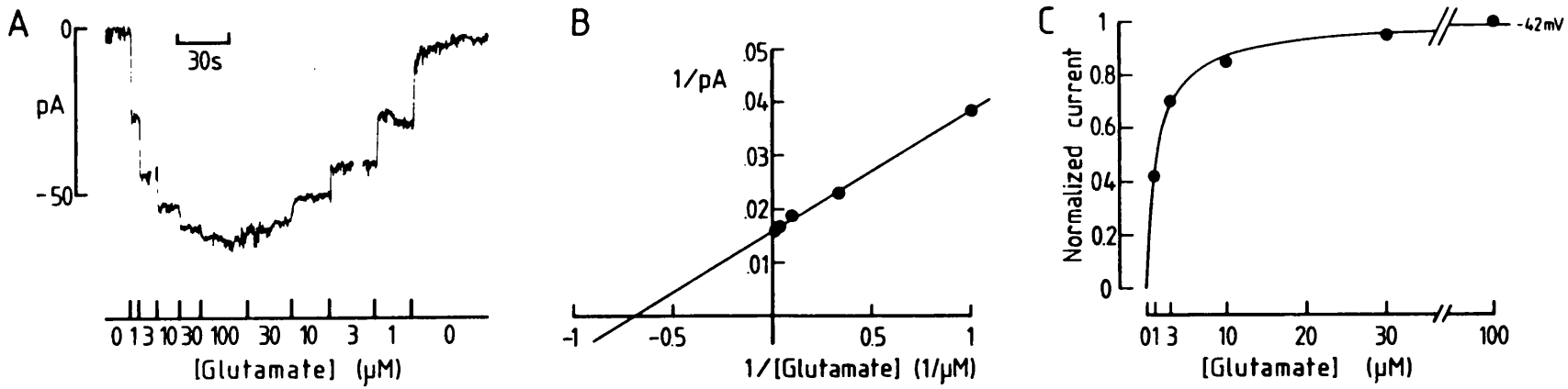
A
0
pA
-50
30s
0 1 3 10 30 100 30 10 3 1 0
[Glutamate] (μM)
B
1/pA
.05
.04
.03
.02
.01
-1
-0.5
0.5
1
1/[Glutamate] (1/μM)
C
Normalized current
1
0.8
0.6
0.4
0.2
0
-42mV
0 1 3 10 20 30 100
[Glutamate] (μM)

Fig. 3.5 Voltage-dependence of glutamate dose-response curves and K_m values for three different voltages, -62mV, -42mV and +28mV.

A Data from Fig. 3.4A, and from similar experiments on the same cell, at -62mV and +28mV, were used to plot the glutamate-induced currents as a function of glutamate concentration (between 1μM and 100μM). The curves through the points were drawn by eye. The dose-response curves look roughly similar in shape at each voltage.

B To check the similarity in shape of the dose response curves, the currents at each voltage were normalized with respect to the current induced at that voltage by 100μM glutamate, and replotted for -42mV (●), -62mV (○) and +28mV (□). The curve through the points is a Michaelis-Menten relation with an apparent K_m of 1.4μM. The fit is not perfect, the dose-response differing most in shape at +28mV.

C K_m values for each voltage calculated from Lineweaver-Burke plots similar to that in Fig. 3.4C. The mean K_m through these points was 1.4μM, and the K_m at each voltage was near to this mean value as expected from the similar shape of the dose-response curves shown in parts **A** and **B**.

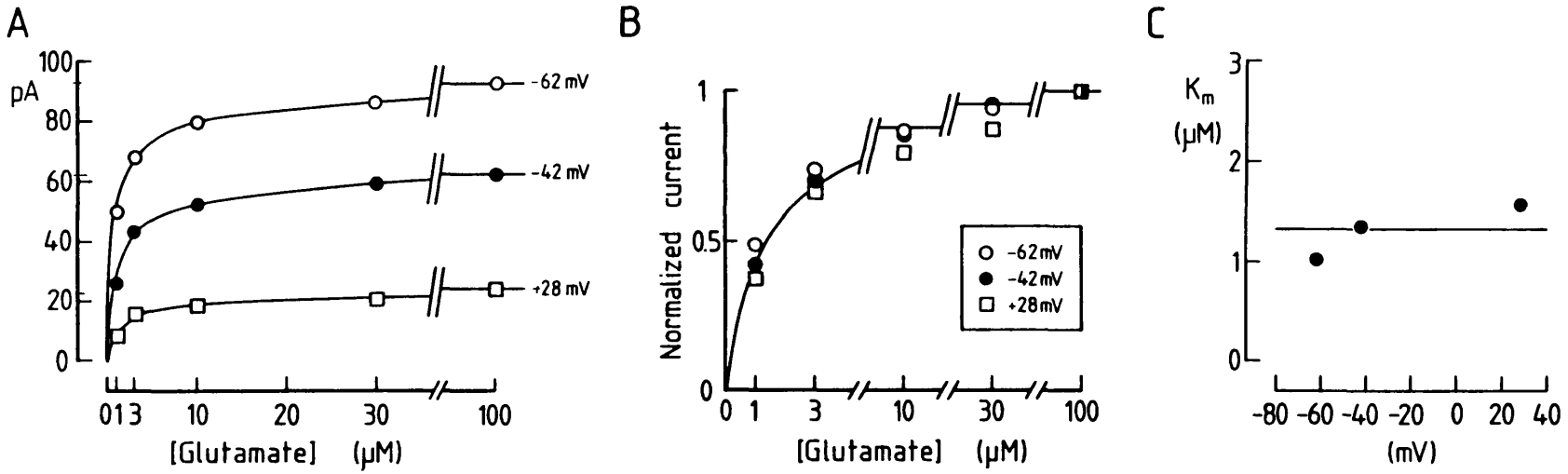
A
pA
100
80
60
40
20
0
-62 mV
-42 mV
+28 mV
0 1 3 10 20 30 100
[Glutamate] (μM)
B
Normalized current
1
0.5
0
0 1 3 10 30 100
[Glutamate] (μM)
-62mV
-42mV
+28mV
C
K_m
(μM)
3
2
1
0
-80 -60 -40 -20 0 20 40
(mV)

to three different potentials (-62mV, -42mV and +28mV). Fig 3.5A shows the data which was obtained (the curves through the points were fitted by eye).

This plot represents only the relative current magnitudes at these potentials, and does not indicate whether the glutamate-induced currents were inward or outward. The glutamate-induced currents were inward at negative potentials, -62mV and -42mV, and outward at +28mV (Fig. 3.2B).

Fig. 3.5B shows the same data after the currents were normalized to the maximal response at each voltage. A Michaelis-Menten curve with a K_m of 1.4μM has been drawn through the points. The shape of the dose-response curve depends only weakly on voltage, which suggests that glutamate binding is not very voltage-dependent over the potential range studied. In Fig. 3.5C, the K_m is plotted for each holding potential (derived from Lineweaver-Burke plots like that shown in Fig. 3.4C). The best fit K_m values show a slow increase with depolarization.

3.3.5 Spatial localization of the glutamate response

In order to determine whether the receptors for the glutamate response were spatially localized in the cone cell membrane, glutamate was iontophoresed onto different regions of the membrane.

Experiments were performed on isolated cones (n=6), voltage-clamped to -40mV. For some recordings normal Ringer's solution was flowing over the cell (towards the synaptic terminal) and for others no Ringer's solution was flowing. Similar results were obtained for each situation.

Fig. 3.6A shows the glutamate-induced currents produced in response to localized glutamate ejection at the sites shown in Fig. 3.6B. The response was largest and fastest in onset (10-50msec) at the synaptic terminal region, and became smaller and slower in onset, as the iontophoretic electrode was moved to other parts of the cell. Presumably this is because of the time taken for glutamate to diffuse from these more distant sites to the synaptic terminal. These data suggest that the response is localized to the cone synaptic terminal. Iontophoresis of glutamate at the end of the outer segment (approximately 50μm from the terminal) produced a response which eventually reached about half of the glutamate

Fig. 3.6 Spatial localization of the glutamate-induced current in cones.

A Current responses to glutamate applied by iontophoresis about 5μm away from a whole-cell patch-clamped cone, at the positions shown in **B**. The patch pipette contained 101mM chloride (solution Cl01, Table 2.2), and the bathing solution was normal Ringer's (solution A, Table 2.1). The timing of iontophoresis is shown by the square trace below the current data. Response amplitudes at each location were measured 50msec (dotted line) after the onset of glutamate iontophoresis for **C** (see below). In 50msec, glutamate can diffuse about 10μm (see section 3.3.5). The response was largest and fastest in onset at the synaptic terminal region, with a time to peak of 100msec (for the short iontophoretic pulse of glutamate). Iontophoresis of glutamate at the outer segment region, after a latency of 300msec, produced a response which was half of the peak response at the terminal.

B Diagram showing the five different positions of the iontophoretic electrode around the cone membrane for the experiment shown in **A**, and the normalized plot shown in **C**. The length of the cone is about 60μm, and the cone proportions are shown roughly correctly.

C Glutamate-induced currents at each of the regions of cell membrane shown in **B**, 50msec after the onset of glutamate iontophoresis, normalized to the magnitude of the current at the synaptic terminal after this short latency. The glutamate-induced current was largest at the synaptic terminal region and became smaller as glutamate was iontophoresed at locations further from the terminal.

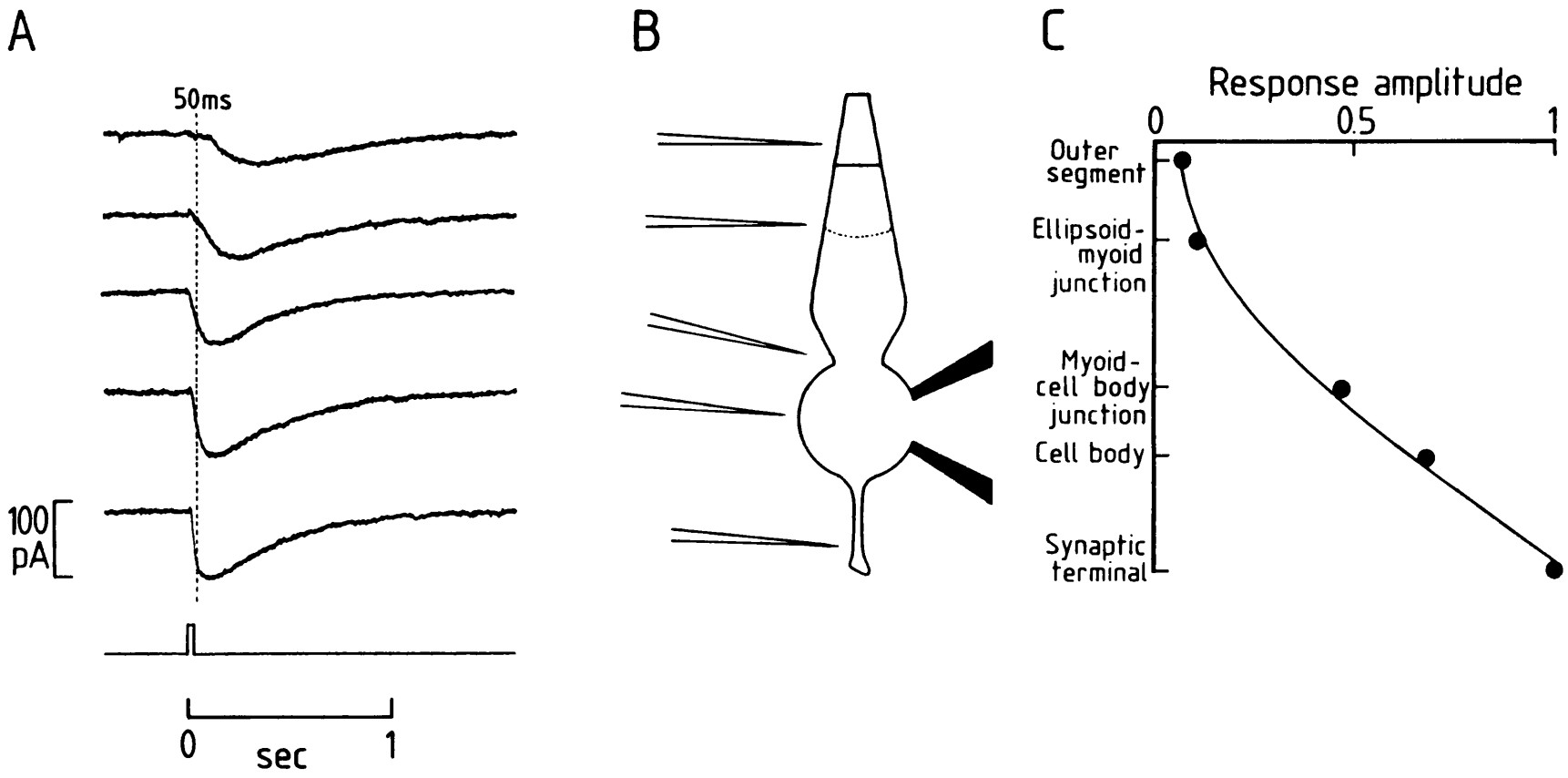
A
50ms
100
pA
0
sec
1
B
C
Response amplitude
0
0.5
1
Outer segment
Ellipsoid-myoid junction
Myoid-cell body junction
Cell body
Synaptic terminal

response produced by iontophoresis near the synaptic terminal. This relatively large (if slow) response presumably reflects the low K_m for glutamate's action (see section 3.3.4): only a little glutamate needs to diffuse from the iontophoretic electrode to the terminal to activate most of the current.

In Fig. 3.6C, currents from Fig. 3.6A were normalized to the size of the maximal response at the synaptic terminal, 50msec after the start of iontophoresis and plotted as a function of membrane region. This short latency was chosen so that glutamate had diffused a limited distance from the iontophoretic electrode. In t=50msec, glutamate will diffuse about 10μm (calculated from the diffusion equation, $x^2 = 2Dt$ (for glutamate applied as a "pulse"), from Crank (1975; p.29, eqn. 3.5) with D, the diffusion coefficient for glutamate, taken as 10^{-9} m^2 s^{-1}, a value similar to that for the diffusion of small ions at 25°C).

Fig. 3.6C shows again that the response is localized to the synaptic terminal of the cone, which in the intact retina is in close contact with the bipolar and horizontal cell dendritic processes, and with Müller cell apical membranes. Cones which had lost their synaptic terminals in the cell isolation procedure did not respond to glutamate.

3.3.6 Dependence of the glutamate-induced current on external sodium concentration

Previous reports of channels gated by glutamate suggest that they are non-specific cation channels, permeable to both sodium and potassium ions (Mayer and Westbrook, 1985). To investigate whether sodium carried any of the glutamate-induced current seen in cones, the sodium concentration was lowered (replaced by choline) in the external solution (barium Ringer's). Patch pipettes contained 101mM chloride (Table 2.2, Chapter 2).

The currents induced by glutamate applied iontophoretically (upper trace shows the timing of iontophoresis) to an isolated cone voltage-clamped to -48mV in different external sodium concentrations (lower trace; solutions Na60-Na2.1, Table 2.1) are shown in Fig. 3.7A and B.

Glutamate induced an inward current of about 80pA when the external sodium concentration was 107mM, which became smaller in 60mM external sodium (Fig. 3.7A). The glutamate-induced current was

Fig. 3.7 The dependence on external sodium of the currents induced by glutamate. Solution Cl01 (Table 2.2) containing 101mM chloride was used to fill the patch pipettes for all parts of the figure.

A Glutamate was repeatedly applied by iontophoresis (top trace) to an isolated cone in barium Ringer's (solution B, Table 2.1), voltage-clamped to -48mV. The inward current evoked by glutamate (centre trace) was reduced by about 30% when the sodium concentration in the external solution was lowered (replaced with choline) from 107mM to 60mM (see Table 2.1, Chapter 2)

B As for **A** except that the external sodium concentration was lowered (bottom trace) from 107mM to 2mM (see Table 2.1, Chapter 2). The inward currents evoked by glutamate (centre trace) applied iontophoretically (top trace), were practically abolished in 2mM external sodium solution. The current response to glutamate regained its original size after applying barium Ringer's (107mM sodium) again.

C Current-voltage relations for the glutamate-induced current in a single cone, in barium Ringer's containing 107, 60, or 2mM sodium. Lowering the external sodium concentration decreased the glutamate-induced current without detectably changing its reversal potential.

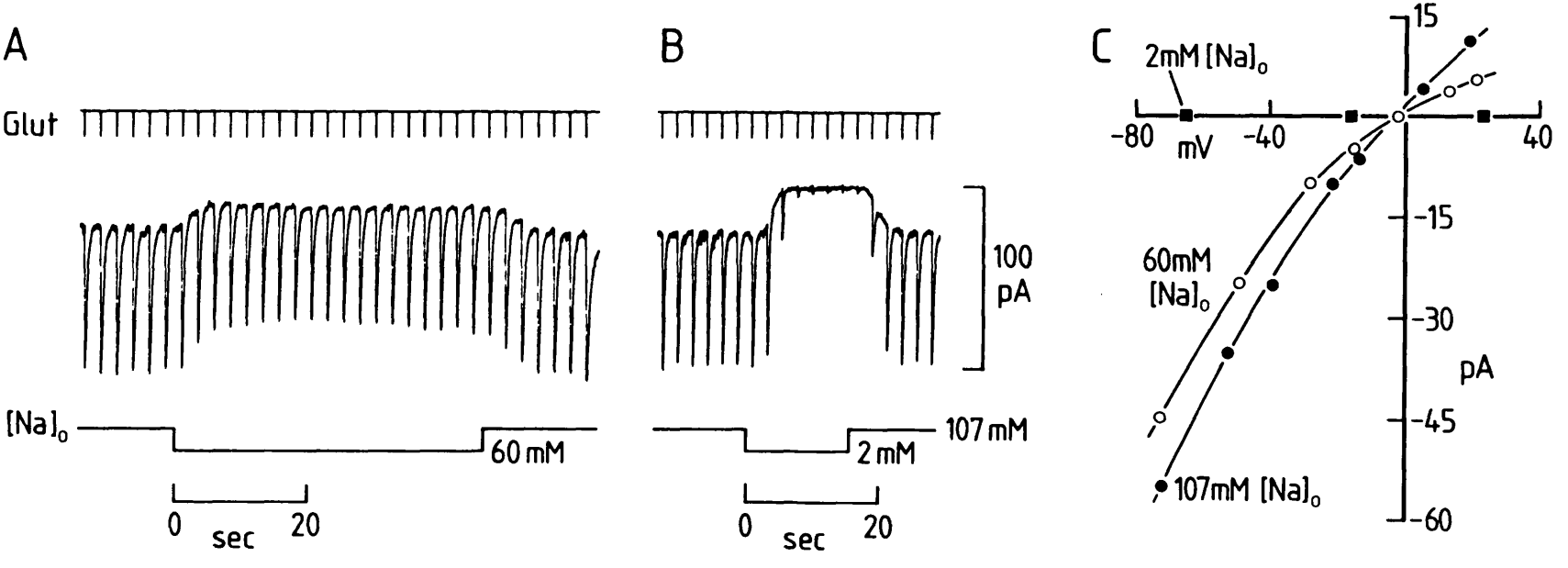
A
Glut
[Na]o
60 mM
0
sec
20
B
100
pA
107 mM
2 mM
0
sec
20
C
2mM [Na]o
15
-80
mV
-40
40
-15
60mM
[Na]o
-30
pA
-45
107mM [Na]o
-60

practically abolished in 2mM external sodium (Fig. 3.7B). Re-applying barium Ringer's containing 107mM sodium produced full recovery of the glutamate response within 8-10 seconds.

The current-voltage relations for glutamate in different external sodium concentrations are plotted in Fig. 3.7C (experiment carried out on 11 cells). Patch pipettes contained 101mM chloride (solution Cl01, Table 2.2). Lowering the external sodium concentration to 60mM, reduced the currents produced by iontophoresis of glutamate at both negative and positive potentials, but did not shift the reversal potential of the response. With an external sodium concentration of 2mM, glutamate produced no measurable currents at either negative or positive voltages. An intermediate sodium concentration of 25mM (data not shown), produced currents smaller than those produced by 60mM sodium, but did not shift the reversal potential of the response.

Thus, the glutamate-induced current in cones was dependent on the external sodium concentration. However, there was no obvious change in the reversal potential for the response, which remained at 0mV (with a patch pipette chloride of 101mM), thus sodium cannot be passing through a putative glutamate-gated cation channel in the cone cell membrane. Sodium must be required in some other way for the glutamate response (see discussion section 7.1.5, Chapter 7).

3.3.7 Dependence of the glutamate-induced current on patch pipette chloride concentration

Glutamate does not always gate cation channels. An invertebrate glutamate-gated anion (chloride) conductance has been reported by Cull-Candy (1976).

To investigate whether the glutamate-induced current seen in cones may be carried by an anion such as chloride, the patch pipette chloride concentration was lowered (replaced with acetate) from 101mM to 30mM (solution C30, Table 2.2) and to 9mM (solution C9, Table 2.2).

In Fig. 3.2 (section 3.3.2), glutamate produced a current with a reversal potential of 0mV with 101mM chloride in the patch pipette. The effect of changing the patch pipette chloride concentration on the current-voltage relation for glutamate is shown in Fig. 3.8. Lowering the pipette chloride concentration to

Fig. 3.8 Dependence of the glutamate-induced current on patch pipette chloride concentration.

A Glutamate-induced currents in a cone voltage-clamped to the potentials shown beside each trace. Timing of glutamate iontophoresis is shown as bottom trace. The patch pipette contained 30mM chloride (solution C30, Table 2.2). The external solution was barium Ringer's (solution B, Table 2.1; $[Cl]_o$ = 126mM). The reversal potential for the response was around -26mV.

B Current-voltage relation for the experiment in **A**. The voltages plotted are corrected for a junction potential of -6mV (see Table 2.2), and the series resistance produced negligible voltage error. The glutamate-induced current reversed at -27mV.

C Currents induced by iontophoresis of glutamate (bottom trace), in a different isolated cone, voltage-clamped to the potentials shown beside each trace. The patch pipette contained 9mM chloride (solution C9, Table 2.2) and the external solution was barium Ringer's ($[Cl]_o$ = 126mM). The current induced by glutamate now reversed at a more negative potential, at around -46mV.

D Current-voltage relation for the experiment in **C**. The voltages are corrected for a junction potential of -7mV (Table 2.2) and the voltage error due to the series resistance was negligible. The interpolated reversal potential is -49mV.

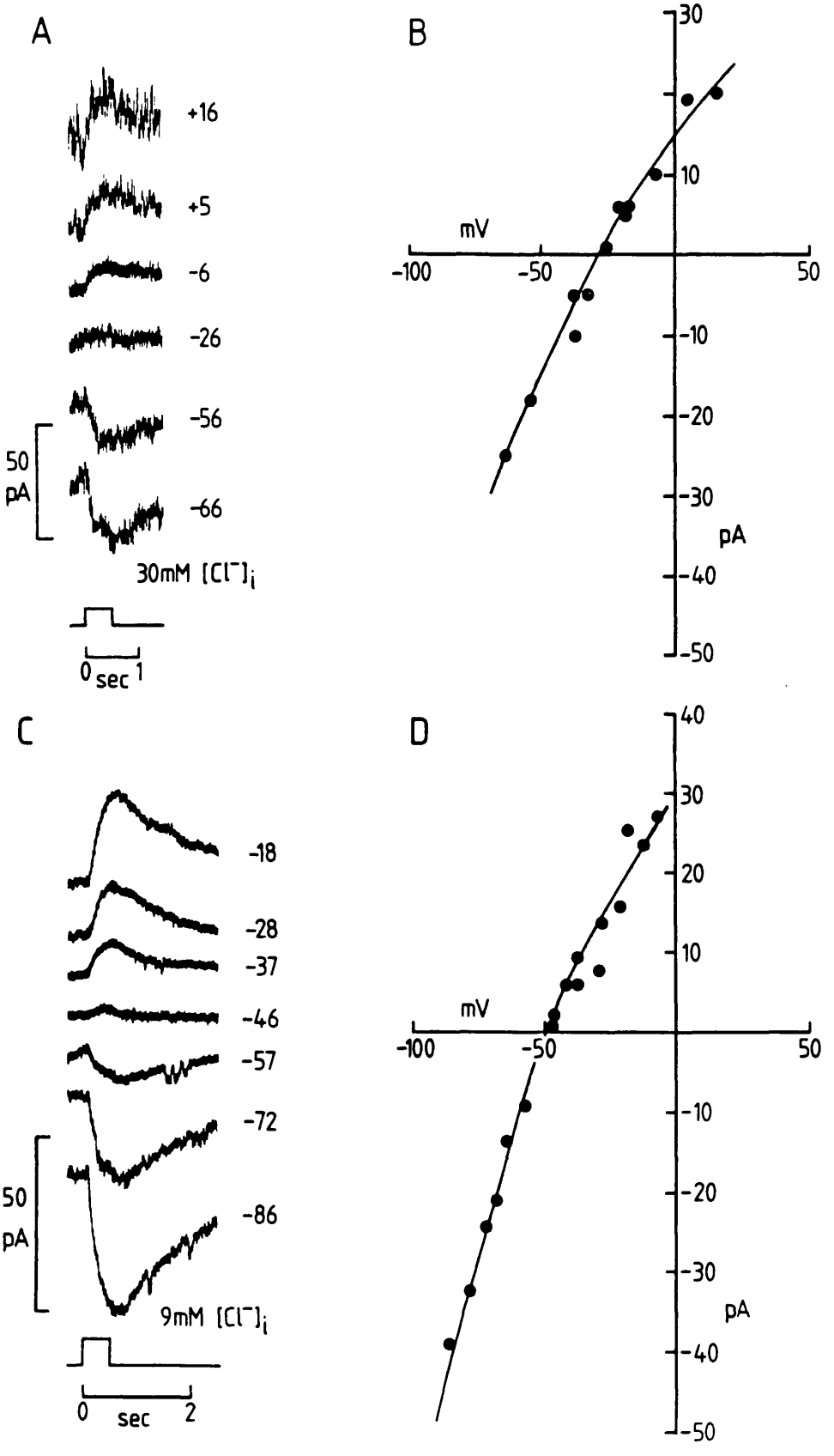
A
+16
+5
-6
-26
-56
-66
50
pA
30mM [Cl⁻]i
0 sec 1
B
30
10
mV
-100
-50
50
-10
-20
-30
pA
-40
-50
C
-18
-28
-37
-46
-57
-72
-86
50
pA
9mM [Cl⁻]i
0 sec 2
D
40
30
20
10
mV
-100
-50
50
-10
-20
-30
pA
-40
-50

* $E_{NEW} = -\frac{RT}{F} \ln\left(\frac{[Cl^-]_o + P_{Ac}/P_{Cl}[AA^-]_o}{[Cl^-]_i + P_{Ac}/P_{Cl}[Ac^-]_i}\right)$

30mM (Fig. 3.8A and B) made the reversal potential more negative, shifting it to -27mV. With 9mM chloride in the patch pipette (Fig. 3.8C and D) the reversal potential shifted to -49mV. This obvious change in the reversal potential of the glutamate response with a change in the patch pipette chloride concentration, implies that chloride ions carry at least part of the current evoked by glutamate. The average reversal potentials (±s.d.) for different patch pipette chloride concentrations were plotted in Fig. 3.9 (filled circles, isolated cells; open square, intact retina: see section 3.3.10). The observed reversal potentials do not fit the Nernst prediction:

$$E_{Cl} = -(RT/F)\ \ln\{[Cl]_o/[Cl]_i\}$$

for a chloride-specific channel (dotted line), with an external chloride concentration ($[Cl]_o$) = 126mM (barium Ringer's).

For each value of patch pipette chloride, the reversal potential was positive to E_{Cl} (see legend to Fig. 3.9). There are three ways in which this situation may be achieved:

1. Positive ions, for example sodium ions, flowing into the cell through the glutamate-gated channels, would shift the reversal potential of the response positive to E_{Cl}. However, it is clear that sodium ions do not pass through the glutamate-gated channel in cones (section 3.3.6).

2. It is possible that the presence of an electrogenic glutamate uptake mechanism (as has been found in Müller cells; Brew and Attwell, 1987), generating an inward current in response to glutamate, in addition to a chloride-specific channel, is responsible for the observed reversal potentials. In this case however, lowering external sodium would be expected to make the reversal potential more negative, and it doesn't (Fig. 3.7).

3. Another negative ion, for example acetate (the other main anion in the internal media) may flow out of the cell through the glutamate-gated channel.

On the basis of the most plausible suggestion above (3), assuming that acetate passes through the channel, the data in Fig. 3.9 were fitted with the Goldman-Hodgkin-Katz equation* (solid curve) for a channel with a permeability ratio of $P_{acetate}/P_{Cl}$ = 0.1. It has yet to be tested whether acetate is indeed the other

Fig. 3.9 Reversal potential of the current induced by glutamate as a function of chloride concentration in the patch pipette.
The dotted line shows the Nernst prediction, $E_{Cl} = -(RT/F) \ln \{[Cl_o]/[Cl_i]\}$ for a chloride-specific channel, with $[Cl]_o = 126mM$. Predicted reversal potentials (in mV) were -66, -36 and -6, for patch pipette chloride concentrations of 9, 30 and 101mM respectively. Points shown as filled circles show the mean and standard deviation of the observed reversal potentials in isolated cones. These were (in mV) -47 ± 2 (n=4), -28 ± 2 (n=6) and -3 ± 6 (n=10), for 9, 30 and 101mM $[Cl_i]$ respectively.

The point shown as an open square gives a mean reversal potential (±s.d.) of -37 ± 1mV, in 3 cells recorded from in the intact retina, with a patch pipette chloride of 16mM (see section 3.3.10). Assuming acetate carries part of the glutamate-induced current in cones (see section 3.3.7), the smooth curve is the Goldman-Hodgkin-Katz equation* for a channel with a permeability ratio $P_{acetate}/P_{chloride} = 0.1$.

$$E_{REV} = -\frac{RT}{F} \ln \left[\frac{[Cl^-]_o + P_{Ac}/P_{Cl}[Ac^-]_o}{[Cl^-]_i + P_{Ac}/P_{Cl}[Ac^-]_i} \right]$$

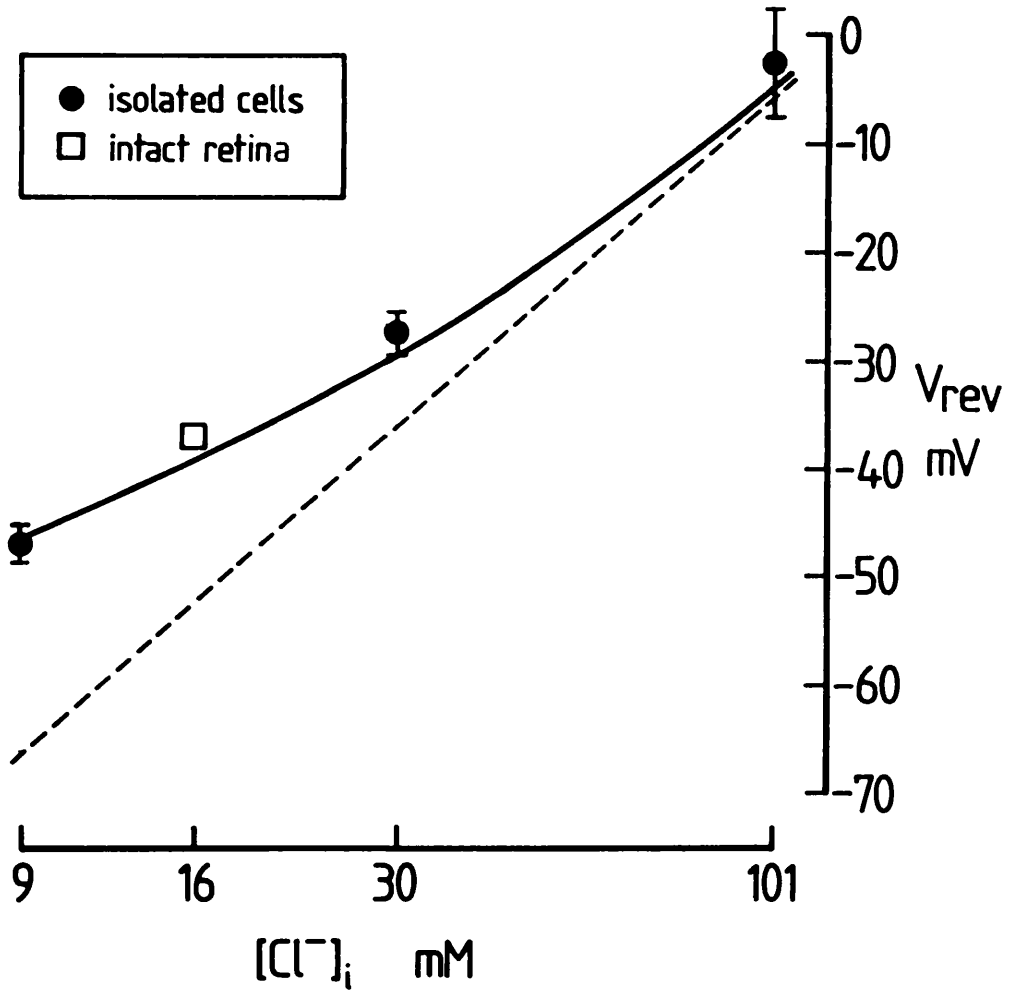
isolated cells
intact retina
0
-10
-20
-30
-40
-50
-60
-70
V_{rev}
mV
9
16
30
101
$[Cl^-]_i$ mM

current carrying ion (see section 7.2.3, Chapter 7).

3.3.8 The glutamate-induced current in cones is blocked by threo-3-hydroxy-DL-aspartate

Fig. 3.10 shows the membrane current of an isolated cone voltage-clamped to -84mV, responding to iontophoretically applied glutamate. The external solution was normal Ringer's and the patch pipette contained 101mM chloride (solution Cl01, Table 2.2). Bath application of 30μM threo-3-hydroxy-DL-aspartate (THDA), a glutamate uptake blocker (Balcar and Johnston, 1972) abolished the glutamate-evoked current (n=3) in about 5 seconds. The glutamate response was recovered on re-applying normal Ringer's.

3.3.9 The glutamate-evoked chloride current in cones is different from the chloride current evoked in cones by gamma-aminobutyric acid (GABA)

I considered the possibility that during the cell isolation procedure, a fragment of horizontal cell becomes encapsulated within the synaptic terminal of the cone (see Fig. 3.11). Fig. 3.11A shows the cone synaptic terminal, or pedicle, containing invaginations into which bipolar and horizontal cell dendrites are inserted in the intact retina. Figs. 3.11B and C show that when glutamate is applied to the isolated cone terminal, it could in principle cause depolarization of a trapped horizontal cell fragment, which may release inhibitory neurotransmitters such as gamma-aminobutyric acid (GABA) or glycine, which in turn may activate a chloride conductance in the cone. GABA has been shown to gate relatively chloride-specific channels in cone photoreceptors (Kaneko and Tachibana, 1986).

If a cell fragment is encapsulated within the cone terminal, it could be as shown in Fig. 3.11B, with no access of the extracellular fluid to the chloride channels in the cone synaptic terminal, or it could be as shown in Fig. 3.11C, with free access of the extracellular fluid to the chloride channels. In fact the second situation must occur, because it has been shown that changing the external chloride concentration changes the reversal potential of the glutamate-evoked current in cones (M. Sarantis, personal communication).

To check that GABA itself did not affect the size of the

Fig. 3.10 Threo-3-hydroxy-DL-aspartate (THDA) blocks the glutamate-induced current. External solution was normal Ringer's (solution A, Table 2.1). Patch pipette contained solution ClOl (Table 2.2). Timing of glutamate iontophoresis is shown in the bottom trace. Application of 30μM THDA for approximately 12 seconds, blocked the glutamate-induced current. This block was reversible on applying Ringer's again.

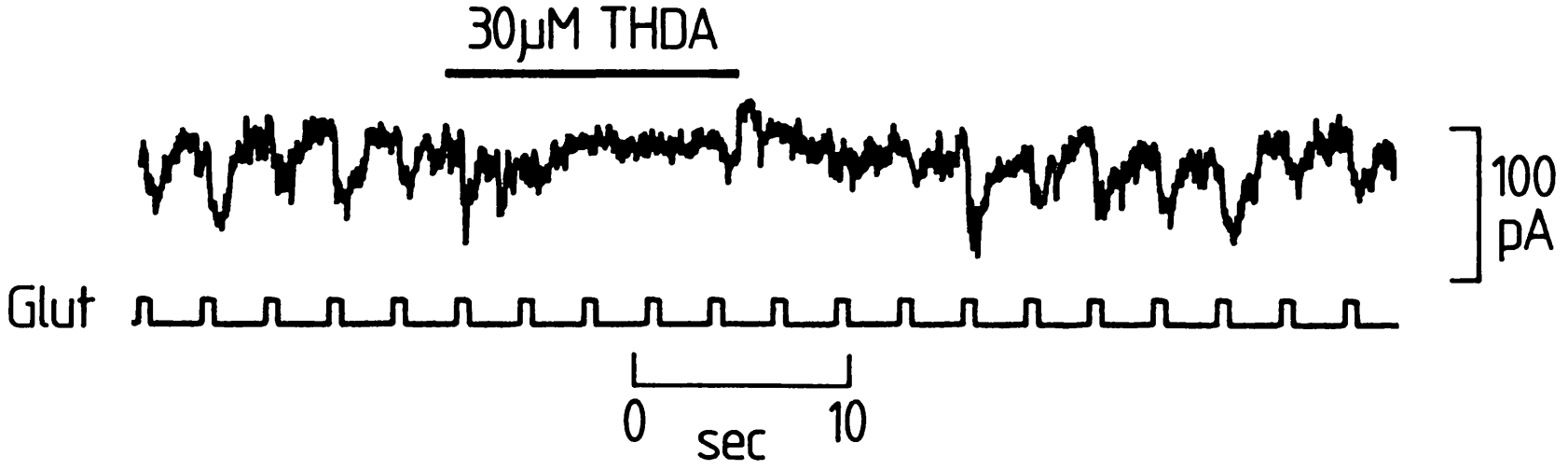
30μM THDA
100
pA
Glut
0
sec
10

Fig. 3.11 Schematic diagram of the cone synaptic terminal in the intact retina (**A**) and hypothetical configurations for a fragment of horizontal cell being trapped in the cone terminal during the cell isolation procedure.

A Drawing of the cone synaptic terminal or pedicle, showing invaginations into which bipolar and horizontal cell dendrites insert in the intact retina.

B Cone isolated from the retina, shown with a horizontal cell fragment trapped within its synaptic terminal, with no solution access between the external medium and the invagination. Glutamate could in principle activate postsynaptic cation channels in the cell fragment, causing release of GABA, which in turn gates chloride channels in the cone terminal membrane.

C Situation as in **B** but with solution access between the external medium and the invagination.

A

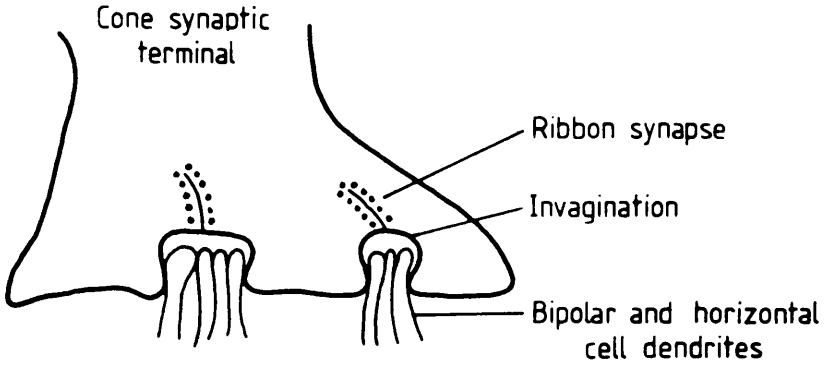
Cone synaptic terminal
Ribbon synapse
Invagination
Bipolar and horizontal cell dendrites

B

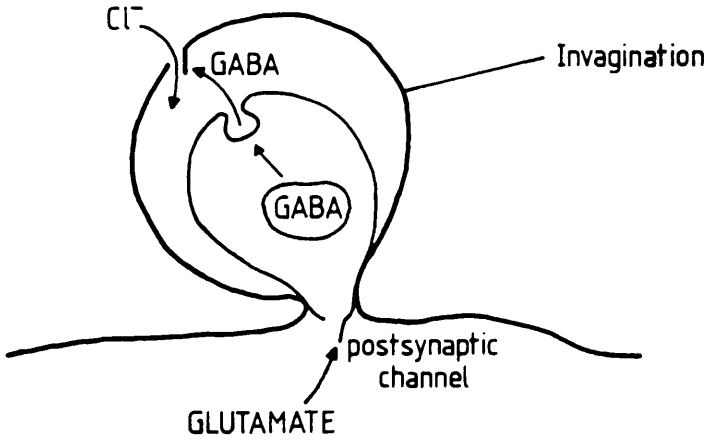
Cl⁻
GABA
Invagination
GABA
postsynaptic channel
GLUTAMATE

C

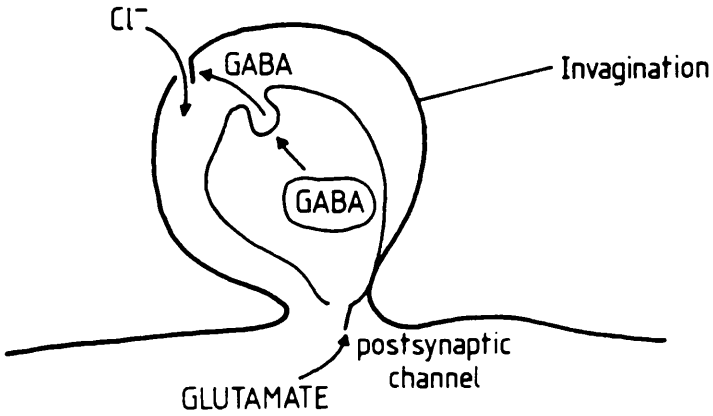
Cl⁻
GABA
Invagination
GABA
postsynaptic channel
GLUTAMATE

glutamate-evoked current in cones, 200μM GABA in barium Ringer's (solution B, Table 2.1) was perfused onto isolated cones while they were responding to glutamate applied by iontophoresis (Fig. 3.12A). Patch pipettes contained 101mM chloride (solution Cl01, Table 2.2). Application of GABA for about 40 secs had no effect on the magnitude of the glutamate response (n=5).

Receptors for GABA which gate chloride channels in the retina have been shown by Kaneko and Tachibana (1986) to be $GABA_A$-type receptors. In Fig. 3.12B, glutamate was applied to an isolated cone in the presence of the $GABA_A$ antagonist, (100μM) bicuculline (and the glycine antagonist, (10μM) strychnine, to block any possible glycinergic input). These antagonists did not markedly affect the magnitude of the glutamate-induced current (n=6).

To check that the antagonists were effective at the doses used, bicuculline and strychnine were applied in turn to different isolated ganglion cells (see section 6.3.2, Chapter 5), to ensure that they blocked the GABA and glycine responses respectively in these cells. The doses of bicuculline and strychnine used were found to be effective in antagonizing the effects of GABA and glycine respectively in isolated ganglion cells (see section 6.3.2, Chapter 6). If the glutamate-induced current seen in cones were even partly due to activation of GABA- or glycine-gated chloride channels, by glutamate, it would be expected that application of these antagonists to a cone, while it is responding to glutamate in the situation shown in Fig. 3.11C, would reduce the magnitude of the current evoked by glutamate. However, this was not seen, suggesting that the glutamate-activated chloride conductance seen in cones, is quite separate from the GABA- or glycine-gated chloride conductance previously reported in cones (Kaneko and Tachibana, 1986).

3.3.10 Glutamate induces a current in cones in the intact retina

The effect of glutamate on cones in the intact retina was investigated to compare it with that seen in isolated cells. The external solution used was based on normal Ringer's and contained 10μM bicuculline to block any response of the cones due to glutamate-activated GABA release from horizontal cells to cones. The patch pipette solution used contained 16mM chloride (solution Cl6, Table 2.2).

Fig. 3.12 Gamma-aminobutyric acid (GABA), bicuculline and strychnine do not affect the size of the glutamate response in cones. External solution was barium Ringer's (solution B, Table 2.1). Patch pipettes contained 101mM chloride (solution Cl01, Table 2.2).

A Glutamate-evoked current in an isolated cone held at -52mV. Bath application of 200μM GABA for the period indicated in the top trace (about 40 seconds), had no effect on the size of the glutamate-evoked current. Timing of glutamate iontophoresis is shown in the lower trace.

B Glutamate-evoked current in an isolated cone held at -62mV. Bath application of 100μM bicuculline and 10μM strychnine for the length of time shown in the top trace (about 80 seconds), had no effect on the magnitude of the glutamate response.

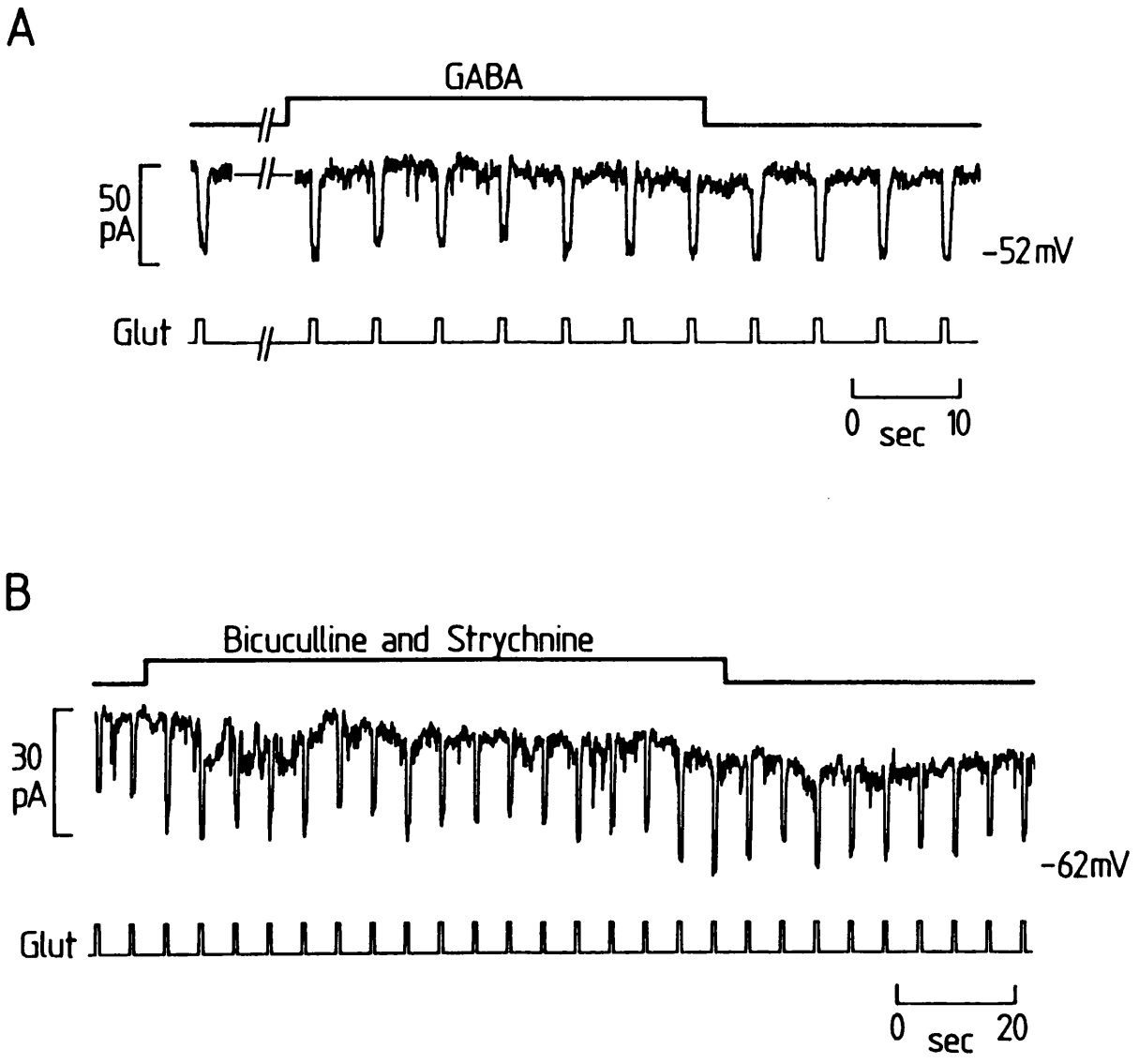
A
GABA
50
pA
-52mV
Glut
0 sec 10
B
Bicuculline and Strychnine
30
pA
-62mV
Glut
0 sec 20

Graded light responses were recorded from dark adapted cones (n=12), voltage-clamped to -40mV, in the intact retina (section 2.1.2, Chapter 2), to ensure that they were viable. Typically, light responses appeared as in Fig. 3.13A. The magnitude of the photocurrent increased as the light intensity increased. The peak photocurrent-$\log_{10}$ (intensity) curve was plotted for this cone in Fig. 3.13B.

All cells tested (n=8) responded to glutamate in the light with an inward current at -60mV. The current-voltage (I-V) relationship for the glutamate-induced current in a single cone in the intact retina is shown in Fig. 3.14. Glutamate (5mM) was applied to the cell voltage-clamped to -40mV. At this potential, glutamate evoked an inward current of 10pA after 1-2mins (this delay reflecting the time needed for the glutamate to diffuse into the retina). The I-V relation shown was obtained by subtracting a control ramped I-V relation in the absence of glutamate, from a ramped I-V relation in the presence of glutamate. The glutamate-induced current was larger at potentials negative to -40mV, reversed at -38mV for this cell, and was outward at more positive potentials. The reversal potential of -38mV is positive to the Nernst prediction of E_{Cl} = -49mV, for a chloride-specific channel with $[Cl]_o$ = 114mM, and $[Cl]_i$ = 16mM.

The average reversal potential (mean data from 3 cells$\pm$s.d.) for this patch pipette chloride concentration was -37$\pm$1mV. This fits very well on the plot of Fig. 3.9 (open square), which shows how the reversal potential of the glutamate-evoked current depends on patch pipette chloride concentration in isolated cones. This suggests that the glutamate-evoked current which I have characterized in isolated cones is also present in intact cones in the retina and is not, for example, induced as an artefact of isolating the cones from the retina.

Fig. 3.13 Photocurrent responses in a dark adapted cone in the intact retina.

A Red light (wavelength 700nm) steps of approximately 1.2 sec duration (controlled by hand) and various intensities were applied to a cone voltage-clamped to -60mV. Numbers are on a $\log_{10}$ scale, where 0.0 = 7.57×10^6 photons/μm^2/sec. Red 0.0 is the brightest light flash. As the light intensity increased, the size of the photocurrent increased in a graded manner.

B Normalized photocurrent (I_{light}/Peak I_{light})-$\log_{10}$ (intensity) curve for the cone in **A**. The peak current at $\log_{10}$ (intensity) = 0 was 32pA.

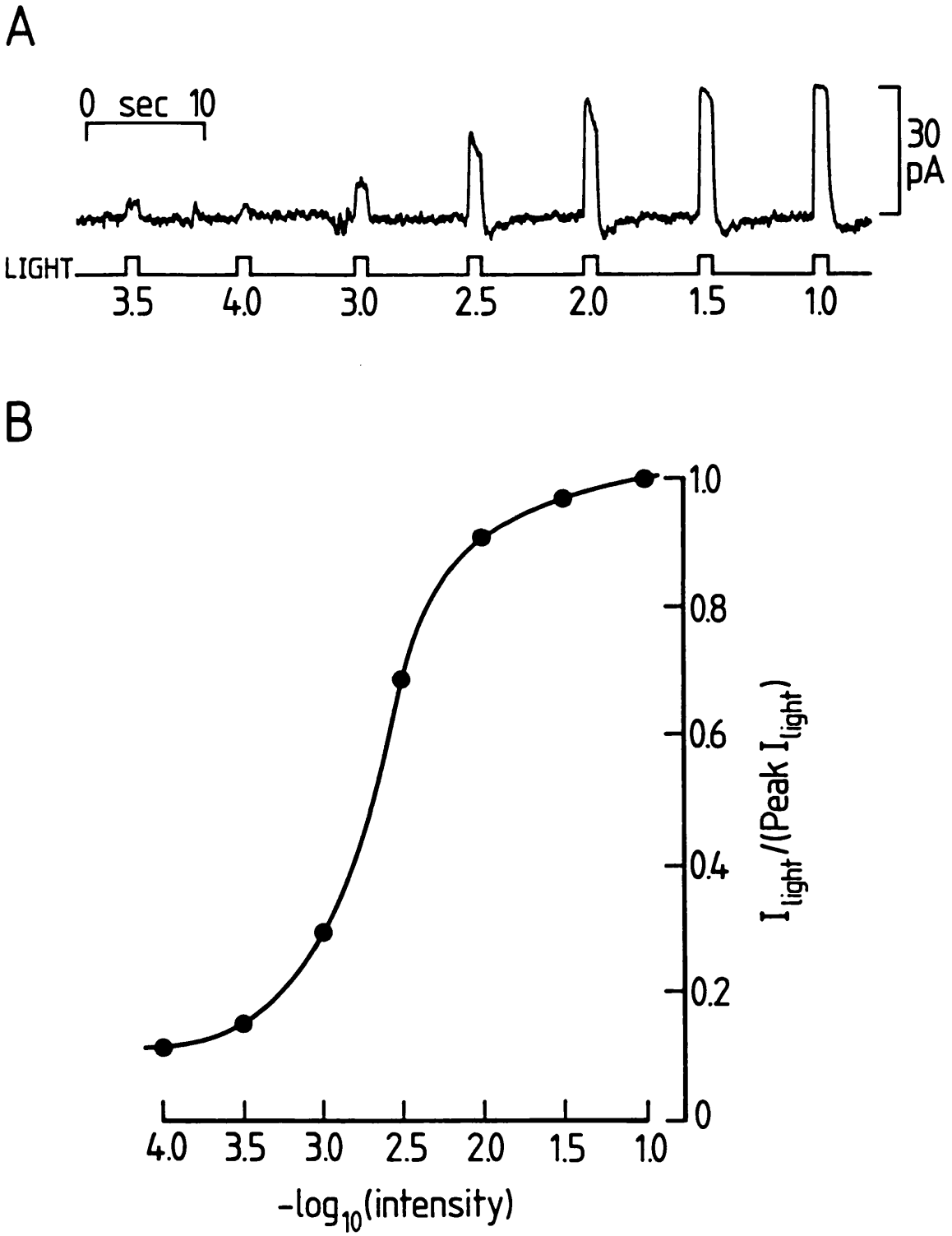
A
0 sec 10
30
pA
LIGHT
3.5
4.0
3.0
2.5
2.0
1.5
1.0
B
1.0
0.8
0.6
0.4
0.2
0
$I_{light}/(Peak\ I_{light})$
4.0
3.5
3.0
2.5
2.0
1.5
1.0
$-\log_{10}(intensity)$

Fig. 3.14 Glutamate produces a current in cones in the intact retina. The external solution was based on normal Ringer's (solution A, Table 2.1), and contained 10μM bicuculline. Patch pipette contained 16mM chloride (solution Cl01, Table 2.2).
A Current-voltage (I-V) relation for the current evoked by 5mM glutamate. Glutamate produced an inward current at the cone dark potential of -40mV, which was larger at more negative potentials. The reversal potential for the glutamate response was -38mV. At more positive potentials the current induced by glutamate was outward. The I-V relation was linear, and the line through the points has been fitted by linear regression, with a slope of 4.4nS and y-intercept of -38mV.

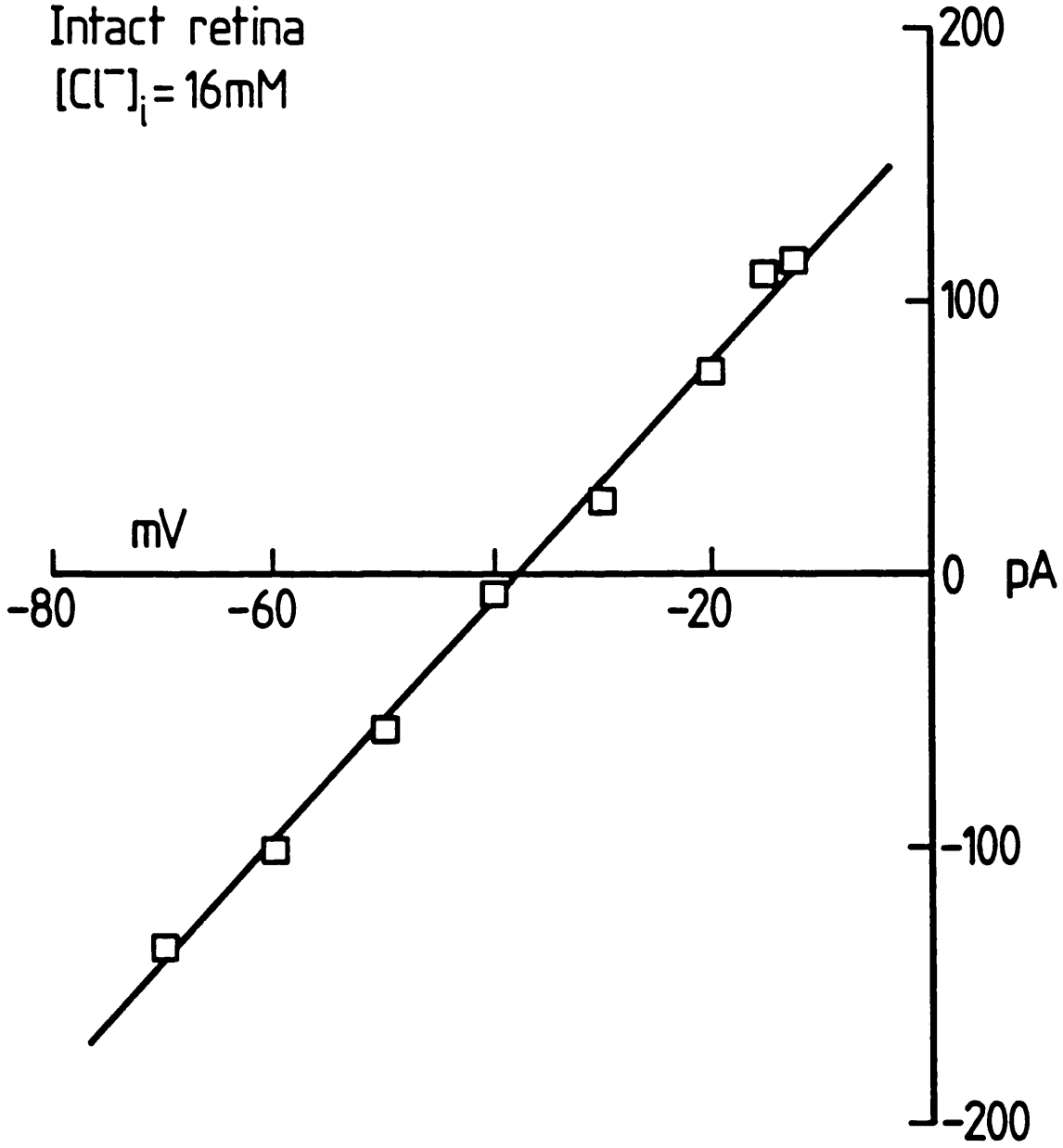
Intact retina
[Cl⁻]i = 16mM
200
100
mV
0 pA
-80
-60
-20
-100
-200

Chapter 4

Voltage-gated membrane currents in retinal ganglion cells

4.1 Introduction

In this chapter I show that both isolated ganglion cells and ganglion cells in the intact retina can be divided into at least two types, based on their response to injected current. Ganglion cells produce either sustained or transient bursts of action potentials in response to depolarizing current injection (mimicking maintained synaptic input from bipolar cells). These types probably correspond to sustained and transient ganglion cell classes shown to exist for both "ON" and "OFF" ganglion cells in response to light (see section 1.2.7, Chapter 1). A preliminary analysis of the voltage-gated currents in isolated ganglion cells is also presented here. These results are important because there is no information concerning the role of voltage-gated currents in the generation of sustained and transient responses in ganglion cells.

The results in this chapter are divided into the following sections: (1) Sustained and transient responses are generated by current injection in identified ganglion cells in the intact retina; (2) Sustained and transient responses can also be generated by current injection in identified isolated ganglion cells; (3) Response properties of isolated cells are not correlated with seal resistance, cell input resistance, pipette series resistance, or resting membrane potential; (4) Voltage-gated membrane currents in isolated ganglion cells; (5) Voltage-dependence and activation range of the sodium, potassium and calcium currents.

These results are used to address the questions raised in section 1.5.3, in Chapter 1, which are presented for discussion in section 7.3 (Chapter 7).

4.2 Methods

Recordings were made from ganglion cells in the intact retinal flatmount (section 2.5.4, Chapter 2), and from isolated cells, dissociated from the enzyme-treated retina (section 2.5.5, Chapter 2). All cells were identified as ganglion cells prior to recording by observation of the fluorescent label, FITC-peroxidase, introduced into cells via their optic nerve axons (sections 2.5.1 and 2.5.2, Chapter 2).

Ganglion cells were whole-cell patch-clamped and recordings were made either in current-clamp (sections 4.3.1 and 4.3.2) or in voltage-clamp (section 4.3.4). The external solution was normal Ringer's (solution A, Table 2.1), and the patch pipettes contained solution GI3 (containing 3mM chloride: Table 2.3, Chapter 2).

In some cases, for cells with a low apparent resting potential during experiments (i.e. before correction for any voltage drop produced by shunting of the cell membrane through the seal resistance), hyperpolarizing current was applied to bring the membrane potential closer to the normal value of -60mV. Recordings were also made from cells with apparent resting potentials which were either positive or negative to -60mV. This did not affect the results obtained (see section 4.3.3).

4.3 Results

4.3.1 Sustained and transient responses are generated by current injection in identified ganglion cells in the intact retina.

Fig. 1A shows a ganglion cell in current-clamp, producing sustained bursts of action potentials in response to injection of depolarizing current steps, from a resting potential of -59mV. As more current is injected, the frequency of action potentials produced increased. However, with larger current injection (+40pA) in this cell), the magnitude of action potentials produced during the current pulse decreased. These smaller action potentials would probably not propagate *in vivo*.

The dependence of action potential frequency on injected current, within the first second of the pulse of current injection, for the data in Fig. 4.1A, is shown in Fig. 4.1B. For low values of injected current, there was a linear relationship between injected current and the number of action potentials produced. For larger current injections, the action potential frequency reached a plateau, and the action potentials became smaller during the current pulse and eventually failed at high injected currents (see discussion, section 7.3.1).

In a different cell, shown in Fig. 4.1C, small depolarizing current injections, from a resting potential of -63mV, produced a single action potential and larger current injections produced only one or two more action potentials which were smaller than the

Fig. 4.1 Depolarizing current injection in current-clamped, whole-cell patch-clamped ganglion cells in the intact flatmounted retina produces sustained or transient bursts of action potentials. The external solution was normal Ringer's (solution A, Table 2.1, Chapter 2) and patch pipettes contained solution GI3 (3mM chloride: Table 2.3, Chapter 2).

A A ganglion cell showing a sustained response to depolarizing current injection (values shown alongside each voltage trace), from a resting potential of -59mV. As more current is injected, the frequency of action potentials produced increases. Larger current injections (in this cell, +40pA), produced a train of action potentials which decreased in size during the pulse.

B Plot of the dependence of action potential frequency on injected current during the first second of the current injection pulse for the data in **A**. For small injected currents (up to +20pA), the relationship between action potential frequency and injected current is linear. However, for larger current injections, the number of action potentials produced reaches a plateau.

C A ganglion cell responding transiently when depolarizing current is injected from a resting potential of -63mV. In this cell, injection of +50pA, produces only a single action potential, and larger current injections produce only one or two more smaller action potentials.

D Plot of variation of action potential frequency with injected current, in the first second of current injection, for the data in **C**. Current injection of +50pA produces a single action potential. Current injection of +60 to +70pA and above, produces one to two more action potentials, but there is no further increase above this, in the number of action potentials produced.

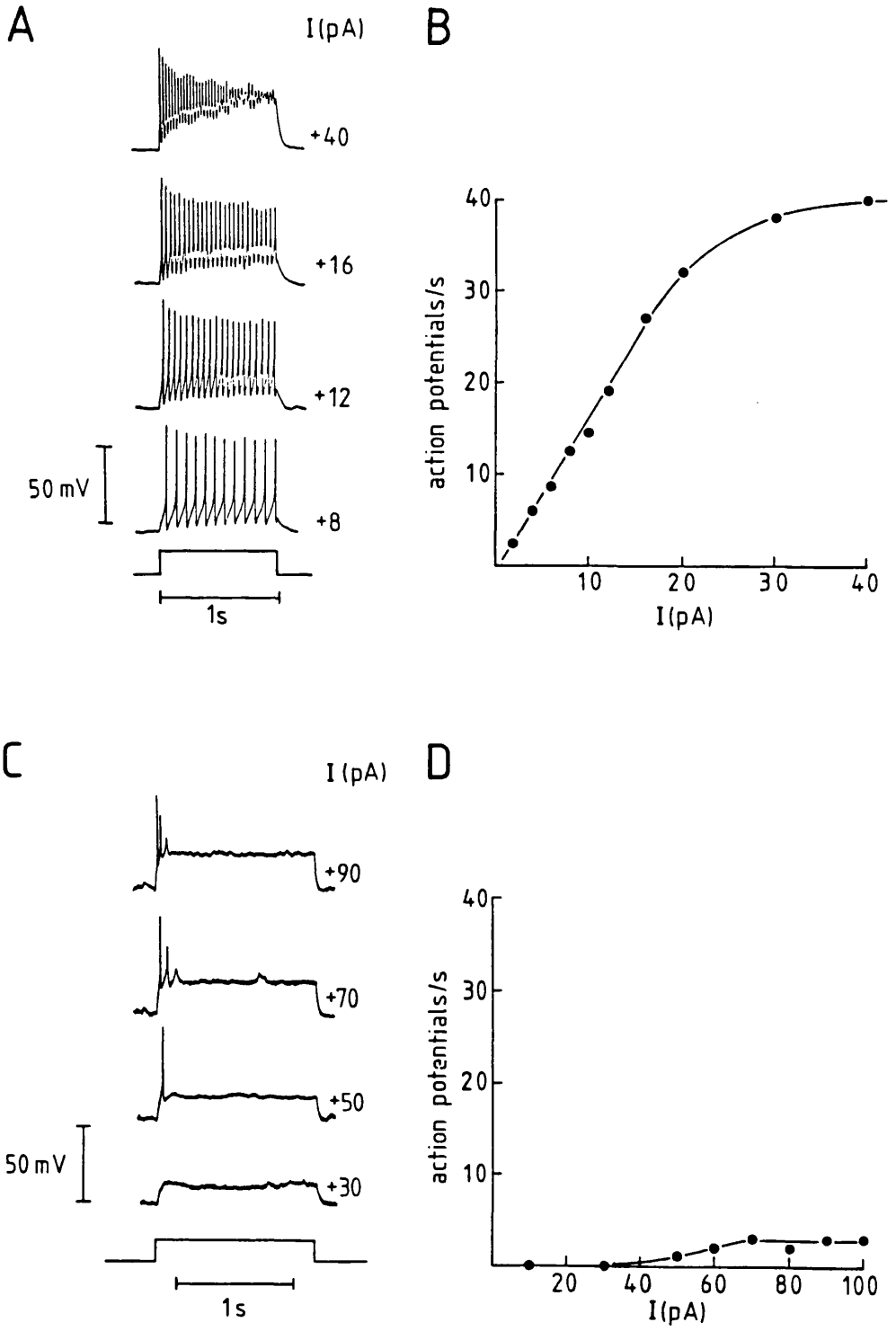
A
I(pA)
+40
+16
+12
+8
50 mV
1s
B
action potentials/s
40
30
20
10
10
20
30
40
I(pA)
C
I(pA)
+90
+70
+50
+30
50 mV
1s
D
action potentials/s
40
30
20
10
20
40
60
80
100
I(pA)

first. The dependence on injected current of the number of action potentials produced in the first second of the pulse of current injection, for this cell, is plotted in Fig. 4.1D.

In 65% of cells recorded from (n=27) depolarizing current pulses evoked sustained trains of action potentials as in Fig. 4.1A, and in 35% of cells current injection produced transient responses as shown in Fig 4.1C. In these cells (data not shown, but see section 4.3.3 for similar data on isolated cells) the occurrence of sustained and transient responses was not correlated with cell input resistance, pipette series resistance, or cell resting potential. For 16 sustained cells, and 7 transient cells, average input resistance (mean±s.e.) was 631±117MΩ and 890±290MΩ, respectively. Pipette series resistance was 97±10MΩ for sustained cells, and 70±5MΩ for transient cells. I considered the possibility that minor differences in pipette series resistance might be significant, since a lower series resistance would allow more rapid equilibration of cell and pipette contents, and thus, might result in washout of certain membrane currents. However, sustained and transient responses were seen within 10 seconds of going into the whole-cell recording mode, and did not change within 5 minutes of recording, suggesting that, for example, equilibration of the cell intracellular medium and the patch pipette solution, leading to time-dependent loss or "washout" of some membrane currents, is probably not responsible for determining whether a cell is sustained or transient. Mean resting potential (±s.e) was -51±4mV for sustained cells, and -49±5mV for transient cells, i.e. not significantly different beween cell types.

4.3.2 Sustained and transient responses are generated by current injection in identified isolated ganglion cells

When depolarizing current pulses were injected into ganglion cells isolated from the retina, sustained and transient response types were obtained as shown in Fig. 4.1A and C for cells in the intact retina. Out of 63 isolated cells recorded from, 48% of cells responded to current injection with sustained bursts of action potentials, and 52% of cells responded with a single action potential, or transient burst of action potentials. As sustained and transient responses similar to those obtained in the intact

retina can be produced in isolated ganglion cells, which are devoid of synaptic input from surrounding retinal cells, it is likely that intrinsic mechanisms within the ganglion cell membrane itself (rather than extrinsic mechanisms such as time course of the synaptic current generated by bipolar and amacrine cells) are largely responsible for the generation of these two response classes.

4.3.3 Response properties of isolated ganglion cells are not correlated with seal resistance, input resistance, pipette series resistance or resting potential.

I investigated whether the occurrence of sustained and transient cells was an artefact produced by differences in seal resistance (which might lead to different amounts of shunting of the cell membrane), differences in input resistance (perhaps reflecting differential damage to cells), differences in pipette series resistance (leading to differences in washout of membrane currents), or differences in membrane potential.

The seal resistances of isolated ganglion cells were measured during cell-attached recording, and plotted against cell number for the range of resistances shown along the abscissa in Fig 4.2A. Transient cells are represented by the hatched bars in each part of Fig. 4.2. Transient cells had seal resistances in the range 1-6GΩ, and most sustained cells also had seal resistances within this range (though a few were much higher, 20 to 30GΩ). The average seal resistance was 8.12 ± 0.62GΩ, (mean±s.e, n=16) for sustained cells, and 2.64 ± 0.05GΩ, (mean±s.e, n=21) for transient cells. For "low" seal resistances (below 6GΩ) both sustained and transient cells were found, ruling out a simple dependence of response class on seal resistance.

Similar plots were made for the cell input resistance, pipette series resistance, and resting membrane potential. In Fig. 4.2B, both sustained and transient cells had input resistances which fell within the range of 0 to 2GΩ. In the 0 to 0.5GΩ range, no cells had an input resistance which was lower than 100MΩ. Since there is also a similar spread of input resistances for both sustained and transient cells, and the average values (mean±s.e) of input resistance are similar for each cell type (1070 ± 40MΩ, n=29, for sustained cells; 840 ± 26MΩ, n=34, for transient cells), it seems

Fig. 4.2 Histograms showing the relationship between the occurrence of sustained (un-shaded histograms) and transient (shaded histograms) responses in isolated ganglion cells in response to current injection and cell seal resistance (**A**), input resistance (**B**), series resistance (**C**) and resting potential (**D**). It appears that there is no convincing dependence of sustained and transient responses on seal resistance, input resistance, pipette series resistance, or resting potential (see section 4.3.3).

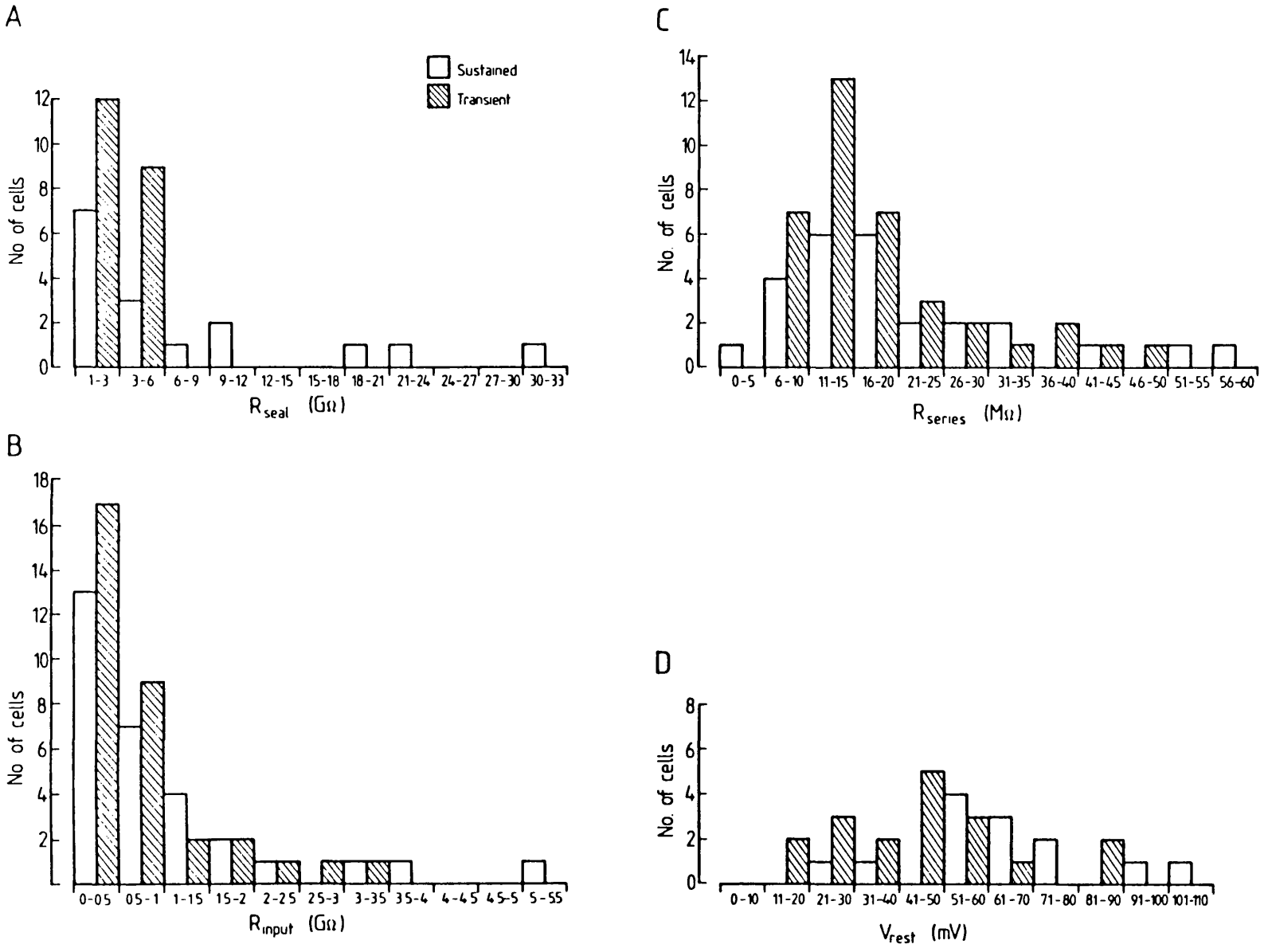
A
Sustained
Transient
No of cells
1-3
3-6
6-9
9-12
12-15
15-18
18-21
21-24
24-27
27-30
30-33
R_{seal} (GΩ)
B
No of cells
0-05
05-1
1-15
15-2
2-25
25-3
3-35
35-4
4-45
45-5
5-55
R_{input} (GΩ)
C
No. of cells
0-5
6-10
11-15
16-20
21-25
26-30
31-35
36-40
41-45
46-50
51-55
56-60
R_{series} (MΩ)
D
No. of cells
0-10
11-20
21-30
31-40
41-50
51-60
61-70
71-80
81-90
91-100
101-110
V_{rest} (mV)

that sustained and transient response types do not reflect differences in input resistance.

The pipette series resistance was measured during the first few seconds of the whole-cell recording configuraton, and is shown for sustained and transient cells in Fig. 4.2C. If the series resistance is high, equilibration of pipette and cell contents will be slow and thus the cell response might change with time. If the series resistance is very low, "washout" of vital membrane currents may occur. Both sustained and transient cell types have a series resistance within the range 6 to 20MΩ. The average series resistance was 20.7±0.6MΩ, (mean±s.e, n=29) for sustained cells, and 17.6±0.3MΩ, (mean±s.e, n=34) for transient cells. Over almost all the range of series resistances found, some cells were transient and others were sustained. In addition, as for ganglion cells in the intact retina, sustained and transient responses were preserved 5-10 minutes after recording had started. These factors, taken together, rule out a simple dependence of response class on series resistance.

Measurement of the apparent resting potential during each recording, and correction for voltage drop produced by the seal conductance (see Methods, section 2.7.1, Chapter 2), produced the data shown in Fig. 4.2D. Average values for resting potential were 64±2mV, (mean±s.e, n=13), for sustained cells, and 49±1mV, (mean± s.e, n=19) for transient cells. Sustained and transient cells were found with true resting potentials over all of the range from -11mV to -90mV. There was, thus, no convincing dependence of response class on resting potential.

Recordings were made from cells with a variety of apparent resting potentials. Depolarizing current was first injected at the apparent resting potential. Most cells responded by producing either transient or sustained bursts of action potentials. Cells were then polarized to -60mV by current injection and their responses to depolarizing current pulses retested. The cells continued to produce either sustained or transient responses. Polarization to -60mV did not convert sustained cells into transient ones or vice versa. The production of sustained or transient responses was uncorrelated with either the apparent resting potential or the resting potential after correction for the

voltage drop produced by the seal conductance.

4.3.4 Voltage-gated membrane currents in isolated ganglion cells

I studied the voltage-gated currents present in isolated ganglion cells to gain some insight into factors which might determine whether ganglion cells respond in a sustained or transient way to injected current.

Voltage-gated membrane currents in identified isolated ganglion cells were studied in voltage-clamp, by applying depolarizing command voltages (usually in steps of 10mV) to cells usually held at around a resting potential of -60mV.

Fig. 4.3A shows the currents which were produced in an isolated ganglion cell, when depolarizing command potentials were applied (shown to the right of each trace) from a holding potential of -63mV. The patch pipette contained solution GI3 ($[Cl^-]$ = 3mM). In the top part of the figure, a rapid (5-10msec) transient inward current was activated at potentials above -40mV, which was smaller at more depolarized potentials. This current is described in more detail below. Depolarization of the cell to -35mV, activated an outward current, which became larger and more transient with further depolarization. In the lower part of the figure, a small inward current was produced in response to step hyperpolarizations from -63mV. These inward and outward currents were seen in both sustained (36%) and transient (64%) cell types (n=28).

Bath application of the sodium channel blocker, 1µM tetrodotoxin (TTX, 1uM), abolished the transient inward current evoked by depolarization in all cells tested (n=11). The effect of TTX was usually completely reversible (n=8: data not shown for the cell in Fig. 4.3A, but see Fig. 4.3B, centre panel). This suggests that the inward current is a sodium current.

The outward current in Fig. 4.3A is probably a potassium current, since this current was absent in other cells recorded from in the presence of the potassium channel blockers, caesium (Cs) and tetraethylammonium (TEA, 10mM) ions, incorporated into the patch pipette medium (Fig. 4.3B, top panel).

For the cell in Fig. 4.3B, depolarizing voltage steps applied from a holding potential of -86mV, produced a fast transient inward current, and a sustained inward current. Bath application of 1µM

Fig. 4.3 Voltage-gated membrane currents in isolated ganglion cells. The external solution was normal Ringer's, and patch pipettes contained the solutions indicated below.

A Depolarizing voltage pulses (upper panel) applied to an isolated ganglion cell, from a holding potential of -63mV, produced a rapid, transient inward current (visible only as a vertical line deflecting downwards on this time scale), which was activated between -40 and -30mV, and a slower transient outward current which activated above -35mV. Hyperpolarizing voltage pulses applied to the same cell, produced a small inward current. The patch pipette contained solution GI3 ($[Cl^-]$ = 3mM).

B Depolarizing voltage pulses applied to a different ganglion cell, from a holding potential of -86mV. Patch pipettes contained solution GI3 containing 10mM tetraethylammonium (TEA) and with potassium chloride replaced by caesium chloride to block any outward potassium current. This left a fast transient inward current, and a sustained inward current (top panel). Application of 1μM TTX (dissolved in Ringer's solution), blocked the fast inward current (a sodium current), to leave a sustained inward current (centre panel). Subsequent application of both TTX and the calcium channel blocker, cobalt (2mM), abolished this sustained current, leaving only a tiny residual current (lower panel).

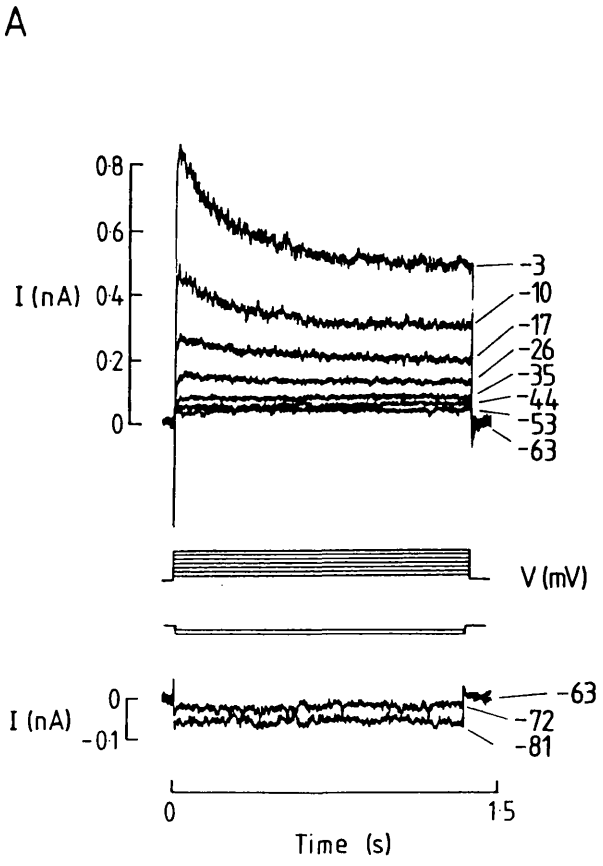
A
0·8
0·6
I (nA) 0·4
0·2
0
-3
-10
-17
-26
-35
-44
-53
-63
V (mV)
I (nA)
0
-0·1
-63
-72
-81
0
1·5
Time (s)

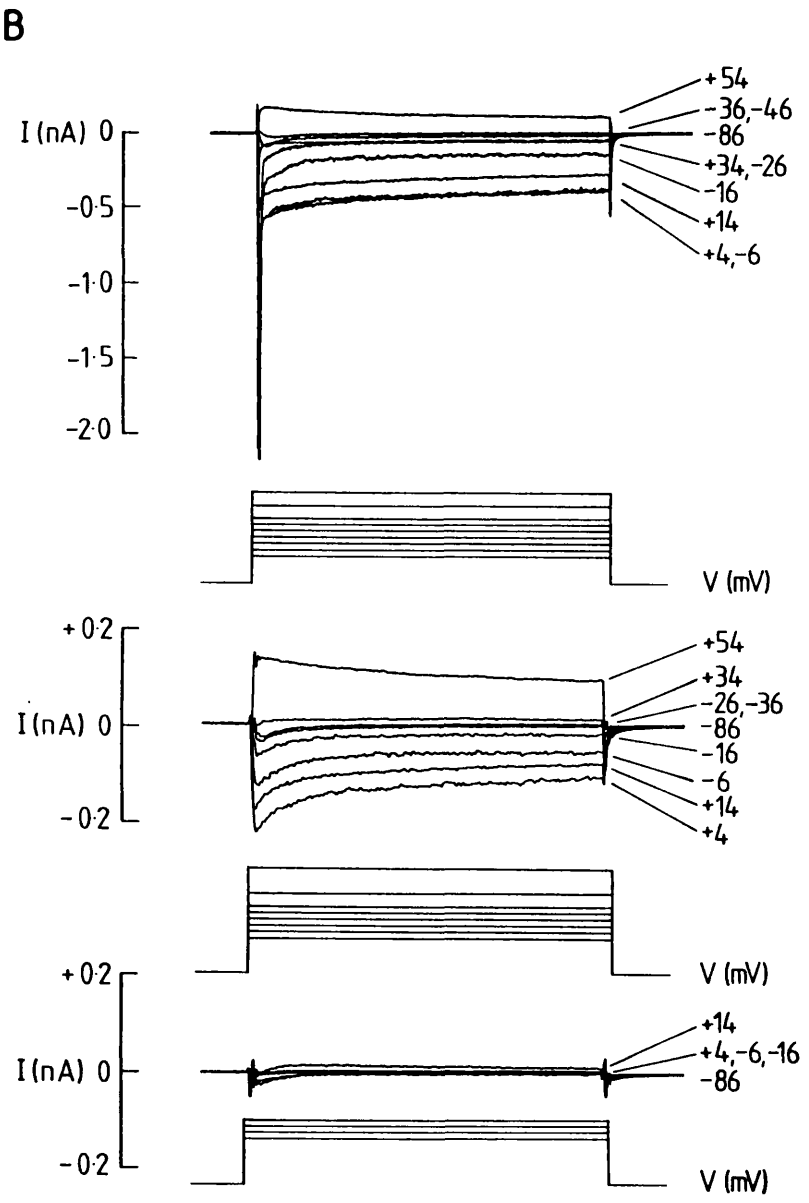
B
I (nA) 0
-0·5
-1·0
-1·5
-2·0
+54
-36,-46
-86
+34,-26
-16
+14
+4,-6
V (mV)
+0·2
I (nA) 0
-0·2
+54
+34
-26,-36
-86
-16
-6
+14
+4
V (mV)
+0·2
I (nA) 0
-0·2
+14
+4,-6,-16
-86
V (mV)

TTX (centre panel) abolished the rapid inward current component (n=10) which is presumably, therefore a sodium current, leaving a residual inward current (n=7). Subsequent bath application of both TTX and the calcium channel blocker, cobalt (2mM), reversibly abolished practically all of this residual inward current (lower panel), suggesting that this was a calcium current (n=6). Incorporation of 100μM leupeptin into the patch pipette (n=6) probably prevented partial "washout" of any calcium current present Leupeptin suppresses an irreversible component of calcium current washout (by inhibiting protease activity), but not a reversible component resulting from dephosphorylation of calcium channels (Chad and Eckert, 1986). The current which remains (lower panel, Fig. 4.3B) may represent residual unblocked voltage-gated currents, or it might in part be a leak current.

Isolated ganglion cells from rat have also been shown to have voltage-gated sodium, calcium and potassium channels, with properties similar to those described here for salamander ganglion cells (Lipton and Tauck, 1987). These authors have also shown that the potassium current is separable into three different components with, properties resembling a delayed outward rectifier, a transient outward current, and a calcium-activated potassium current.

4.3.5 Voltage-dependence and activation range of the sodium, potassium and calcium currents

The dependence on membrane potential of the peak sodium current (I_{Na}, lower curve) and the steady-state potassium current (I_K, upper curve), are plotted in Fig. 4.4A, for a different ganglion cell to that shown in Fig. 4.3. There was no caesium/TEA present in the patch pipette solution which was GI3 (3mM chloride).

Values for the peak I_{Na} at different potentials were obtained by computer subtraction of the currents produced in the presence of 1μM TTX, from currents obtained in the absence of TTX. Since TTX blocks I_{Na}, and since any calcium current present is probably much smaller than either the sodium or potassium current (compare sizes of I_{Na} and I_K in Fig. 4.4A with I_{Ca} in Fig 4.5A), the remaining current is likely to be mostly due to potassium. Thus, values for the steady-state I_K were estimated approximately by measuring the currents which remained in the presence of TTX.

Fig. 4.4 Voltage-dependence and activation range of the sodium and potassium currents in an isolated ganglion cell. The external solution was normal Ringer's (solution A, Table 2.1, Chapter 2), and the patch pipette contained solution GI3 ($[Cl^-]_i$=3mM) from Table 2.3 (Chapter 2).

A Current-voltage relation for the peak sodium current (lower curve) and steady-state potassium current (upper curve). Values for the peak sodium current were obtained by computer subtraction of currents produced by depolarizing voltage steps in the presence of TTX, from currents produced in the absence of TTX (section 4.3.5). The sodium current activated sharply over the range -35 to -20mV, with the largest inward current at about -22mV, and reversed at +51mV. The potassium current activated slowly from -50mV, and was always outward at potentials above this.

B Upper part, normalized potassium conductance, $g_K = I_K/(V-V_{rev})$, representing the fraction of channels activated (0 = no channels activated; 1 = all channels activated), plotted against voltage. The potassium current begins to be activated at -50mV, is 50% activated at -5mV, and fully activated at +40mV. Lower part, normalized sodium conductance, $g_{Na} = I_{Na}/(V-V_{rev})$, plotted against membrane potential. The sodium current activates sharply over the range -40 to -25mV. Both of these activation ranges are only approximations to the true curves, because of unavoidable voltage errors caused by series resistance in the patch pipette.

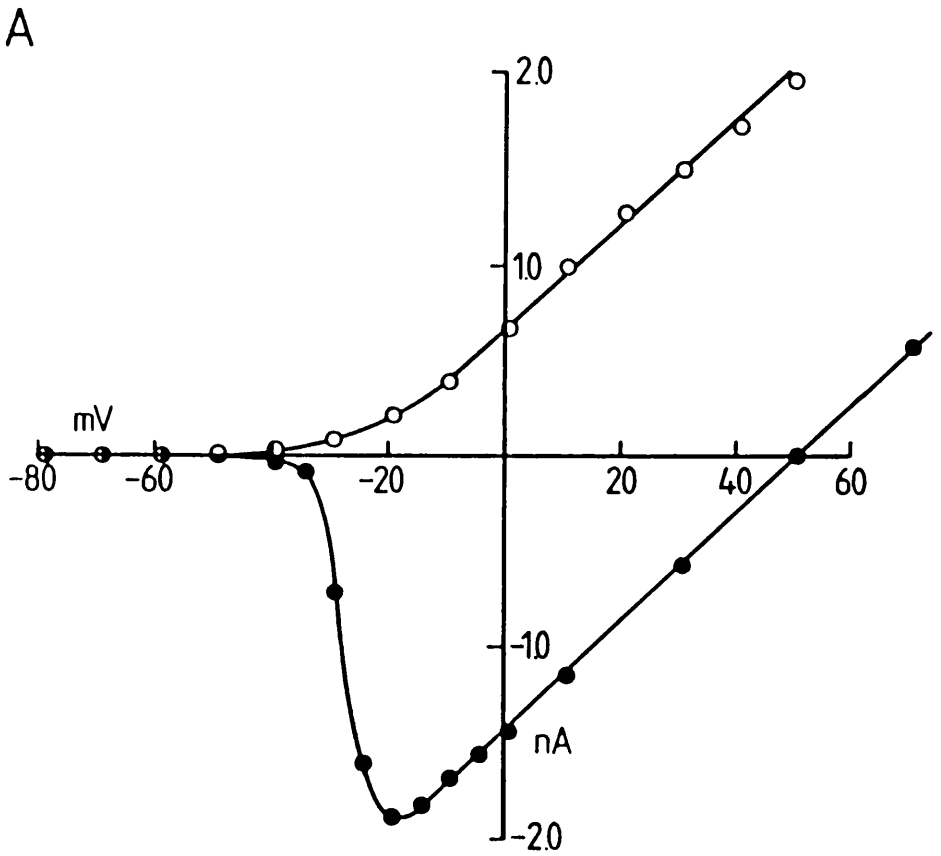
A
2.0
1.0
mV
-80
-60
-20
20
40
60
-1.0
nA
-2.0

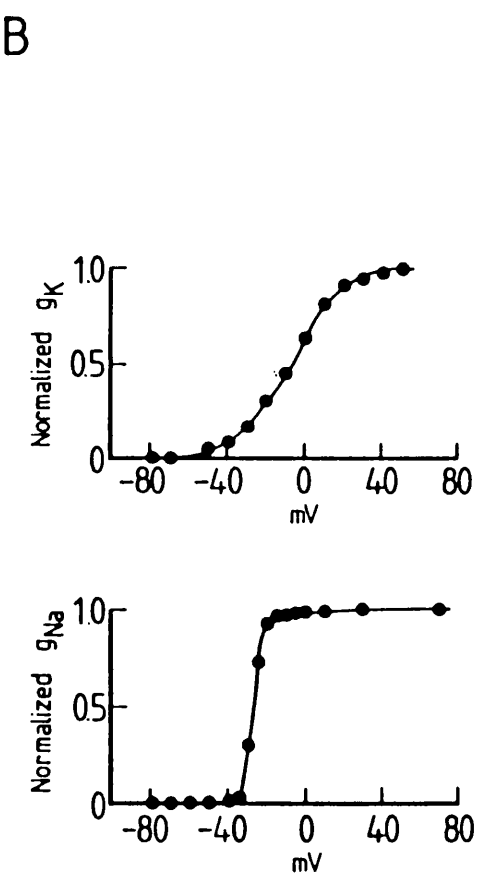
B
Normalized g_K
1.0
0.5
0
-80
-40
0
40
80
mV
Normalized g_{Na}
1.0
0.5
0
-80
-40
0
40
80
mV

The sodium current was sharply activated over the range -35 to -25mV. Fig. 4.4B (lower part) shows the normalized conductance, $g_{Na} = I_{Na}/(V-V_{rev})$, representing the fraction of channels activated over the range of voltages shown. For this cell, I_{Na} began to be activated at -40mV, was 50% activated at -25mV, and was practically fully activated at -20mV. The largest peak sodium current was nearly 2nA, at -22mV in this cell (Fig. 4.4A), and the current reversed at +51mV, close to that predicted by the Nernst equation, $E_{Na} = RT/F \log_{10} \{[Na]_o/[Na]_i\}$, of +59mV, with $[Na]_o$=107mM, and $[Na]_i$=10mM.

The voltage-dependence of the steady-state potassium current shows that I_K was activated relatively slowly over the range -50 to 0mV, and was always outward above -50mV. The fraction of potassium channels activated, given as the normalized conductance g_K = steady-state $I_K/(V-V_{rev})$, is plotted against membrane potential in the upper part of Fig. 4.4B. The potassium channels start to activate at just below -50mV, 50% are activated at -5mV, and all channels are only activated by depolarization to around +40mV. Compared to the rapid activation of sodium channels, potassium channel activation is slow, and in this cell, sodium and potassium channel activation ranges clearly overlap.

It should be noted that, because of the large size of the sodium and potassium currents, large voltage drops are produced across the pipette series resistance when these currents flow. For a typical series resistance of 19MΩ, a 1nA current will produce a 19mV voltage error. These errors must distort the shape of the activation curves (see section 7.4.3, Chapter 7, for further experiments).

Fig. 4.5 shows the voltage-dependence and activation range of the calcium current in Fig. 4.3B. Values for the peak calcium current (I_{Ca}) at different voltages were obtained by computer subtraction of the current which remains in the presence of TTX and cobalt (lower panel, Fig. 4.3B), from the residual inward current left after applying TTX alone (centre panel, Fig. 4.3B). The largest peak calcium current was about 200pA at +5mV, and the current reversed at +40mV.

The activation range of the calcium current is shown in Fig. 4.5B. The fraction of channels activated is given as the normalized

Fig. 4.5 Voltage-dependence and activation range of the calcium current in an isolated ganglion cell (for the data shown in Fig. 4.3B). The external solution was normal Ringer's (solution A, Table 2.1, Chapter 2), and the patch pipettes contained solution GI3 (Table 2.3, Chapter 2), with 10mM tetraethylammonium (TEA) added, and potassium chloride replaced by caesium chloride.

A Current-voltage relation for the peak calcium current (I_{Ca}), (obtained as described in section 4.3.5), shows that it activated over the range -70 to +5mV, with the largest inward current at +5mV. The current had a reversal potential of +35mV.

B Plot of fraction of channels activated (normalized conductance, $g_{Ca} = I_{Ca}/(V-V_{rev})$), against membrane potential, for the cell in **A**. 0 = no channels activated; 1 = all channels activated. Calcium channels started to activate slowly from -70mV, were 50% activated at -5mV, and all were fully activated at around +5mV.

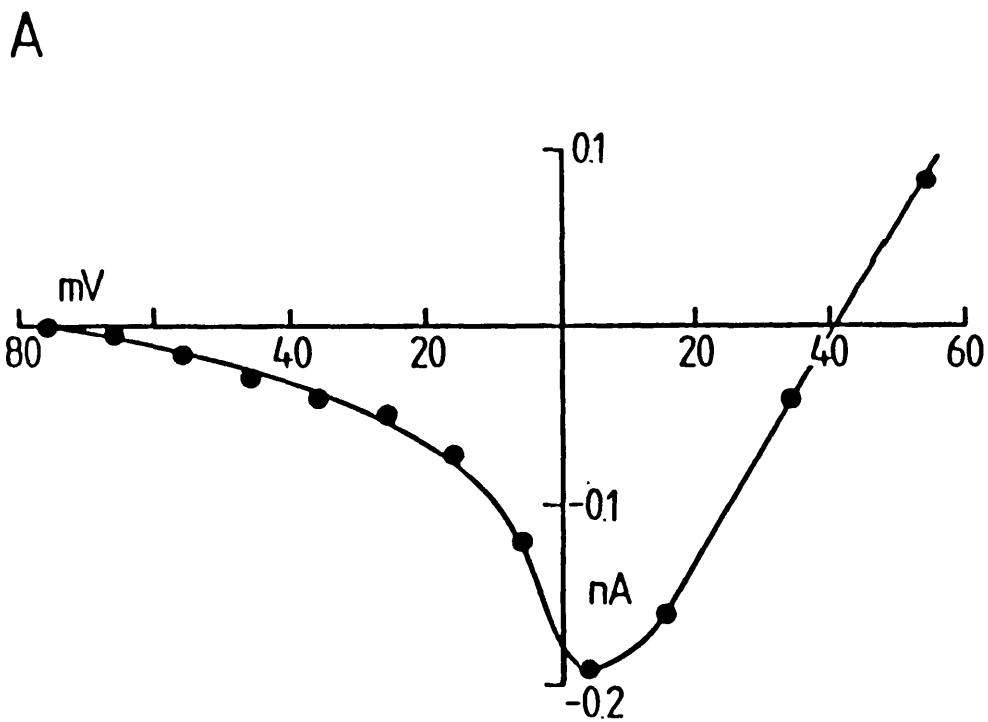
A
mV
80
40
20
20
40
60
0.1
-0.1
nA
-0.2

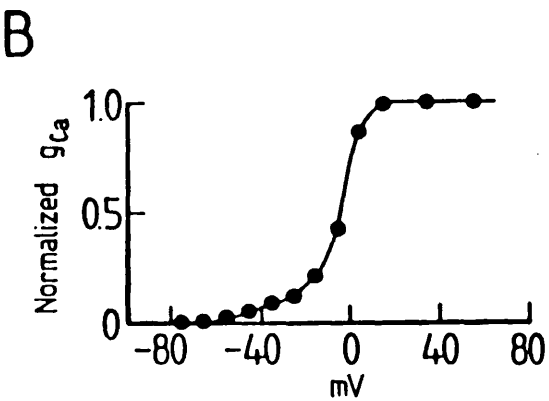
B
Normalized g_{Ca}
1.0
0.5
0
-80
-40
0
40
80
mV

conductance, $g_{Ca} = I_{Ca}/(V-V_{rev})$, and plotted against the voltage. The calcium current seemed to activate gradually from around -70mV, to 50% activation at -5mV, and then rapidly reached complete activation by further depolarization to +5mV.

Chapter 5

Properties of currents induced by excitatory amino acids in ganglion cells

5.1 Introduction

This chapter describes the effects of L-glutamate and its analogues, kainate, quisqualate (Quis), and N-methyl-D-aspartate (NMDA), on isolated ganglion cells. The results are used to address the questions raised in section 1.5.3 in Chapter 1. These questions are presented for discussion in section 7.5 (Chapter 7).

The results (in section 5.3 of this chapter) are divided into the following sections; (1) In isolated ganglion cells, L-glutamate evokes a current which has a linear voltage-dependence; (2) Noise changes associated with the glutamate-induced current; (3) Spatial localization of the glutamate response; (4) The pharmacology of the glutamate response (5) Voltage-dependence of the current induced by kainate; (6) Voltage-dependence of the current induced by quisqualate; (7) Voltage-dependence of the current induced by NMDA; (8) NMDA responses in isolated ganglion cells in the absence of extracellular magnesium; (9) Ganglion cells in the intact retina respond to NMDA; (10) Voltage-dependence of the current induced by NMDA in the intact retina.

5.2 Methods

All experiments were performed on isolated ganglion cells (section 2.5.5), except for those described in sections 5.3.9 and 5.3.10 on ganglion cells in the intact retina. In all experiments, cells were voltage-clamped and recordings were made using the whole-cell variant of the patch-clamp technique. The external solution was normal Ringer's (solution A, Table 2.1, Chapter 2). For bath perfusion of L-glutamate and its analogues, substances were dissolved in Ringer's solution A. Glutamate was often applied by iontophoresis (section 2.6.2, Chapter 2). Patch pipettes contained solution G3, containing 3mM chloride (Table 2.3, Chapter 2) unless otherwise indicated. This solution was used because it has been suggested that the internal chloride concentration of ganglion cells *in vivo* is low (Miller and Dacheux, 1983).

5.3 Results

5.3.1 In isolated ganglion cells, glutamate evokes a current which has a linear voltage-dependence

Application of glutamate by iontophoresis (Fig 5.1A, Fig. 5.2A) or by bath perfusion (Figs. 5.4 and 5.5) to isolated whole-cell patch-clamped ganglion cells, produced an inward current in 67% of cells (n=120) voltage-clamped to their resting potential of approximately -60mV. The current response varied in magnitude between 30 and 300pA at -60mV. Fig. 5.1A shows the currents induced by iontophoretic application of L-glutamate in an isolated ganglion cell voltage-clamped to various potentials (shown alongside each trace). The external solution was normal Ringer's and the patch pipette contained solution G3, containing 3mM chloride (Table 2.3, Chapter 2). The inward current produced by glutamate was larger at more negative potentials, reversed at about -6mV, and was outward at potentials positive to this.

The relation between the peak glutamate-induced current and voltage for the data in Fig. 5.1A, is plotted in Fig. 5.1B. The line drawn through the points (fitted by linear regression) has a slope conductance of 0.67nS, and a reversal potential of -7mV. For iontophoresis of glutamate, I-V relations (n=10) were generally linear (n=7) although outward rectification was seen in some ganglion cells (n=3). The average reversal potential for the glutamate-induced current produced by iontophoresis was -16 ± 8mV (mean$\pm$s.d.). Current-voltage relations were also obtained for glutamate applied by bath perfusion at a concentration of 100μM (n=5). The current-voltage relation was linear in four cells, and showed outward rectification in one cell. The average reversal potential for the current induced by bath applied 100μM glutamate was -16 ± 9mV (mean$\pm$s.d.) with an average slope conductance ($\pm$s.d.) of 2.4 ± 1.4nS (n=10). Typically, the average conductance of isolated ganglion cells in the absence of glutamate was around 1.2 ± 1.1nS, near the resting potential, for cells with a resting potential within the range -55 to -75mV (n=17; see sections 4.3.2 and 4.3.3, Chapter 4). Thus, glutamate significantly increases the cell conductance and *in vivo* glutamate released from bipolar cells might be expected to significantly alter the ganglion cell potential.

Fig. 5.1 The voltage-dependence of currents induced by glutamate applied by iontophoresis in an isolated ganglion cell. The external solution was normal Ringer's (solution A, Table 2.1). The patch pipette contained solution G3 (3mM chloride; Table 2.3, Chapter 2). This low concentration of chloride in the patch pipette was used because it is suggested that the internal chloride concentration of ganglion cells in vivo is low (Miller and Dacheux, 1983).

A Glutamate-induced currents in an isolated ganglion cell voltage-clamped to the potentials shown alongside each trace. Timing of glutamate iontophoresis is shown by the square trace immediately below the current data. The currents evoked by glutamate were clearly inward below -15mV, and outward above -6mV.

B Current-voltage relation for the glutamate-induced currents in **A**. Peak glutamate-induced currents were plotted as a function of membrane potential. The reversal potential of the current response was -7mV. (correlation coeff. = 0.993)
(x-intercept at y = 0 = -7.5; y-intercept at x=0 = 4.9.)

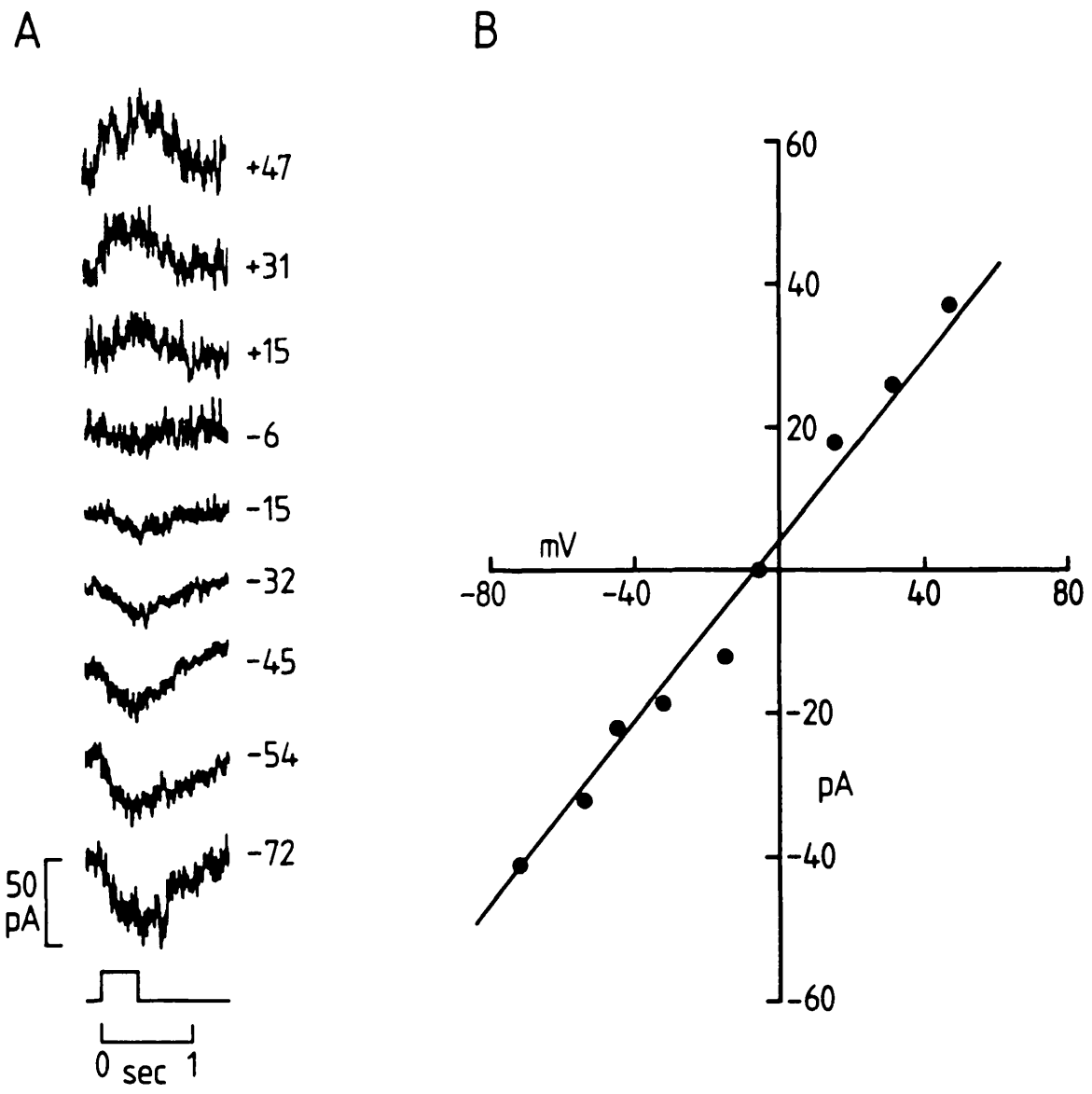
A
+47
+31
+15
-6
-15
-32
-45
-54
-72
50
pA
0 sec 1
B
60
40
20
mV
-80
-40
40
80
-20
pA
-40
-60

5.3.2 Noise changes associated with the glutamate-induced current

Analysis of the noise associated with the current evoked by glutamate reveals some information about the properties of the channels gated by glutamate.

Fig. 5.2A (upper trace) shows the inward current response to iontophoretically applied glutamate in an isolated ganglion cell held at -60mV. The external solution was normal Ringer's and the patch pipette contained G3 (3mM chloride). The lower, high pass filtered trace shows that there is an increase in current fluctuations (noise) associated with the change in current produced by glutamate. The current noise is presumably due to glutamate opening ion channels in the membrane. Part B of Fig. 5.2 shows that glutamate induces a substantial increase in the variance of the membrane current noise (from almost nothing to about $70pA^2$). Fig. 5.2C shows the variance of the glutamate-induced current noise changes (in the range 4-1000Hz) as a function of the mean glutamate-induced current flowing. The relationship between the noise variance and the mean current flowing is approximately linear, implying that the probability of channel opening is low (Colquhoun and Hawkes, 1977). Making the assumption that there is only one type of glutamate-gated channel present, having only one open state, the current flowing through a single channel opened by glutamate can be calculated from the ratio of the variance to the mean current flowing, i.e. from the slope of the line plotted through the points. This gives a single channel current of -0.26pA and hence a single channel conductance of 5.6pS (with "lost variance" at >1000Hz and <4Hz taken into account by extrapolating a sum of two Lorentzians fitted to the power spectrum of the glutamate-induced noise). However, in practice, there are complications in interpreting the data in this way. Glutamate may in fact, activate a channel which has different subconductance states (Cull-Candy and Usowicz, 1987; Jahr and Stevens, 1987), or there may be more than one type of channel activated by glutamate. For example, these ganglion cells may have glutamate-gated channels selectively activated by glutamate analogues, kainate, quisqualate and NMDA. Noise variance produced by opening and closing of channels, does so with a certain rate around a mean frequency. The net power spectrum of current noise for this cell (i.e. the

Fig. 5.2 Noise changes associated with the glutamate-induced current.

A Upper trace shows the inward current (low pass filtered at 1000Hz) produced by prolonged iontophoretic application of glutamate in an isolated ganglion cell, voltage-clamped to -60mV. The external solution was normal Ringer's (solution A, Table 2.1, Chapter 2) and the patch pipette contained solution G3 (3mM chloride; Table 2.3, Chapter 2). The lower trace shows the trace in **A** on a larger scale, high pass filtered (4Hz), to reveal an increase in the magnitude of current fluctuations (noise) associated with the inward current produced by glutamate.

B Upper trace shows the same data as in **A** (top trace). The lower trace shows the increase in the variance (pA^2) of the glutamate-induced current noise (between 4 and 1000Hz) as a function of time.

C Plot to show the variance change associated with the mean glutamate-evoked current flowing (frequency range as in **B**). The line was calculated by linear regression from stretches of data during glutamate application, and during control periods before and after glutamate application, and has a slope of 0.26pA. This represents an estimate of the magnitude of the current flowing through a single glutamate-gated channel (but see text, section 5.3.2).

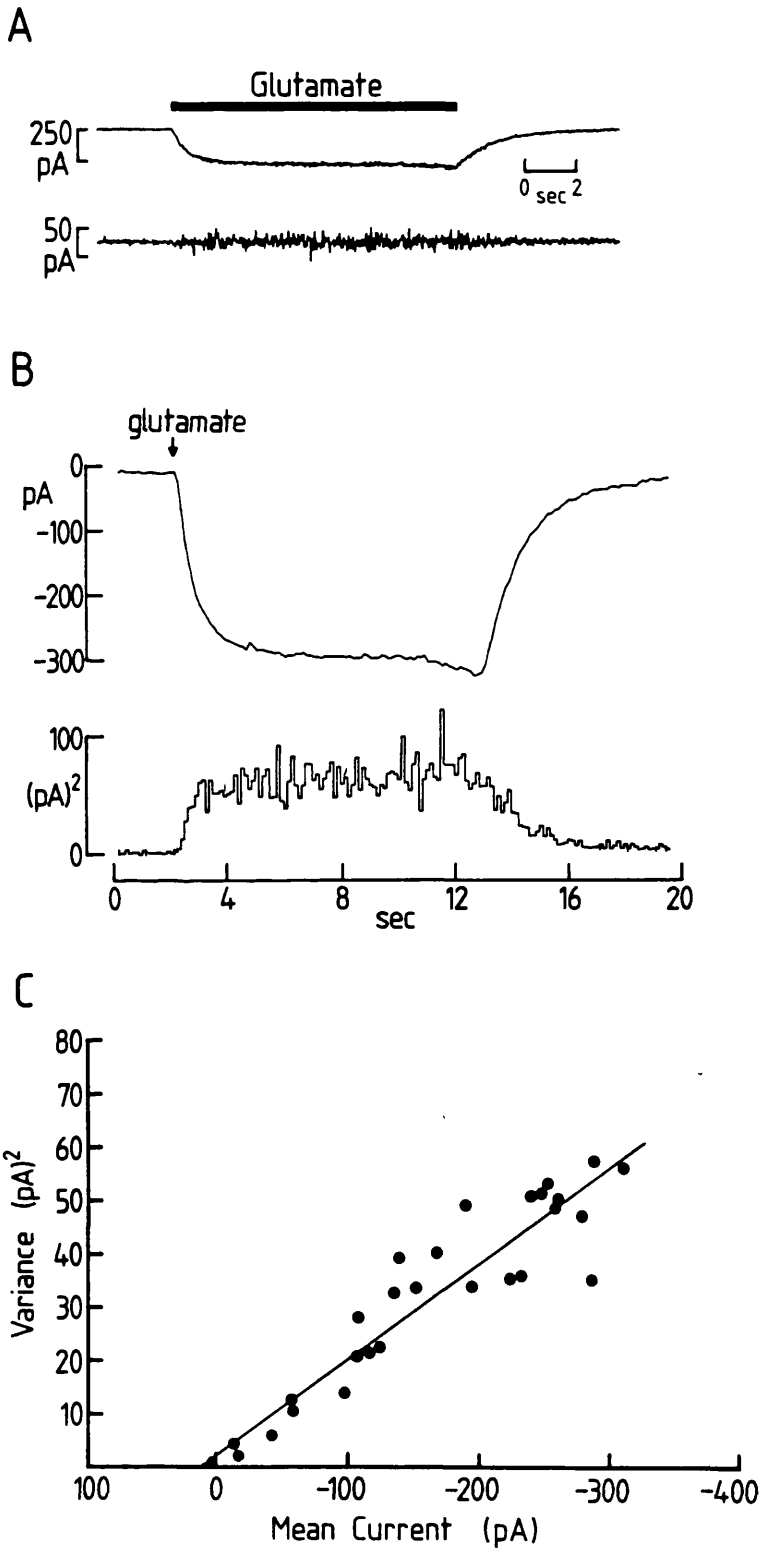
A
Glutamate
250 pA
0 sec 2
50 pA
B
glutamate
0
pA
-100
-200
-300
100
(pA)²
0
0
4
8
12
16
20
sec
C
80
70
60
50
40
30
20
10
Variance (pA)²
100
0
-100
-200
-300
-400
Mean Current (pA)

difference between the spectrum of noise evoked by application of glutamate and the control spectrum) was fitted with the sum of two Lorentzians with half power frequencies of 10 and 200Hz. These frequency values can be used to obtain estimates of the rates of opening and closing of channels and the mean channel open and closed times.

5.3.3 Spatial localization of the glutamate response

To investigate whether the response to glutamate was localized to certain regions of the ganglion cell membrane, glutamate was applied by iontophoresis to different membrane regions of isolated ganglion cells (n=2), as indicated in Fig. 5.3B. Cells were voltage-clamped to -60mV, and the external solution was normal Ringer's which was flowing continuously across the cell in Fig. 5.3B, from left to right. The patch pipette contained solution G42 ($[Cl^-]_i$=42mM, Table 2.3, Chapter 2). There was some difficulty in measuring the response to glutamate at distal dendritic regions, due to visible movement of the dendrites as the Ringer's solution flowed past. However, attempts to overcome this were made by positioning the iontophoretic electrode as close as possible to the site under investigation, with continual observation of the cell during glutamate application to ensure that dendrite movement was not too extensive. Despite this problem, Fig. 5.3A shows that the response to glutamate is largest (approximately 50pA) and fastest in onset at dendrites furthest from the cell body. Each current trace shown is an average of 5 responses. The glutamate-induced current became smaller and slower in onset as the iontophoretic electrode was repositioned nearer to the cell body. Iontophoresis of glutamate at the axon produced the smallest response (8-10pA). The responses disappeared when the iontophoretic pipette was moved laterally (approximately 50μm) away from the whole cell.

Fig. 5.3C shows the currents from Fig. 5.3A normalized to the maximum response at the distal dendrites, measured 30msec after the start of iontophoresis and plotted against membrane region. This short latency was chosen to minimize the distance that glutamate diffuses from the site of application. In 30msec, glutamate will have diffused only about 8μm from the tip of the iontophoretic electrode (calculated from the diffusion equation, $x^2=2Dt$, with diffusion coefficient, $D=10^{-9}m^2s^{-1}$; see section 3.3.5, Chapter 3).

Fig. 5.3 Spatial localization of the glutamate-induced current in isolated ganglion cells.

A Glutamate-evoked currents in response to iontophoresis, in an isolated ganglion cell voltage-clamped to -60mV, for each of the five positions indicated in **B**. Each trace is an average of five responses. The patch pipette contained solution G42 (42mM chloride; Table 2.3, Chapter 2), and the external solution was normal Ringer's (solution A, Table 2.1). The direction of flow of Ringer's solution was across the cell from left to right. The timing of iontophoresis is shown by the square trace immediately below the current data. Response amplitudes were measured 30msec (dotted line) after the onset of glutamate iontophoresis, and normalized to the maximum after this time for **C** (see below).

B Diagram to show the relative positions of the iontophoretic electrode around the ganglion cell membrane for the experiment in **A**. The total length of the ganglion cell is about 200μm, and the cell proportions are approximately correct.

C Glutamate response amplitudes at each of the cell membrane regions indicated in **B**, measured 30msec after the start of iontophoresis, and normalized to the maximum (at the distal dendrites) after this latency. The glutamate-evoked current is largest at the distal dendrite region, and has its fastest onset at that region (see **A**), implying that the receptors for glutamate are localized to this dendrite region.

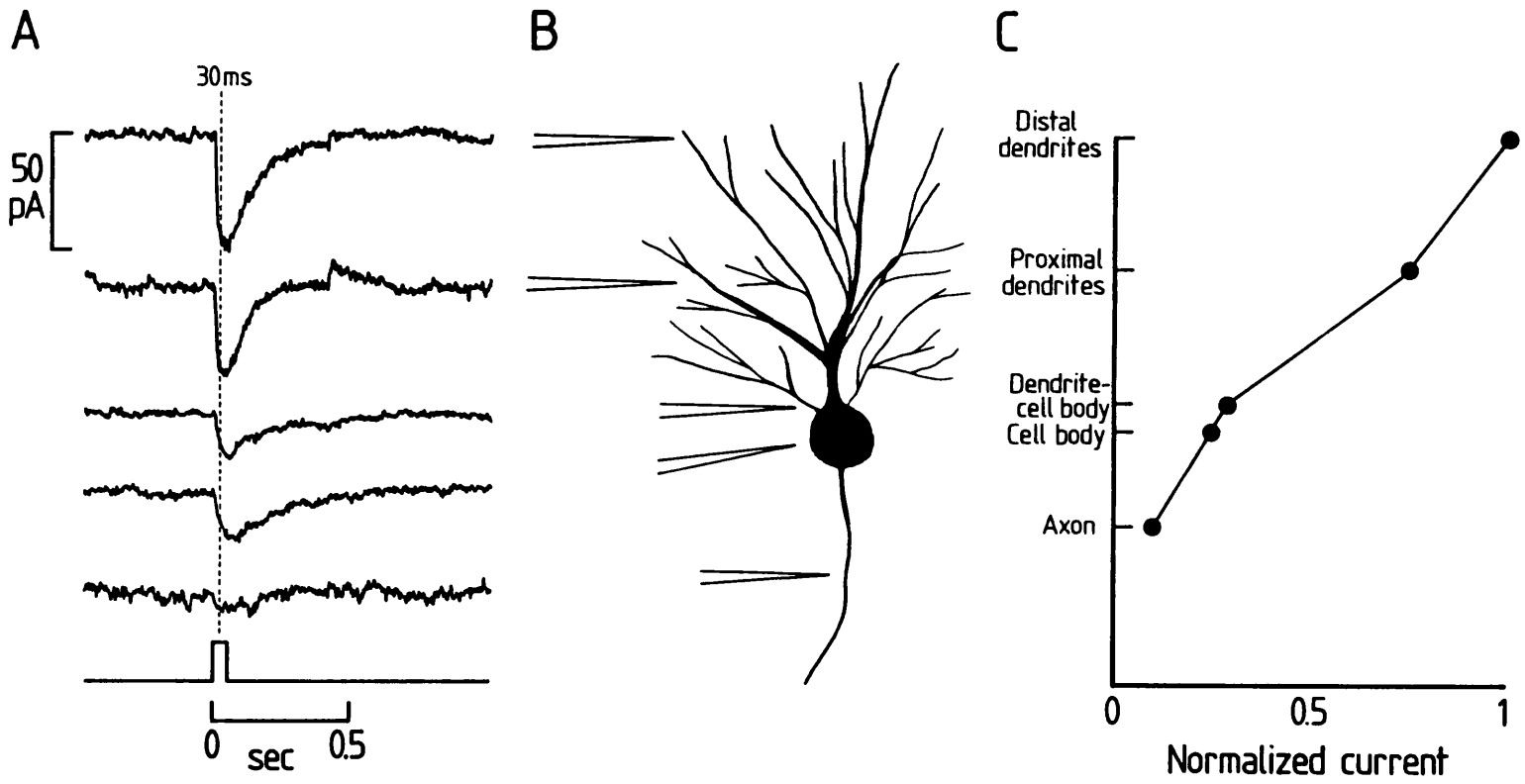
A
30ms
50
pA
0
sec
0.5
B
C
Distal
dendrites
Proximal
dendrites
Dendrite-
cell body
Cell body
Axon
0
0.5
1
Normalized current

This can be compared to the total length of the cell in Fig. 5.3B (including axon and dendrites), which was approximately 200μm. Thus, the response to glutamate measured after this short latency seems to be largest at distal dendrites.

The data suggest that the receptors for glutamate are localized to the distal regions of the ganglion cell dendrites, since the response to glutamate has its fastest onset at this region. This implies that the receptors are localized in the appropriate position for receiving neurotransmitter glutamate released from bipolar cell axons. It is worth noting that, although detailed mapping of the glutamate response was carried out in only 2 cells, isolated ganglion cells having just one or two dendrites responded to glutamate, and those without dendrites, but with an axon, did not respond to glutamate.

5.3.4 The pharmacology of the glutamate response

Fig. 5.4 shows the current responses in an isolated ganglion cell, voltage-clamped to -40mV, to bath applied L-glutamate and L-aspartate, and their stereoisomers D-glutamate and D-aspartate, at a concentration of 100μM. The external solution was normal Ringer's and the patch pipette contained solution G42 (42mM chloride; Table 2.3, Chapter 2).

This cell produced a small inward current (20pA) in response to L-glutamate at this potential, and also responded to L-aspartate with an inward current of about the same magnitude. There was little or no response to D-glutamate or D-aspartate. Out of 12 cells tested, all responded to L-glutamate, sometimes with currents as large as 200pA at -40mV. However, only four of these responded to L-aspartate, and no convincing currents were seen in response to D-glutamate or D-aspartate. For all cells, L-glutamate and analogues were each applied several times to the same cell.

In other preparations, for example spinal cord, it has been shown that responses to L-aspartate and D-aspartate are moderately sensitive, and responses to D-glutamate very sensitive, to N-methyl-D-aspartate (NMDA) channel blockers, much more so than are responses to L-glutamate (Watkins and Evans, 1981). This suggests that these glutamate analogues may generate a current by activating NMDA receptors. The presence of magnesium (0.5mM) in the external

Fig. 5.4 Currents induced by L-glutamate and glutamate analogues D-glutamate, L-aspartate and D-aspartate. The external solution was normal Ringer's (solution A, Table 2.1). The patch pipette contained solution G3 (3mM chloride; Table 2.3, Chapter 2).
In this cell, which was voltage-clamped to -40mV, bath applied L-glutamate and L-aspartate at a concentration of 100μM, produced small inward current responses of about 20pA. D-glutamate and D-aspartate (100μM) produced no convincing current responses in this cell.

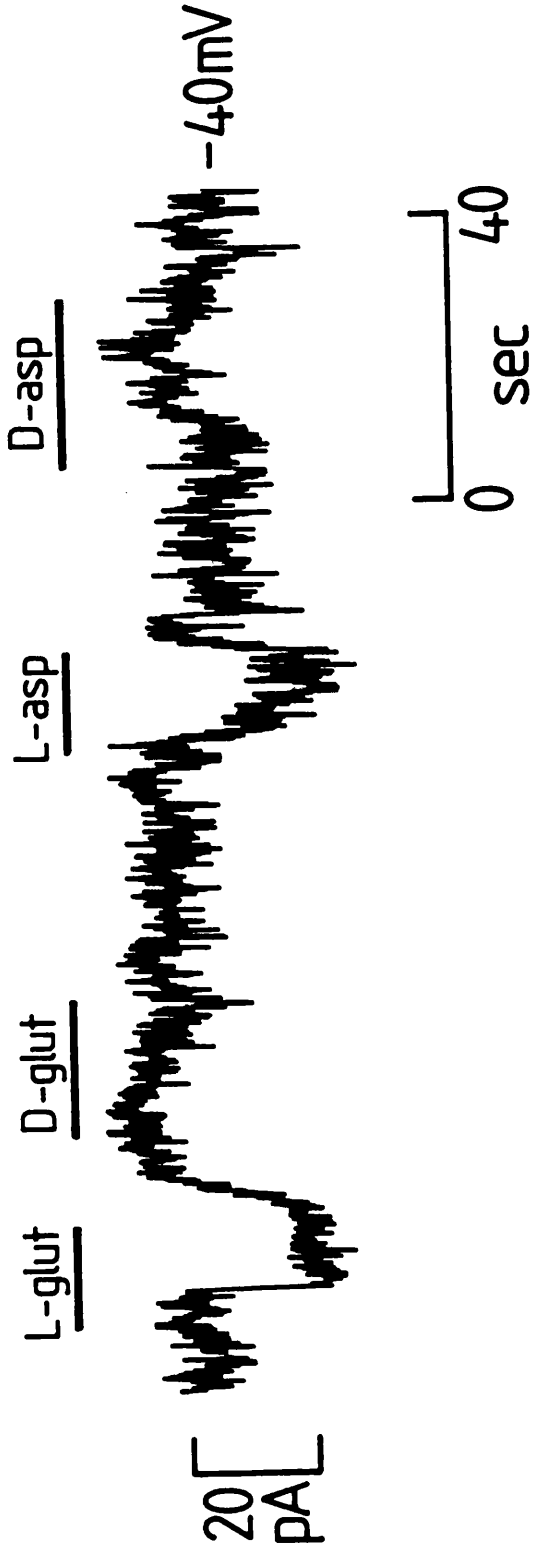
L-glut
D-glut
L-asp
D-asp
-40mV
20 pA
0 sec 40

Ringer's solution may prevent NMDA channel activation by these glutamate analogues, and hence may explain the lack of current responses observed to application of D-aspartate and D-glutamate.

To examine the pharmacology of the glutamate response in more detail, in a different set of experiments the glutamate analogues kainate, quisqualate (Quis) and N-methyl-D-aspartate (NMDA), were applied by bath perfusion to isolated ganglion cells, voltage-clamped to around their resting potential (Fig. 5.5). Substances were dissolved in normal Ringer's which contained 0.5mM magnesium. Patch pipettes contained solution G3 (3mM chloride; Table 2.3, Chapter 2). Fig. 5.5A shows the responses of an isolated ganglion cell held at -60mV, responding to glutamate and its analogues, bath applied at a concentration of 10μM. This cell responded to kainate with a non-desensitizing inward current, and to quisqualate with an apparently rapidly desensitizing current response. Not all cells responded to 10μM quisqualate with a current that had a desensitizing component (but this early component may only be seen in cells for which the solution perfusion rate was high). This cell did not respond to NMDA. Six out of twelve cells tested showed an inward current (at -60mV) in response to bath application of 10μM glutamate. The same 6 cells responded both to kainate and quisqualate, but only one of these cells showed a small response to NMDA. At this concentration, the currents produced by L-glutamate, kainate, quisqualate and NMDA had relative magnitudes 0.26:1:0.75:0.03 (mean data from 6 cells).

In a different cell to that shown in A, bath application of a higher concentration (100μM) of glutamate and glutamate analogues produced the current responses shown in Fig. 5.5B. The responses to glutamate, quisqualate and kainate were usually non-desensitizing, although in this cell current responses to these agonists may show slow desensitization with time (the sag may also be due to run down of the currents). There was a small response to NMDA in this cell. Out of 14 cells recorded from, all responded to glutamate and kainate, and 13 responded to quisqualate with an inward current at this voltage. Only two cells responded to NMDA with a small inward current of 10-15pA. At this concentration, the currents produced at -60mV by L-glutamate, kainate, quisqualate and NMDA had relative magnitudes 0.15:1:0.16:0.005 (mean data from 14 cells tried).

Fig. 5.5 Current responses to glutamate and the analogues kainate, quisqualate and N-methyl-D-aspartate (NMDA) in isolated ganglion cells. Glutamate and analogues were dissolved in normal Ringer's (solution A, Table 2.1) to give a concentration of 10μM in **A** and 100μM in **B**. The patch pipettes contained solution G3 (3mM chloride; Table 2.3, Chapter 2).

A Isolated ganglion cell voltage-clamped to -60mV, responding to 10μM glutamate, kainate, quisqualate and NMDA applied by bath perfusion. The response to kainate was larger than that to glutamate or quisqualate, and there was no detectable response to NMDA in this cell. Responses to glutamate and kainate were non-desensitizing for the duration of application as indicated by the bars above each current trace. The response to quisqualate seems to show early desensitization (see section 5.3.4).

B A different isolated ganglion cell to that shown in **A**, voltage-clamped to -60mV, responding to glutamate (glut), kainate, quisqualate (quis) and NMDA, bath applied at a concentration of 100μM. The response to kainate was largest, as in **A** above, however, this concentration of glutamate, kainate and quisqualate produced currents which showed slight desensitization during the period of application as indicated by the bars above each current trace. There was a small detectable current response to NMDA.

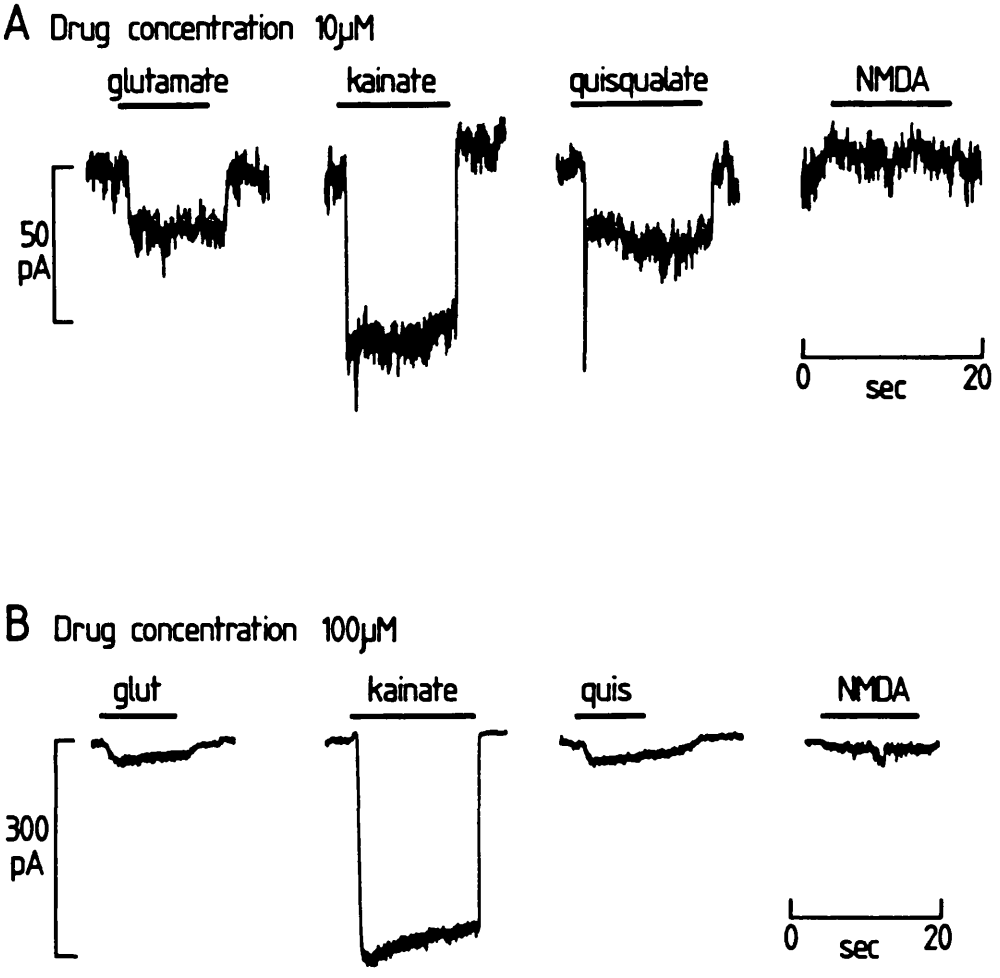
A Drug concentration 10μM
glutamate
kainate
quisqualate
NMDA
50
pA
0
sec
20
B Drug concentration 100μM
glut
kainate
quis
NMDA
300
pA
0
sec
20

Thus, for both low (10μM) and high doses (100μM) of glutamate and glutamate analogues, the largest average response was always produced by kainate, so it seems likely that most of the receptors for glutamate in these ganglion cells are kainate-sensitive.

Only three out of 24 cells tried showed any response to NMDA. The frequency with which NMDA responses were detected was not increased even when NMDA was applied to cells voltage-clamped to very positive potentials (+70mV) to alleviate the voltage-dependent open channel block which is thought to be produced at negative potentials by the magnesium present in the external solution (Nowak et al., 1984). In a different set of experiments, NMDA (100μM) was applied to isolated ganglion cells after magnesium was removed from the extracellular solution (n=5). Responses to NMDA were detected in three of these cells (see section 5.3.8). However, subsequent experiments in which 100μM NMDA was perfused onto voltage-clamped ganglion cells in the intact retinal flatmount (section 2.5.4, Chapter 2) in the absence of external magnesium (n=5), showed that all cells recorded from responded to NMDA, with currents ranging from -60 to -90pA at a negative holding potential of -60mV (see section 5.3.9).

This suggests that the lack of NMDA responses detected in isolated cells might have been due largely to enzymatic degradation of NMDA receptors during dissociation of the cells, or to loss of cell processes containing receptors for NMDA. Dissociating retinae with trypsin instead of papain did not increase the frequency with which NMDA responses were detected (n=3).

5.3.5 Voltage-dependence of the current induced by kainate

Fig. 5.6A (top trace) shows the inward current evoked in an isolated ganglion cell voltage-clamped to -80mV, in response to bath-applied 100μM kainate. Kainate was dissolved in normal Ringer's and the patch pipette contained solution G3 (3mM chloride; Table 2.3, Chapter 2). In this cell, the response to kainate was non-desensitizing, but in other cells perfusion of 100μM kainate for a similar period of time seemed to produce a slowly desensitizing current response (see Fig. 5.5B). The response to glutamate in the same cell is shown in the lower trace for comparison.

Fig. 5.6B shows the current-voltage (I-V) relation for kainate

Fig. 5.6 Voltage-dependence of the kainate-induced current. External solution was normal Ringer's (solution A, Table 2.1) and the patch pipette contained G3 (3mM chloride; Table 2.3, Chapter 2).

A Top trace shows an isolated ganglion cell held at -80mV, responding with a large inward current to 100μM kainate (dissolved in normal Ringer's) applied by bath perfusion. Bottom trace shows the response to bath applied 100μM glutamate in the same cell.

B Current-voltage (I-V) relation in kainate for the cell in **A**. Peak kainate-induced currents are plotted against voltage. The kainate-induced I-V relation was obtained by subtracting a control ramped I-V relation in Ringer's solution alone, from a ramped I-V in the presence of kainate. In this cell, the reversal potential of the current was -3mV. (correlation coeff. = 0·998; (x-intercept at $y=0$ = −2·52; y-int. at $x=0$ = 7·84)

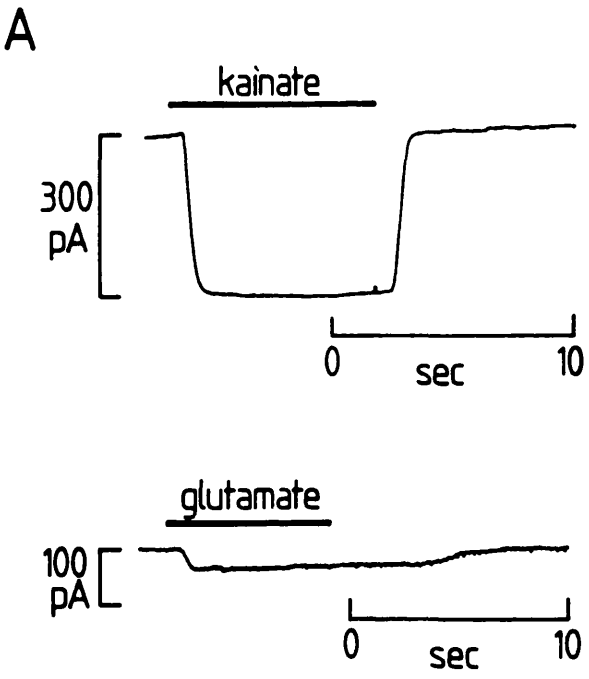
A
kainate
300
pA
0
sec
10
glutamate
100
pA
0
sec
10

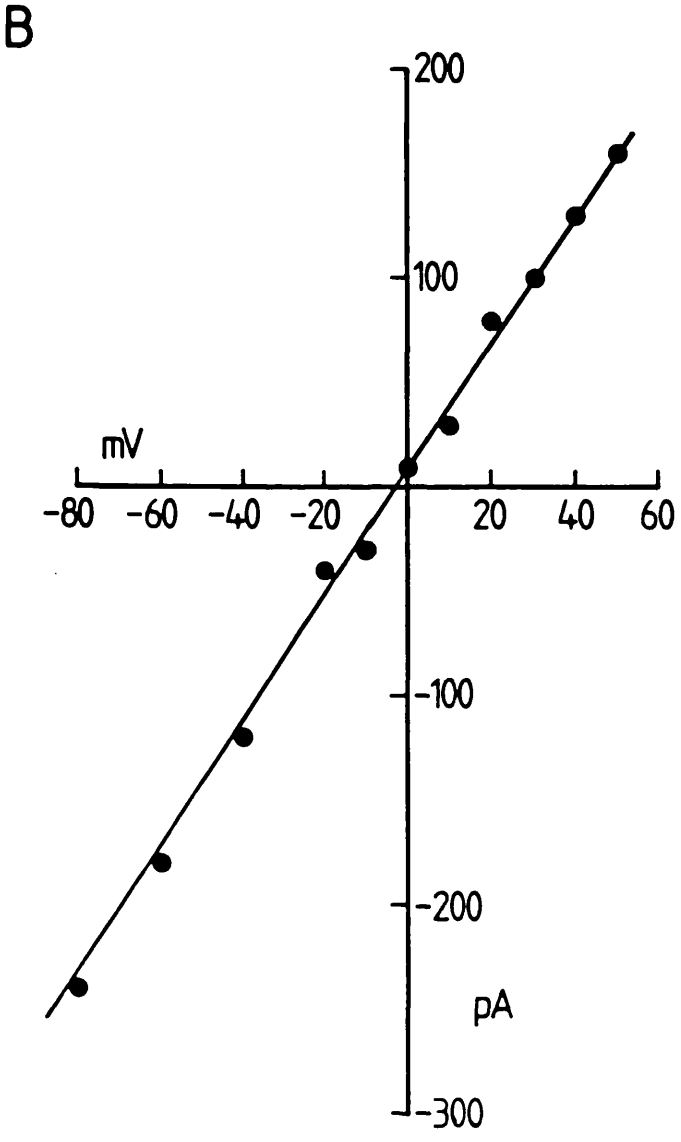
B
200
100
mV
-80
-60
-40
-20
20
40
60
-100
-200
pA
-300

in this cell. This was obtained by subtracting a control ramped I-V relation in Ringer's solution alone, from a ramped I-V in the presence of kainate. A subsequent ramped I-V, obtained on reflowing Ringer's solution alone, superimposed on the control I-V relation, showing that the effect of kainate was fully reversible. Application of kainate at -80mV produced a large inward current of 300pA. The kainate-induced current was smaller, but still inward, at less negative potentials, reversed at around -3mV, and was outward at potentials positive to this. The I-V relation was linear, with the line drawn through the points fitted by linear regression having a slope conductance of 3.09nS. The reversal potentials for the current induced by kainate in the two cells were -3mV and -12mV, similar to those found for the glutamate-induced current (section 5.3.1 above). This method of producing I-V relations is not the most accurate, since ramping the voltage is likely to activate voltage-gated time-dependent currents in the ganglion cell membrane so the I-V relation produced will depend critically on the speed of the voltage ramp. However, it gives a reasonable indication of the way in which the drug-induced current depends on voltage. In section 5.3.10 of this chapter, I-V relations for the NMDA-induced current in ganglion cells in the intact retina were obtained by this method and by a more reliable method, in which the drug was perfused onto the cell held at several different potentials. The current-voltage relations obtained were almost identical.

5.3.6 Voltage-dependence of the current induced by quisqualate

Current-voltage (I-V) relations (n=2) for the maintained quisqualate-induced current (data not shown) in isolated ganglion cells responding to quisqualate with an initial desensitizing phase, were obtained as described for the kainate-induced current (section 5.3.5). Patch pipettes contained solution G3 (3mM chloride, Table 2.3, Chapter 2). The magnitude of the inward current (10pA) produced increased as the cell was voltage-clamped to more negative potentials. The I-V relations were linear over the potential range studied (-110 to -30mV), and linear regression lines were fitted to the points, and extrapolated, to obtain the reversal potential of the response. The reversal potentials for the

maintained component of the quisqualate-induced currents in the two cells were -23mV and -24mV.

5.3.7 Voltage-dependence of the current induced by N-methyl-D-aspartate (NMDA)

Fig. 5.7A (top trace) shows the inward current (15pA) in response to bath applied 100μM N-methyl-D-aspartate, in an isolated ganglion cell voltage-clamped to -60mV. The external solution was normal Ringer's containing 0.5mM magnesium, and the patch pipette contained solution G3 (3mM chloride; Table 2.3, Chapter 2). The response to NMDA at this dose is non-desensitizing. The response to bath applied glutamate in the same cell, at a concentration of 100μM, is shown for comparison in the lower trace.

The current-voltage (I-V) relation in the presence of extracellular magnesium (0.5mM in normal Ringer's) for the cell in A, is shown in Fig. 5.7B. The method used to obtain the I-V was that described for kainate (section 5.3.5) and quisqualate (section 5.3.6). Inward currents in response to 100μM NMDA were very small (15pA) over the negative potential range -90 to -30mV. The reversal potential for the response was -25mV, and currents become outward at potentials positive to this. The outward rectification observed for this cell in the presence of external magnesium could be due to a voltage-dependent open channel block by magnesium ions.

5.3.8 NMDA responses in isolated ganglion cells in the absence of extracellular magnesium

In section 5.3.4, application of 100μM NMDA to isolated ganglion cells voltage-clamped to -60mV produced a detectable inward current in only two out of 14 cells tried. In another set of experiments, in the absence of external magnesium (Fig. 5.8), 3 out of 5 cells responded to NMDA with an inward current at -60mV.

Fig 5.8A shows an isolated ganglion cell responding to glutamate in the presence of 1mM external magnesium, with an inward current of nearly 400pA at a holding potential of -61mV (left hand trace). When held at -50mV, application of NMDA in the absence of external magnesium, produced an inward current of 50pA (right hand trace). Application of NMDA in the presence of 1mM external magnesium produced no detectable response in all cells tested (n=5).

Fig. 5.7 Voltage-dependence of the current induced by NMDA. The external solution was normal Ringer's (solution A, Table 2.1) containing 0.5mM magnesium. Solution G3 (3mM chloride; Table 2.3, Chapter 2) was used to fill the patch pipette.

A An isolated ganglion cell voltage-clamped to -60mV, responding with an inward current to bath applied 100μM NMDA (top trace) and glutamate (lower trace). The period of application is shown by the bars. The response to both NMDA and glutamate is non-desensitizing at this dose.

B Current-voltage relation for the current induced by NMDA for the cell in **A**, obtained by subtracting ramped I-V relations in the presence and absence of NMDA. The current-voltage relation shows considerable outward rectification, and the reversal potential for the NMDA-induced current was -25mV.

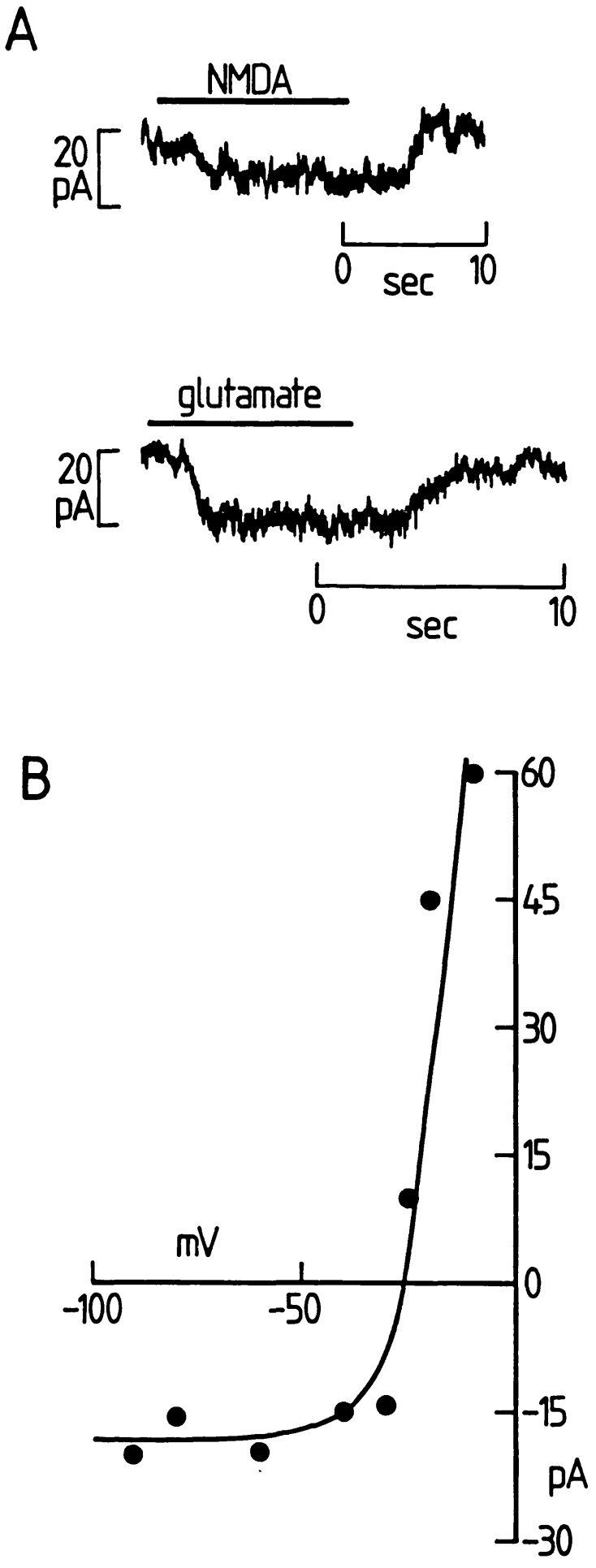
A
NMDA
20
pA
0
sec
10
glutamate
20
pA
0
sec
10
B
60
45
30
15
mV
0
-100
-50
-15
pA
-30

Fig. 5.8 Current responses to NMDA in the absence of external magnesium. External solution was based on normal Ringer's (solution A, Table 2.1) and contained either 1mM magnesium or zero magnesium. Substances were applied by bath perfusion, dissolved in Ringer's solution. Patch pipettes contained solution G3 (3mM chloride; Table 2.3, Chapter 2).

A An isolated ganglion cell voltage-clamped to the potentials shown alongside each current trace, shown responding to bath applied 100μM glutamate in normal Ringer's, and to 100μM NMDA, in the absence of external magnesium. The concentration of external magnesium is shown in the top trace. Glutamate produced an inward current of nearly 400pA at -61mV (left hand trace), and NMDA induced a current of about 50pA at -50mV (right hand trace).

C An isolated ganglion cell voltage-clamped to -60mV, shown responding to 100μM glutamate alone (left hand trace), and to the same concentration of glutamate, coapplied with 1μM glycine. The external solution contained zero magnesium. The response to glutamate in this cell was small (20pA), and glycine, at this concentration had no effect on the magnitude of the glutamate response.

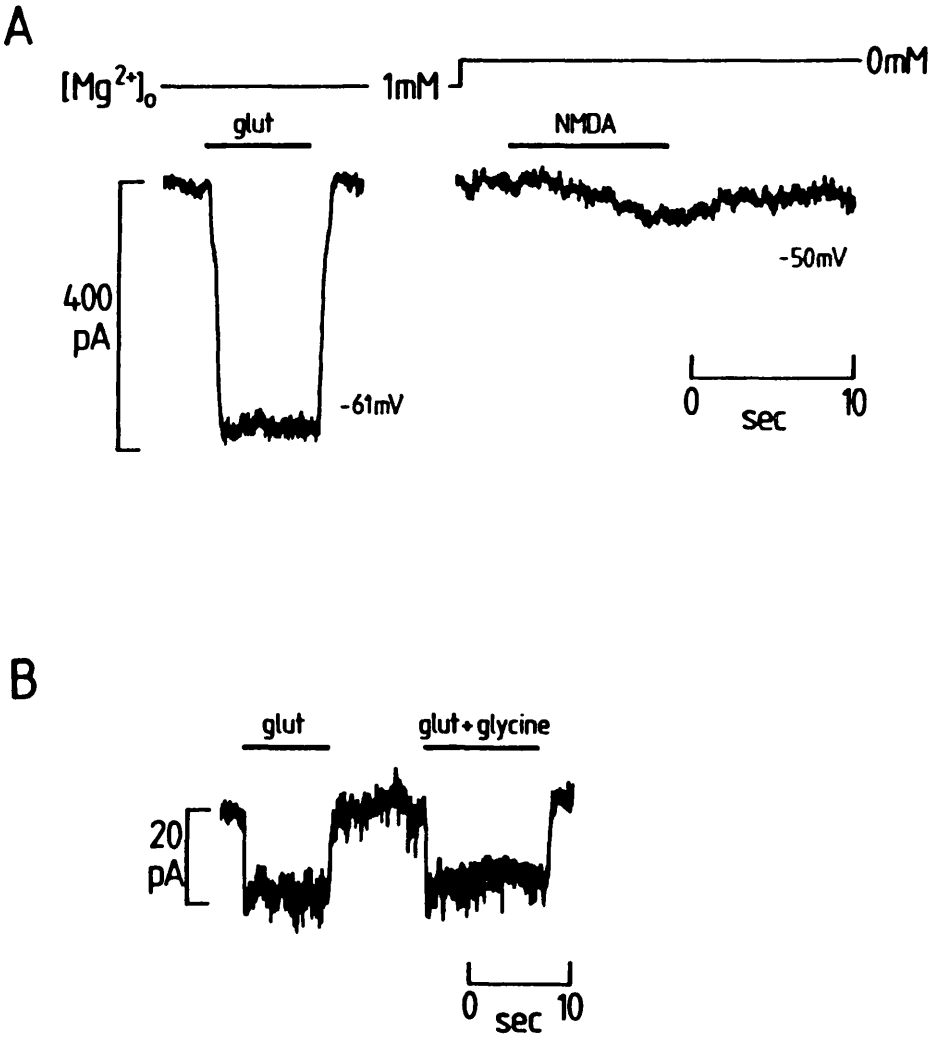
A
[Mg2+]o
1mM
0mM
glut
NMDA
400
pA
-61mV
-50mV
0
sec
10
B
glut
glut+glycine
20
pA
0
sec
10

Since low doses (0.1μM) of glycine are known to potentiate the response to glutamate via a regulatory site on the NMDA receptors in cultured mouse brain neurones (Johnson and Ascher, 1987), and in neocortical slices (Thomson et al., 1989), the possibility that glycine potentiates the glutamate response was investigated as an indirect measure of the presence of NMDA receptors in these ganglion cells.

Fig. 5.8B shows a small inward current response to 100μM glutamate applied by bath perfusion (left hand trace) to an isolated ganglion cell voltage-clamped to -60mV. The external solution (based on normal Ringer's) contained no magnesium. Removal of external magnesium did not affect the size of the glutamate response (n=12). Co-application of 100μM glutamate and 1μM glycine by bath perfusion (right hand trace) did not affect the magnitude of the current response to glutamate (n=12). This was true for cells responding to glutamate with different response sizes, ranging from 20pA (shown here), to 900pA.

The dipeptide N-acetylaspartylglutamate (NAAG) has been identified by immunohistochemical methods within ganglion and amacrine cells of the cat retina (Tieman et al., 1987), and in cultured mouse spinal neurones high concentrations of NAAG (above 300μM) are shown to selectively activate NMDA receptors (Westbrook et al., 1986). Thus, it was thought possible that salamander ganglion cells might also express receptors for NMDA and respond to applied NAAG. However, application of 10, 100, and 500μM NAAG to isolated ganglion cells in the absence of external magnesium, produced no detectable response in all cells tested (n=5). This appears only to further imply a lack of ganglion cell receptors for NMDA.

5.3.9 Ganglion cells in the intact retina respond to NMDA

To investigate whether the inability to detect responses to NMDA in isolated cells might be partly due to loss of dendritic branches containing receptors for NMDA, recordings were made from voltage-clamped ganglion cells in the flatmounted intact retina. (section 2.5.4, Chapter 2). Patch pipettes contained solution G42 (42mM chloride, Table 2.3, Chapter 2).

Bath application of 100μM NMDA, dissolved in Ringer's solution containing zero magnesium (based on solution A, Table 1), produced a convincing current response in all cells tested (n=5). When

voltage-clamped to -60mV, all cells responded to NMDA with an inward current of 60-90pA (see Fig. 5.9A).

There was always a considerable delay between the time of application of NMDA, and the onset of the response. This varied from 4 to 15 seconds, and presumably represents the time taken for the NMDA to reach the flatmounted retina from the solution inlet. The response to NMDA appeared non-desensitizing in each case, although this might not reflect the true situation, as it was unlikely that any early transient component would be detected, with the response having such a slowly developing onset.

All cells showed an increase in current fluctuations associated with the current induced by NMDA. Fig. 5.9A shows the increase in current fluctuations (lower trace) associated with the current produced by NMDA (upper trace). Fig. 5.9B shows the NMDA-induced current noise variance in the range 4-1000Hz, as a function of the mean current flowing, for the current response in Fig. 5.9A. The ratio of the variance to the mean current flowing, gives a value of 0.11pA for the single channel current flowing through NMDA-activated channels. The single channel current measured in this way varied from 0.09pA to 0.15pA at -60mV, and in one cell, was 0.17pA at +32mV, indicating slight outward rectification in the single channel current. ($\gamma \approx 12pS$)

5.3.10 Voltage-dependence of the NMDA-induced current in the intact retina

Current-voltage (I-V) relationships were obtained for NMDA responses in 3 out of the 5 ganglion cells recorded from in the intact retina. Fig. 5.10 shows I-V relations obtained by two different methods, for two different ganglion cells (A and B). In each case, 100μM NMDA was applied by bath perfusion, dissolved in magnesium-free Ringer's solution (as in section 5.3.8 above). Patch pipettes contained G42 (42mM chloride; Table 2.3, Chapter 2).

The current-voltage relation shown in Fig. 5.10A, was obtained by subtracting a control ramped I-V in Ringer's solution only, from a ramped I-V in the presence of NMDA. There was a clear inward current of 50pA at -60mV, which became slightly larger at more negative potentials, reversed around -20mV, and became outward at

Fig. 3.9 NMDA induces a current in voltage-clamped ganglion cells in the intact retina. The NMDA-induced current is associated with an increase in noise. The external solution was based on normal Ringer's (solution A, Table 2.1) and contained no magnesium. Patch pipettes contained solution G42 (42mM chloride; Table 2.3, Chapter 2).

A Current response to 100μM NMDA, applied by bath perfusion in a ganglion cell voltage-clamped to -60mV in the intact retina. NMDA was applied for the length of time indicated in the top trace. NMDA produced a current response (low pass filtered at 1000Hz) of 70pA at this voltage (middle trace). The lower trace (high pass filtered at 4Hz) shows that there is an increase in current fluctuations (noise) associated with the current induced by NMDA.

B Plot of the variance change associated with the mean glutamate-induced current flowing between 4 and 1000Hz. The ratio between the variance and the mean current flowing gives the single channel current flowing, which is 0.11pA for this cell at -60mV.

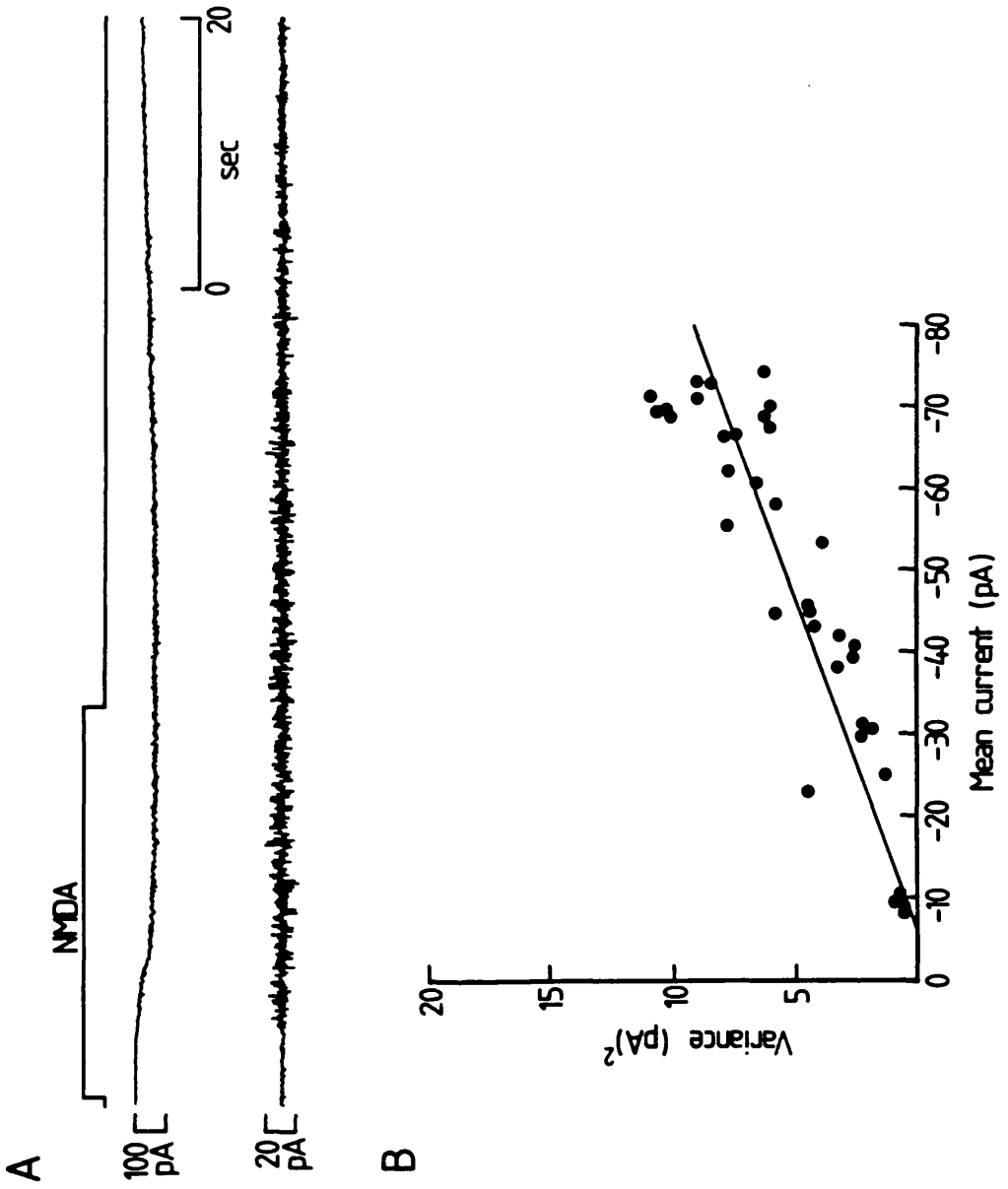
A
NMDA
100 pA
20 pA
0
sec
20
B
Variance (pA)²
Mean current (pA)
0
-10
-20
-30
-40
-50
-60
-70
-80
5
10
15
20

Fig. 5.10 Voltage-dependence of the current induced by NMDA in the intact retina. External solution was based on normal Ringer's (solution A, Table 2.1) but contained no magnesium. Patch pipettes contained solution G42 (42mM chloride; Table 2.3, Chapter 2).
A Current-voltage (I-V) relation for the current induced by 100μM NMDA, obtained by subtracting a control ramped I-V in Ringer's solution alone, from a ramped I-V in the presence of NMDA. The I-V relation showed some outward rectification, and reversed at -20mV.
B Current-voltage (I-V) relation for the NMDA-induced current. Peak NMDA-induced currents were measured and plotted against voltage, for perfusion of NMDA at different holding potentials. The I-V relation rectifies outwardly in a similar manner to that seen in **A**, and the reversal potential of the response was -18mV.

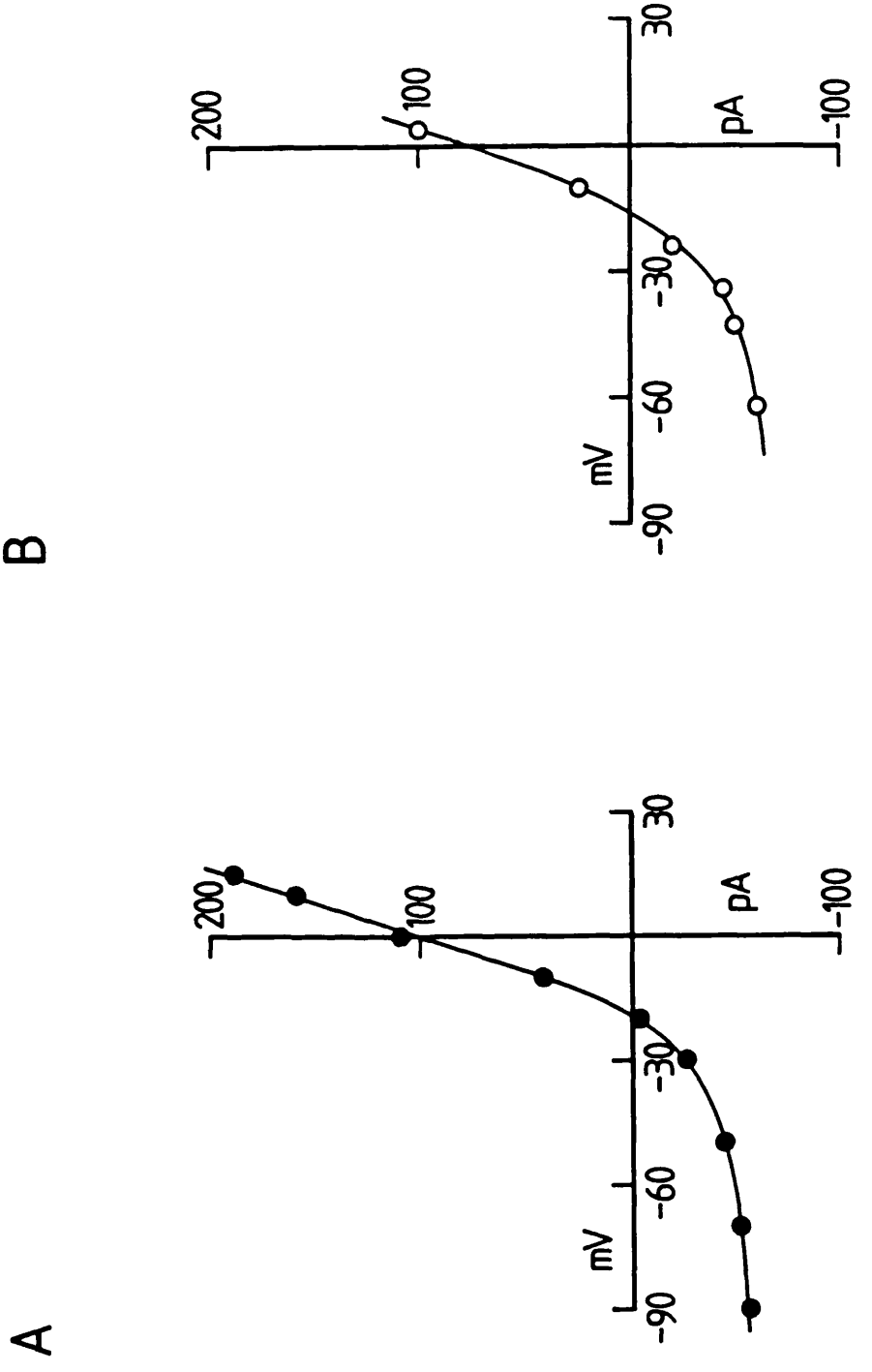
A
B
200
100
30
pA
-100
-30
-60
mV
-90

rectification in the I-V relation, although it is not as strong as that seen in the I-V for the current induced by NMDA in an isolated cell (section 5.3.7). In addition, the inward currents detected in response to NMDA in the intact retina are five times larger than those produced for the isolated cell in section 5.3.7. In some other cells, this method of ramping the voltage produced hysteresis during the ramping, probably due to activation of voltage-gated currents in the ganglion cell membrane, making it difficult to measure true current sizes. Fig 5.10B shows the current-voltage relation for NMDA, in a different ganglion cell, obtained by perfusing 100μM NMDA onto the cell, while it was voltage-clamped to several different holding potentials. This more reliable method gave a current-voltage relation which looked almost identical to that shown in Fig. 5.10A, and had a similar reversal potential (-18mV). The average reversal potential (±s.d.) for the current induced by NMDA (n=3) in the intact retina was -18.3±1.7.

Since all cells in the intact retina responded to NMDA, in the absence of external magnesium, it seems that difficulty in detecting responses to NMDA in some isolated cells, probably results mostly from loss of receptors for NMDA during the cell isolation procedure (see discussion, section 7.5.2, Chapter 7). However, although I have assumed here that NMDA is acting directly on the cell recorded from, I cannot rule out the possibility that it acts for example, on amacrine cells that send synaptic input to the ganglion cell recorded from.

Chapter 6

Properties of currents induced by inhibitory amino acids in ganglion cells

6.1 Introduction

This chapter begins an investigation of the effects of the inhibitory amino acids, gamma-aminobutyric acid (GABA) and glycine on isolated ganglion cells. The results presented are used to address the questions raised in section 1.5.3 (Chapter 1) which are discussed in section 7.7 (Chapter 7).

The results in this chapter are divided into the following sections; (1) Gamma-aminobutyric acid (GABA) and glycine evoke a current in isolated ganglion cells; (2) Bicuculline and strychnine block current responses to GABA and glycine respectively; (3) Voltage-dependence of the current induced by GABA; (4) Voltage-dependence of the current induced by glycine; (5) Dependence of the GABA- and glycine-induced currents on internal chloride concentration; (6) Dependence of the glycine-evoked current on extracellular glycine concentration; (7) The peptide, substance P, evokes a current in isolated ganglion cells.

6.2 Methods

All experiments were performed on isolated ganglion cells (section 2.5.5). Cells were voltage-clamped and recordings were made using the whole-cell variant of the patch-clamp technique. The external solution was normal Ringer's (solution A, Table 2.1). GABA and glycine were applied either by iontophoresis (section 2.6.2), or dissolved in Ringer's solution and applied by bath perfusion. The GABA antagonist bicuculline, the glycine antagonist strychnine, glutamate and substance P were applied by bath perfusion. Patch pipettes contained various solutions (Table 2.3, Chapter 2) as indicated in the text.

6.3 Results

6.3.1 Gamma-aminobutyric acid (GABA) and glycine evoke a current in isolated ganglion cells

In the retinae of lower vertebrates, biochemical, autoradiographic and electrophysiological studies have shown that amacrine cells (which synapse onto ganglion cells) contain GABA or glycine (amongst many other substances) (Ehinger, 1972; Voaden et al., 1974). It would be

Fig. 6.1 GABA and glycine evoke a current in isolated ganglion cells. External solution was normal Ringer's (solution A, Table 2.1) and patch pipettes contained solution G42 (42mM chloride) in **A** and **B**, and G102 (102mM chloride) in **C** (Table 2.3, Chapter 2).

A Current response (top trace) to prolonged iontophoretic application of glycine (lower trace) in an isolated ganglion cell voltage-clamped to -40mV. The peak glycine-evoked inward current is 750pA, which desensitizes to a smaller maintained inward current of about 40pA.

B Current response to 100μM glycine applied by bath perfusion to a different isolated ganglion cell to that shown in **A**, voltage-clamped to -50mV. Timing of glycine application is shown by the bar. Glycine produces an inward current which peaks at 1nA, and desensitizes fairly rapidly with time, as in **A**.

C Current response (top trace) to iontophoretically applied GABA, for the length of time indicated in the lower trace, in an isolated ganglion cell voltage-clamped to -50mV. The large inward current response to GABA has a rapid onset, peaks at 1.2nA and desensitizes to a smaller maintained inward current of about 100pA. The series resistance for the pipette used to clamp the cell was 20MΩ, producing a voltage error of 30mV for a 1.5nA current, so at the peak of the response the cell voltage will actually have been -80mV (similarly for **A** and **B**).

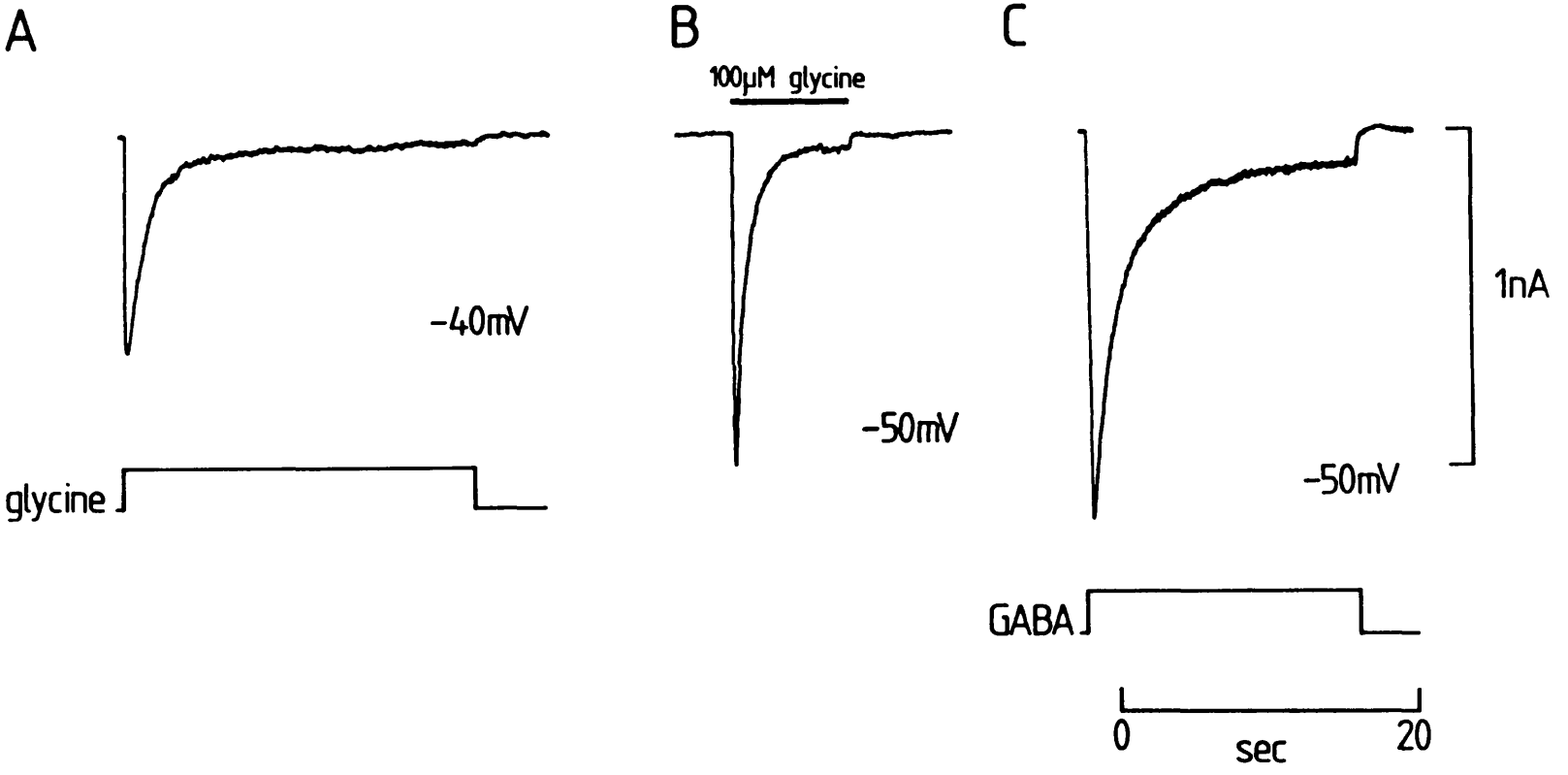
A
-40mV
glycine
B
100µM glycine
-50mV
C
1nA
-50mV
GABA
0
sec
20

interesting to see what effects, if any, these inhibitory amino acids might have when applied to salamander ganglion cells.

Fig. 6.1 shows the current responses to glycine applied by iontophoresis (A), or by bath perfusion (B), and to GABA applied by iontophoresis (C), in three different ganglion cells, voltage-clamped to the potentials shown alongside each current trace. The external solution was normal Ringer's and the patch pipette contained solution G42 (42mM chloride) in A and B, and solution G102 (102mM chloride) in C (see Table 2.3, Chapter 2, for patch pipette solutions).

Prolonged iontophoretic application of glycine or GABA, produced a large peak current with a rapid onset which then desensitized with time. In Fig. 6.1B, bath perfusion of 100μM glycine to an isolated ganglion cell held at -50mV, produced an inward current similar to that produced by iontophoretically applied glycine (Fig. 6.1A). Out of a total of 24 cells tested, all responded to glycine. Similarly, out of 16 cells tested with GABA, all responded. Since all cells responded either to the application of GABA or glycine, it seems highly likely that these ganglion cells have receptors for both inhibitory amino acids (although both drugs were not applied to the same cell to test this explicitly).

6.3.2 Bicuculline and strychnine block the current response to GABA and glycine respectively

Fig. 6.2A shows an isolated ganglion cell voltage-clamped to around -50mV, responding to iontophoretically applied GABA (lower trace) in normal Ringer's solution. The patch pipette contained 102mM chloride (solution G102, Table 2.3, Chapter 2). GABA produced an inward current of 340pA in this cell at this voltage. Bath application of 100μM bucuculline for about 20 seconds (as shown by the bar), blocked most of the current response to GABA, with recovery of the response on reflowing Ringer's solution (n=5).

Fig. 6.2B shows a different isolated ganglion cell, voltage-clamped to -40mV, responding to iontophoretically applied glycine (lower trace). Glycine produced an inward current of 550pA at this voltage, which was rapidly and reversibly abolished by bath application of 10μM strychnine.

Fig. 6.2 Bicuculline and strychnine block the current response to GABA and to glycine respectively. The external solution was normal Ringer's (solution A, Table 2.1). Bicuculline (100μM) and strychnine (10μM) were bath applied, dissolved in Ringer's solution. Patch pipettes contained solution G102, containing 102mM chloride (Table 2.3, Chapter 2).

A GABA-induced inward currents (top trace) in an isolated ganglion cell voltage-clamped to -50mV. GABA was applied by iontophoresis (lower trace). Bath application of 100μM bicuculline (for the length of time indicated by the bar) almost completely blocked the response to GABA. This block was reversible and on reflowing Ringer's solution without bicuculline, the current response to GABA returned.

B Currents induced by glycine (top trace) applied by iontophoresis (lower trace) in an isolated ganglion cell held at -40mV. Glycine produced an inward current, which was practically abolished in the presence of 10μM strychnine, applied for the length of time indicated by the bar. The response to glycine recovered on reflowing Ringer's solution without strychnine.

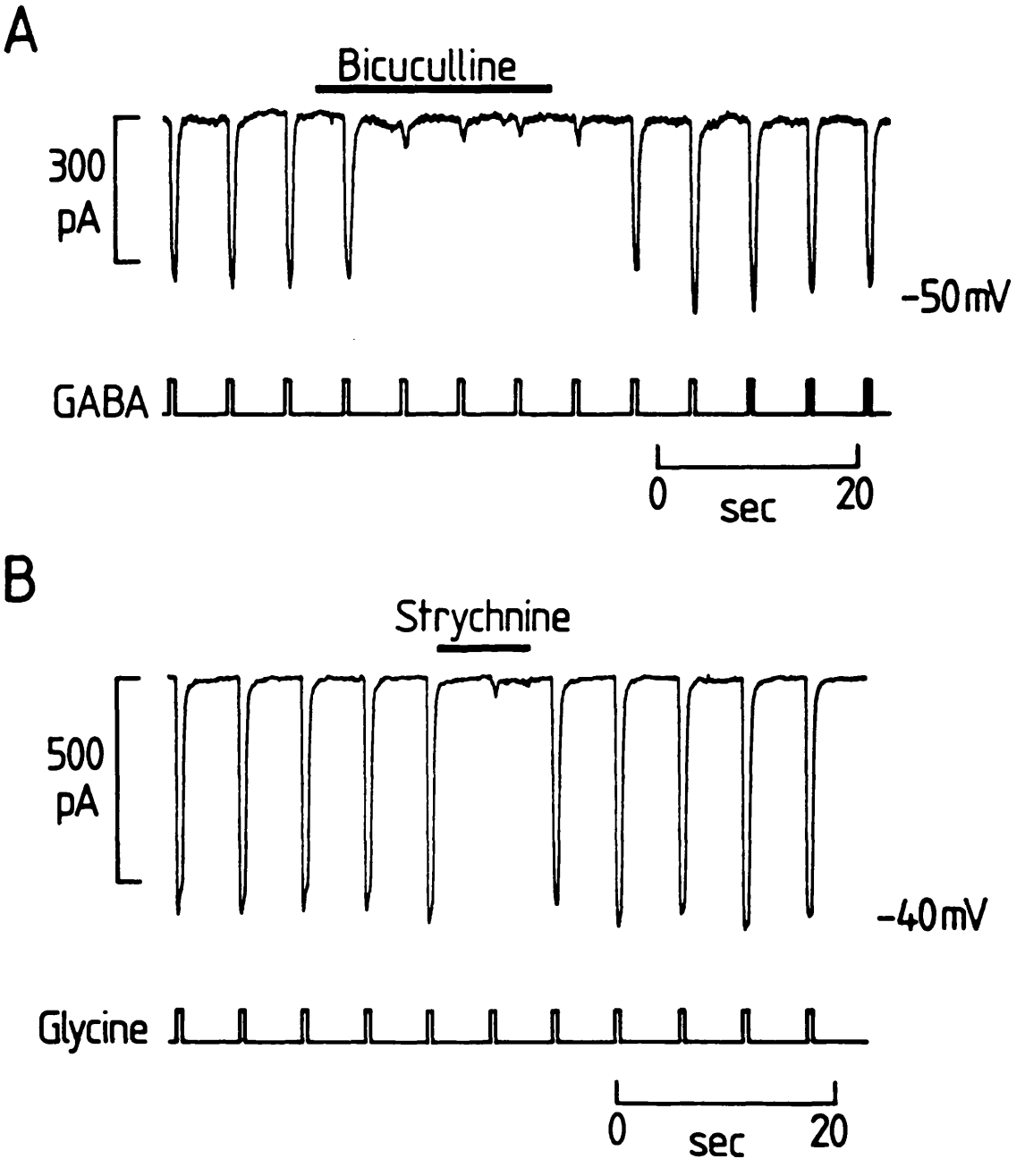
A
Bicuculline
300
pA
-50mV
GABA
0
sec
20
B
Strychnine
500
pA
-40mV
Glycine
0
sec
20

6.3.3 Voltage-dependence of the current induced by GABA

To investigate whether the voltage-dependence of the GABA-induced current was similar to that seen for other cell types, GABA was applied by iontophoresis to isolated ganglion cells voltage-clamped to several different potentials. Fig. 6.3A shows the currents induced by GABA in a ganglion cell voltage-clamped to the potentials shown alongside each trace. The external solution was normal Ringer's and the patch pipette contained solution G42, which contained 42mM chloride (Table 2.3, Chapter 2). GABA evoked a large inward current of 800pA at -56mV, around the cell's resting potential. The inward current was larger at more negative potentials, reversed around -27mV and was outward at potentials positive to this. The relation between the peak GABA-evoked current and voltage (I-V) was plotted for the data in A, in Fig. 6.1B. A linear regression line through the points gave a slope conductance of 21.8nS and the reversal potential of the response was -27mV. Voltages plotted were corrected for voltage errors produced by the patch pipette series resistance (section 2.7.1, Chapter 2), which were found to be significant at large voltage displacements from the reversal potential, but negligible near the reversal potential. For consistency, when estimating the reversal potential of the response, straight lines were drawn through the data. However, in some cases (n=5/16), the data could be just as well fit with a curve, showing slight outward rectification of the response, as has been seen for GABA-gated chloride channels in other cell types. (see discussion, section 7.7.2, Chapter 7). Mean reversal potentials (section 6.3.5) were obtained for patch pipette chloride concentrations of 102mM (n=4), 42mM (n=3) and 3mM (n=5).

6.3.4 Voltage-dependence of the current induced by glycine

To investigate whether the glycine-induced current in isolated ganglion cells might have a similar voltage-dependence to that seen in other cell types, glycine was applied by iontophoresis to isolated ganglion cells voltage-clamped to various potentials as shown in Fig. 6.4A. The external solution for the cell in this figure was normal Ringer's and the patch pipette contained solution G102 (102mM chloride; Table 2.3, Chapter 2). With this patch pipette chloride (n=4), glycine evoked an inward current of about 200pA, at around the ganglion cell resting potential of -65mV. The

Fig. 6.3 Voltage-dependence of the current induced by GABA. The external solution was normal Ringer's (solution A, Table 2.1) and patch pipettes contained solution G42 (42mM chloride; Table 2.3, Chapter 2)

A GABA-induced currents in an isolated ganglion cell voltage-clamped to the potentials shown alongside each trace. Timing of GABA iontophoresis is shown by the square trace immediately below the current data. GABA evokes an inward current at around the ganglion cell resting potential of -56mV. The current was larger at more negative potentials, reversed around -27mV and was outward at potentials positive to this. Currents have been plotted against voltages which have been corrected for voltage drop across the series resistance.

B Current-voltage (I-V) relation for the GABA-induced currents in **A**. Peak GABA-induced currents were plotted as a function of membrane potential. The linear regression line through the points gave a reversal potential of -27mV for the current response.
(x-intercept at $y=0 = -27.5$; y-intercept at $x=0 = 600.2$; correlation coefficient $= 0.990$.)

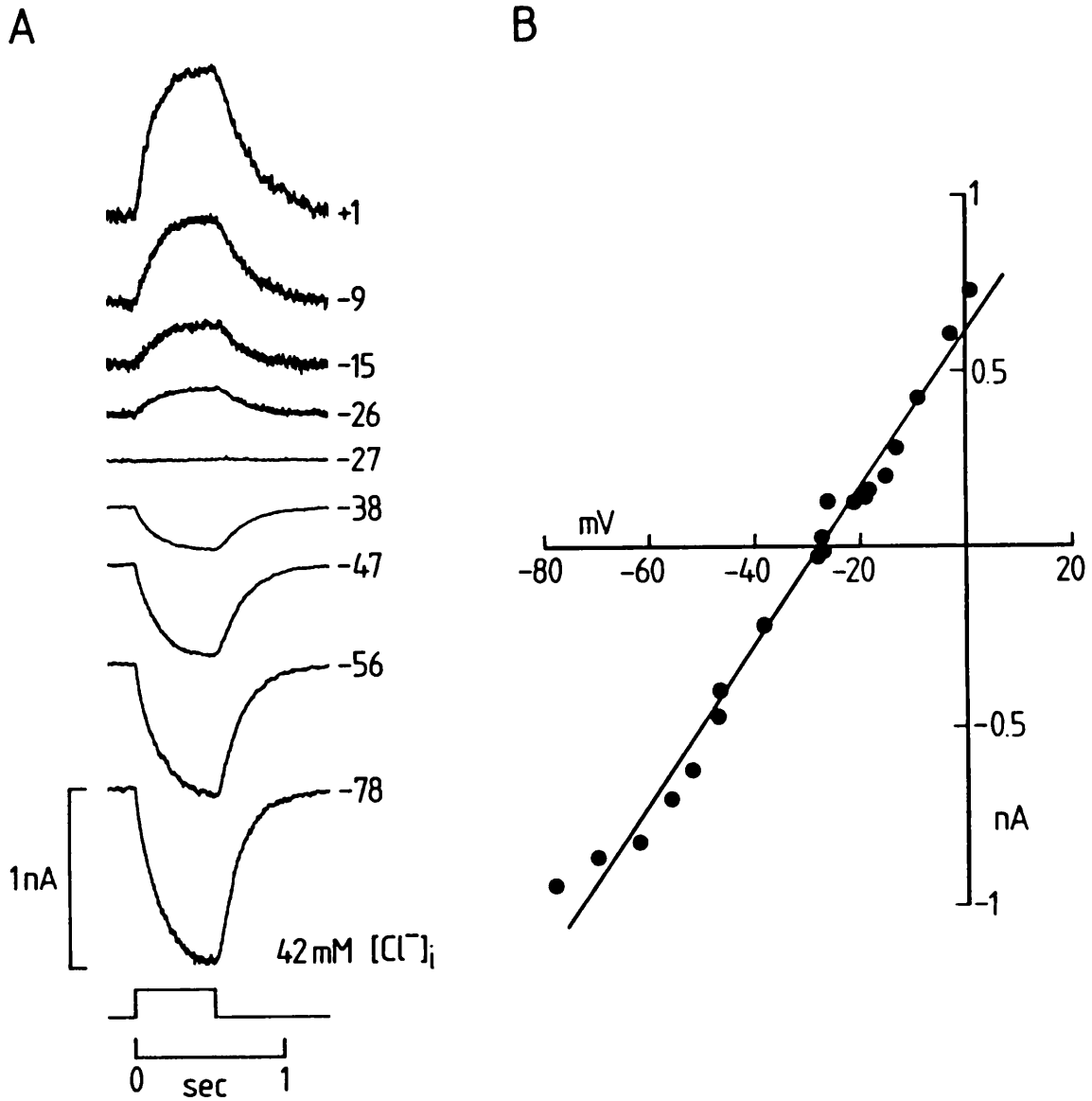
A
+1
-9
-15
-26
-27
-38
-47
-56
-78
1nA
42 mM [Cl⁻]i
0
sec
1
B
mV
-80
-60
-40
-20
20
1
0.5
-0.5
-1
nA

Fig. 6.4 Voltage-dependence of the current induced by glycine. The external solution was normal Ringer's (solution A, Table 2.1) and the patch pipette contained solution G102 (102mM chloride; Table 2.3, Chapter 2).

A Currents evoked by glycine in an isolated ganglion cell voltage-clamped to the potentials shown alongside each trace. Timing of glycine iontophoresis is shown by the square trace immediately below the current data. Glycine evokes an inward current at -65mV with G102 (102mM chloride) in the patch pipette. The current was larger at more negative potentials, reversed around -7mV and was outward at potentials positive to this. Currents have been plotted against voltages which were corrected for voltage drop across the pipette series resistance.

B Current-voltage (I-V) relation for the glycine-induced currents shown in **A.** Peak glycine-evoked currents were plotted against voltage. The linear regression line through the points gave a reversal potential of -6mV.

(x-intercept at $y=0$ = -6; y-intercept at $x=0$ = 17.4; Correlation coeff. = 0.996)

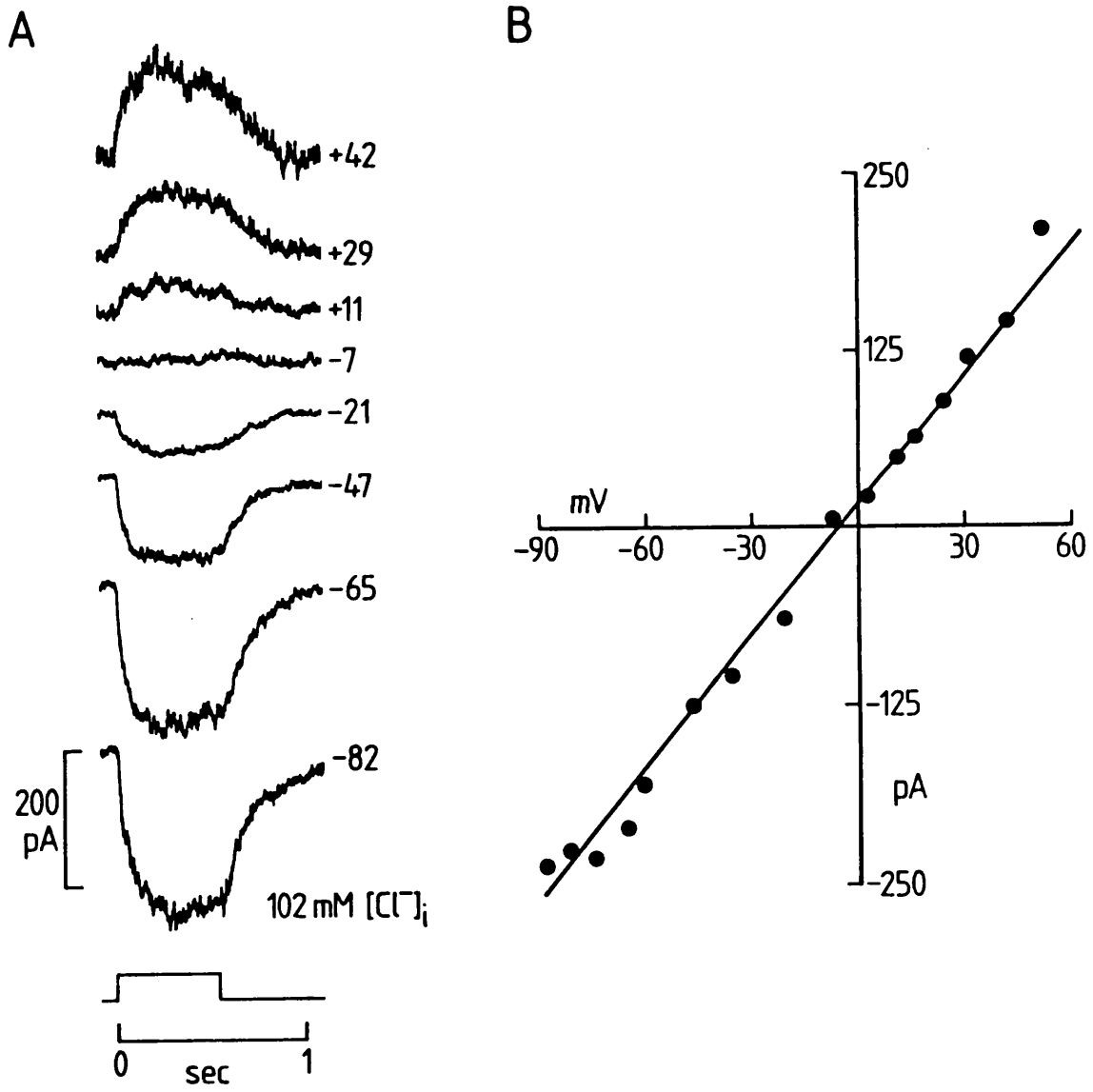
A
+42
+29
+11
-7
-21
-47
-65
-82
200 pA
102 mM [Cl⁻]ᵢ
0
sec
1
B
250
125
-125
-250
mV
-90
-60
-30
30
60
pA

$$* \; E_{rev} = -\frac{RT}{F} \ln \left[\frac{[Cl^-]_o + P_{Ac}/P_{a}[Ac^-]_o}{[Cl^-]_i + P_{Ac}/P_{a}[Ac^-]_i} \right]$$

glycine-evoked current was larger at more negative potentials, reversed around -6mV, and was outward at more positive potentials.

The current-voltage (I-V) relation shown in Fig. 6.4B was linear, with a slope conductance of 3.17nS and an interpolated reversal potential of -6mV. Current-voltage relations for glycine-induced currents were also obtained for patch pipette chloride concentrations of 42mM (n=3), 17mM (n=2) and 3mM (n=4), with chloride ions replaced by acetate. As for GABA, current-voltage relations were generally linear and data points were fitted with a straight line to estimate the reversal potential (but see discussion, section 7.7.2, Chapter 7).

6.3.5 Dependence of the GABA- and glycine-induced current reversal potentials on patch pipette chloride concentration

To see if GABA and glycine gated conventional chloride channels in salamander ganglion cells, the average reversal potentials measured for different patch pipette chloride concentrations (chloride replaced with acetate) were compared with the Nernst potential for chloride. This is shown for GABA in Fig 6.5A and for glycine in Fig. 6.5B. Mean reversal potentials (±s.d.) for GABA are given in Table 6.1, and for glycine in Table 6.2.

In Fig. 6.5A, the dotted line represents the Nernst prediction, $E_{Cl} = -RT/F \ln\{[Cl^-]_o/[Cl^-]_i\}$, with $[Cl^-]_o$ = 114mM (normal Ringer's). The data points shown (average reversal potentials±s.d.) deviated from the Nernst equation, especially for low values of patch pipette chloride, e.g 3mM, in which the observed reversal potential was about 20mV positive to the predicted value of E_{Cl}. Since GABA-gated chloride channels in mouse cultured spinal neurones have been shown to be slightly permeable to acetate as well as to chloride ($P_{acetate}/P_{Cl}$ = 0.08; Bormann et al., 1987) the smooth curve through the points was a Goldman-Hodgkin-Katz equation* fit with a permeability ratio $P_{acetate}/P_{Cl}$ = 0.034, assuming that acetate passed through the channel with chloride.

Fig. 6.5B reveals a similar deviation of the observed reversal potential (mean±s.d.) for the glycine-induced current from the Nernst prediction (dotted line), for four different patch pipette chloride concentrations. As for GABA, glycine-gated chloride

Fig. 6.5 Dependence of the reversal potential of the GABA and glycine-induced currents on patch pipette chloride concentration. The external solution was normal Ringer's (solution A, Table 2.1). Patch pipettes contained the following solutions (with chloride concentrations in brackets); G102 (102mM); G42 (42mM); G17 (17mM); or G3 (3mM), with chloride replaced by acetate to give the final chloride concentrations above (Table 2.3, Chapter 2).

A Reversal potential of the GABA-induced current as a function of pipette chloride concentration ($[Cl^-]_i$). Points represent 5, 3 and 4 cells studied for 3, 42 and 102mM $[Cl^-]_i$. Data do not fit the Nernst prediction for a chloride-specific channel (dotted line). Bars show mean reversal potential±s.d. (see Table 6.1). Smooth curve is the Goldman-Hodgkin-Katz equation* for a channel with a permeability ratio $P_{acetate}/P_{Cl}$ = 0.034.

B Reversal potential of the glycine-induced current as a function of pipette chloride concentration. Points represent 4, 2, 3 and 4 cells studied for 3, 17, 42 and 102mM $[Cl^-]_i$. Bars show mean reversal potentials±s.d. (see Table 6.2). As for GABA in **A**, data do not fit the Nernst prediction for a chloride-specific channel (dotted line) and are best fit by the smooth curve which is a Goldman-Hodgkin-Katz equation fit for a channel with a permeability ratio $P_{acetate}/P_{Cl}$ = 0.024.

C Reversal potential of the glycine-induced current as a function of pipette chloride concentration, with patch pipette acetate replaced by a larger anion, gluconate. Points represent 6 and 3 cells studied for 3 and 42mM $[Cl^-]_i$ and bars show mean reversal potential±s.d. (see Table 6.3). The data do not fit the Nernst prediction for a chloride-specific channel and the smooth curve is a Goldman-Hodgkin-Katz equation fit with a permeability ratio $P_{gluconate}/P_{Cl}$ = 0.028. These data suggest that the glycine-gated chloride channel is as permeable to gluconate as it is to acetate.

* $E_{rev} = -\frac{RT}{F} \ln \left[\frac{[Cl^-]_o + P_{Ac}/P_{Cl}[Ac^-]_o}{[Cl^-]_i + P_{Ac}/P_{Cl}[Ac^-]_i} \right]$

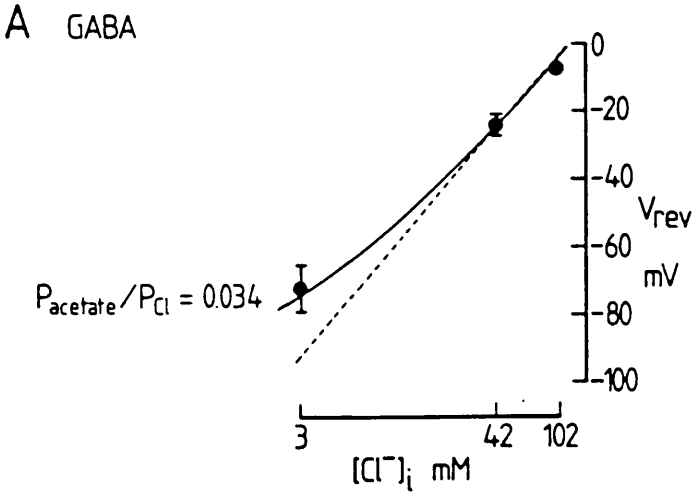
A GABA
$P_{acetate}/P_{Cl}$ = 0.034
0
-20
-40
-60
-80
-100
V_{rev}
mV
3
42
102
$[Cl^-]_i$ mM

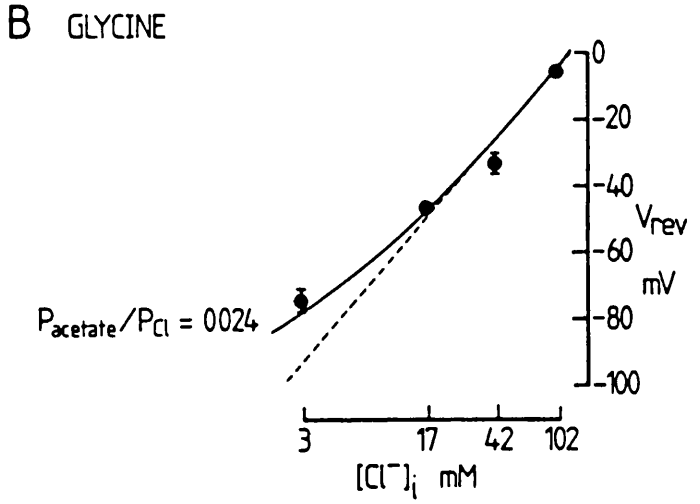
B GLYCINE
$P_{acetate}/P_{Cl}$ = 0.024
0
-20
-40
-60
-80
-100
V_{rev}
mV
3
17
42
102
$[Cl^-]_i$ mM

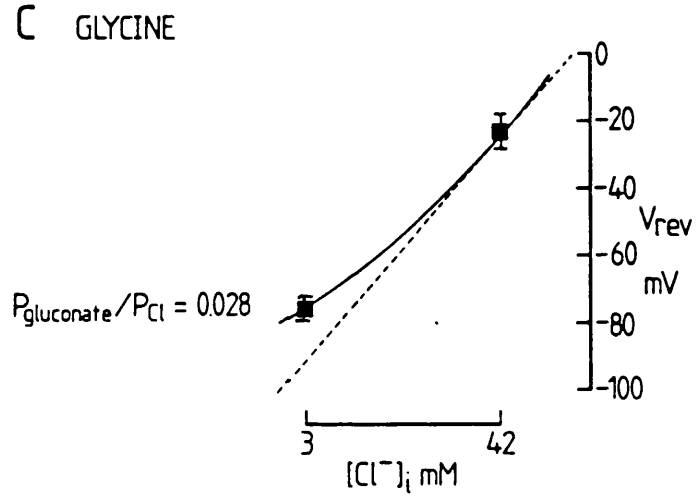
C GLYCINE
$P_{gluconate}/P_{Cl}$ = 0.028
0
-20
-40
-60
-80
-100
V_{rev}
mV
3
42
$[Cl^-]_i$ mM

channels in mouse neurones were slightly permeable to acetate ($P_{acetate}/P_{Cl}$ = 0.035, Bormann et al., 1987). Thus, assuming that acetate also carried part of the glycine-induced current in ganglion cells, the smooth curve drawn through the points was a Goldman-Hodgkin-Katz equation fit with a permeability ratio $P_{acetate}/P_{Cl}$ = 0.024. As in mouse neurons, the ganglion cell GABA-gated chloride channel is more permeable to acetate than the glycine-gated channel.

In an attempt to prove that acetate was indeed the other current carrying ion, the acetate in the pipette medium was replaced by another anion, gluconate, which is larger and therefore, presumably impermeant. Fig. 6.5C shows a plot of the mean reversal potentials (±s.d.) of the response to glycine, for patch pipette chloride concentrations of 3mM (n=6) and 42mM (n=3), with acetate replaced by gluconate (see Table 6.3). The observed reversal potentials still deviated from the Nernst prediction for a chloride-specific channel, and the data was best fit by the smooth curve, which is a Goldman-Hodgkin-Katz equation fit with a permeability ratio $P_{gluconate}/P_{Cl}$=0.028. This suggests only that the glycine-gated chloride channel is just as permeable to gluconate as it is to acetate.

6.3.6 Dependence of the glycine-evoked current on extracellular glycine concentration

Fig. 6.6A shows the currents produced in an isolated ganglion cell voltage-clamped to -60mV, by different concentrations of glycine applied by bath perfusion. The external solution was normal Ringer's and the patch pipette contained solution G42 (42mM chloride, Table 2.3, Chapter 2). To estimate the maximum response, for each concentration of glycine, cells were moved close to the solution inlet, since the response to local (iontophoretic) application of glycine desensitizes rapidly (Fig. 6.1A and B, section 6.3.1). In addition, a multiple barrelled inflow tube was used to minimize the response time to peak.

A small inward current of about 10pA was evoked by 10μM glycine, and the peak currents (I) were larger with higher glycine concentrations, up to 1mM (n=3). For concentrations higher than 10μM, the response to glycine rapidly desensitized. Note that the size of the current response to 1mM glycine is slightly smaller

Fig. 6.6 Currents induced by concentrations of glycine between 10μM and 1mM. The external solution was normal Ringer's (solution A, Table 2.1) and the patch pipette contained solution G42 (42mM chloride; Table 2.3, Chapter 2).

A Currents induced in an isolated ganglion cell voltage-clamped to -60mV, by glycine applied to the cell by bath perfusion. The current produced by glycine at all concentrations tested (above 10μM), was desensitizing. The lowest concentration of glycine to produce a detectable current was 10μM.

B Dose-response curve for the data in **A**. The peak glycine-evoked currents were normalized to the maximum (in this case, the maximum current was evoked by 500μM glycine). The curve drawn through the points is a Michaelis-Menten relation, having the form, $I/I_{max} = [glycine]^2/\{[glycine]^2 + K_m^2\}$, with a K_m of 84μM. Thus at least 2 glycine molecules must bind to open each channel (but see also text, section 6.3.7).

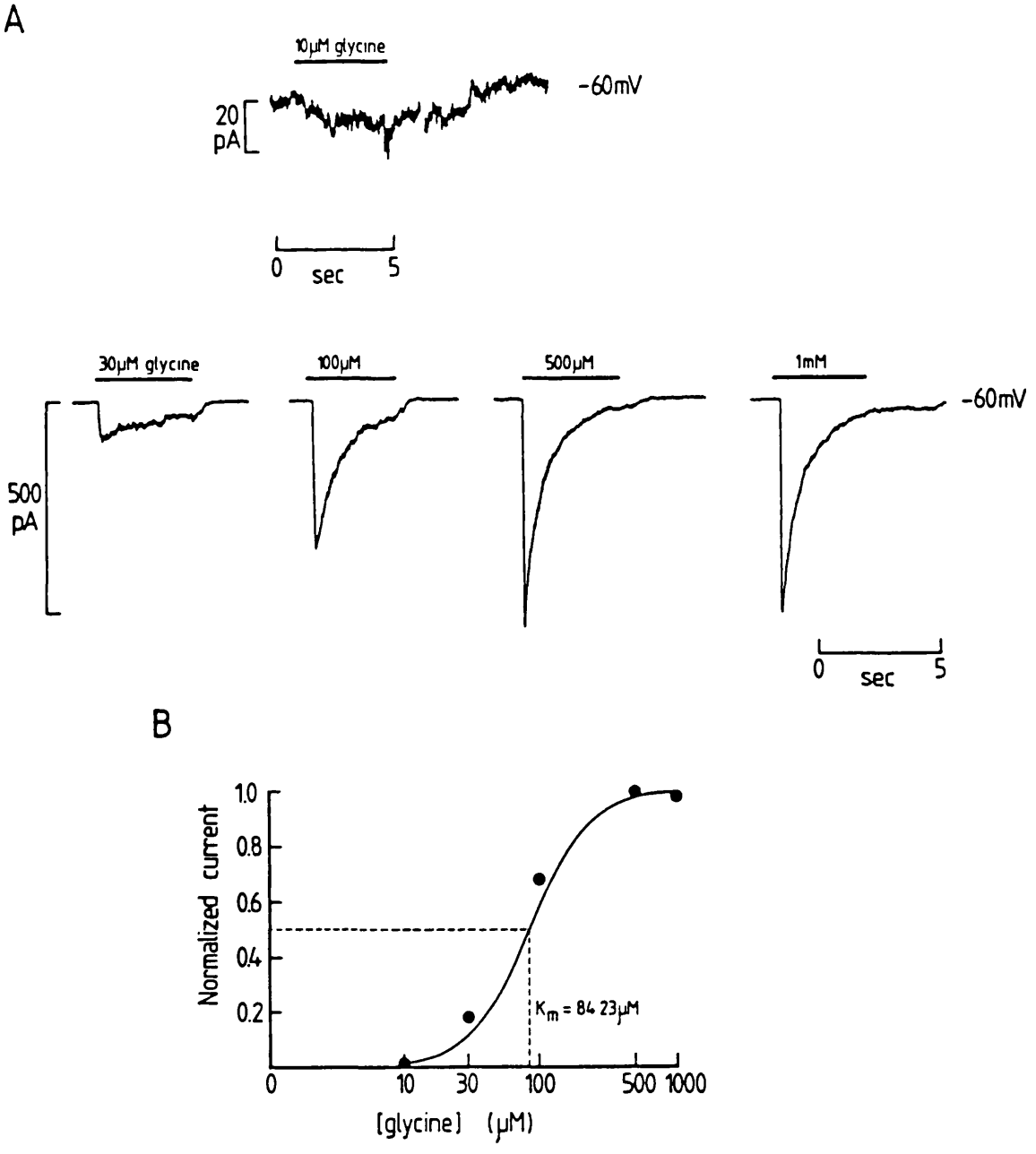
A
10μM glycine
-60mV
20 pA
0 sec 5
30μM glycine
100μM
500μM
1mM
-60mV
500 pA
0 sec 5
B
Normalized current
1.0
0.8
0.6
0.4
0.2
K_m = 84.23μM
0 10 30 100 500 1000
[glycine] (μM)

than that to 500μM glycine, possibly because some receptors for glycine were still desensitized after exposure to 500μM glycine, because desensitization occured more quickly with 1mM than with 500μM glycine (i.e. during the rising phase of the response), or because the flow rates of the different solutions were slightly different. In order to try and overcome such problems, the following protocol was enforced. Trials of 60 seconds (3 x 20 sec) were used for each glycine concentration. Glycine was applied for 4sec, and then Ringer's solution was perfused for 16 seconds. This was repeated 3 times for each concentration, to ensure that the peak response amplitude was the same. Each current response in Fig. 6.6A is the third response to glycine in each 60sec trial for each concentration.

Fig. 6.6B shows the curve relating the normalized peak response amplitude to the external concentration of glycine, for the currents shown in A. The dose that produced a half-maximal response was 84μM (from a Lineweaver-Burke plot of 1/I against $1/[\text{glycine}]^2$. The curve through the points was drawn according to the relation,

$$I/I_{max} = [\text{glycine}]^2/\{[\text{glycine}]^2 + K_m^2\}$$

with a K_m of 84μM.

In another cell, the dose-response data were better fit with a curve of the form,

$$I/I_{max} = [\text{glycine}]^3/\{[\text{glycine}]^3 + K_m^3\}$$

with a K_m of 48μM. The sigmoid onset of these dose response curves implies that at least two glycine molecules bind to each receptor.

The discrepancy in the value of K_m and the shape of the dose-response curve for different cells probably reflects some difficulty in measuring the true peak responses to glycine, despite using the protocol described above.

6.3.7 The peptide, substance P, evokes a current in isolated ganglion cells

Substance P has been localized to retinal amacrine cells of the pigeon (Karten and Brecha, 1980) and bullfrog (Eskay et al., 1981) and has been shown to enhance light-evoked excitation of

ganglion cells (Dick *et al*, 1988; Djamgoz *et al*, 1988).

In Fig. 6.7, substance P and glutamate were bath applied to the same isolated ganglion cell, voltage-clamped to -50mV and -60mV respectively. The external solution was normal Ringer's and the patch pipette contained solution G42 (42mM chloride; Table 2.3, Chapter 2). 100μM glutamate (applied for the length of time indicated by the bar) produced an inward current of 50pA at -60mV (right hand trace). The same cell responded to 100nM substance P at -50mV, with a small inward current of about 18pA (left hand trace). In 3 out of 5 cells recorded from, substance P produced an inward current of 10-20pA at around -50mV, with solution G42 in the patch pipettes.

In another cell, application of 10mV pulses before and during substance P application, enabled detection of any change in the cell membrane input resistance produced by substance P. In this cell, substance P decreased the the membrane input resistance, by approximately half, from 330 to 140MΩ. So, it appears that substance P opens ion channels in the ganglion cell membrane. Further experiments on isolated ganglion cells may reveal more details of the action of substance P on the ganglion cell membrane (section 7.8.3, Chapter 7) and might provide some insight as to how this peptide could act as a neuromodulator in the inner retina.

Fig. 6.7 The peptide, substance P evokes a current in isolated ganglion cells. External solution was normal Ringer's (solution A, Table 2.1) and patch pipettes contained solution G42 (42mM chloride; Table 2.3, Chapter 2).

Bath application of 100nM substance P (for the length of time indicated by the bar) to an isolated ganglion cell voltage-clamped to -50mV, produced a small inward current response of 18pA. (left hand trace). Application of 100μM glutamate to the same cell held at -60 mV (right hand trace), produced an inward current of about 50pA.

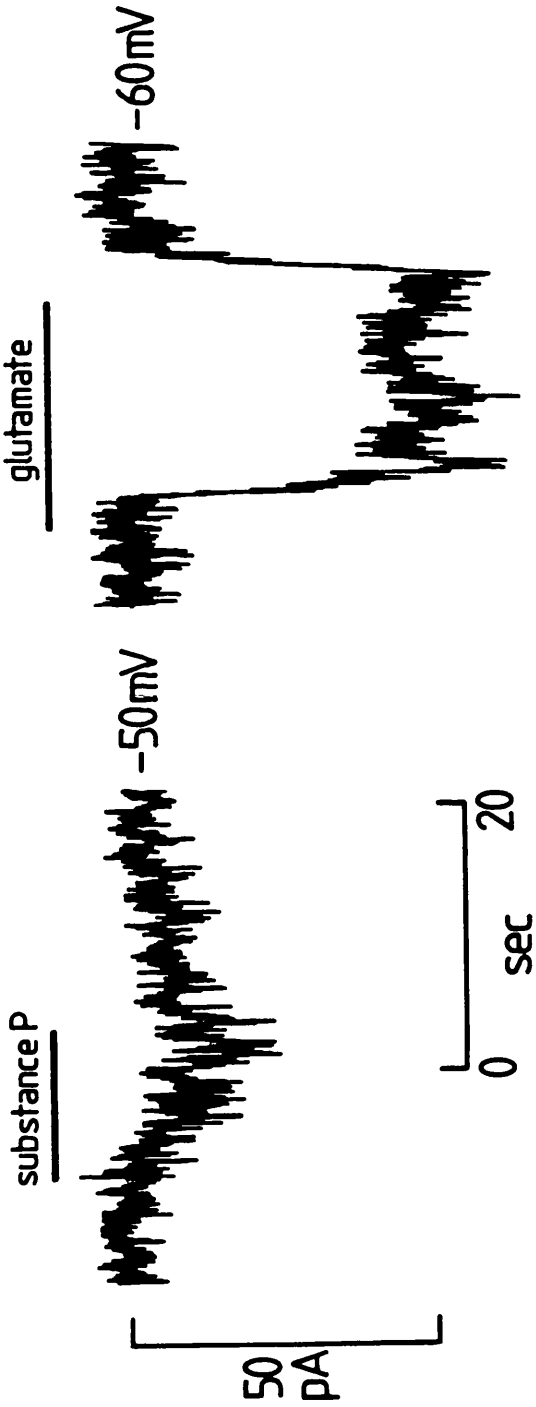
-60mV
glutamate
-50mV
substance P
0
20
sec
50
pA

Table 6.1

GABA: chloride replaced by acetate

Patch pipette $[Cl^-]$ (mV)	No. of cells	V_{rev} (±s.d.) with acetate (mV)	V_{rev} predicted from Nernst eqn. (mV)
3	5	-72±7	-92
42	3	-24±3	-25
102	4	-8±1	-3

Table 6.2

Glycine: chloride replaced by acetate

Patch pipette $[Cl^-]$ (mM)	No. of cells	V_{rev} (±s.d.) with acetate (mV)	V_{rev} predicted from Nernst eqn. (mV)
3	4	-74±4	-92
17	2	-46±1	-48
42	3	-33±4	-25
102	4	-5±1	-3

Table 6.3

Glycine: chloride replaced by gluconate

Patch pipette $[Cl^-]$ (mM)	No. of cells	V_{rev} (±s.d.) with gluconate (mV)	V_{rev} predicted from Nernst eqn. (mV)
3	6	-75±6	-92
42	3	-24±4	-25

Chapter 7
Discussion of results

7.1 Discussion of Chapter 3

7.1.1 Does L-glutamate evoke a current in cone photoreceptors?

Previous reports have suggested that glutamate has no effect on rods and cones (Murakami et al., 1972), or that it hyperpolarizes photoreceptors (Cervetto and MacNichol, 1972). Application of L-glutamate to isolated cones (section 3.3.1), voltage-clamped to their resting potential, produced an inward current when the patch pipette contained 101mM chloride. Glutamate produced a current in single cones and in both principal and accessory members of double cones, but so far I have not been able to demonstrate a glutamate-gated conductance in salamander rods. Glutamate also produced a current in cones in the intact retina (section 3.3.10). Contrary to previous suggestions, my results suggest that glutamate depolarizes (tiger salamander) cones over most of the voltage range of the cone light response (for discussion, see section 7.1.7, Chapter 7).

7.1.2 Does L-glutamate activate channels or an electrogenic carrier mechanism in the cone membrane?

Glutamate gates ion channels in postsynaptic bipolar and horizontal cells, suggesting that glutamate could also generate a current in cones by opening ion channels. However, glutamate uptake into photoreceptors has been demonstrated from radiotracing experiments (White and Neal, 1976; Miller and Schwartz, 1983) and such uptake might be electrogenic, as in retinal Müller cells, and thus generate a current when glutamate is applied.

The glutamate-evoked current in cones showed a clear reversal potential (Figs. 3.2 and 3.14), and was associated with an increase in current noise (section 3.3.3), implying that at least part of the glutamate-evoked current was produced by glutamate opening ion channels. The glutamate-induced current in bipolar and horizontal cells has also been shown to be accompanied by an increase in current fluctuations (Ishida and Neyton, 1985; Attwell et al., 1987; Murase et al., 1987), which is usually associated with an increase in opening and closing of ion channels. In addition, changing the external or internal chloride concentration has no

*However, the possibility that the cone response to glutamate (section 3.3.8) is related to glutamate reuptake at the cone terminal, cannot be excluded, since the glutamate responses were abolished by the glutamate uptake blocker, threo-3-hydroxy-DL-aspartate.

effect on the glutamate-evoked current produced by the glutamate uptake carrier in Müller cells (Barbour et al., 1988), but has a large effect on the magnitude and reversal potential of the glutamate-evoked current in cones (section 3.3.7). Thus, most of the current produced by glutamate in cones probably results from glutamate-activated anion channels (see below).*

7.1.3 Which ions carry the current evoked by glutamate?

Changing the internal and external chloride concentrations revealed that chloride was the principle ion carrying the current evoked by glutamate. This is in contrast to other glutamate-gated channels seen in vertebrates which are non-specific cation conductances. It is also in contrast to that found by Tachibana and Kaneko (1988), who describe a glutamate-gated current in turtle photoreceptors, with similar properties to that described here (e.g. the current is sodium-dependent and localized to the synaptic terminals of the photoreceptors) except that their data suggest that the glutamate-gated channel is a cation channel. Although it is unusual that glutamate should gate an anion channel, glutamate-gated chloride conductances have previously been shown to exist in locust muscle fibres (Cull-Candy, 1976) and in snail neurones (Szczepaniak and Cottrell, 1973).

The reversal potential for the glutamate response did not indicate a purely chloride-specific conductance. It is assumed that another anion present in the patch pipette, acetate (shown by Bormann et al., (1987) to be permeant through GABA- and glycine-gated chloride channels), carries the current with chloride. The dependence of the reversal potential of the glutamate response on pipette chloride concentration, can be explained if the channel permeability to these ions has a ratio $P_{acetate}/P_{Cl} = 0.1$. With a physiological internal chloride concentration of between 12-24mM (in turtle, Kaneko and Tachibana, 1986), the glutamate-evoked current will reverse in the voltage range -34 to -43mV, close to the cone dark potential of -40mV (Attwell et al., 1982).

The glutamate-gated anion conductance in cones was quite different from the gamma-aminobutyric acid (GABA)-gated chloride-

specific conductance observed by Kaneko and Tachibana (1986) in turtle cones, and from glycine-gated chloride conductances seen in other cell types. The glutamate-induced current in cones was unaffected by bicuculline (100μM) or strychnine (10μM), as in Fig. 3.12, at doses which reduced or abolished chloride currents evoked in isolated ganglion cells by iontophoresis of GABA or glycine (section 6.3.2, Chapter 6). The chloride current evoked by glutamate in cones showed inward rectification around the reversal potential, unlike the slight outward rectification observed for GABA-gated chloride currents in cones (Kaneko and Tachibana, 1986) and in other cell types, for example, mouse spinal neurones (Bormann et al., 1987) In addition, the glutamate-gated channels in cones were less chloride-selective than those activated by GABA in other retinal neurones (Attwell et al., 1987). Acetate is impermeant through GABA-gated channels in salamander bipolar cells (Attwell et al., 1987) and Bormann et al., (1987) show that in cultured mouse spinal neurones, the permeability of GABA- and glycine-gated channels to acetate is lower than for the glutamate-gated channels in cones.

7.1.4 How does the glutamate-induced current depend on the external glutamate concentration?

The dose-response data for glutamate show that a significant proportion of the current was activated by 1μM glutamate, compared to the minimal detectable response in turtle photoreceptors evoked by 5μM glutamate (Tachibana and Kaneko, 1988). The data points approximated a Michaelis-Menten relation, i.e. it appears that one glutamate molecule binds to open each channel. Glutamate binds with higher affinity (K_m = 1-6μM) to receptors in the salamander cone membrane, than to glutamate receptors in turtle photoreceptors (K_m = 40μM; Tachibana and Kaneko, 1988), or to the glutamate uptake carrier in Müller cells (K_m = 22μM; Brew and Attwell, 1987).

7.1.5 How does the glutamate-induced current depend on the external sodium concentration?

When the external concentration of sodium was reduced by replacing sodium with equimolar concentrations of choline, the current response to glutamate was reduced (section 3.3.6), but there was no change in the reversal potential of the response.

Thus, although sodium ions do not carry the current produced by glutamate, sodium was essential for the glutamate response. There are three possible reasons for this dependence on sodium:

(1) It may be that removal of external sodium inhibits sodium-calcium exchange in the membrane, resulting in accumulation of calcium inside the cell. This increase in intracellular calcium may close the glutamate-gated ion channels, possibly via a calcium-dependent phosphorylation mechanism, preventing further movement of ions through the channel.

(2) An increase in intracellular calcium concentration has been shown to decrease the affinity of receptors for GABA in sensory neurones from the bullfrog (Inoue et al., 1986) and acetylcholine in pond snail neurones (Chemeris et al., 1982). A similar mechanism might be operating in cones, such that elevated intracellular calcium concentration decreases the affinity of cone receptors for glutamate.

(3) Sodium may simply be required externally in some way, for glutamate to bind to its receptor.

Further experiments are required (see section 7.2.2, Chapter 7) to investigate which, if any, of these possibilities might be correct.

7.1.6 Are the glutamate-gated channels localized to specific regions of the cone cell membrane?

As shown in Fig. 3.6 (section 3.3.5), iontophoresis of glutamate to different regions of the cone cell membrane, showed that the response to glutamate was largest and fastest in onset at the cone synaptic terminal. This implies that the receptors for glutamate are localized to the cone terminal. This localization suggests that glutamate released from a cone may have a feedback action on its own terminal, modulating its own release (i.e. an autoreceptor effect). The magnitude of this current will depend on how close the cone glutamate receptors are to the sites of glutamate release. It may also be the case that glutamate released from neighbouring rods could activate the glutamate receptors at the cone terminal (see Fig. 7.1), since there is ultrastructural evidence for a synapse from rods to cones in the salamander retina (Lasansky, 1973), and chemical evidence in the turtle retina

(Normann et al., 1984), for a synapse between different cone types. Whichever the case, the glutamate receptors are presynaptic (with respect to transmission of information from photoreceptors to second order neurons).

Presynaptic glutamate receptors have previously been suggested to exist in invertebrates (Thieffrey and Bruner, 1978; Thieffrey et al., 1979), and in vertebrate hippocampus (Errington et al., 1987) and olfactory cortex (Collins et al., 1983). In general, autoreceptors mediate a negative feedback action (with the exception of receptors at the terminals of noradrenergic neurons) on the release of neurotransmitter (Starke, 1981). The presynaptic glutamate receptors at the cone terminal could initiate a positive feedback mechanism, serving to increase the gain of cone phototransduction as described below.

7.1.7 What might be the functional significance of receptors for glutamate at the cone synaptic terminal?

Evidence shows that photoreceptors probably release glutamate as a neurotransmitter when electrically stimulated, or when they are depolarized by elevating the extracellular potassium concentration (Miller and Schwartz, 1983; Copenhagen and Jahr, 1989). Glutamate is one of five chemical substances shown to be released from toad photoreceptors (Miller and Schwartz, 1983). Out of these five, only glutamate has an effect on second order neurons (Tachibana, 1985; Attwell et al., 1987).

Fig. 7.1 summarizes the sites of action of glutamate released from the cone terminal. Glutamate gates ion channels in postsynaptic bipolar and horizontal cells. This neurotransmitter action of glutamate is terminated, at least in part, by uptake of glutamate into Müller cells. Some glutamate is probably recycled for further use by uptake into photoreceptors and some glutamate probably simply diffuses away, to be taken up by cells further away. Based on the experiments presented in Chapter 3, I suggest that glutamate released from the cone can also activate presynaptic receptors in the cone terminal.

The functional significance of the glutamate-induced current in the cone terminal is obviously dependent on the normal reversal potential of the current in vivo. The chloride concentration in turtle cones has been estimated (Kaneko and Tachibana, 1986) to be

Fig. 7.1 Schematic diagram summarizing the actions of glutamate released from a cone photoreceptor terminal.

Glutamate is released from the cone when it is depolarized. Activation of voltage-gated calcium channels in the membrane, leads to a rise in intracellular calcium, which results in stored glutamate being released from the terminal, probably by exocytosis.

Glutamate gates postsynaptic channels in bipolar and horizontal cells, and uptake of glutamate back into cone (and rod) terminals and into retinal glial (Müller) cells, assists in terminating the neurotransmitter action of glutamate, recycling it for further use. Glutamate released from the cone may also activate presynaptic channels in the cone membrane, initiating a mechanism which could enhance the amount of glutamate released from the cone. Some glutamate, probably simply diffuses away, to be taken up by cells further away.

Glutamate could also be released from neighbouring rod or cone photoreceptors to the cone terminal, possibly activating the "presynaptic receptors" there. In addition, the cone receives inhibitory synaptic input (GABA) from horizontal cells.

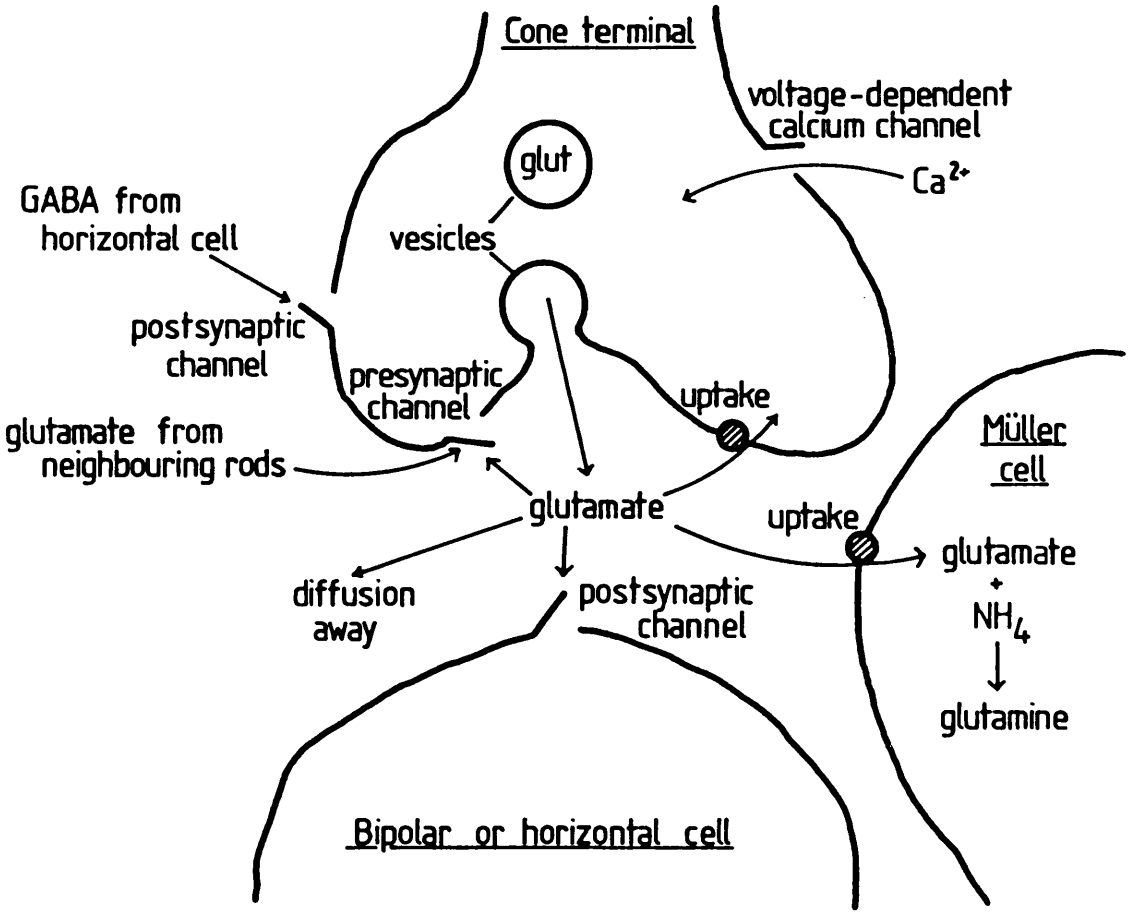
Cone terminal
voltage-dependent calcium channel
glut
Ca^{2+}
GABA from horizontal cell
vesicles
postsynaptic channel
presynaptic channel
uptake
glutamate from neighbouring rods
Müller cell
glutamate
uptake
glutamate
+
NH_4
glutamine
diffusion away
postsynaptic channel
Bipolar or horizontal cell

between 12 and 24mM (assuming the intracellular acetate, or other permeant anion, concentration is the same in vivo as is present inside the patch pipettes), suggesting a reversal potential for the glutamate-evoked current of between -34 and -43mV. Thus, glutamate will produce an inward current, over most, or all of the cone light response range (-40 to -65mV).

This statement would stand more firmly if the exact reversal potential of the glutamate-gated current in vivo was known. If, for example, the permeability of the actual intracellular anions other than chloride was higher than that of acetate, used in the ion substitution experiments described in section 3.3.7 (Chapter 3), then the reversal potential would be more positive than predicted here. This would imply that glutamate would produce an inward current over all of the cone light response range. If, however, the permeability of the actual intracellular anions other than chloride is lower than that of acetate, the reversal potential of the glutamate response would be more negative. Thus, the feedback mechanism mediated by cone receptors for glutamate would probably be negative, rather than positive, over part of the cone light response range.

Maximum glutamate release from photoreceptors in the intact retina occurs in the dark, at the cone dark potential of -40mV. Light-induced hyperpolarization of photoreceptors, decreases the amount of glutamate released (Cervetto and Piccolino, 1974). When a cone is brightly illuminated and polarized to (say) -65mV, so there is no glutamate release, a slight dimming of the light will depolarize the cone, activating voltage-gated calcium channels (see Fig. 7.1), initiating the release of glutamate. The feedback action of the glutamate released will produce an inward current in the synaptic terminal of the cone, depolarizing it further, and causing further release of glutamate. Thus, for a certain change in light intensity, there will be a greater change in the cone voltage, and in the amount of glutamate released, than would occur in the absence of glutamate autoreceptors. This will result in an increase in the gain for the conversion of changes in light intensity into changes in glutamate release. This can be quantified as follows:

If a change of light intensity generates a current change, ΔI_{light}, in the cone outer segment, the change of cone voltage, ΔV,

which results, will be determined by the cone resistance, R, and by the current change evoked by glutamate (ΔI_{glut}), binding to the cone terminal autoreceptors:

$$\Delta V = R(\Delta I_{light} + \Delta I_{glut})$$

If it is assumed that for small changes of light intensity, the change in current evoked by glutamate is proportional to the local change in the concentration of glutamate, which in turn is proportional to the change of membrane potential (so that $\Delta I_{glut} = k\Delta V$ with k a constant), then;

$$\Delta V = R.\Delta I_{light}/(1-kR)$$

so, for kR<1 (i.e. the strength of the feedback loop is too weak to produce a regenerative change of voltage), the changes in cone voltage and the amount of glutamate released are increased by a factor of 1/(1-kR) relative to the situation with no autoreceptors (k=0). This gain increase could be significant, because the glutamate-gated conductance in cones (e.g. 1nS for the cell in Fig. 3.8C and D) is comparable to the light-modulated conductance (0.94nS: Attwell et al., 1982).

It might be expected that such a positive feedback loop could lead to runaway depolarization in the cone. However, in theory, this should not occur as long as the strength of the feedback loop is low enough, compared to the whole-cell resting conductance of the cone membrane (i.e. kR<1 in the equation above). The strength of the feedback mechanism itself depends on several factors, including the magnitude of the glutamate-induced current (compared to the magnitude of the light-induced current), and the voltage-dependence of glutamate released. In addition, depolarization above the cone resting potential is probably counteracted by activation of outward potassium currents (Bader et al., 1982), and in the intact retina release of inhibitory transmitters (e.g. GABA) from horizontal cells onto cones (Fig. 7.1), and uptake of glutamate into photoreceptors and Müller cells, might together help to antagonize the depolarizing effect of glutamate on cones.

Previous studies have shown that cones are not depolarized as described above, when glutamate is perfused onto the intact retina. This may be because (in the dark) the reversal potential for the

glutamate-gated current is close to the cone dark potential, and because (in the light) the glutamate applied to the retina, depolarizes horizontal cells (Miller and Slaughter, 1986), causing release of inhibitory neurotransmitter, for example, GABA, which gates ion channels in cones leading to cone hyperpolarization (Wu, 1986; Kaneko and Tachibana, 1986). For bulk perfusion of glutamate, there will be a large change in voltage in the horizontal cells, and the inhibitory action on cones which results may outweigh the direct depolarizing action of glutamate seen here in isolated cells. However, for spatially restricted changes in illumination, there will be little voltage change in the horizontal cells as a result of changes in transmitter release from one or a few cones (i.e. only a small fraction of the cones projecting to each horizontal cell), and the positive feedback loop for glutamate will not be outweighed by inhibitory inputs from horizontal cells.

7.2 Further experiments to be carried out

7.2.1 Pharmacological profile for the glutamate-induced current

Retinal bipolar and horizontal cells have glutamate-gated channels. They are activated by much lower concentrations of L-glutamate than L-aspartate (Lasater et al., 1984; Ishida et al., 1984; Attwell et al., 1987) and seem to be mainly kainate-type glutamate receptors: that is, they are activated by L-glutamate and its analogues, kainate and quisqualate, but not by NMDA or D-aspartate (Lasater et al., 1984; Ishida, 1984).

Glutamate uptake into retinal Müller cells is activated by L- and D-aspartate, as well as L-glutamate, but not by the glutamate analogues kainate, quisqualate or NMDA (Brew and Attwell, 1987).

Application of these glutamate analogues to salamander cones would allow a test of my conclusion that the glutamate-evoked current is generated largely by ion channels and not by glutamate uptake. The glutamate-evoked current in turtle photoreceptors (Tachibana and Kaneko, 1988) could also be produced by activators of glutamate uptake (i.e L-glutamate, L-aspartate and D-aspartate), and by activators of glutamate-gated ion channels such as kainate (Kaneko and Tachibana, 1987). However, the photoreceptor glutamate-evoked current was not suppressed by the broad band glutamate receptor blocker, kynurenic acid at a concentration of 1mM, but was partially blocked

by 200μM p-chloromercuriphenylsulfonate (PCMPS), a glutamate uptake inhibitor (Balcar and Johnston, 1972). It seems that a proportion, at least, of the current generated by glutamate in turtle photoreceptors, probably results from activation of a glutamate uptake carrier.

It would also be interesting to see whether the proposed presynaptic receptors for glutamate were of the kainate-type, since Ferkany et al., (1982) have shown that kainate stimulates release of excitatory transmitters at presynaptic glutamatergic receptors in mouse cerebellum.

7.2.2 How could the dependence of the glutamate-induced current on external sodium be investigated further?

It would be possible to distinguish between at least two of the postulated reasons for the observed sodium-dependence of the glutamate response (section 7.1.5), by removing external sodium while the external concentration of calcium is low. If sodium removal inhibits a sodium-calcium exchanger in the membrane, causing an increase in the intracellular calcium concentration which inhibits the response to glutamate, then removal of external sodium in the absence of external calcium, should not induce a rise in intracellular calcium concentration, and the glutamate response should remain. If, however, sodium is simply required externally for glutamate to bind to its receptor, then removal of external calcium while sodium is absent should have no effect and the glutamate response will still be abolished.

7.2.3 Does the anion acetate carry any of the current induced by glutamate?

To determine whether part of the glutamate-induced current is carried by acetate ions, acetate ions could be replaced by a larger, presumably impermeant anion species, such as gluconate, for different values of patch pipette chloride. If acetate carries the other part of the current not carried by chloride ions, then replacing acetate with gluconate should shift the observed reversal potentials much closer to the chloride equilibrium potentials for each value of patch pipette chloride.

7.2.4 Do the glutamate-gated channels increase the gain of cone phototransduction?

If the pharmacological analysis suggested above reveals specific blockers of the glutamate-gated channels in the cone synaptic terminal, application of these blockers in the intact retina would allow a test of whether the postulated positive feedback loop increases the gain for conversion of light into a voltage change.

7.3 Discussion of Chapter 4

7.3.1 What is the functional significance of the difference in response properties of sustained and transient ganglion cells in response to injected current?

Ganglion cells in the intact retina and isolated ganglion cells can respond in a sustained or transient way to injection of depolarizing current (sections 4.3.1 and 4.3.2, Chapter 4). These sustained and transient response cell types are similar to those which have been shown respectively to respond in a sustained way to maintained illumination or darkness, and those that generate only a transient response when a light is turned on or off.

It has been suggested that sustained cells may be used for encoding fine differences of light intensity in an image, and that transient cells play a role in movement detection: transient ganglion cells will only generate a response signalling that a change in light intensity has occurred.

This can be seen from Fig. 4.1, in which the dependence of action potential frequency on injected current within the first second of the current injection pulse, is different for sustained (Fig. 4.1B) and transient cells (Fig. 4.1D). Sustained ganglion cells respond to different sizes of injected current (mimicking synaptic current injected from bipolar cells) by generating more action potentials, as the size of current injected increases. However, this only occurs over a limited response range, at frequencies over a 20-fold range (in this cell between 2-40 action potentials/sec), with the number of action potentials produced being proportional to the size of injected current for low currents (up to 20pA in this cell), and the number of action potentials produced saturating at higher currents. Transient cells generate a brief response at the onset of current injection which does not increase with further increases in current amplitude, suggesting that they do, indeed, generate a response which simply signals a change in synaptic input.

It has recently been shown that the size range of the synaptic current (up to 300pA) measured in response to light of different intensities, in ganglion cells in retinal slices, is comparable to the range of injected currents used here (200-300pA of current was injected into some ganglion cells) to investigate the response

properties of both isolated ganglion cells, and ganglion cells recorded from in the intact retinal flatmount (Mobbs et al., manuscript in preparation). In fact, these authors report that the range of synaptic currents generated by light (up to 300pA) is much larger than the range of currents that even sustained ganglion cells can convert into different action potential frequencies (Fig. 4.1). Thus, sustained (Fig. 4.1B) and transient (Fig. 4.1D) ganglion cell responses to current injection would appear to saturate at injected currents which are well below the corresponding maximum synaptic input. This suggests that ganglion cells can only convert the part of the bipolar synaptic input resulting from low light intensities, into different frequencies of action potentials, and larger light-evoked signals will be clipped at the bipolar to ganglion cell synapse. A similar signal clipping mechanism is seen at the photoreceptor to bipolar cell synapse (Attwell et al., 1987).

7.3.2 Can isolated ganglion cells be divided into sustained and transient cell types in response to current injection?

It has previously been suggested that the division of ganglion cells into sustained and transient classes is a result of different types of excitatory synaptic input to sustained and transient cells (Ikeda and Sheardown, 1982). However, section 4.3.2 in Chapter 4 shows that cells isolated from the retina and thus devoid of synaptic input from neighbouring cells, can produce sustained or transient bursts of action potentials in response to injected current. The occurrence of sustained and transient response types was not correlated with cell seal resistance, input resistance, pipette series resistance, or resting membrane potential for both isolated ganglion cells and ganglion cells recorded from in the intact retina. This implies that whether a ganglion cell is sustained or transient may depend to a large extent on the inherent properties of the ganglion cell membrane itself.

7.3.3 Which voltage-gated currents are present in the isolated ganglion cell membrane?

Using whole-cell patch-clamping techniques and applying depolarizing voltage steps to identified isolated ganglion cells under voltage-clamp (section 4.3.4, Chapter 4), it was possible to show the existence of at least three voltage-gated currents in

salamander ganglion cells, a sodium current (I_{Na}), a calcium current (I_{Ca}) and a potassium current (I_K).

Each membrane current was separated by its characteristic voltage-dependence and by a differential sensitivity to various specific channel blockers. I_{Na} was reversibly blocked by external application of 1μM TTX, and showed classical Hodgkin-Huxley type activation (the sodium current activated steeply over the voltage range -35 to -25mV, similar to that seen for the sodium current isolated in rat retinal ganglion cells; Lipton and Tauck, 1987). I_{Ca} was suppressed externally by the divalent cation cobalt (2mM), and a patch pipette solution with potassium ions replaced by caesium ions, plus TEA (10mM), blocked the outward potassium current which was activated at potentials depolarized from the resting potential. The blocking ability of these concentrations of TTX, TEA, caesium and cobalt, on their respective conductances, must have been almost complete since a combination of these specific drugs left only a tiny residual current component (Fig. 4.3B, lowest panel).

I_K activated relatively slowly over the range -60 to +20mV (with the fastest rate of activation in the range -20 to 0mV). The behaviour of I_K in ganglion cells resembled that of the transient outward potassium current (A-current) described in marine gastropod neurons by Connor and Stevens (1971b), in that I_K was activated at potentials above -50mV (in gastropod neurons, above -40mV, a delayed outward potassium current, called K-current by Connor and Stevens (1971a, 1971b), is activated). Further, like the A-current, once activated, I_K in ganglion cells rose rapidly to a peak and decayed exponentially during depolarization, and the peak current amplitude increased as the cell was stepped to more depolarized potentials. However, it can be seen from Fig. 4.3A (section 4.3.4, Chapter 4), that I_K decays to a plateau level, which is dependent on the voltage step, over the time scale shown, whereas the A-current (inactivated over a similar range of depolarized potentials) decays essentially to zero within 200 to 700msec.

These observations might suggest that the potassium current observed in ganglion cells might have more than one outward current component. For example, a combination of a transient outward current (or A-current), which is activated from -60mV, and a

delayed outward K-current, activated from more depolarized potentials (around -30mV), could respectively explain the initial transient outward current component, and the maintained outward current which follows.

The calcium current in Fig. 4.3B (centre panel), shows an initial transient component, followed by a more prolonged component. Karschin and Lipton (1989) have recently shown that the calcium current of isolated rat retinal ganglion cells has a similar shape, that is attributable to two separable components; a transient component that is activated between -50mV and -30mV, and a prolonged sustained current component that activates above -40mV. These components respectively resembled the T- and L-type calcium channels which have been described in mouse neuroblastoma cells (Narahashi et al., 1987), on the basis of differences in voltage-sensitivity and pharmacology of channel block. I suggest that two similar components might be present in salamander ganglion cells, to explain the shape of the calcium current and the dependence of the current on voltage.

7.3.4 How might these voltage-gated currents account for the division of ganglion cells into sustained and transient classes?

Exactly what differences in voltage-gated currents result in some ganglion cells being "sustained" and some being "transient" remains to be determined. However, it is possible to speculate on how specific relationships between the membrane currents present in ganglion cells might produce these cell classes.

One explanation is suggested by the properties of amacrine cells in the tiger salamander retina. These have a sodium current, calcium current, and a calcium-dependent outward potassium current. The role of these voltage-gated currents in the generation of the amacrine cell transient response, at the onset or offset of illumination, has been investigated by examining the properties of the currents present (Barnes and Werblin, 1986), and by carrying out computer simulations of the voltage response to current injection (Eliasof et al., 1987).

Barnes and Werblin (1986) found that the production of a transient response in amacrine cells was mediated by a specific non-overlapping relationship between the potential ranges for sodium current inactivation (between -60 and -20mV) and potassium

current activation (positive to -20mV). Thus, a maintained depolarizing current step elicits an initial action potential, but subsequent activation of the potassium current does not hyperpolarize the cell enough to remove much sodium inactivation. Consequently, a depolarization from this level, would not generate enough inward sodium current to initiate another action potential.

In ganglion cells, the extent to which the sodium and potassium currents overlap may vary in different cells, so that if some ganglion cells have a non-overlapping and some have an overlapping relationship between I_{Na} inactivation and I_K activation, the occurrence of sustained and transient ganglion cell classes might be explained. However, so far, no correlative study of the range of overlap of these currents with "sustained" or "transient" responses has been performed.

In simulated models of the salamander amacrine cell voltage response to current injection, alteration of various parameters makes it possible to convert a "transient" response into a "sustained" one (Eliasof et al., 1987). For example, increasing the magnitude of the sodium conductance by a factor of 5, on the simulated voltage response to injected current, permits a greater sodium current, allowing the membrane to depolarize further, leading to generation of more action potentials and thus simulating the behaviour of a "sustained" cell. It may be that a similar situation exists in ganglion cells. Different densities of voltage-gated currents might be present in different ganglion cells; cells having more sodium channels, and hence a larger sodium current (with respect to the size of the potassium current), may behave as "sustained " cells, for the reason described above, and ganglion cells with fewer sodium channels may thus exhibit transient behaviour. In isolated ganglion cells, it was found that I_{Na} was slightly larger with respect to I_K in cells which responded in a sustained way to injected current.

It might be that slow activation of a calcium-dependent potassium current, contributes to the generation of a transient response. The magnitude of any calcium-dependent potassium current has so far not been correlated with the occurrence of "sustained" or "transient" behaviour in ganglion cells. To distinguish between these possible explanations for the basis of sustained and

transient response classes, more detailed experiments on the properties of ganglion cell currents are necessary (see section 7.4.3).

7.4 Further experiments to be carried out

7.4.1 Can the potassium current be pharmacologically separated into different components?

Since all potassium currents are blocked by application of TEA to the intracellular membrane surface, and hence internal cell receptors for TEA are probably the same in all cells, incorporation of TEA into the patch pipette (as for the ganglion cell in Fig. 4.3B, section 4.3.4, Chapter 4), blocked the outward potassium current but revealed no further information about different types of potassium current that might be present.

As Thompson (1977) has shown in molluscan neurones, it is possible to separate three different potassium currents pharmacologically, on the basis of their sensitivity to external application of TEA and other drugs. The pyridine, 4-aminopyridine blocks the transient A-current, but has little effect on the delayed outward potassium (K) current (which contains a calcium-dependent current component). TEA reversibly block the delayed outward K-current, but at similar concentrations, is much less effective in blocking the calcium-dependent potassium current, or the A-current. Cobalt or manganese ions, or removal of calcium from the external medium, reversibly blocks the slow calcium-dependent delayed outward potassium current, without affecting either of the other two types of potassium current. A similar pharmacological analysis of I_K in salamander ganglion cells could be performed in this way.

7.4.2 Can the calcium current be separated into different components?

From known activation and inactivation ranges of transient (T-type) and long-lasting (L-type) calcium channels, an attempt to separate the salamander calcium current into similar components could be made by trying to inactivate any rapid transient component by holding the membrane at a depolarized potential (above -40mV, for example). This should preserve the more prolonged calcium current component.

Possible pharmacological separation of T- and L-type current components could be tried by applying 1,4-dihydropyridines, such as nifedipine, or cadmium ions, which are more selective for L-type calcium channels. There are fewer selective antagonists for T-type calcium channels. Nickel, and low doses of cobalt (e.g 1mM; Narahashi et al., 1987) could be tried.

7.4.3 Are the properties of the voltage-gated currents different in "sustained" and "transient" ganglion cell types?

In both isolated ganglion cells and ganglion cells in the intact retina, a correlative study could be made of the occurrence of sustained and transient cell response types with, for example, the degree of overlap of I_{Na} inactivation and I_K activation ranges, the relative sizes of I_{Na} and I_K, and the size of I_{Ca} (section 7.3.4). Quantifying these currents in the intact retina is further complicated by the fact that it is more difficult to adequately voltage-clamp the cells. An attempt to record from cells while blocking most of the large currents (I_{Na} and I_K) under study would reduce voltage error due to series resistance and enable a more accurate estimation of activation and inactivation kinetics.

7.5 Discussion of Chapter 5

7.5.1 Do ganglion cells have receptors for L-glutamate?

If the putative bipolar to ganglion cell transmitter is glutamate, then isolated ganglion cells should express receptors for glutamate and thus respond to applied glutamate.

L-glutamate was applied by iontophoresis or bath perfusion to isolated salamander ganglion cells voltage-clamped to their resting potential of around -60mV. This isolated cell preparation allowed observation of the direct effects of glutamate (and glutamate analogues), on identified ganglion cells, in the absence of possible confounding synaptic input from other retinal cells.

Glutamate produced an inward current at -60mV, in 67% of cells tried (n=120). Glutamate has also been shown to have a similar effect on ganglion cells isolated from the rat retina (Aizenman et al., 1988a), and ganglion cells in the intact rabbit retina (Massey and Miller, 1988). The ganglion cell response to glutamate (in tiger salamander) was usually non-desensitizing, for perfusion of doses up to 100μM, or iontophoresis of glutamate onto the cells.

Immunocytochemical localization of the enzyme aspartate amino transferase (which can convert glutamate into aspartate), shows that its activity is high in the inner retina of the rat (Lin, 1983). In addition, aspartate has been shown to have excitatory effects on rabbit retinal ganglion cells, which are as potent as those produced by glutamate (Bloomfield and Dowling, 1985). This suggests that aspartate, as well as glutamate, might function as a neurotransmitter to ganglion cells.

L-aspartate (100μM) produced a small current (20pA) in isolated ganglion cells, comparable to that produced by glutamate (35pA) at the same dose. It is interesting that these ganglion cells respond to both aspartate and glutamate, because it has been suggested that L-aspartate may be the excitatory transmitter mediating light excitation of sustained ganglion cells but not transient cells in the cat retina in vivo (Ikeda and Sheardown, 1982).

7.5.2 How do any glutamate receptors present respond to the glutamate analogues kainate, quisqualate and NMDA?

Application of L-glutamate to isolated ganglion cells revealed the presence of receptors for glutamate. Since L-glutamate is known

to be a rather non-selective agonist, activating kainate, quisqualate and NMDA receptor subtypes in other preparations (Westbrook and Mayer, 1984), kainate, quisqualate and NMDA were applied in turn to isolated ganglion cells.

This revealed that for concentrations up to 100μM, kainate was the most effective agonist (section 5.3.4, Chapter 5), both in the number of cells which responded (all cells responding to glutamate also responded to kainate, but not all responded to quisqualate or NMDA), and in the magnitude of the kainate-induced currents (which were always larger than those produced by glutamate). However, at lower doses of glutamate agonists (10μM), the response to quisqualate was sometimes larger than that to kainate.

Bath perfusion of NMDA at concentrations of up to 100μM, produced tiny (10-15pA) currents in only a few isolated ganglion cells tested, with magnesium present in the extracellular solution. The presence of magnesium might have prevented detection of responses to NMDA at negative potentials, due to a voltage-dependent open channel block by external magnesium ions, as has been shown in mouse neurons by Nowak et al. (1984). This might be the case, since application of lower doses (50μM) of NMDA to isolated rat ganglion cells (Aizenman et al., 1988a) in the absence of extracellular magnesium, produced detectable currents of 30 to 40pA in the negative potential range over which magnesium is known to block the NMDA receptor open channel. These authors also found that only about 60% of cells tested responded to NMDA.

However, application of NMDA to unresponsive salamander ganglion cells held at very positive potentials (+70mV) to remove any voltage-dependent block by magnesium produced responses in only 12% of cells tested (n=24). Removal of magnesium from the extracellular solution, produced responses in 60% of cells tested (although the number of cells tested was not as great, n=5).

Another explanation for lack of ganglion cell responses to NMDA might be that different types of retinal ganglion cells have different populations, or distributions of each receptor subtype, such that lack of response to NMDA reflects a real lack of receptors for NMDA on those ganglion cells studied. This is feasible, since Lukasiewicz and McReynolds (1985) propose that glutamate activates NMDA receptors on sustained ganglion cells, and

may act at non-NMDA receptors on transient ganglion cells.

It is also possible that NMDA receptors may have been lost, (through loss of dendrites containing receptors for NMDA), or became inactive during the cell isolation procedure. It is known that enzyme treatment can remove receptors or render them inactive (Lee et al., 1977). Enzyme-treated rat hippocampal neurons selectively lose their sensitivity to NMDA, whereas mechanically dissociated neurons were responsive to all excitatory amino acids (Akaike et al., 1988). Loss of ganglion cell receptors for NMDA during cell isolation by enzyme treatment, or loss of dendrites containing NMDA receptors, probably explains the lack of ganglion cell responses to NMDA, since application of NMDA to ganglion cells in the intact retinal flatmount produced current responses in all cells tested (n=5; section 5.3.9). Surprisingly, the voltage-dependence of this NMDA-induced current showed strong outward rectification although the Ringer's used contained nominally zero magnesium. Normally, the outward rectification of NMDA responses is attributed to a voltage-dependent block by magnesium at negative voltages.

For low doses of glutamate and agonists (10μM), the order of agonist potency was kainate > quisqualate > glutamate > NMDA, or quisqualate > kainate > glutamate > NMDA. The former is similar to that seen in ganglion cells in the intact retina in mudpuppy (Slaughter and Miller, 1983c), and rabbit (Bloomfield and Dowling, 1985). For higher doses (100μM), the pharmacological selectivity was always kainate > quisqualate > glutamate > NMDA, as seen for ganglion cells in the intact rabbit retina (Massey and Miller, 1985). The presence of all three glutamate receptor subtypes has also been shown in isolated rat retinal ganglion cells, with glutamate receptors being most selective for kainate, (Aizenman et al., 1988a), and the glutamate and glutamate analogue-induced currents having similar properties to those described here.

It seems, therefore, that receptors for glutamate on isolated ganglion cells of the inner retina are primarily of the kainate type, not altogether a surprising finding, since outer retinal neurons (bipolar and horizontal cells) also express kainate-type receptors for glutamate.

7.5.3 Is the response to glutamate localized to appropriate regions of the ganglion cell membrane?

Iontophoresis of glutamate to different regions of the ganglion cell membrane showed that the response to glutamate was largest and fastest in onset at the tips of the dendrites. This suggests that the receptors for glutamate are localized to this membrane region, in an appropriate position for receiving neurotransmitter glutamate released from presynaptic bipolar cell synaptic terminals.

7.5.4 Could different classes of glutamate receptors be localized to different regions of the ganglion cell membrane?

As shown in section 5.3.4 (Chapter 5), for low doses (10μM) of glutamate analogues, some isolated ganglion cells responded maximally to kainate and others responded maximally to quisqualate. For higher doses (100μM) of these drugs, kainate always produced the largest response. Thus, it appears as though kainate-type receptors are preferentially activated on ganglion cells.

However, it may be that different ganglion cell types express different populations of glutamate receptor subtypes, or glutamate receptor subtypes are localized to different regions of the ganglion cell membrane. The latter has been demonstrated in rat cerebellar type-2 astrocytes, which have glutamate receptor channels which are activated by kainate or quisqualate, but not by NMDA (Usowicz *et al.*, 1989). Cull-Candy *et al.* (1989) show by iontophoretic mapping of the response to kainate and quisqualate in these cells, that the response to kainate was largest at the dendrites, and that to quisqualate, on the cell body.

It has also been shown recently by Jones and Baughman (1988), that NMDA as well as non-NMDA receptors are highly localized along different regions of dendrites in cerebral cortex cells. These cells had a response to glutamate which consisted of an NMDA component and a non-NMDA component. Dendritic "hot spots" two to three times more sensitive to glutamate than neighbouring regions of dendrites, were shown to result from either an enhanced NMDA component, a larger non-NMDA component, or a strengthening of both components.

If glutamate receptor subtypes were localized in ganglion cells in this way, then possible loss of certain glutamate receptor

subtypes might explain why, for example, some isolated ganglion cells responded maximally to quisqualate rather than to kainate, and others were unresponsive to NMDA.

The possibility that glutamate receptors for kainate, quisqualate and NMDA might be localized in a similar way in retinal ganglion cells, could easily be tested using the above method (see also section 7.6.3).

7.5.5 Is it possible that desensitization of ganglion cell receptors for glutamate contributes to the generation of transience in the light response of ganglion cells?

If the release of the bipolar cell neurotransmitter is tonic, then one possible mechanism of generation of transience in the ganglion cell light response, might be by desensitization of ganglion cell receptors for glutamate with time, such that applied glutamate only changes the ganglion cell membrane potential sufficiently to generate a burst of action potentials at the start of glutamate application.

Although the synaptic current evoked by light in both sustained and transient ganglion cell types exhibits a degree of transience (Mobbs et al., manuscript in prep.), in general, application of the putative transmitter, glutamate, by iontophoresis or by bath perfusion, produced non-desensitizing current responses in isolated ganglion cells. This implies that desensitization of the ganglion cell response to glutamate is probably not a mechanism by which transience may be introduced into the light response of ganglion cells.

In section 5.3.2 (and Fig. 5.2), application of glutamate by iontophoresis to a ganglion cell held at its resting potential, produced an inward current of 250pA, and bath perfusion of 100uM kainate produced an inward current of about 300pA in other cells (section 5.3.4). These large inward currents would be sufficient to significantly depolarize ganglion cells, allowing production of bursts of action potentials. Taking the cell of Fig. 5.2 as an example, for a 250pA change in current in this cell, which had an input resistance of 200MΩ, there would be a voltage change (depolarization) in the cell of 50mV, large enough to depolarize the ganglion cell far enough from its resting potential of -60mV,

to fully activate sodium channels in the membrane (section 4.3.5, Chapter 4), resulting in action potential generation.

Indeed, isolated ganglion cells held in current-clamp, were seen to respond to iontophoretically applied glutamate with a large depolarization from around the resting potential, accompanied by the production of a sustained burst of action potentials (n=3; data not shown). These sustained ganglion cell responses were similar to those obtained by current injection (sections 4.3.1 and 4.3.2, Chapter 4). Further experiments are required, to see if the ganglion cell response to glutamate is always sustained. If so, this would support the above conclusion that desensitization of ganglion cell receptors for glutamate does not contribute to generation of transience in the ganglion cell light response. However, this does not eliminate the possibilty that sustained and transient ganglion cells (in response to injected current or to light), might each express receptors for different putative excitatory neurotransmitters, as has been previously suggested (Ikeda and Sheardown, 1982; Lukasiewicz and McReynolds, 1985).

Although the isolated ganglion cell response to glutamate was usually non-desensitizing, the response to kainate (at 100μM) and quisqualate (at both 10μM and 100μM), sometimes showed varying degrees of desensitization. The response to high concentrations of kainate showed continual slow desensitization during the period of drug application (see Fig. 5.5B). This concentration of quisqualate also introduced desensitization into the response, and for the cell in Fig. 5.5B, the glutamate-induced current also showed slight desensitization with time. In rat retinal ganglion cells, 100μM concentrations of glutamate and quisqualate, but not kainate, introduced a desensitizing phase into the response (Aizenman et al., 1988a). Desensitization was only introduced into the rat ganglion cell response to NMDA at higher (500μM) drug concentrations. In salamander, for lower concentrations of quisqualate (10μM), some cells responded with a non-desensitizing current, but others showed a rapidly desensitizing component, occuring within about 40msec, followed by a non-desensitizing phase. It may be that this early component was only seen in cells for which the perfusion rate was sufficiently high. Rapidly desensitizing responses to quisqualate, occuring over a similar

time scale (desensitizing within 100msec to a maintained level) have also been seen in other neurons e.g. in mouse hippocampal neurons (Mayer et al., 1989). As most salamander ganglion cells respond to glutamate with a sustained current, even at high doses, it is rather difficult to explain transience in, for example, the quisqualate response.

It has been suggested that rat retinal ganglion cells can express two distinct receptors for quisqualate, based on the inhibitory actions of kynurenate (a general excitatory amino acid receptor antagonist), and CNQX (6-cyano-2,3 dihydroxy-7-nitroquinoxaline, a kainate and quisqualate, but not NMDA receptor antagonist) on responses produced by quisqualate and another agonist, AMPA, in these cells (Aizenman et al., 1988b). Further experiments are required to clarify the situation in salamander ganglion cells, possibly by correlating sustained and transient ganglion cell response types with receptor subtypes present (see section 7.6.4).

7.6 Further experiments to be carried out

7.6.1 Is glutamate the bipolar to ganglion cell transmitter in salamander?

It might be possible to show that an excitatory amino acid (maybe glutamate) is released from isolated salamander bipolar cells, using the technique described recently by Copenhagen and Jahr (1989) for detecting excitatory amino acid release from turtle photoreceptors. In a preparation of isolated salamander bipolar and ganglion cells, outside-out membrane patches from (labelled as in section 2.5.1, Chapter 2) ganglion cells, could be held in close apposition to intact bipolar cell synaptic terminals, in an attempt to detect any release of substances released from bipolar cells when they are electrically stimulated. A change in the frequency of channel openings in the ganglion cell membrane patch, would indicate a postsynaptic effect of any substance released from a bipolar cell. Although the open channel conductance could be measured and compared to that seen for excitatory amino acid-gated conductances in other cell types, the conclusion would certainly be complicated by the fact that several substances are probably co-released from bipolar cells, as in photoreceptors (Miller and Schwartz, 1983).

7.6.2 Further pharmacology of the ganglion cell glutamate response

A more complete pharmacological profile for the ganglion cell glutamate response would be obtained by investigating the actions of excitatory amino acid antagonists on isolated ganglion cells. Both broad spectrum antagonists such as kynurenate (Ganong et al., 1983), and other antagonists which have more specific actions on different glutamate receptor subtypes (Watkins and Olverman, 1987) could be tried. For example, kynurenate has been shown to block (at 300μM) the response to kainate and NMDA, but not that to quisqualate, in isolated rat retinal ganglion cells (Aizenman et al., 1988a). The response to NMDA in these cells was also blocked by the NMDA receptor-specific blocker, APV (2-amino-5-phosphonovalerate; Davies et al., 1980), The quinoxaline compounds, CNQX and DNQX (Drejer and Honore, 1988), which are much more potent antagonists at quisqualate and kainate receptor sites than NMDA receptor sites, have been shown to block the quisqualate- and kainate-induced excitation of sustained cat ganglion cells, in the optically intact in vivo eye (Ikeda et al., 1989).

However, although application of agonists and antagonists helps to define the relationship between agonist, receptor and antagonist, the situation has recently become more complicated. Reports show that quisqualate, as well as acting as an agonist on some (rat) ganglion cells, can also antagonize the response to kainate in cells which have little or no response to quisqualate alone (Aizenman et al., 1988a). Karschin et al. (1988) have shown that NMDA can also act as a (competitive) antagonist for kainate receptors.

7.6.3 Localization of glutamate receptor subtypes to different regions of the ganglion cell membrane

By applying glutamate analogues individually by iontophoresis, to isolated ganglion cells, it would be possible to map the distribution of receptors for kainate, quisqualate or NMDA. This has been done for kainate and quisqualate receptors in rat cerebellar type-2 astrocytes, showing that kainate receptors are localized to the dendrites, and quisqualate receptors localized to the cell body (Cull-Candy et al., 1989).

7.6.4 Could sustained and transient ganglion cell types express different receptors for glutamate?

The possible differences between synaptic input to sustained and transient ganglion cells, could be investigated by correlating sustained and transient isolated ganglion cell responses (to current injection) with the pharmacological actions of excitatory amino acid agonists and antagonists on each cell type. This is interesting because the origins of this difference in ganglion cell response properties has previously been suggested to be at least partly due to different types of synaptic input to sustained and transient cells (Ikeda and Sheardown, 1982; Lukasiewicz and McReynolds, 1985).

7.6.5 Do glutamate analogues produce responses in ganglion cells in the intact retina with properties similar to those seen in isolated ganglion cells?

Ganglion cells in the intact retinal flatmount respond to bath application of 100μM NMDA (in the absence of external magnesium), in a similar way to a few isolated ganglion cells responding to NMDA (sections 5.3.9 and 5.3.10). The actions of other glutamate analogues may be investigated by perfusing the retinal flatmount with cobalt or manganese (to block calcium-dependent transmitter release from second order neurons), and perfusing glutamate agonists and antagonists, in turn, to patch-clamped ganglion cells. (Note, however, that cobalt blocks NMDA receptor channels (Mayer & Westbrook, 1987). A study of the possible correlation between sustained and transient ganglion cell responses (to injected current) and the pharmacology of glutamate agonists and antagonists in each cell type, could also be performed in the intact retina as for isolated ganglion cells.

7.6.6 Are the properties of the glutamate-induced current similar to those of the synaptic current evoked by light in ganglion cells?

By recording from dark-adapted neurons in the ganglion cell layer of the retinal slice, it would be possible to investigate the properties of the synaptic current evoked by light in these cells, and hence compare these with the properties of the current evoked by the putative neurotransmitter, glutamate, in isolated ganglion cells.

It would not be possible to unequivocally identify neurons as

ganglion cells with the fluorescent stain used to identify isolated ganglion cells and ganglion cells in the intact retina because the retina must remain dark-adapted in order to preserve the cells' light responses. However, 70% of cells in the ganglion cell layer are ganglion cells (Cook and Mobbs, 1988), thus most recordings would probably be from ganglion cells.

Mobbs et al. (unpublished results) have shown that the light-evoked synaptic current has a waveform which is transient, unlike the response to glutamate, which is usually maintained (non-desensitizing). The current-voltage relation for the light-evoked current has an average reversal potential (-13±3mV for 5 cells, with 30mM chloride in the patch pipette) similar to that seen for glutamate in isolated ganglion cells (-16±7mV for 10 cells, with 3mM chloride in the patch pipette).

Although the light-evoked current showed transience, both sustained and transient cells (in responses to light) had a similar degree of transience in the synaptic current evoked by light. Thus it seems unlikely that transience in ganglion cells (in response to light, or injected current) is generated by transience in the synaptic input.

7.7 Discussion of Chapter 6

7.7.1 Do isolated ganglion cells have receptors for GABA and/or glycine?

All isolated ganglion cells tested responded to iontophoretic application of GABA or glycine, with a current response in whole-cell patch-clamp mode which desensitized over several seconds during sustained application of the agonists. Cells were not tested for the presence of both GABA and glycine receptors, but virtually all ganglion cell types (ON, OFF and ON-OFF in response to light) in the intact mudpuppy retina respond to both agonists (Miller et al., 1981, Belgum et al., 1984).

The response to glycine was dose-dependent in the range 10μM to 1mM (section 6.3.6, Chapter 6), with a half-maximal peak response at 84μM. This can be compared to the value of 700μM, found for both GABA and glycine-gated channels in the intact retina of mudpuppy (Belgum et al., 1984). However, the actual concentration at synaptic sites in the intact retina is probably less, due to uptake and rapid metabolism by neurons and glia.

Receptors for GABA have been shown to be of the $GABA_A$ subtype, which gate chloride channels in the outer (Kaneko and Tachibana, 1986) and inner retina (Miller et al., 1981; Ishida and Cohen, 1988). Application of the $GABA_A$ antagonist, bicuculline methiodide, to isolated salamander ganglion cells, blocked the GABA-evoked chloride current (section 6.3.2) indicating that receptors for GABA in these cells are also probably $GABA_A$ receptors. Glycine responses were consistently and reversibly blocked by the glycine antagonist, strychnine.

It has been suggested that amacrine cells in Necturus (mudpuppy) retina are either GABA- or glycine-releasing (Miller et al., 1977). In addition, perfusion of strychnine over the intact retina of mudpuppy blocks the transient, but not the sustained response of ganglion cells to light (Belgum et al., 1984). Perfusion of GABA antagonists had no effect on the transient ganglion cell response to light. These facts together suggest that GABA and glycine may mediate functionally different kinds of inhibitory synaptic inputs to ganglion cells, since transient and sustained inhibitory inputs to mudpuppy ganglion cells may be mediated by different inhibitory neurotransmitters.

7.7.2 Do GABA and glycine gate conventional chloride channels in salamander ganglion cells?

Currents activated by both GABA and glycine were demonstrated to be chloride-dependent, by investigating the dependence of the current reversal potential (V_{rev}) on patch pipette chloride concentration. For both GABA and glycine, the dependence of the current reversal potential on chloride concentration deviated from that predicted by the Nernst equation. Assuming acetate carried part of the agonist-induced current, permeability ratios $P_{acetate}/P_{Cl}$ were 0.034 and 0.024 for GABA and glycine respectively. Thus, acetate seems to pass more easily through the GABA-gated chloride channel, an observation consistent with that found for GABA-gated chloride currents in some other cell types (Bormann et al., 1987), but contrary to that found recently in isolated goldfish ganglion cells, in which the GABA-gated current was chloride-specific (Ishida and Cohen, 1988; Cohen et al., 1989). It has yet to be proven conclusively that acetate is indeed the other current-carrying ion in salamander ganglion cells.

To calculate the GABA and glycine-induced current reversal potentials, straight lines were always fitted to the data for consistency (sections 6.3.3 and 6.3.4). The majority of cells showed perfect linear behaviour (with the calculated best fit line for their current-voltage relation having a correlation coefficient of 1), although in some cases it was clear that the points could be just as well fitted with a curve showing outward rectification. A straight-line fit to the data will tend to make the reversal potential more negative than the actual value, in cases where outward rectification was seen. The magnitude of this error, if present, was usually only 2-3mV, although in two cells responding to glycine with 42mM patch pipette chloride, this error was much larger (8-10mV).

Outward rectification has also been observed for similar chloride conductances in mouse spinal neurones (Bormann et al., 1987) and mammalian dorsal root ganglion cells (Robertson et al., 1989). This property is attributed to the voltage-dependence of channel gating in these cells. i.e. that the probability of channel opening increases with depolarization.

Outward rectification in salamander ganglion cells might

result from low internal chloride, since there would be fewer ions to carry inward current than there would be to carry outward current. However, rectification was not only seen in ganglion cells patched with a low pipette chloride, but was also seen for higher patch pipette chloride concentrations, making this suggestion unlikely. Further experiments are required to investigate the exact nature of this difference in voltage-dependence between cells.

7.7.3 How are chloride ions important for inhibition in the retina?

The relation between the reversal potential for chloride ions and the resting membrane potential of ganglion cells provides a framework for understanding inhibition in the retina. An increase in chloride conductance associated with the actions of GABA or glycine, could produce inhibition (suppression of action potential production) in ganglion cells by any one of the mechanisms discussed in section 1.3.7 (Chapter 1).

1. Application of GABA to ganglion cells in the intact retina produces a hyperpolarization below their resting potential. This implies that the intracellular chloride concentration *in vivo* is low. Miller and Dacheux (1983) have shown using intracellular chloride electrodes that the measured chloride concentration in ganglion cells is indeed low. Inhibitory amino acid neurotransmitters will only induce a hyperpolarization when the reversal potential for chloride ions is negative to the resting potential of that cell. In mudpuppy, inhibition of ganglion cells by GABA or glycine occurs by this mechanism (Miller *et al.*, 1981) and it is likely that a similar mechanism produces inhibition in salamander ganglion cells.

2. Movement of chloride ions out of the ganglion cell could keep the cell sufficiently depolarized to prevent removal of sodium current inactivation and thus, inhibit action potential production.

3. Shunting inhibition occurs when the reversal potential for chloride ions is close to the cell resting potential so there is no net movement of chloride ions into or out of the cell. An increase in chloride conductance produced by GABA or glycine can greatly reduce the cell membrane resistance without changing the membrane potential. This mechanism has been shown to operate in mudpuppy

amacrine cells (Miller et al., 1981). The cells are inhibited because the voltage change resulting from a given amount of charge movement is reduced, so that a larger excitatory input is required to produce a certain depolarization.

7.7.4 Do ganglion cells have receptors for the peptide, substance P?

Immunohistochemical studies have localized the peptide, substance P, to amacrine cells in the retinae of lower and higher vertebrates (Eskay et al., 1981; Karten and Brecha, 1980). It has also been shown that substance P can be released in a calcium-dependent way from bullfrog retina by depolarization with high external potassium (Eskay et al., 1980). If substance P is used as a neurotransmitter or neuromodulator from amacrine to ganglion cells, then exogenously applied substance P should influence the electrophysiological properties of ganglion cells.

Extracellular recordings made from ganglion cells (ON, OFF and ON-OFF in response to light) in the intact retina, are affected by local application of substance P. This peptide has been shown to excite ON-ganglion cells (i.e. enhances light-evoked excitation) and inhibit OFF-ganglion cells in carp retina (Glickman et al., 1982; Djamgoz et al., 1983), but excites all ganglion cell types (ON, OFF, ON-OFF) in mudpuppy retina (Dick et al., 1980).

Direct application of substance P (100nM) to isolated ganglion cells of tiger salamander produced a conductance increase (implying that substance P opens ion channels in the ganglion cell membrane) which was concomitant with the production of a small inward current (section 6.3.7, Chapter 6). Hence isolated tiger salamander ganglion cells may have receptors for this peptide. Substance P is thought to act on ganglion cells through a specific receptor which is separate from those mediating other neurotransmitter inputs to ganglion cells (Eskay et al., 1980).

The function of substance P in the retina and the physiological conditions of its release from amacrine cells are unknown, but the long duration of its action (up to 15mins) makes it likely that substance P is involved in changing the excitability of the retina, and thus functions as a neuromodulator.

Some idea of the function of retinal peptides has come from

other studies in which other peptides, e.g. enkephalins, have been shown to be co-localized with GABA in retinal amacrine cells and are released on cell depolarization (Watt et al., 1984). These authors also show that exogenous enkephalins inhibit GABA release from amacrine cells of chicken. A similar effect is produced by exogenous application of opiates in goldfish (Djamgoz et al., 1981). Further experiments are required to assess the possible function of receptors for substance P in tiger salamander ganglion cells (see section 7.8.3).

7.7.5 Is it possible that release of inhibitory amino acids from amacrine cells to ganglion cells, delayed with respect to release of glutamate from bipolar cells, may contribute to the generation of transience in the light response of ganglion cells?

Transmission of information from photoreceptors to ganglion cells occurs with a synaptic delay via the amacrine cell pathway, with respect to the straight-through pathway from bipolar to ganglion cells. Werblin (1977) suggested that the initial excitatory effect of bipolar cell transmitter on ganglion cells in the mudpuppy is inhibited by later synaptic input from amacrine cells. It seems likely that the excitatory effect of bipolar cell glutamate in salamander ganglion cells could be inhibited later on by release of GABA or glycine from amacrine cells.

Alternatively, inhibitory amino acids released from amacrine cells may affect release of bipolar cell neurotransmitters and thus have an effect which is presynaptic with respect to ganglion cells. Lukasiewicz et al. (1988) have recently shown that the synaptic current of ganglion cells measured when bipolar cells were depolarized by pressure ejection of kainate, was reduced by perfusion of GABA. This implies that release of the bipolar cell transmitter is reduced by GABA. So, it is possible that modulation of bipolar cell glutamate release by GABA from amacrine cells might also provide a mechanism by which transience may be introduced into the ganglion cell response.

7.8 Further experiments to be carried out

7.8.1 Which other ion carries the current with chloride through GABA- and glycine-gated channels in ganglion cells?

GABA and glycine gate channels in the ganglion cell membrane

which are not chloride-specific, showing some permeability to acetate and gluconate (substituted for chloride in turn; section 6.3.5, Chapter 6). By substituting chloride in the patch pipette for a larger polyatomic anion such as phosphate or propionate, (shown by Bormann et al., (1987) to be impermeant through glycine-gated channels in mouse spinal neurons), it might be possible to find out whether or not acetate carries part of the current induced by these agonists in ganglion cells.

7.8.2 Can the properties of GABA or glycine-gated channels be modulated by other putative neurotransmitters?

It would be interesting to see if glutamate (released from bipolar cells) could affect the strength of GABA-mediated synaptic inhibition in ganglion cells since it has been shown that the GABA response in hippocampal neurons is potentiated by low concentrations (50μM) of glutamate and several glutamate analogues (Stelzer and Wong, 1989). This effect appears to result from an increase in the conductance of the GABA-activated chloride channel.

In preliminary experiments, isolated ganglion cell responses to iontophoretically applied GABA were not affected by subsequent perfusion of 50μM glutamate (n=3). This was the case for a range of voltage-clamp potentials (-80 to +15mV). This lack of effect may be because novel receptors for glutamate are restricted to certain cell locations or indeed species, or the receptors, like those for NMDA, are lost.

7.8.3 What are the detailed actions of the peptide substance P on ganglion cell membranes?

Although it is known that substance P excites ganglion cells (Dick et al., 1980; Djamgoz et al., 1983) the details of its action on cell membranes is unknown. Using an isolated ganglion cell preparation, the properties of the current induced by substance P could be investigated. For example, substance P may activate a channel or a carrier mechanism to produce a current, or may itself be transported across the cell membrane. Knowledge of properties such as the current-voltage relation and possible ionic selectivity of a channel or carrier may provide some insight into explaining the established effects of substance P in the intact retina (see section 7.7.4).

References

Aizenman, E., Frosch, M. P. & Lipton, S. A. (1988a) Responses mediated by excitatory amino acid receptors in solitary retinal ganglion cells from rat. J. Physiol. 396, 75-91.

Aizenman, E., Karschin, A. & Lipton, S. A. (1988b) Two distinct quisqualate receptors in isolated retinal ganglion cells from rat. Soc. Neurosci. Abs. 14, 789.

Akaike, N., Kaneda, M., Hori, N. & Krishtal, O. A. (1988) Blockade of N-methyl-D-aspartate receptors in enzyme-treated rat hippocampal neurons. Neurosci. Letters 87, 75-79.

Ariel, M. & Daw, N. W. (1982) Pharmacological analysis of directionally sensitive rabbit retinal ganglion cells. J. Physiol. 324, 162-185.

Ashmore, J. F. & Copenhagen, D. R. (1980) Different postsynaptic events in two types of retinal bipolar cell. Nature 288, 84-86.

Attwell, D. (1986) Ion channels and signal processing in the outer retina. Quart. J. Exp. Physiol. 71, 497-536.

Attwell, D., Borges, S., Wu, S. M. & Wilson, M. (1987) Signal clipping at the rod output synapse. Nature 328, 522-524.

Attwell, D., Werblin, F. S. & Wilson, M. (1982) The properties of single cones isolated from the tiger salamander retina. J. Physiol. 328, 259-283.

Attwell, D. & Wilson, M. (1980) Behaviour of the rod network in the tiger salamander retina mediated by membrane properties of individual rods. J. Physiol. 309, 287-315.

Attwell, D., Mobbs, P., Tessier-Lavigne, M. & Wilson, M. (1987) Neurotransmitter-induced currents in retinal bipolar cells of the axolotl, Ambystoma mexicanum. J. Physiol. 387, 125-161.

Ayoub, G. S. & Lam, D. M.-K. (1984) The release of gamma-aminobutyric acid from horizontal cells of the goldfish (Carassius auratus) retina. J. Physiol. 355, 191-214.

Ayoub, G. S., Korenbrot, J. I. & Copenhagen, D. R. (1988) Glutamate

* Anderson, C. R. & Stevens, C. F. (1973) Voltage-clamp analysis of ACh produced end-plate current fluctuations at frog neuromuscular junction. J. Physiol. Lond. 235, 655-691.

is released from individual photoreceptors. Invest. Ophthalmol. Vis. Sci. (Suppl) 29, 273.

Bader, C. R., Bertrand, D. & Schwartz, E. A. (1982) Voltage-activated and calcium-activated currents studied in solitary rod inner segments from the salamander retina. J. Physiol. 331, 253-284.

Bader, C. R., Macleish, P. & Schwartz, E. A. (1979) A voltage-clamp study of the light response in solitary rods of the tiger salamander. J. Physiol, 296, 1-26.

Balcar, V. J. & Johnston, G. A. R. (1972) The structural specificity of the high affinity uptake of L-glutamate and L-aspartate by rat brain slices. J. Neurochem. 19, 2657-2666.

Balcar, V. J. & Johnston, G. A. R. (1973) High affinity uptake of transmitters: studies on the uptake of L-aspartate, GABA, L-glutamate and glycine in cat spinal cord. J. Neurochem. 20, 529-539.

Barbour, B., Brew, H. & Attwell, D. (1988) Electrogenic glutamate uptake in glial cells is activated by intracellular potassium. Nature 335, 433-435.

Barlow, H. B. (1981) The Ferrier Lecture 1980. Critical limiting factors in the design of the eye and the visual cortex. Proc. Roy. Soc. Lond. B. 212, 1-34.

Barlow, H. B. & Levick, W. R. (1965) The mechanism of directionally selective units in the rabbit's retina. J. Physiol. 178, 477-504.

Barnes, S. & Werblin, F. (1986) Gated currents generate single spike activity in amacrine cells of the tiger salamander retina. Proc. Natl. Acad. Sci. USA. 83, 1509-1512.

Belgum, J. H., Dvorak, D. R. & McReynolds, J. S. (1982) Sustained synaptic input to ganglion cells of mudpuppy retina. J. Physiol. 326, 91-108.

Belgum, J. H., Dvorak, D. R. & McReynolds, J. S. (1983) Sustained and transient synaptic inputs to ON-OFF ganglion cells in the mudpuppy retina. J. Physiol. 340, 599-610.

Belgum, J. H., Dvorak, D. R. & McReynolds, J. S. (1984) Strychnine blocks transient but not sustained inhibition in mudpuppy retinal ganglion cells. J. Physiol. 354, 273-286.

Bloomfield, S. A. & Dowling, J. E. (1985) Role of aspartate and glutamate in synaptic transmission in rabbit retina. II. Inner plexiform layer. J. Neurophysiol. 53, 714-725.

Bormann, J., Hamill, O. P. & Sakmann, B. (1987) Mechanism of anion permeation through channels gated by glycine and gamma-amino-butyric acid in mouse cultured spinal neurones. J. Physiol. 385, 243-286.

Brandon, C. & Lam, D. M.-K. (1983) L-glutamic acid: A neurotransmitter candidate for cone photoreceptors in human and rat retinas. Proc. Natl. Acad. Sci. USA 80, 5117-5121.

Brew, H. & Attwell, D. (1987) Electrogenic glutamate uptake is a major current carrier in the membrane of axolotl retinal glial cells. Nature 327, 707-709.

Cajal, S. R. (1893) La retine des vertebres. La Cellule 9, 17-257.

Cervetto, L. & MacNichol, E. F. (1972) Inactivation of horizontal cells in turtle retina by glutamate and aspartate. Science 178, 767-768.

Cervetto, L. & Piccolino, M. (1974) Synaptic transmission between photoreceptors and horizontal cells in the turtle retina. Science 183, 417-419.

Chad, J. E. & Eckert, R. (1986) An enzymatic mechanism for calcium current inactivation in dialysed Helix neurones. J. Physiol. 378, 31-51.

Chemeris, N. K., Kazachenko, V. N., Kislov, A. N. & Kurchikov, A. L. (1982) Inhibition of acetylcholine responses by intracellular calcium in Lymnaea stagnalis neurones. J. Physiol. 323, 1-19.

Cohen, B. N., Fain, G. L. & Fain, M. J. (1989) GABA and glycine channels in isolated ganglion cells from the goldfish retina. J. Physiol. 417, 53-82.

Coleman, P. A. & Miller. R. F. (1989) Measurement of passive membrane parameters with whole-cell recording from neurons in the intact amphibian retina. J. Neurophysiol. 61, 218-230.

Collins, G. G. S., Anson, J. & Surtees, L. (1983) Presynaptic kainate and N-methyl D-aspartate receptors regulate excitatory amino acid release in the olfactory cortex. Brain Res. 265, 157-159.

Colquhoun, D. & Hawkes, A. G. (1977) Relaxation and fluctuations of membrane currents that flow through drug-operated channels. Proc. Roy. Soc. Lond. B. 199, 231-262.

Connor, J. A. & Stevens, C. F. (1971a) Inward and delayed outward membrane currents in isolated neural somata under voltage-clamp. J. Physiol. 213, 1-19.

Connor, J. A. & Stevens, C. F. (1971b) Voltage clamp studies of a transient outward membrane current in gastropod neural somata. J. Physiol. 213, 21-30.

Cook, A. & Mobbs, P. (1988) Application of FITC-peroxidase to optic nerve identifies viable ganglion cells in slice and isolated cell preparations of the tiger salamander retina. J. Physiol. 401, 8P.

Copenhagen, D. R., Ashmore, J. F. & Schnapf, J. L. (1983) Kinetics of synaptic transmission from photoreceptors to horizontal and bipolar cells in turtle retina. Vision Res. 23, 363-369.

Copenhagen, D. R. & Jahr, C. E. (1989) Release of endogenous excitatory amino acids from turtle photoreceptors. Nature 341, 536-539.

Cull-Candy, S. G. (1976) Two types of extrajunctional receptors in locust muscle fibres. J. Physiol. 255, 449-464.

Cull-Candy, S. G., Mathie, A., Symonds, C. J. & Wyllie, D. J. A. (1989) Distribution of quisqualate and kainate receptors in rat type-2 astrocytes and their progenitor cells in culture. J. Physiol. 418, 195P.

Cull-Candy, S. G. & Usowicz, M. M. (1987) Multiple-conductance channels activated by excitatory amino acids in cerebellar neurons.

Nature 325, 525-528.

Del Castillo, J. & Katz, B. (1954) The effects of magnesium on the activity of motor nerve endings. J. Physiol. 124, 553-559.

Davies, J., Francis, A. A., Jones, A. W. & Watkins, J. C. (1980) 2-amino-5-phosphonovalerate (2APV) a highly potent and specific antagonist at spinal NMDA receptors. Br. J. Pharmacol. 70, 52-53.

Daw, N. W., Brunken, W. J. & Parkinson, D. (1989) The function of synaptic transmitters in the retina. Ann. Rev. Neurosci. 12, 205-225.

Dick, E., Miller, R. F. & Behbehani, M. M. (1980) Opioids and substance P influence ganglion cells in amphibian retina. Invest. Ophthalmol. Vis. Sci. (Suppl). 19, 132.

Djamgoz, M. B. A, Downing, J. E. G. & Prince, D. J. (1983) Physiology of neuroactive peptides in vertebrate retina. Biochem. Soc. Trans. 11, 686-689.

Djamgoz, M. B. A., Stell, W. K., Chin, C.-A. & Lam, D. M.-K. (1981) An opiate system in the goldfish retina. Nature 292, 620-623.

Dowling, J. E. (1987) The retina: An approachable part of the brain. The Belknap Press of Harvard University Press.

Dowling, J. E. & Ehinger, B. (1975) Synaptic organization of the amine-containing interplexiform cells of the goldfish and Cebus monkey retinas. Science 188, 270-273.

Dowling, J. E. & Ripps, H. (1973) Neurotransmission in the distal retina: the effect of magnesium on horizontal cell activity. Nature 242, 101-103.

* Drejer, J. & Honore, T. (1988) New quinoxalinediones show potent antagonism of quisqualate responses in cultured mouse cortical neurons. Neurosci. Letters 87, 104-108.

Ehinger, B. (1972) Cellular location of the uptake of some amino acids into the rabbit retina. Brain Res. 46, 297-311.

Ehinger, B. (1982) Neurotransmitter systems in the retina. Retina 2, 305-321.

* Dowling, J. E. & Werblin, F. S. (1969) Organization of the retina of the mudpuppy, Necturus maculosus. I. Synaptic structure, J. Neurophysiol. 32, 315 – 338.

Eliasof, S., Barnes, S. & Werblin, F. (1987) The interaction of ionic currents mediating single spike activity in retinal amacrine cells of the tiger salamander. J. Neurosci. 7, 3512-3524.

Enroth-Cugell, C. & Robson, J. G. (1966) The contrast sensitivity of retinal ganglion cells of the cat. J. Physiol. 187, 517-522.

Errington, M. L., Lynch, M. A. & Bliss, T. V. P. (1987) Long-term potentiation in the dentate gyrus: Induction and increased glutamate release are blocked by D(-) aminophosphonovalerate. Neuroscience 20, 279-284.

Eskay, R. L., Furness, J. F. & Long, R. T. (1981) Substance P activity in the bullfrog retina: Localization and identification in several vertebrate species. Science 212, 1049-1051.

Eskay, R. L., Long, R. T. & Iuvone, P. M. (1980) Evidence that TRH, somatostatin and substance P are present in neurosecretory elements of the vertebrate retina. Brain Res. 196, 554-559.

Fain, G. L., Ishida, A. T. & Callery, S. (1983) Mechanisms of synaptic transmission in the retina. Vision Res. 23, 1239-1249.

Fenwick, E. M., Marty, A. & Neher, E. (1982) A patch-clamp study of bovine chromaffin cells and of their sensitivity to acetylcholine. J. Physiol. 331, 577-597.

Ferkany, J. W., Zaczek, R. & Coyle, J. T. (1982) Kainic acid stimulates excitatory amino acid neurotransmitter release at presynaptic receptors. Nature 298, 757-759.

Fesenko, E. E., Kolesnikov, S. S. & Lyubarsky, A. L. (1985) Induction by cyclic GMP of cationic conductance in plasma membrane of retinal rod outer segment. Nature 313, 310-313.

* Furukawa, T. & Hanawa, I. (1955). Japanese J. Physiol. 5 289-300.

Ganong, A. H., Jones, A. W., Watkins, J. C. & Cotman, C. W. (1983) Kynurenic acid inhibits synaptic and acidic amino acid-induced responses in the rat hippocampus and spinal cord. Brain Res. 273, 170-174.

Glickman, R. D.m Adolph, A. R. & Dowling, J. E. (1982) Inner plexiform circuits in the carp retina: Effects of cholinergic

agonists, GABA and substance P on the ganglion cells. Brain Res. 234, 81-99.

Hagins, W. A., Penn, R. D. & Yoshikami, S. (1970) Dark current and photocurrent in retinal rods. Biophysical J. 10, 380-412.

Hamill, O. P., Marty, A., Neher, E., Sakmann, B. & Sigworth, F. J. (1981) Improved patch-clamp techniques for high-resolution current recording from cells and cell-free membrane patches. Pflügers Archiv. 391, 85-100.

Hartline, H. K. (1938) The response of single optic nerve fibres of the vertebrate eye to illumination of the retina. Am. J. Physiol. 121, 400-415.

Ikeda, H. (1985) Transmitter action at cat retinal ganglion cells. In: Retinal research 4, 1-32 (eds. N. N. Osborne & G. J. Chader).

Ikeda, H. & Sheardown, M. J. (1982) Aspartate may be an excitatory transmitter mediating visual excitation of "sustained" but not "transient" cells in the cat retina: Iontophoretic studies in vivo. Neuroscience 7, 25-36.

Ikeda, H., Kay, C. D. & Robbins, J. (1989) Properies of excitatory amino acid receptors in the cat retina. Neuroscience 32, 27-38.

Inoue, M., Oomura, Y., Yakushiji, T. & Akaike, M. (1986) Intracellular calcium ions decrease the affinity of the GABA receptor. Nature 324, 156-158.

Ishida, A. T. (1984) Responses of solitary retinal horizontal cells to L-glutamate and kainic acid are antagonized by D-aspartate. Brain Res. 298, 25-32.

Ishida, A. T. & Cohen, B. N. (1988) GABA-activated whole-cell currents in isolated retinal ganglion cells. J. Neurophysiol. 60, 381-396.

Ishida, A. T., Kaneko, A. & Tachibana, M. (1984) Responses of solitary retinal horizontal cells from Carassius auratus to L-glutamate and related amino acids. J. Physiol. 348, 255-270.

Ishida, A. T. & Neyton, J. (1985) Quisqualate and L-glutamate inhibit retinal horizontal cell responses to kainate. Proc. Natl.

Acad. Sci. USA. 82, 1837-1841.

Jahr, C. E. & Stevens, C. F. (1987) Glutamate activates multiple single channel conductances in hippocampal neurones. Nature 325, 522-525.

Johnson, J. W. & Ascher, P. (1987) Glycine potentiates the NMDA response in cultured mouse brain neurones. Nature 325, 529-531.

Jones, K. A. & Baughman, R. W. (1988) Iontophoretic mapping of NMDA and non-NMDA receptors on inhibitory and excitatory cell types of cerebral cortex. Soc. Neurosci. Abs. 14, 789.

Kaneko, A. & Tachibana, M. (1985) A voltage-clamp analysis of membrane currents in solitary bipolar cells dissociated from Carassius auratus. J. Physiol. 358, 131-152.

Kaneko, A. & Tachibana, M. (1986) Effects of gamma-aminobutyric acid on isolated cone photoreceptors of the turtle retina. J. Physiol. 373, 443-461.

Kaneko, A. & Tachibana, M. (1987) Effects of L-glutamate on isolated turtle photoreceptors. Invest. Ophthalmol. Vis. Sci. (Suppl) 28, 50.

Karschin, A., Aizenman, E. & Lipton, S. A. (1988) The interaction of agonists and non-competitive antagonists at the excitatory amino acid receptors in rat retinal ganglion cells in vitro. J. Neurosci. 8, 2895-2906.

Karschin, A. & Lipton, S. A. (1989) Calcium channels in solitary retinal ganglion cells from postnatal rat. J. Physiol. 418, 379-396.

Karten, H. J. & Brecha, N. (1980) Localisation of substance P immunoreactivity in amacrine cells of the retina. Nature 283, 87-88.

Konishi, S., Tsunoo, A. & Otsuka, M. (1981) Enkephalin as a transmitter for presynaptic inhibition in sympathetic ganglia. Nature 294, 80-82.

Kuffler, S. W. (1953) Discharge patterns and functional

organization of mammalian retina. J. Neurophysiol. 16, 37-68.
Lamb. T. D. (1976) Spatial properties of horizontal cells in the turtle retina. J. Physiol. 263, 239-256
Lamb, T. D. (1986) Transduction in vertebrate photoreceptors: The roles of cGMP and calcium. TINS 9, 224-228.

Langdon, R. B. & Freeman, J. A. (1986) Antagonists of glutaminergic neurotransmission block retinotectal transmission in goldfish. Brain Res. 398, 169-174.

Lasansky, A. (1973) Organization of the outer synaptic layer in the retina of the larval tiger salamander. Proc. Trans. Roy. Soc. B. 265, 471-489.

Lasater, E. M. & Dowling, J. E. (1982) Carp horizontal cells in culture respond selectively to L-glutamate and its agonists. Proc. Natl. Acad. Sci. USA. 79, 936-940.

Lasater, E. M., Dowling, J. E. & Ripps, H. (1984) Pharmacological properties of isolated horizontal and bipolar cells from the skate retina. J. Neurosci. 4, 1966-1975.

Lee, K. S., Akaike, N. & Brown, A. M. (1977) Trypsin inhibits the action of tetrodotoxin on neurones. Nature 265, 751-753.

Levick, W. R. (1967) Receptive fields and trigger features of ganglion cells in the visual streak of the rabbit's retina. J. Physiol. 188, 285-307.

Lin, C. T., Li, H. Z., & Wu, J. Y. (1983) Immunocytochemical localization of L-glutamate decarboxylase, gamma-aminobutyric acid transaminase, cysteine sulfinic acid decarboxylase, aspartate amino transferase and somatostatin in rat retina. Brain Res. 270, 273-283.

Lipton, S. A. & Tauck, D. L. (1987) Voltage-dependent conductances of solitary ganglion cells dissociated from the rat retina. J. Physiol. 385, 361-391.

Lukasiewicz, P. D. & McReynolds, J. S. (1985) Synaptic transmission at N-methyl-D-aspartate receptors in the proximal retina of the mudpuppy. J. Physiol. 367, 99-115.

Lukasiewicz, P., Maple, B., Maguire, G. & Werblin, F. (1988) $GABA_A$ modulation of synaptic release from tiger salamander bipolar cells.

Invest. Ophthalmol. Vis. Sci. 29, 255.

Marc, R. E. & Lam, D. M.-K. (1981) Uptake of aspartic and glutamic acids by photoreceptors in the goldfish retina. Proc. Natl. Acad. Sci. USA. 78, 7185-7189.

Marc, R. E. & Liu, W.-L. S. (1984) Horizontal cell synapses onto glycine-accumulating interplexiform cells. Nature 312, 266-268.

Marc, R. E., Stell, W. K., Bok, D. & Lam, D. M.-K. (1978) Gaba-ergic pathways in the goldfish retina. J. Comp. Neurol. 182, 221-246.

Marr, D. (1982) Vision. W. H. Freeman & Co. San Francisco.

Massey, S. C. & Miller, R. F. (1985) Differing effects of glutamate analogues and antagonists in the rabbit retina. Soc. Neurosci. Abs. 11, 823.

Massey, S. C. & Miller, R. F. (1988) Glutamate receptors for ganglion cells in the rabbit retina: evidence for glutamate as a bipolar cell transmitter. J. Physiol. 405, 635-655.

Massey, S. C. & Redburn, D. A. (1982) A tonic GABA-mediated inhibition of cholinergic amacrine cells in rabbit retina. J. Neurosci. 2, 1633-1643.

Massey, S. C. & Redburn, D. A. (1987) Transmitter circuits in the vertebrate retina. Prog. in Neurobiol. 28, 55-96.

Mayer, M. L. & Westbrook, G. L. (1985) The action of N-methyl-D-aspartic acid on mouse spinal neurones in culture. J. Physiol. 361, 65-90.
Mayer, M. L. & Westbrook, G. L. (1987) Prog. Neurobiol. 28, 197-276.
Mayer, M. L., Vyklicky Jr., L. & Clements, J. (1989) Regulation of NMDA receptor desensitization in mouse hippocampal neurons by glycine. Nature 338, 425-427.

Miller, R. F. & Dacheux, R. F. (1983) Intracellular chloride in retinal neurons: measurement and meaning. Vision Res. 23, 399-411.

Miller, R. F., Dacheux, R.F & Frumkes, T. E. (1977) Amacrine cells in Necturus retina: Evidence for independent gamma-aminobutyric acid and glycine releasing neurones. Science 198, 748-750.

Miller, R. F., Frumkes, T. E., Slaughter, M. & Dacheux, R. F. (1981) Physiological and pharmacological basis of GABA and glycine action on neurons of mudpuppy retina. II. Amacrine and ganglion cells. J. Neurophysiol. 45, 764-782.

Miller, A. M. & Schwartz, E. A. (1983) Evidence for the identification of synaptic tranmitters released by photoreceptors of the toad retina. J. Physiol. 334, 325-349.

Miller, R. F. & Slaughter, M. M. (1986) Excitatory amino acid receptors of the retina: diversity of subtypes and conductance mechanisms. TINS 9, 211-218

Mobbs, P., Everett, K. & Cook, A. (1990) Signal shaping by voltage-gated currents in retinal ganglion cells (manuscript in preparation).

Murakami, M., Ohtsu, K. & Ohtsuka, T. (1972) Effects of chemicals on receptors and horizontal cells in the retina. J. Physiol. 227, 899-913.

Murakami, M., Ohtsuka, T. & Shimazaki, H. (1975) Vis. Res. 15, 456-458.

Murase, K., Usui, S. & Kaneko, A. (1987) Neurosci. Res. Suppl. 6, 175-190.

Naka, K.-I. (1976) Neuronal circuitry in the catfish retina. Invest. Ophthalmol. 15, 926-934.

Narahashi, T., Tsunoo, A. & Yoshii, M. (1987) Characterization of two types of calcium channels in mouse neuroblastoma cells. J. Physiol. 383, 231-249.

Nawy, S. & Copenhagen, D. R. (1987) Multiple classes of glutamate receptors on depolarizing bipolar cells in retina. Nature 325, 56-58.

Newman, E. A. (1985) Voltage-dependent calcium and potassium channels in retinal glial cells. Nature 317, 809-811.

Nistri, A., Sivilotti, L. & Bunce, N. (1988) Pharmacological block of excitatory synaptic transmission in the frog optic tectum in vitro. Br. J. Pharmac. 95, 891P.

Normann, R. A., Perlman, I., Kolb, H., Jones, J. & Daly, S. J.

(1984) Direct interactions between cones of different spectral types in the turtle retina. Science 224, 625-627.

Nowak, L., Bregestovski, P., Ascher, P., Herbet, A. & Prochiantz, A. (1984) Magnesium gates glutamate-activated channels in mouse central neurones. Nature 307, 462-465.

Ripps, H. & Witkovsky, P. (1985) Neuron-glia Interaction in the brain and retina. 181-219.

Robertson, B. (1989) Characteristics of GABA-activated chloride channels in mammalian dorsal root ganglion neurons. J. Physiol. 411, 285-300.

Rothman, S. M. & Olney, J. W. (1987) Excitotoxicity and the NMDA receptor. TINS 10, 299-302.

Sarthy, P. V., Hendrickson, A. E. & Wu, J.-Y. (1986) L-glutamate: A neurotransmitter candidate for cone photoreceptors in the monkey retina. J. Neurosci. 6, 637-643.

Sarthy, V. J. & Lam, D. M.-K. (1978) Biochemical studies of isolated glial (Müller) cells from the turtle retina. J. Cell. Biol. 78, 675-684.

Schiller, P. H., Sandell, J. H. & Mannsell, J. H. (1986) Functions of the ON and OFF channels of the visual system. Nature 322, 824-825.

Schiells, R. A., Falk, G. & Naghshineh, S. (1981) Action of glutamate and aspartate analogues on rod horizontal and bipolar cells. Nature 294, 592-594.

Schmidt, M., Humphrey, M. F. & Wassle, H. (1987) Action and localization of acetylcholine in the cat retina. J. Neurophysiol. 58, 997-1015.

Schwartz, E. A. (1986) Synaptic transmission in amphibian retinae during conditions unfavourable for calcium entry into presynaptic terminals. J. Physiol. 376, 411-428.

Slaughter, M.M. & Miller, R.F. (1981) Science 211, 182-185.

Slaughter, M. M. & Miller, R. F. (1983a) Bipolar cells in the mudpuppy retina use an excitatory amino acid neurotransmitter.

Nature 303, 537-538.

Slaughter, M. M. & Miller, R. F. (1983b) An excitatory amino acid antagonist blocks cone input to sign-conserving second-order retinal neurons. Science 219, 1230-1232.

Slaughter, M. M. & Miller, R. F. (1983c) The role of excitatory amino acid transmitters in the mudpuppy retina: an analysis with kainic acid and N-methyl aspartate. J. Neurosci. 3, 1701-1711.

Slaughter, M. M. & Miller, R. F. (1985a) Characterization of an extended glutamate receptor of the ON bipolar neuron in the vertebrate retina. J. Neurosci. 5, 224-233.

Slaughter, M. M. & Miller, R. F. (1985b) Identification of a distinct synaptic glutamate receptor on horizontal cells in mudpuppy retina. Nature 314, 96-97.

Srinivasan, M. V., Laughlin, S. B. & Dubs, A. (1982) Predictive coding: a fresh view of inhibition in the retina. Proc. Roy. Soc. Lond. B. 216, 427-459.

Stallcup, W. B., Bulloch, K. & Baetge, E. E. (1979) Coupled transport of glutamate and sodium in a cerebellar nerve cell line. J. Neurochem. 32, 57-65.

Starke, K. (1981) Presynaptic receptors. Ann. Rev. Pharmacol. Toxicol. 21, 7-30.

Stelzer, A. & Wong, R. K. S. (1989) $GABA_A$ responses in hippocampal neurons are potentiated by glutamate. Nature 337, 170-173.

Stone, J. & Hoffman, K.-P. (1972) Very slow conduction ganglion cells in the cat's retina: A major new functional type? Brain Res. 43, 610-616.

* Szczepaniak, A. C. & Cottrell, G. A. (1973) Biphasic action of glutamic acid and synaptic inhibition in an identified serotonin-containing neurone. Nature New Biol. 241, 62-64.

Tachibana, M. (1985) Permeability changes induced by L-glutamate in solitary retinal horizontal cells isolated from Carassius auratus. J. Physiol. 358, 153-167.

* Svaetichin, G. (1953) The cone action potential. Acta. Physiol. Scand. 29 565 - 600.

Tachibana, M. & Kaneko, A. (1988) L-glutamate-induced depolarization in solitary photoreceptors: A process that may contribute to the interaction between photoreceptors in situ. Proc. Natl. Acad. Sci. USA 85, 5313-5319.

Tessier-Lavigne, M., Attwell, D., Mobbs, P. & Wilson, M. (1988) Membrane currents in retinal bipolar cells of the axolotl. J. Gen. Physiol. 91, 49-72.

Tieman, S. B., Cangro, C. B. & Neale, J. H. (1987) N-acetylaspartylglutamate immunoreactivity in neurons of the cat's visual system. Brain Res. 420, 188-193.

Thieffrey, M. & Bruner, J. (1978) Direct evidence for a presynaptic action of glutamate at a crayfish neuromuscular junction. Brain Res. 156, 402-406.

Thieffrey, M., Bruner, J. & Personne, P. (1979) The presynaptic action of L-glutamate at the crayfish neuromuscular junction. J. Physiol. Paris 75, 635-639.

Thompson, S. H. (1977) Three pharmacologically distinct potassium channels in molluscan neurones. J. Physiol. 265, 465-488.

Thomson, A. M., Walker, V. E. & Flynn, D. M. (1989) Glycine enhances NMDA-receptor mediated synaptic potentials in neocortical slices. Nature 338, 422-425.

Toyoda, J. I. (1973) Vision Res. 13, 283-294.

Usowicz, M. M., Gallo, V. & Cull-Candy, S. G. (1989) Multiple conductance channels in type-2 cerebellar astrocytes activated by excitatory amino acids. Nature 339, 380-383.

Voaden, M. J., Marshall, J. & Murani, N. (1974) The uptake of [^{3}H]-gamma-aminobutyric acid and [^{3}H]-glycine by the isolated retina of the frog. Brain Res. 67, 115-132.

Watkins, J. C. & Evans, R. H. (1981) Excitatory amino acid transmitters. Ann. Rev. Pharmacol. Toxicol. 21, 165-204.

Watkins, J. C. & Olverman, H. J. (1987) Agonists and antagonists for excitatory amino acid receptors. TINS 10, 265-272.

Watt, C. B., Su, Y. T. & Lam, D. M.-K. (1984) Interactions between enkephalin and GABA in avian retina. Nature 311, 761-763.

Werblin, F. S. (1972) Lateral interactions at inner plexiform layer of vertebrate retina: antagonistic responses to change. Science 175, 1008-1010.

Werblin, F. (1973) Control of sensitivity in the retina. Sci. Am. 228, 71-79.

Werblin, F. (1977) Regenerative amacrine cell depolarization and formation of ON-OFF ganglion cell response. J. Physiol. 264, 767-785.

* Westbrook, G. L. & Mayer, M. L. (1984) Glutamate currents in mammalian spinal neurons: Resolution of a paradox. Brain Res. 301, 375-379.

Westbrook, G. L., Mayer, M. L., Namboodiri, A. A. & Neale, J. H. (1986) High concentrations of N-acetylaspartylglutamate (NAAG) selectively activate NMDA receptors on mouse spinal neurones in cell culture. J. Neurosci. 6, 3385-3392.

White, R. D. & Neal, M. J. (1976) The uptake of L-glutamate by the retina. Brain Res. 111, 79-93.

Witkovsky, P., Shakib, M. & Ripps, H. (1974) Interreceptoral junctions in the teleost retina. Invest. Ophthalmol. 13, 996-1009.

Wu, S. (1986) Effects of gamma-aminobutyric acid on cones and bipolar cells of the tiger salamander retina. Brain Res. 365, 70-77.

Yazulla, S., Studholme, K. M., Vitorica, J. & DeBlas, A. L. (1987) Localization of GABA receptors on photoreceptor synaptic terminals in goldfish and chicken retinas by immunocytochemistry. Soc. Neurosci. Abs. 13, 1054.

* Werblin f. S. & Dowling J. E. (1969) Organization of the retina of the Mudpuppy, Necturus maculosus, II. Intracellular Recording J. Neurophysiol. 32: 339-355.